VEÐURSTOFA ÍSLANDS

Report
01001

Ragnar Stefánsson, Françoise Bergerat, Maurizio Bonafede,
Reynir Böðvarsson, Stuart Crampin, Kurt L. Feigl, Frank Roth,
Freysteinn Sigmundsson, Ragnar Slunga

PRENLAB-TWO – final report

April 1, 1998 - June 30, 2000

VÍ-JA01
Reykjavík
February 2001

Report - Greinargerð
01001

Ragnar Stefánsson, Françoise Bergerat, Maurizio Bonafede,
Reynir Böðvarsson, Stuart Crampin, Kurt L. Feigl, Frank Roth,
Freysteinn Sigmundsson, Ragnar Slunga

PRENLAB-TWO – final report

April 1, 1998 - June 30, 2000

VÍ-JA01
Reykjavík
February 2001

Earthquake–prediction research in a natural laboratory –

THE PRENLAB–2 PROJECT

April 1, 1998 – June 30, 2000

Ragnar Stefánsson, Francoise Bergerat, Maurizio Bonafede, Reynir Böðvarsson, Stuart Crampin, Kurt L. Feigl, Frank Roth, Freysteinn Sigmundsson, Ragnar Slunga

4 methods and algorithms for warnings

Shear–wave splitting, stress changes
Strike of horizontal compressions
Slunga warnings – seismicity and source radius
SAG – spectral amplitude grouping

New base for studying crustal processes

Microearthquake technology
Paleoseismology
Modelling – multidisciplinary
Continuous GPS and SAR
Role of fluids
Visualization
Real–time research

Warnings during the project period

M=5 earthquake, November 1998
Hekla eruption, February 2000
Two M=6.6 SISZ earthquakes, June 2000

Continuation towards new risk mitigation projects

Building an early warning system (Icelandic project)
Developing stress monitoing sites SMSITES (EU project)
Continuation of PRENLAB–2

Contents

1 Summary **9**

1.1 Activity overview 9

1.2 Significant achievements as concerns short-term warnings, hazard assessments and understanding crustal processes related to earthquakes 10

1.2.1 New methods and algorithms have been developed and are applied - a basis for earthquake warnings 10

1.2.2 New observations and new understanding of earthquake related crustal processes, a basis for long-term as well as real-time interpretations . . 12

1.2.3 Significant warnings and other risk mitigating information during the project period 14

1.2.4 Continuation towards new research projects and enhanced warning service based on the results of the PRENLAB projects 16

1.3 Meetings and workshops 17

2 The role of the responsible institutions **19**

2.1 IMOR.DG: Icelandic Meteorological Office, Department of Geophysics 19

2.2 UUPP.DGEO: Uppsala University, Department of Geophysics 19

2.3 UEDIN.DGG: University of Edinburgh, Department of Geology and Geophysics 20

2.4 GFZ.DR.DBL: Stiftung GeoForschungsZentrum Potsdam - Solid Earth Physics and Disaster Research - Earthquakes and Volcanism 20

2.5 NVI: Nordic Volcanological Institute 21

2.6 CNRS.TT: Centre National de la Recherche Scientifique, Delegation Paris B - Département de Géotectonique 21

2.7 UBLG.DF: University of Bologna, Department of Physics 21

2.8 CNRS.DTP: Centre National de la Recherche Scientifique, UPR 0234 - Dynamique Terrestre et Planétaire 22

3 Summary of scientific achievements by subprojects and tasks **23**

3.1 Subproject 1: Monitoring crustal processes for reducing seismic risk 23

3.1.1 Task 1: Database development and service for other scientists 24

3.1.2 Task 2: Enhancing the basis for alerts, warnings and hazard assessments 29

3.1.3 Task 3: Modelling of near-field ground motions in catastrophic earthquakes in Iceland 30

3.1.4 Task 4: Mobile stations for shear-wave splitting monitoring 31

3.1.5 Task 5: Extending the alert system functions by real-time research . . 33
3.1.6 Task 6: To prepare the SIL system and the alert system for use in other risk areas 37
3.1.7 References 37
3.2 Subproject 2: Applying new methods using microearthquakes for monitoring crustal instability 40
3.2.1 Real-time mass evaluation of relative locations 40
3.2.2 The Spectral Amplitude Grouping method (SAG) for analyzing crustal stress conditions. A potential for intermediate-term warnings 42
3.2.3 Real-time inversion of stress tensor 44
3.2.4 References 44
3.3 Subproject 3: Using shear-wave splitting to monitor stress changes before earthquakes and eruptions 45
3.3.1 Task 1: Continuous monitoring of shear-wave splitting 45
3.3.2 Task 2: Analysis of shear-wave splitting measurements 53
3.3.3 Task 3: Establish shear-wave splitting map of Iceland 54
3.3.4 Task 4: Calibrate techniques and behaviour if and when changes are identified 54
3.3.5 Task 5: Incorporate shear-wave splitting interpretations into routine analysis 55
3.3.6 Meetings and conferences 55
3.3.7 References 55
3.4 Subproject 4: Borehole monitoring of fluid-rock interaction 56
3.4.1 Geophysical logging 56
3.4.2 Task 1: Repeated logging in borehole Nefsholt 58
3.4.3 Tasks 2, 3, and 4: Cross correlation of logs of the same type from different campaigns and earlier loggings; comparison of changes in logs of different type; comparison of changes in logs with changes in seismicity, etc. 63
3.4.4 Acknowledgements 80
3.4.5 References 80
3.5 Subproject 5: Active deformation determined from GPS and SAR 81
3.5.1 Subpart 5A: SAR interferometry study of the South Iceland seismic zone 82
3.5.2 Subpart 5B: GPS measurements of absolute displacements 86
3.5.3 References 90
3.6 Subproject 6: Effects of stress fields and crustal fluids on the development and sealing of seismogenic faults 91
3.6.1 Task 1: Determination of the paleostress fields associated with the test areas from fault-slip data 92
3.6.2 Task 2: Reconstruction of the current stress field associated with the test areas 95
3.6.3 Task 3: Present–day deformation from GPS network and interferograms of ERS-SAR scenes 100

3.6.4 Task 4: Effects of fluid pressure on faulting 103
3.6.5 Task 5: Numerical models on faults and fault populations 106
3.6.6 Task 6: Analyzing the fracture properties of Icelandic rocks in the laboratory 107
3.6.7 Conclusions 112
3.6.8 References 112
3.7 Subproject 7: Theoretical analysis of faulting and earthquake processes 114
3.7.1 Subpart 7A: Ridge-fault interaction in Iceland employing crack models in heterogeneous media 114
3.7.2 Subpart 7B: Modelling of the earthquake related space–time behaviour of the stress field in the fault system of southern Iceland 122
3.7.3 References 143

4 Publications **145**

Chapter 1

Summary

The PRENLAB-2 project started on April 1, 1998, and ended on June 30, 2000. It was a continuation of the PRENLAB project lasting from March 1, 1996, to February 28, 1998.

1.1 Activity overview

The project has successfully been carried out in accordance with the workprogramme. The individual subprojects have been carried out successfully in accordance with the general outlines in the workprogramme, as confirmed in reports on individual subprojects. Earth activity, seismic and volcanic, has been extremely high in Iceland during the time of the project. Therefore it was necessary to put much emphasis in enhancing the monitoring system and collection of data. Consequently, it was possible to study crustal processes related to earthquakes to an extent far beyond what was originally expected. The increased earth activity as well as scientific progress, not least of the PRENLAB projects, led to an increased interest and thus increased support of the government of Iceland for monitoring earthquake- and volcano-related crustal processes.

Successes in providing useful warnings have led to increased confidence of the public as well as of authorities of Iceland in the possibilities of seismology and related sciences in mitigating risks, as well as in the significance of the PRENLAB projects. The earth activity in Iceland led to slight shifts in the emphasis within individual tasks of the workprogramme in order to grasp the opportunities nature provided to carry forward the main objectives of the project, which are to understand better where, when and how earthquakes occur.

An earthquake sequence in the Hengill-Ölfus area in SW-Iceland (Figure 1) and associated deformation lead to concentration of the PRENLAB-2 activity in this area which, because of these events, became the most significant part of the natural laboratory during the first part of PRENLAB-2.

Two eruptions occurred in southern part of Iceland during the period of the project.

Two large earthquakes which occurred in the South Iceland seismic zone (SISZ), both magnitude 6.6 (Ms), near the end of the project period, were a test for the state of risk mitigation and earthquake prediction research in Iceland at present, and reveal new possibilities for the progress of such a research. These two earthquakes and related observed earth activity are of enormous significance for the progress of many parts of the PRENLAB-2 project far beyond its objectives.

1.2 Significant achievements as concerns short-term warnings, hazard assessments and understanding crustal processes related to earthquakes

1.2.1 New methods and algorithms have been developed and are applied - a basis for earthquake warnings

Iceland is divided into 34 basic alert regions. When number or size, etc., of small earthquakes in these regions changes beyond predefined levels scientists are alerted to take a closer look at the ongoing activity, to try to see if it might be premonitory for hazards.

Within PRENLAB-2 several algorithms have been developed to add to the alert functions and to base short-term warnings on. The limited understanding of earthquake processes as well as of their variability, requests many methods, based on our understanding of the physics of earthquake sources, or experience.

Following four methods are presently applied at IMOR.DG, for testing and as a basis for warnings.

1.2.1.1 Changes of shear-wave splitting time to observe changes of stress

By observing changes in shear-wave splitting time of local earthquakes, changes of stress can be observed in the ray path of waves radiated from the sources. Near source regions of frequent local earthquakes it is possible to observe stress changes, possibly in the build-up period of large earthquakes or eruptions. The method has already been applied in a successful stress forecast before an earthquake, and changes seen in hindsight before other events are promising for the usefulness of the method. The method has been developed within Subproject 3 at UEDIN.DGG. The method is applied for observing stress changes in seismic data from Iceland at UEDIN.DGG in close co-operation with IMOR.DG, for possibly preparing stress forecasts of earthquakes or volcanic eruptions, and for testing, as further described in Subproject 3.

1.2.1.2 Short-term warnings based on continuous observation of the strike of horizontal compressions from fault plane solutions of microearthquakes

A short-term warning algorithm has been developed which is based on completely automatic evaluations of automatically located small earthquakes and automatic fault plane solutions. This algorithm is already in continuous operation at IMOR.DG for some areas of Iceland, for short-term warning and for testing. It shows stable strike directions during a long period of time, changing however when there is a change in the mode of microearthquake activity. There are examples of precursory changes of this parameter before large earthquakes. A description of the method and results is found under Subproject 1. The method has been developed at IMOR.DG on basis of methods for fault plane solutions based on spectral amplitudes by Ragnar Slunga at UUPP.DGEO.

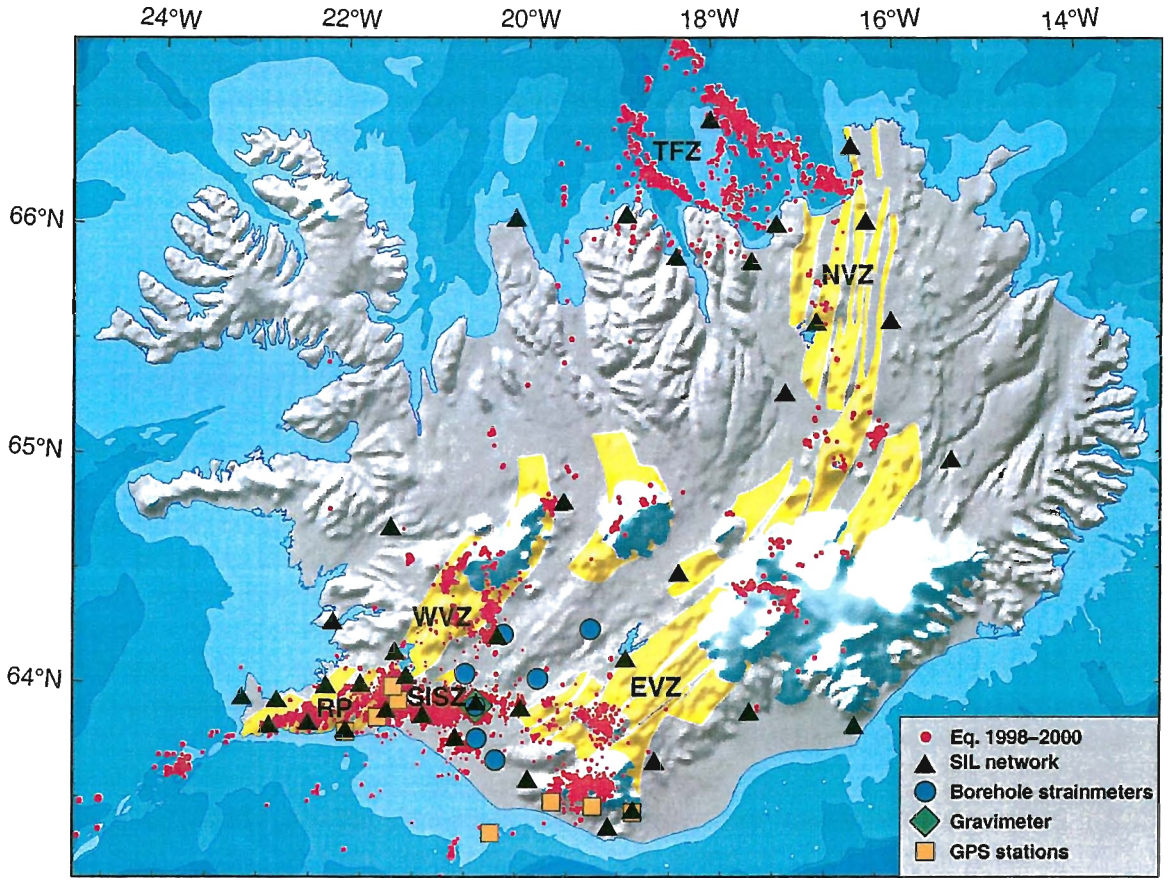

Figure 1. *Iceland, with its rift zones and volcanic zones, which delineate the mostly NS elongated mid-Atlantic ridge through Iceland. The EW plate divergency across the mid-Atlantic ridge and upwelling mantle plume below Iceland (Hotspot) are responsible for the seismicity and the volcanism. The observational network for continuous monitoring, used in the project, is shown. Volcanic zones are shown in yellow, i.e. the very active eastern volcanic zone (EVZ), the less active western volcanic zone (WVZ), and Reykjanes peninsula (RP). Large earthquakes occur along the EW elongated South Iceland seismic zone (SISZ) and in the Tjörnes fracture zone (TFZ) off the north coast. Glaciers are shown in bluish-white. The Hengill-Ölfus area, frequently mentioned in this report, is at the triple junction between SISZ, RP and WVZ.*

1.2.1.3 Slungawarning, an algorithm for alerting about time and site of impending earthquakes

The Slungawarning algorithm is based on watching seismicity of small earthquakes as well as of their source dimensions. The idea behind this is that the minimum size of source radius of earthquakes (microearthquakes) varies in time and space in the faulting area. A special case is the preparatory period of large earthquakes. Observations in hindsight of earthquake activity since 1991, after the start of the SIL system, by this algorithm provide short-term alarms for the larger events with few false alarms. This algorithm is now applied routinely for testing and gradually for short-term warnings at IMOR.DG. The method has been developed at UUPP.DGEO (see Subproject 2).

1.2.1.4 SAG, spectral amplitude grouping, a method for monitoring general stress increase in an area

It is often observed that increased stresses or closeness to fracture criticality in an area is reflected in an increase in the frequency of small earthquakes. Much of the seismic activity is, however, independent of the general stress changes, i.e. they have local energy sources and are not necessarily signs of general stress increase. By SAG spectral amplitudes of various phases of microearthquakes are used to group together earthquakes which are close to identical, and leave them out when seismicity is observed versus time. It is a better measure of closeness to fracture criticality to observe only singular events versus time than to observe all registered earthquakes. The method is a promising tool to observe the general stress level on a regional basis over a longer period of time, i.e. useful for medium-term assessments of the state of stress. It can be applied on a routine basis at IMOR.DG. It is developed in Subproject 2 at UUPP.DGEO.

1.2.2 New observations and new understanding of earthquake related crustal processes, a basis for long-term as well as real-time interpretations

The basic objective of the PRENLAB-2 project is to provide knowledge about earthquakes and related earth processes which can be basis for reducing seismic risk. The approach is physical and multidisciplinary. New measurements have been introduced and new understanding has been created to help in carrying forward these objectives.

1.2.2.1 The build-up of continuous GPS measurements in Iceland and observations of active deformation preceding earthquakes

Most significant extension of the observational network is that continuous monitoring of deformation has been initiated in Iceland by the installation of continuous GPS for observation at 8 sites in an area of high seismic and possibly volcanic activity in SW-Iceland.

These 8 stations are linked to observations of two former continuous GPS stations, which create a reference base for the local deformation monitoring. The cost of the equipment has been paid by Icelandic authorities, but the development of the observations and of the observational technology has to a large extent been a part of the PRENLAB-2 project. The

continuous GPS measurements which have only been carried out for one to two years, have already recorded significant land deformations, either preceding or coinciding with earthquake occurrence, as further described below. The significant results of these observations are gradually creating a basis for funding more stations for continuous monitoring. The continuous GPS measurements provide new constraints in using the activity in this area as a basis for modelling earthquake processes. This work has basically been carried out in cooperation between Subproject 1 and Subproject 5 and is further described under Subproject 1.

1.2.2.2 Seismic and interseismic deformation observed by interferometric analysis of Synthetic Aperture Radar (InSAR) images

Satellite radar interferometry has been used to conduct extensive investigations of crustal deformation in SW-Iceland. The Hengill volcanic area has been the main target area, and there a series of interferograms show clearly a concentric fringe pattern, indicative of uplift of 19 mm/year from 1993 to 1998. The uplift is due to an expanding pressure source located at 7 km depth, and is interpreted to be result of magma accumulation. The inflation causes stresses that exceed the Couloumb failure critertion, and the results indicate that inflow of magma into the crust can furnish the primary driving force to actually break rocks on a fault in an earthquake. Furthermore, a new technique has been developed to combine GPS and satellite radar interferometry results in order to produce three-dimensional motion maps, that give an unprecedented view of plate motions. Significant results in applying SAR technique are described under Subprojects 5 and 6.

1.2.2.3 The significance of paleoseismology for catching the variability of seismicity in time and space

Geological studies of exposed parts of the fracture and fault zones in Iceland in conjunction with microearthquakes studies have revealed significant new understanding of the variability of fault zones and faulting in time and space. Established fault zones reveal significant perturbations in stress field.

Both the South Iceland seismic zone (SISZ) and the Tjörnes fracture zone (TFZ) show large variations in mechanical decoupling during short time spans. Comparable variability is also observed on a much shorter time scale. Repeated GPS measurements as well as observations by SAR have during repeated measurements since 1995 revealed variability in time and space as well as the interaction of areas, with different mode of tectonics, in governing the crustal processes. During the 5 years of observations it has been revealed that the dangerous Húsavík-Flatey fault is at present locked above the ductile brittle boundary, below which it has enormously variable creep velocity. It has been modelled how magmatic activity in adjacent volcanic zones can influence the probability of earthquakes in the fault zones. This variability in time highlights the necessity of continuous GPS measurements for risk mitigation in these areas in addition to the seismic methods. The results are described in Subproject 6.

In the SISZ borehole measurements to obtain the horizontal stress directions indicate stability in these since in the 1970s as described under Subproject 4.

1.2.2.4 Laboratory studies of rock samples and fluid activity in the fault zones

Experimental studies on Icelandic rocks demonstrate that due to the high temperature gradient and low lithostatic stress, thermal cracking may be an important process in controlling fracture in the Icelandic crust. This leads to fast increasing permeability. Field observations of mineral-filled veins in exposed deep parts within the TFZ indicate that fluid pressures due to faulting there may be as high as 20 MPa above the least compressive stress. By implication this is thought to be similar in the SISZ. This means that the driving shear stress needed to trigger fault slip is low, only 4-6 MPa. However, for triggering an earthquake the stress conditions along the entire fault plane must be homogenized, for example by fluid flow. This can be of significance for forecasting large earthquakes, if the homogenization process can be monitored. The results are described in Subproject 6.

1.2.2.5 Modelling of processes in earth realistic heteorogenic crust

Geological and geophysical techniques aim to reveal crustal processes by observing various derived changes. This would be relatively simple if the earth could be assumed to be rheologically homogeneous in all cases. However, simplifying such conditions may be very misleading. Within the PRENLAB projects there has been significant success in applying analytic crack theory to explain the response to applied stresses in proximity of rheological discontinuities. Models which have been developed help to interprete induced seismicity in rift zones in response to stress changes. Other models help to interprete faulting and deformation at depth based on surface observations. Such results are described in Subproject 7, Subpart 7A.

A model was created of the space-time development of stress field in the SISZ on basis of historical earthquakes and expected tectonic loading. Modelling of stress field due to plate motion and the sequence of strong earthquakes since 1706 showed that the events released stress in the whole volume of the E-W trending SISZ despite that they take place on N-S faults. The earthquakes in most cases occurred in areas where the model shows relatively high stress at the time of the events. This was also partly true for the two large earthquakes of June 2000 as described under Subproject 7, Subpart 7B.

1.2.3 Significant warnings and other risk mitigating information during the project period

The PRENLAB projects have in many ways increased understanding of crustal processes, as well as the awareness that it is possible to mitigate risks by warnings preferably ahead of a hazardous event. Three examples will be described in the following.

1.2.3.1 Stress forecast before the magnitude 5 earthquake on November 13, 1998

On basis of experience in studying shear-wave splitting time patterns in the very active Hengill-Ölfus area in SW-Iceland a successful stress forecast was issued by Stuart Crampin at UEDIN.DGG, on November 10, 1998, to IMOR.DG. This forecast said that an earthquake of magnitude 5-6 could occur anytime between the issuing of the forecast (M=5) and the end

of February 1999 (M=6) if stress kept increasing. An earthquake of magnitude 5 occurred near the center of the region included in the forecast on November 13. Although this kind of forecast is far from being a complete earthquake prediction this is a step forward for short-term warnings. It does not in itself specify the epicenter of the earthquake. In this case the most likely epicenter and size had been guessed based on former activity, i.e. to complete an ongoing seismic cycle, as had been described by IMOR.DG scientists. In hindsight it was observed that the earthquake of November 13 had foreshock activity, which in fact defined the most likely epicenter for the earthquake, and also indicated that it was impending within short. Of course it is always a question if a sequence of microearthquakes is a foreshock activity or not. However, the pattern and characteristics of the foreshock activity in this case and methods for automatic evaluations of observations, give hopes that procedures can be developed to complete such a stress forecast by observations which aim at finding the place and the time of the earthquake nucleation before it ruptures.

1.2.3.2 Short-term prediction and warning before the Hekla eruption starting on February 26, 2000

The eruption of the volcano Hekla, that started on February 26, 2000, was predicted. An hour before the eruption the National Civil Defence of Iceland was warned that an eruption in Hekla was probably imminent. 20-25 minutes before the start of the eruption it was declared to the Civil Defence that an eruption would certainly start within 15-20 minutes. The warnings were based on observed microearthquakes of magnitude 0-1 which started 80 minutes before the eruption and on observations of a volumetric strainmeter in a borehole 15 km from the volcano. This warning was very significant as the ash plume reached 10 km height in a few minutes, which also was predicted. It was also significant because tourists could possibly be hiking on the mountain, which in fact showed no signs of an impending eruption except for the last 80 minutes prior to its start. The successful prediction was based on good cooperation between scientists at IMOR.DG and at UICE.SI, both involved in the PRENLAB projects. The prediction is described in Subproject 1.

1.2.3.3 Short-term warning about size and location of a magnitude 6.6 earthquake in the South Iceland seismic zone (SISZ)

Two large earthquakes occurred in the South Iceland seismic zone on June 17 and June 21, 2000, both of magnitude 6.6 (Ms). No short-term warning was issued before the first earthquake, although the sites of the two earthquakes were within 5 km of the location that had been estimated as most likely for the two next large earthquakes in the earthquake zone. This was mainly based on lack of release of moment in historical earthquakes in these two areas.

Short-term warning was issued 24 hours before the second earthquake, predicting the approximate size and the most likely area of maximum destruction within a kilometer. In hindsight very significant observations were also made before the first earthquake which may be very significant for warning in the future. The most significant observations of precursory activity were microearthquakes, water height or pressure in hot water boreholes, continuous GPS measurements and borehole strainmeters.

Warnings were issued by scientists at IMOR.DG. A fuller description is provided under Subproject 1.

1.2.4 Continuation towards new research projects and enhanced warning service based on the results of the PRENLAB projects

The results of the PRENLAB projects have paved the road for further efforts to enhance warnings and other hazards-related service. Two significant projects have started which are a direct continuation of PRENLAB-2.

1.2.4.1 A project for building an early warning system in Iceland

A project has started in Iceland for creating an early warning database and an early warning information system, with the objective to be able to utilize all available knowledge about earthquakes or volcanic hazards to mitigate risks, if possible in advance of the event, but otherwise as soon as possible after the onset of the hazard. The basis of this project is on one hand the enormous new information which is available, based on research and multidisciplinary monitoring, and on the other hand modern information technology for communication among scientists and with the public and the authorities. This project is supported by the Iceland Science Foundation. It is lead by IMOR.DG with participation of specialists on information technology from the University of Iceland and a private company.

1.2.4.2 Developing a stress monitoring site near Húsavík, N–Iceland

The town Húsavík, N-Iceland, is situated in a seismic zone of earthquakes reaching magnitude 7. Based on the success within the PRENLAB projects of monitoring stress changes by observing shear-wave splitting from local small earthquakes, a test site has been set up near Húsavík where active sources of seismic waves will be applied to observe changes in shear-wave splitting. Other observational methods, research results and experience gained in the PRENLAB projects will also be applied in this project which is supported by EU. This project (SMSITES) is shortly described under Subproject 3.

1.2.4.3 Continuation of PRENLAB-2 research based on observations of the two large SISZ earthquakes in June 2000

The multidisciplinary observations of the two large South Iceland seismic zone earthquakes in June 2000 will be of enormous significance for understanding earth processes leading to and involved in large earthquakes. Research work has started to a minor extent within the PRENLAB-2 project. The earthquakes occurred just before the end of the project. But such earthquakes were the main target of the project and thus a PRENLAB-3 would be a natural continuation of PRENLAB-2 applying the new understanding and enormous amount of data.

1.3 Meetings and workshops

The results and progress of the project were demonstrated and discussed at internal PRENLAB-2 workshops and at other workshops, and international scientific conferences, some coinciding with the PRENLAB workshops, others not.

- A whole day planning workshop was organized during the XXIII EGS General Assembly in Nice, France, April 20-24, 1998.
- The second PRENLAB-2 workshop was held in Húsavík, Iceland, July 30, 1998, attended by participants of the project in addition to several Icelandic and other European geophysicists, who are active in research related to the Húsavík fault. The workshop was also attended by representatives from the Húsavík community. The main topics of the workshop were to discuss the probability of a possibly impending destructive earthquake near Húsavík and action to be taken for research in the area as well as for enhancing the basis for providing warnings by increased monitoring.
- The third PRENLAB-2 workshop was held on March 31, 1999, coinciding with the tenth biennial EUG meeting in Strasbourg, France.
- The fourth PRENLAB-2 workshop was held on June 27, 1999, coinciding with the second EU-Japan workshop on seismic risk, Reykjavík, Iceland.
- The fifth PRENLAB-2 workshop was held on April 27, 2000, in Nice, France, coinciding with the XXV EGS General Assembly.

Among other conferences where progress of PRENLAB-2 was presented were:

- The EU-Japan workshop on seismic risk, Chania, Crete, Greece, March 24-26, 1998.
- XXIII EGS General Assembly, Nice, France, April 20-24, 1998.
- XXVI ESC General Assembly, Tel Aviv, Israel, August 23-28, 1998.
- Early Warning Conference (EWC 98), Potsdam, Germany, September 7-11, 1998.
- Workshop on recurrence of great intraplate earthquakes and its mechanism, Kochi, Shikoku, Japan, January 20-21, 1999.
- Tenth biennial EUG meeting, Strasbourg, France, March 28 - April 1, 1999.
- The conference of the Seismological Society of America, Seattle, Washington, USA, May 2-5, 1999.
- SEISMODOC and SERGISAI workshop, Brussel, Belgium, May 3, 1999.
- The second EU-Japan workshop on seismic risk, Reykjavík, Iceland, June 23-27, 1999.
- XXII IUGG General Assembly, Birmingham, United Kingdom, July 18-30, 1999.

- AGU fall meeting, San Francisco, California, USA, December 13-17, 1999.
- The third EU-Japan workshop on seismic risk, Kyoto, Japan, March 27-30, 2000.
- XXV EGS General Assembly, Nice, France, April 25-29, 2000.
- AGU spring meeting, Washington D.C., USA, May 30 - June 3, 2000.
- XXVII ESC General Assembly, Lissabon, Portugal, September 10-15, 2000.

Results and progress are described at the PRENLAB website:

http://www.vedur.is/ja/prenlab/

Chapter 2

The role of the responsible institutions

2.1 IMOR.DG: Icelandic Meteorological Office, Department of Geophysics

IMOR.DG did coordinate the PRENLAB-2 project and was responsible for Subproject 1, *Monitoring crustal processes for reducing seismic risk.* The commitments of the first year of PRENLAB-2 workprogramme have been fulfilled as detailed below.

The coordinator and contractor was Ragnar Stefánsson. IMOR.DG was responsible for a significant extension of the seismic network, of build-up of the new continuous GPS network and others available for the project, and for operating these networks. It has carried out extensive work in extending, refining and standardizing the earthquake databases as well as related databases on slow changes, where continuous borehole strainmeters are most significant, together with the emerging continuous GPS measurements. It served the other subprojects with data from these databases. It was continuously working on mapping of active faults, in studying seismicity patterns, in enhancing the alert system in Iceland, for developing and testing new algorithms and methods to cope with steadily increasing data acquisition and for enhancing the automatic data evaluation processes. It did cooperate closely with all the other subprojects, and through its coordination all the subprojects were well linked together.

Work has been carried out according to the time schedule of the workprogramme, although there has been more achieved in the data collection than planned, both because of significant earthquake sequences that had to be very well observed and because the observational system has expanded more than had been planned, also because of this increased activity.

2.2 UUPP.DGEO: Uppsala University, Department of Geophysics

UUPP.DGEO was responsible for Subproject 2, *Applying new methods using microearthquakes for monitoring crustal instability.*

The contractor, Reynir Böðvarsson, has fulfilled his commitments according to the schedule of the workprogramme. As detailed in the first annual report of PRENLAB-2 all tasks were carried out according to schedule except Task 4, which has not been carried out in the way which was planned. The Task was implementation of these new methods in a second EU country with high seismic risk. The plan was to implement these methods within the Seismological Laboratory, University of Patras in Greece. However, the leading scientist in Patras, which was a contact person in this cooperation moved to a new position in Athens,

and it has not been successful so far to re-establish the practical contact for carrying out the implementation. On the other hand the necessary preparations for being able to apply the SIL procedures at other sites have been in good advance by the contractor, both in cooperation with Subproject 1 but also in connection with the build-up of a SIL system in Sweden. The build-up of the SIL system in Sweden has to be considered a great advance for the Subproject and will further make it more feasible to export the SIL procedures to other sites.

During the second half of the project period significant new methods and algorithms have been developed by the contractor which integrate the development within the various tasks of the Subproject.

In all tasks above the closest cooperator was IMOR.DG. There has also been cooperation with UEDIN.DGG in using microearthquakes for studying shear-wave splitting.

2.3 UEDIN.DGG: University of Edinburgh, Department of Geology and Geophysics

UEDIN.DGG was responsible for Subproject 3, *Shear-wave splitting to monitor in situ stress changes before earthquakes and eruptions.* The contractor was Stuart Crampin. UEDIN.DGG has fulfilled its commitments in the workprogramme as a whole. However, frequent earthquakes in the Hengill-Ölfus area in SW-Iceland made it significant to change the emphasis of individual tasks to be carried out. This was reflected later in this report, in detailing the work carried out. All the problems addressed in the workprogramme are however addressed in the work carried out. The emphasis on continuous survey of temporal variations of shear-wave splitting from local earthquakes at a few stations in SW-Iceland has shown that it may be possible in many cases to see stress changes related to build-up of earthquakes or volcanic eruptions. In particular, observed temporal variations in shear-wave splitting in SW–Iceland was a basic observation in the successful forecast of the time and magnitude of a magnitude M=5 earthquake in SW-Iceland in November 1998. The success of this Subproject in explaining the relation between shear-wave splitting variations and effects of stress changes, as well as the successful stress forecast has initiated a new EU project within "Support for research infrastructures" (SMSITES: Developing stress monitoring sites and infrastructure for forecasting earthquakes, contract no. EVR1-CT1999-40002), which began on January 1, 2000. In all tasks above there was a close cooperation with IMOR.DG as concerns basic evaluation of and in providing data and applying the forecasts.

2.4 GFZ.DR.DBL: Stiftung GeoForschungsZentrum Potsdam - Solid Earth Physics and Disaster Research - Earthquakes and Volcanism

GFZ.DR.DBL was responsible for Subproject 4 as a whole, *Borehole monitoring of fluid–rock interaction.* Commitments of the workprogramme have been satisfactorily fulfilled. Tasks 1-4 were in direct continuation of the loggings carried out during the PRENLAB project,

and have been successfully continued during PRENLAB-2, significant results obtained and reported.

GFZ.DR.DBL was also responsible for Subpart 7B, *Modelling the earthquake related space-time behaviour of the stress field in the fault system of southern Iceland.* Close co-operation was with IMOR.DG. Subpart 7B has been successfully carried out in accordance with the workprogramme.

2.5 NVI: Nordic Volcanological Institute

NVI was responsible for Subproject 5, *Active deformation determined from GPS and SAR.* NVI has fulfilled its commitments in the workprogramme, with some well justified modifications in the carrying out the individual tasks.

The Subproject was divided into two Subparts, 5A and 5B.

Subpart 5A, *SAR interferometry study of the South Iceland seismic zone*, was managed by associated contractor Kurt Feigl of the CNRS.DTP in close cooperation with Freysteinn Sigmundsson, contractor of NVI. Subpart 5A has been carried out with some modifications as compared to the workprogramme. In accordance with the high seismic activity in the Hengill-Ölfus area at the western end of the South Iceland seismic zone, the main emphasis was on observing this activity with the SAR technology.

Subpart 5B, *GPS measurements of absolute displacements*, was managed by the contractor Freysteinn Sigmundsson of NVI, in cooperation with Páll Einarsson, subcontractor, UICE.SI, and with IMOR.DG. The work has basically been carried out in accordance with workprogramme although there was some reorientation of priorities in accordance with obtained results and because of necessary concentration of activities to the Hengill-Ölfus area because of the intensive seismic and deformation processes there.

2.6 CNRS.TT: Centre National de la Recherche Scientifique, Delegation Paris B - Département de Géotectonique

CNRS.TT was responsible for Subproject 6, *Effects of stress fields and crustal fluids on the development and sealing of seismogenic faults*, and has fulfilled its commitments in the workprogramme. All the tasks have been carried out in accordance with the workprogramme, by the contractor Francoise Bergerat of CNRS.TT, and the subcontractors Jacques Angelier of the CNRS.TT, Ágúst Guðmundsson of the University of Bergen, Norway, Thierry Villemin of Université de Savoie, France, and Philip Meredith, University College London, United Kingdom, and their coworkers.

2.7 UBLG.DF: University of Bologna, Department of Physics

UBLG.DF was responsible for Subproject 7, *Theoretical analysis of faulting and earthquake processes.* This Subproject was divided in two Subparts, 7A and 7B.

Subpart 7A, *Ridge-fault interaction in Iceland employing crack models in heterogeneous media*, was managed by contractor Maurizio Bonafede of UBLG.DF. All the tasks of the

Subpart 7A has been carried out successfully by the contractor and his coworkers at the same institute.

Subpart 7B, *Modelling the earthquake related space-time behaviour of the stress field in the fault system of southern Iceland*, was managed by associated contractor Frank Roth of GFZ.DR.DBL (see 2.4). Close cooperation was with IMOR.DG. Subpart 7B has been carried out in accordance with the workprogramme.

2.8 CNRS.DTP: Centre National de la Recherche Scientifique, UPR 0234 - Dynamique Terrestre et Planétaire

See 2.5.

Chapter 3

Summary of scientific achievements by subprojects and tasks

3.1 Subproject 1: Monitoring crustal processes for reducing seismic risk

Coordinator/contractor:

Ragnar Stefánsson
Department of Geophysics
Icelandic Meteorological Office
Bústaðavegur 9
150 Reykjavík
Iceland
Tel: +354-522-6000
Fax: +354-522-6001
E-mail: ragnar@vedur.is

Reseachers:

Kristján Ágústsson
E-mail: kri@vedur.is
Þóra Árnadóttir
E-mail: thora@vedur.is
Pálmi Erlendsson
E-mail: pe@vedur.is
Halldór Geirsson
E-mail: hg@vedur.is
Gunnar B. Guðmundsson
E-mail: gg@vedur.is
Páll Halldórsson
E-mail: ph@vedur.is
Steinunn S. Jakobsdóttir
E-mail: ssj@vedur.is
Einar Kjartansson
E-mail: eik@vedur.is
Sigurður Th. Rögnvaldsson
E-mail: sr@vedur.is
Þórunn Skaftadóttir
E-mail: thorunn@vedur.is
Kristín Vogfjörð

E–mail:kristinv@vedur.is
Bergþóra S. Þorbjarnardóttir
begga@vedur.is
Barði Þorkelsson
E–mail: bardi@vedur.is
All at Department of Geophysics
Icelandic Meteorological Office

3.1.1 Task 1: Database development and service for other scientists

3.1.1.1 Task 1.1: Data collection

Much more work was carried out in data collection and data evaluation than anticipated when the workprogramme was prepared.

This was partly due to general extensions of the applied monitoring systems, but partly due to very high seismic, volcanic and deformation activity at various places in southern Iceland.

The high seismic and deformation activity that started in 1994 in the Hengill-Ölfus area in SW-Iceland, culminated in June and November 1998, with magnitude 5 earthquakes (Figure 1).

Enormously significant data were collected in this area which contain earthquake premonitory activity and short-term precursors to earthquakes. The data collection and evaluations carried out in relation to this activity have been of basic significance in understanding crustal processes leading to earthquakes, and for creating algorithms for short–term warnings, for modelling motions involved in earthquakes and for understanding large-scale stress modifications that were caused by the two earthquakes. Most of the participants of the project have been making use of these data (Rögnvaldsson et al. 1998c). Other significant earth activity which have created significant data are the eruptions in Grímsvötn in the Vatnajökull glacier in December 1998, and the eruption in volcano Hekla in February 2000 (Stefánsson et al. 2000a; Ágústsson et al. 2000). Since July 1999 there has been a volcanic crisis in volcano Katla and in nearby volcanoes (Stefánsson et al. 2000b; Geirsson et al. 2000), based on observed activity, and on the threat which these volcanoes are for the inhabitants of the area and travellers on the nearby roads.

The two large earthquakes in the South Iceland seismic zone (SISZ) in June 2000, shortly before the end of this project and the data collected from these are of enormous significance for earthquake prediction research in general (Figure 4). Earthquakes in the SISZ, which can reach magnitude 7 have been a threat for the inhabitants in this area. Understanding large earthquakes in this area has been a basic objective for the PRENLAB projects (Stefánsson et al. 2000c). The seismic data and GPS data of the hazards shortly described here above have all been used in research actions as well as of other actions. Also significant warnings and information about these events have been provided, so significant experience has also been gained in predictions and early warnings to the public and to authorities.

The extension of the SIL acquisition and evaluation system, the SIL system, has continued during the year. The number of operating SIL stations was increased from 33 to 41.

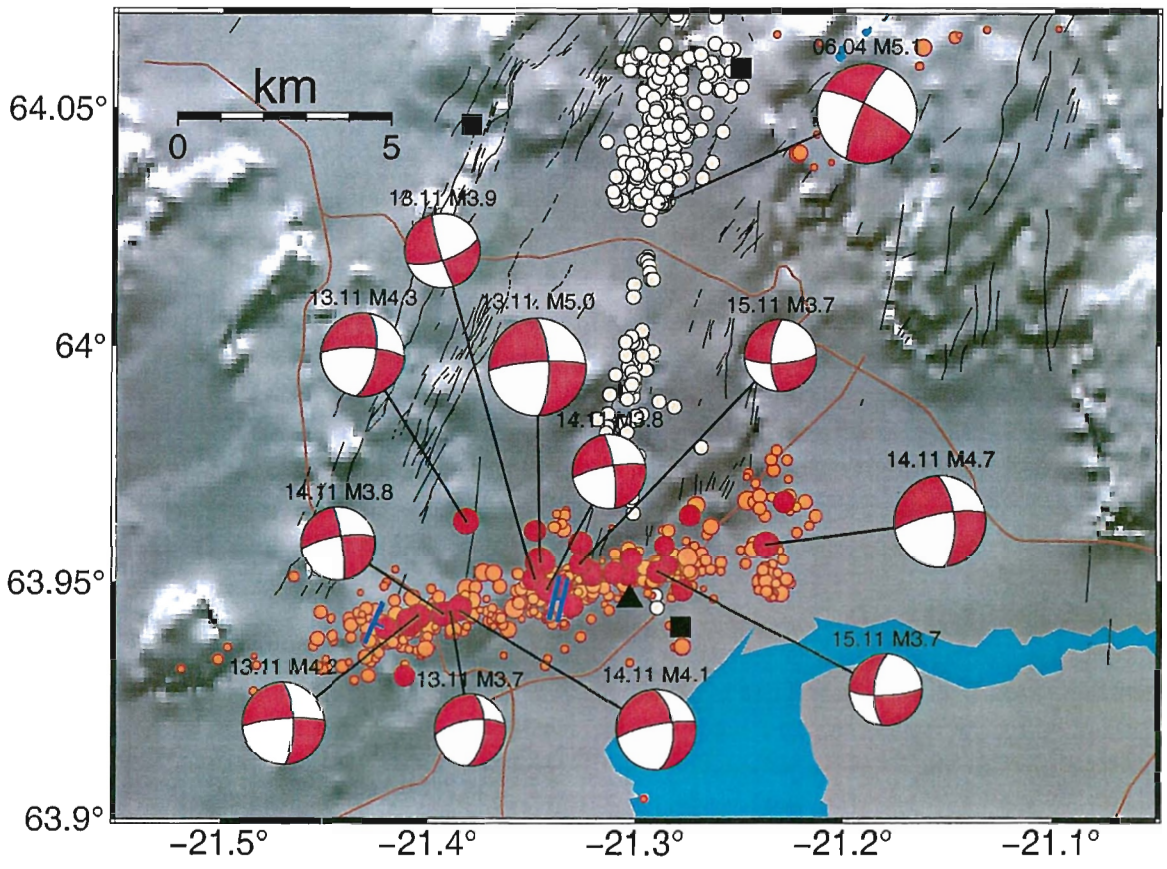

Figure 2. *Yellow and red circles show well located earthquakes (horizontal error less than 1 km and vertical error less than 2 km) from November 13-15, 1998, in Ölfus, SW-Iceland. The largest earthquake had magnitude 5.0. Red and white spheres present fault plane solutions in a conventional manner. Active faults found by accurate relative location of groups of microearthquakes are shown as blue line segments. White circles show locations of a few hundred earthquakes of the preceding earthquake swarm in Hengill in June 1998, maximum magnitude 5.1. The course of events was such that seismic activity had mostly been concentrated in the Hengill area since 1994, but ripped a fault to the south on June 4, 1998, followed by high seismic activity in an E-W elongated zone in Ölfus on November 13-15, 1998.*

Quite often during high earthquake activity the incoming data of small earthquakes is so high in the SIL system that the communication system and the computers have problems to cope with the data stream, and jams were created, which sometimes could delay the data, so the system evaluation was delayed. This could even lead to loss of data. As it is very significant to gather earthquake data down to the smallest earthquakes that provide information about crustal conditions, it was necessary to design and implement more effective procedures for doing this. For this purpose a new compression algorithm was developed for the system, i.e. the bit compression. This algorithm compresses the data very effectively at the site stations and the compressed data go directly into the evaluation procedures at the SIL center, much faster than the earlier procedures.

A new format for saving the digital earthquake waveform data will be described shortly in following:

The output of the seismometer digitizer is a series of integer values. The sample-to-sample variation is usually much less than the maximum values, which for most of SIL stations are between +/−3276800. In the AH format which was used by the SIL software, each value is stored in 32 bits.

A reduction in size of the data files of approximately a factor of 5 is achieved by storing the sample-to-sample variation in packed, variable size integers.

The access to data is thus much faster than to data that is compressed using general purpose compression programs such as *gzip* or *compress* and the files are typically 2-3 times smaller.

This new bit-compress format (bc) (Kjartansson 1996) was incorporated into the data acquisition in the SIL system during the autumn of 1998. The software on each station writes in ascii files in format that is called the SIL format. The program bc-tool can convert these files to the bc-format and back. All information in the headers are preserved.

The bc-files are then transferred to the SIL center (currently using uucp). All files from each day are kept together, with a directory for each station. An index file that contains a list of all waveforms for each day is maintained.

The index files are stored on binary form, and are sorted by the programs that read them. A major performance bottleneck in previous version resulted from sorting index files on ascii form, each time that waveform data arrived.

The new software is able to keep up with much larger levels of earthquake activity than previous software. Because the routines that read and uncompress the data are very fast and files are small, performance of all programs that use the data has been improved.

There are now 7 continuous GPS stations in S-Iceland. These stations collected valuable data during the June 2000 earthquake sequence. Although the installation cost of these stations is paid by Icelandic authorities, PRENLAB-2 has contributed significantly to the build-up and development of these measurements. The continuous monitoring of these stations has provided data which are significant for the objectives of the PRENLAB-2 project for data collection. Four of the continuous GPS stations were installed in the Hengill-Ölfus area, two south of Mýrdalsjökull and one south of Eyjafjallajökull volcanic area, as shown in Figure 3.

The project of building the continuous GPS measurements is a collaboration between IMOR.DG, NVI, and UICE.SI, with significant support for development work from PRENLAB-

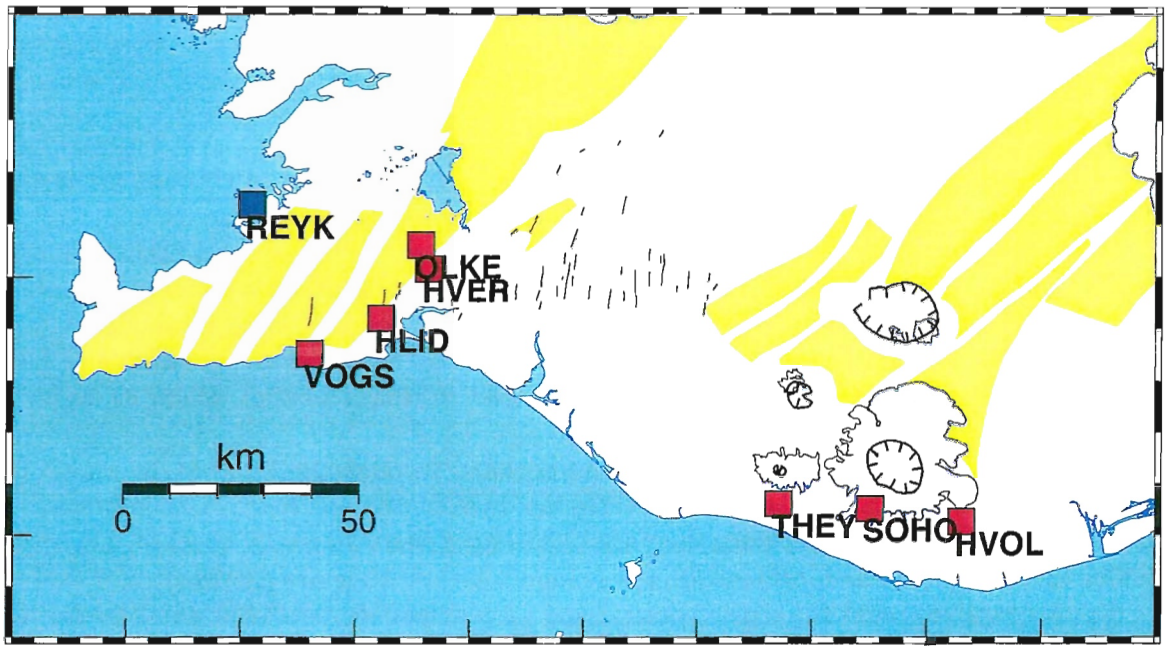

Figure 3. *Location of the continuous GPS stations in S-Iceland (red squares). The continuous GPS station in Reykjavík (REYK) is shown with a blue square. Thin black lines denote mapped faults (Einarsson and Eiríksson 1982; Einarsson and Sæmundsson 1987; Erlendsson and Einarsson 1996). The yellow areas are volcanic fissure swarms, and the calderas are shown with black lines with tick marks.*

2. The funding for purchasing the equipment comes from the Icelandic government and the Reykjavík Municipal District Heating Service. We use Trimble 4700 CORS and Trimble 4000 SSI dual frequency receivers, and Trimble Choke Ring antennas, to ensure the best data quality.

The data are automatically downloaded once every 24 hours to IMOR.DG via phone lines. Data from the IGS stations Reykjavík (REYK) and Höfn (HOFN) are included in our analysis. The data are automatically processed at IMOR.DG using the Bernese v4.2 software, and Center for Orbit Determination in Europe (CODE) predicted orbits. The displacements relative to REYK are calculated and the results posted automatically on the IMOR.DG website. The URL is http://www.vedur.is/ja/gps.html. A description of the network, data processing and results from the first year of observations are described by Árnadóttir et al. (2000).

Stations for continuous monitoring of conductivity at depth are presently operated at three sites in Iceland. A station was installed at Skrokkalda in the central highland of Iceland in July 1999, after being operated for a year at a site at the eastern end of the SISZ. This station is linked to the SIL seismic system and real-time observations are made at the SIL

center at IMOR.DG. A second station is operated at Húsafell in Borgarfjörður, W-Iceland, since spring 2000, and a station started operation in Tjarnarland in Eyjafjörður, N-Iceland at the beginning 2000. This work has been carried out through cooperation between Axel Björnsson at the University of Akureyri, and IMOR.DG. The two last continuous MT stations operate off-line.

3.1.1.2 Task 1.2: Data access

Extensive work has been carried out within the PRENLAB-2 project in creating an earthquake database with easy access. The database structure used is INGRES.

Work has started in creating an early warning system, including a multidisciplinary early warning database. The objective of this system and its database is to merge together all available information that can be significant to have in case of large earthquakes and eruptions. Also to make relevant information and warnings based on them available as fast as possible to other scientists, authorities and the public, in case of an approaching or ongoing hazard situation.

SIL network seismic data since 1991 can be accessed through the Internet, by search in a simple relational database table. This table has hypocenter and magnitude information on SIL measured earthquakes since July 1991 that have been manually checked, i.e. over 160000 earthquakes. Search options for area, magnitude and time are provided.

The preparatory work for a new, general and easy accessible relational database for all seismic data is completed and the inclusion of data in the database is in good progress.

Included in the database now or in the near future is:

- Information based on historical information. This information has been gathered over the years and will be inserted into the database.

- Information on instrumentally measured earthquakes from 1926 to 1991. Available parameter data for earthquakes during the period 1926-1974 has been extracted from catalogues and inserted into relational database tables. Parameter data for the period 1975-1986 have also been inserted into relational database tables but are not complete. Work on filling gaps in time and for areas for this period is in progress. Work on 1987-1990 data is also in progress and will be inserted within short.

  Information on earthquakes that were felt but not recorded is also inserted into the tables.

- Information on SIL parameter data from 1991 to present. The data have been checked and updated to ensure compatible processing from different recording systems. The insertion of parameter data, both observed and derived, into relational database tables is up-to-date. Information on over 160000 earthquakes is now accessible through a standardized SQL database.

- Information on station parameters, such as coordinates, instrument characteristics and time corrections at each respective time of measuring. Relational database tables have been developed.

Beside preparing this general database much work has been carried out in providing the various other subprojects with earthquake data, in accordance with the progress of the research work.

The early warning system is being built up in continuation of the significant results and data collection of the PRENLAB projects. It has been shown during recent high activity in Iceland that scientists can now provide information and warnings that are very significant for mitigating risks. Thus it is a pressing need to make, as fast as possible, use of all acquired understanding for that purpose. The IMOR.DG website is already now a significant center for the very much needed fast communication among scientists, with the public and the authorities, foremost the National Civil Defence of Iceland.

3.1.2 Task 2: Enhancing the basis for alerts, warnings and hazard assessments

This work has been carried out in relation to providing information and warnings about ongoing activity. It has been linked with increased probability of the occurrence of large earthquakes, on one hand in SW-Iceland and on the other hand near the Húsavík earthquake fault in N-Iceland.

Much work which concerns all aspects of Task 2 has been devoted to the Hengill-Ölfus area in SW-Iceland (Figure 1). An earthquake sequence has been ongoing in this region since 1994, related on one hand to E-W transversal motion across the plate boundary, and on the other to an expansion source at 8-10 km depth below the Hengill area. The largest earthquakes of this sequence took place on June 4, 1998, magnitude 5.1, and on November 13, 1998, magnitude 5. This sequence of events, as observed seismologically and geodetically, is of enormous significance for understanding the build-up of stress before earthquakes and for understanding the nucleating process or the short-term precursor activity before earthquakes (Figure 2) (Ágústsson 1998; Rögnvaldsson et al. 1998c; Tryggvason et al. 2000; Stefánsson et al. 2000d). Description of work developed on data from the Hengill-Ölfus area is also found in Subprojects 2, 3 and 4.

After the earthquake of June 4, 1998, and the following earthquake sequence and deformation, stress was modified up to 50 km distance to east and west from the epicenter, along the E-W plate boundary. This appeared in widespread seismic activity, but also in increases in shear-wave splitting delay time, which lead to an earthquake forecast (Crampin et al. 1999).

Work which is concerned with the possibility of an impending large earthquake, i.e. earthquake of magnitude 7, near the town Húsavík in N-Iceland (Figure 1), was discussed at a special PRENLAB-2 workshop in Húsavík on July 30, 1998. Work is going on under several subprojects with risk related research in this region. Subproject 1 has besides providing seismological data, taken initiative in planning new observations to be made in the area, on basis of the results of ongoing work. The objective is to provide observations which can create a better basis for modelling of the Húsavík earthquake, for an improved hazard assessment and for better real-time monitoring possibly involving short-term warnings (Stefánsson et al. 1998). IMOR.DG has been much involved in preparing and starting a new project, SMSITES, an EU project within "Support for Research Infrastructures", which is based

on the results of the PRENLAB projects (see further Subproject 3). This involves seismic measurements and evaluations as well as monitoring of changes of water elevations in hot water boreholes in the area. Work is ongoing within Subproject 1 regarding the Tjörnes fracture zone in general (Rögnvaldsson et al. 1998b).

Increased activity in the volcanic complex of Katla (see position in Figure 4), Mýrdalsjökull and Eyjafjallajökull in S-Iceland from summer 1999 which has involved increased research and monitoring as well as multidisciplinary cooperation, was aimed at being able to provide useful warnings in case of a suddenly occurring of a possibly very dangerous eruption there. The website of IMOR.DG has gradually developed into a center of early warning and information activities in Iceland (http://www.vedur.is/ja/jar_inn).

The progress of this work on this task was put under test in the two large earthquakes in the South Iceland seismic zone, on June 17 and 21, 2000, as well as in the Hekla eruption which started February 26, 2000 (Figure 4). These events involved decision about warnings or predictions as further described and referred in Subsection 3.1.5.3.

3.1.3 Task 3: Modelling of near-field ground motions in catastrophic earthquakes in Iceland

The M=5.1 earthquake on June 4, 1998, at Hellisheiði in the Hengill area (Figure 2) provided excellent geodetic and seismic data for modelling of near-field displacements of the largest earthquake in the area since 1955.

Results from modelling GPS data spanning the M=5.1 earthquake, June 4, 1998, were described in the first PRENLAB-2 annual report and by Árnadóttir et al. (1999). Preparations are ongoing for modelling near-field ground motions expected in large South Iceland seismic zone earthquakes on basis of GPS data, strong motion and records of the SIL network for the earthquakes on June 17 and June 21, and on basis of historical documentation of near-field destruction in historical South Iceland seismic zone earthquakes.

The modelling of ground motions expected in large South Iceland seismic zone earthquakes has been done for the M_S=7.1 earthquake of August 14, 1784, and written in a report (Árnadóttir and Olsen 2000). We use a finite-difference method to simulate the M_S=7.1 earthquake of August 14, 1784, which occurred in the South Iceland seismic zone, believed to have been the largest historical earthquake in Iceland. The August 14 earthquake was followed two days later by a M_S=6.7 event located approximately 30 km to the west.

We simulate a rupture on a N–S, vertical, right-lateral, strike-slip fault, vary the fault geometry, slip distribution and rupture velocity, and compare the peak velocities calculated at the surface obtained for the different models to a reference model. We find that the simulated peak velocities depend significantly on the depth to the top of the fault. The fault-parallel and vertical peak velocities decrease significantly if the fault does not break the surface, while the fault-perpendicular component is less affected. A model with a heterogeneous slip distribution yields a very different pattern and lower magnitude of surface peak velocities than uniform moment models (Figure 5). This is partly due to the variable slip at shallow depth in the distributed slip model.

We calculate the static Coulomb stress change for two models of the August 14, 1784, earthquake to examine if it is likely to have triggered the second large earthquake on August 16, 1784. We find that the stress change caused by a 20 km long fault is larger in the

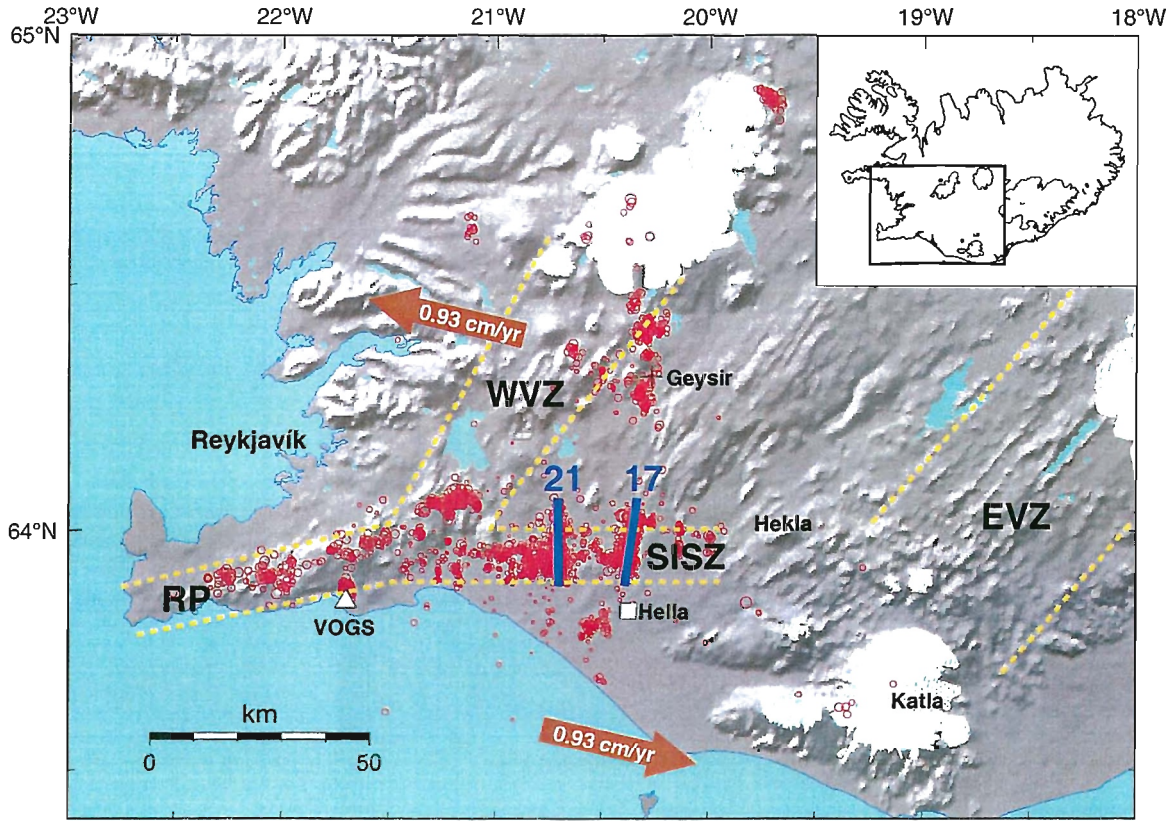

Figure 4. *The figure shows the southwestern part of Iceland. Iceland as a whole is shown in the upper right corner. Dotted yellow lines denote the western volcanic zone (WVZ) and the presently more active eastern volcanic zone (EVZ). South Iceland seismic zone (SISZ) is indicated as well as its prolongation in the Reykjanes peninsula (RP). The direction of the relative plate motion is shown by arrows. The faults of the earthquakes on June 17 and 21 are indicated by 17 and 21 respectively. Red dots, which are epicenters of small shocks following the large earthquakes, describe the area seismically activated.*

hypocentral region of the second earthquake than that for a 50 km long fault. This indicates that if the M_S=7.1 earthquake occurred on a short rather than a long fault, it is likely to have triggered the second large earthquake.

3.1.4 Task 4: Mobile stations for shear-wave splitting monitoring

The objective of this task is to investigate more in detail the shear-wave splitting effects of the crust and the spatial distribution of the observed anisotropy. Seven three-component mobile seismometers of ORION type were borrowed for this purpose from UUPP.DGEO. The seismometers were operated as a dense network near to the SIL station SAU for this purpose, from May 13 to July 5, 1998, and again from July 23 to August 13. This is in the middle of the South Iceland seismic zone and it is very significant for future use of shear-wave

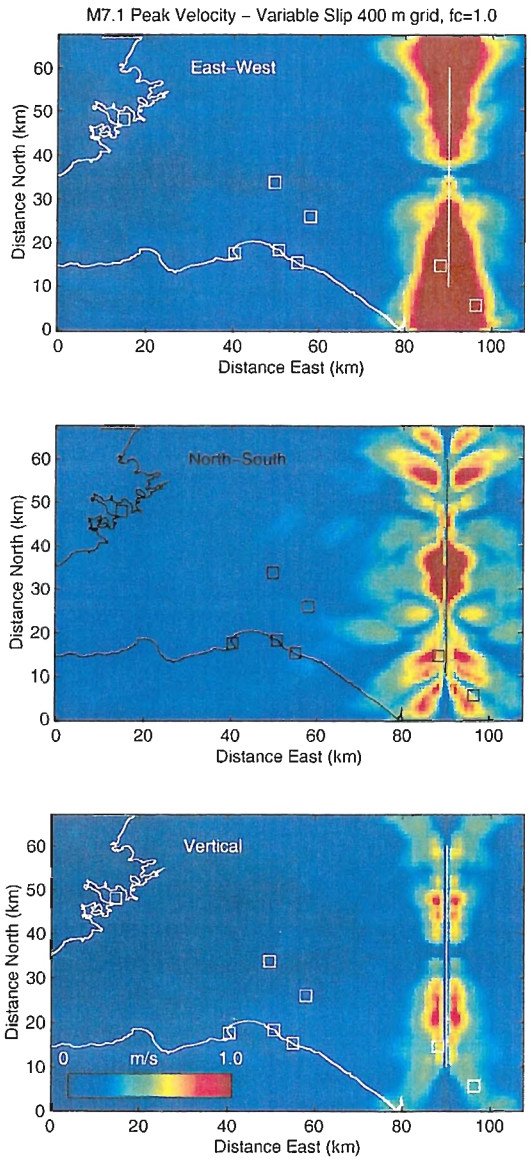

Figure 5. *Peak velocities for a model with variable slip distribution. The top panel shows the E-W component, the center panel shows the N-S component, and the bottom panel shows the vertical component. The color scale extends from 0 m/s (dark blue) to 1.0 m/s (red). The N-S line shows the surface trace of the fault model. The fault is 50 km long and extends from the surface down to 15 km depth. The rupture starts at the center of the fault at 10 km depth, and propagates bilaterally with a constant rupture velocity of 2.7 km/s. In general, the largest peak velocities correspond to areas of large slip in the model. The squares depict current locations of towns (Árnadóttir and Olsen 2000).*

splitting methods in this earthquake-prone area to carry out this study. Data were collected for this period and preparations are going on to evaluate these data. It has taken some work to merge these data with the SIL data evaluation system algorithms. This is necessary for best results, and so the high level evaluation processes of the SIL system can be utilized in full. Work on this task is ongoing, but the enormous seismic and volcanic activity in southern Iceland during the last two years has delayed this work as it has been considered more significant to save and to evaluate data of the recent large hazard events.

3.1.5 Task 5: Extending the alert system functions by real-time research

Automatic alert system at IMOR.DG as well as information from other scientific institutions and the public alert the scientists at IMOR.DG about a possibly approaching seismic or volcanic hazard. In evaluating the alert it is of enormous significance to have preprepared tools and easily accessible multidisciplinary database to help the scientists in as fast decision making as possible. The high earth activity in Iceland lately has pushed forward such a development.

Algorithms have been developed for quick visualization of direct observations, as well as of results of evaluations by many new algorithms developed within the project. Most of these tools for real-time research are available now for the scientists on the IMOR.DG website. The visualization procedures span time graphs and maps of seismic activity as well as graphs of strainmeter changes, on real-time basis as well as for comparison with earlier observations.

Several algorithms for evaluating crustal processes have been developed in the PRENLAB projects to be used on a routine basis in order to provide short-term warnings as well as for real-time research. They are used on a routine basis and are of significance for short-term warnings and thus for real-time research, as will be described in the following sections.

3.1.5.1 Methods tested and applied for short- and medium-term warnings

Following algorithms have been used and checked in Subproject 1 and will be applied at IMOR.DG in the future:

- **Monitoring stress changes from local earthquakes:**

  Stress monitoring by observing changes in shear-wave splitting time from local small earthquakes. The routine observations are carried out by UEDIN.DGG (see Subproject 3). The results are checked and discussed with IMOR.DG (see Subproject 1).

- **Variations with time in the horizontal compressions of fault plane solutions:**

  Based on automatic fault plane solutions, horizontal compressions of individual fault planes of earthquakes down to magnitude 0 are observed in real-time. It shows that the strike of the horizontal compression axis is often very stable in Iceland. Exceptions of this have been observed in the preparatory stage of large earthquakes. These variations can be observed directly in real-time on the IMOR.DG website for some areas. A tool is available on the website to monitor other areas and time periods. This work is done

both on completely automatic evaluated data as well as on manually checked data (Stefánsson et al. 2000d).

- **Slungawarning:**

  This algorithm defines time and place of a possibly approaching earthquake, on basis of seismicity rate and on sizes of fault planes of small earthquakes. The method has been developed under Subproject 2 and is described there. The algorithm has been checked at IMOR.DG and is routinely used there. See further in Subproject 2.

- **SAG:**

  Spectral amplitude grouping (SAG) is a monitoring algorithm that can be a good indicator of long-term evolution of stress. Two previous algorithms are based on fault plane solutions of earthquakes. The fault plane solutions are based on spectral amplitudes of P- and S-waves, and signs of the P-waves. SAG is based on grouping the earthquakes by using spectral amplitudes of many different phases at some seismic stations. The method is applied to monitor the of state of stress in a region as described in Subproject 2.

- **Monitoring rock stress tensor:**

  Inversion for rock stress tensor based on microearthquake locations and fault plane solutions is a very significant tool in real-time investigations. Algorithms for this are available and routinely applied at the IMOR.DG, and described under Subproject 2.

- **Subcrustal mapping of faults:**

  An algorithm for relative location based on multievent location technique is available for investigation and testing at IMOR.DG. By this technique which provides relative locations for groups of microearthquakes with an error within 10 m, it is possible even to discriminate between the fault plane and the auxiliary plane (Rögnvaldsson et al. 1998b).

3.1.5.2 An early warning system and an early warning database

In case of a dangerous earthquake or a dangerous eruption it is vital to be able to access as soon as possible all available observations and knowledge to try to mitigate risks. This is significant during the often short time between the first suspicious signs of an impending hazard and the hazard itself. But it is also significant even if no prewarning can be given. Communication between scientists, the public and authorities is enormously significant during such times.

An early warning system is in development at IMOR.DG to serve such needs. Although it is only in its initial ages of development it is already applied in practice for supplying warnings and information and for testing (Stefánsson 2000a; Halldórsson et al. 2000; Stefánsson 2000b). This project is lead by IMOR.DG in cooperation with participation of specialists on information technology from the University of Iceland and a private company. The project is supported by the Iceland Science Foundation and the government of Iceland.

3.1.5.3 Warnings for hazards in practice

The experience gained in warning service is maybe the most significant in extending the alert system and for developing real-time research. During the PRENLAB-2 period there were three eruptive crisis in Iceland, two of which have already ended with eruptions and two earthquake sequences occurred in S-Iceland where warnings and information was significant.

- **Short-term warning and information before the eruption in volcano Hekla, February 2000:**

  The eruption that started in the volcano Hekla in S-Iceland at approximately 18:17-18:19 GMT on February 26, 2000, was preceded by precursory signals on seismographs and volumetric strainmeters during the last 79 minutes prior to the outbreak.

  The National Civil Defence of Iceland was warned of a probable imminent eruption about an hour before the ash plume was observed. By time the precursory signals became more prominent and at 17:53 a prediction was issued to the Civil Defence claiming that an eruption was certainly to be expected within 15-20 minutes, with the recommendation that a warning should be issued and broadcast to the public. The main immediate hazard caused by recent Hekla eruptions is the 10 km high ash plume during the first minutes of the eruption that endangers flight traffic. Therefore, well before the final prediction was made, probable ash trajectories were calculated and the Civil Aviation Administration was notified that an ash plume from Hekla could be expected to rise to cruising altitudes of air traffic within short. The first signs of the coming eruption were seen at 17:00 from a seismometer situated within 2 km of the top of the volcano. These were earthquakes of magnitude below 1. The earthquake swarm became more intense in the next half hour and events were located by the automatic location system and detected by the alert system at 17:29. Earthquake sequences of similar size are unknown at Hekla except as a prelude to eruptions. A volumetric strainmeter at a distance of 15 km from Hekla showed rapidly increasing contraction starting 30 minutes before the eruption. Based on modelling of the 1991 Hekla eruption this was a clear sign of an opening of a feeding dyke for an eruption. This observation was used to refine the timing of the final prediction. The rapid response to the premonitory signals of the eruption was possible because of a combination of improved instrumentation in the region of Hekla, improved facilities for real-time analysis and alerting, and raised general alert caused by recent unrest in the neighbouring volcanoes, mainly Katla and Eyjafjallajökull (Stefánsson et al. 2000b; Ágústsson et al. 2000).

- **Stress forecast before the magnitude 5 earthquake in November 13, 1998, in the Ölfus area:**

  The Hengill-Ölfus area in SW–Iceland (Figure 1) was a very significant research and test area for the PRENLAB-2 project as it was for the PRENLAB project for development of warning algorithms as well as for general understanding of earthquake related crustal processes (Rögnvaldsson et al. 1998a) (Figure 2).
  The reason is basically the very high seismic activity in this area since 1994. It has been possible to carry out deformation measurements of various kinds to keep track of the deformation, both by GPS and SAR in addition to very detailed observations

of frequent seismic swarms and individual earthquakes up to 5.1 in magnitude. Stress modifications related to the largest earthquakes have been observed. Thus an earthquake cycle has been observed from the start time of build-up of stress on June 4, 1998, in a large area towards concentration of stress in a focal region and foreshocks of an earthquake that occurred on November 13, 1998. After the earthquake of November 13, it was then observed how an E-W fault zone served as a stress guide, and how a sequence of earthquakes was observed related to that guide.

On basis of experience in studying shear-wave splitting time patterns in this area and on basis of the general understanding achieved of crusal processes there, stress forecast was issued by Stuart Crampin at UEDIN.DGG, on November 10, 1998, to IMOR.DG. This forecast said that an earthquake of magnitude 5-6 could occur anytime between the issuing of the forecast (M=5) and the end of February 1999 (M=6) if stress kept increasing. An earthquake of magnitude 5 occurred near the center of the region included in the forecast on November 13. Although this kind of forecast is far from being a complete earthquake prediction this is a step forward for short-term warnings. It does not in itself specify the epicenter of the earthquake. In this case the most likely epicenter and size had been guessed based on former activity, i.e. to complete an ongoing seismic cycle, as had been described by IMOR.DG scientists. In hindsight it was observed that the earthquake of November 13 had foreshock activity, which in fact defined the most likely epicenter for the earthquake, and also indicated that it was impending within short. Of course it is always a question if a sequence of microearthquakes is a foreshock activity or not. However, the pattern and characteristics of the foreshock activity in this case and methods for automatic evaluations of observations, give hopes that procedures can be developed to complete such a stress forecast by observations which aim at finding the place and the time of the earthquake nucleation before it ruptures (see further Subproject 3).

- **Hazard assessments and short-term warning related to the two M=6.6 earthquakes in the South Iceland seismic zone in June 2000:**

  In June 2000 two earthquakes with magnitude 6.6 (Ms) struck in the central part of the South Iceland seismic zone (SISZ), immediately followed by seismic activity along zones of 100 km length (Stefánsson et al. 2000c). This occurred after 88 years of relative quiescence in the 70 km long EW transform zone in SW-Iceland (Figure 4).

  Earthquakes in this region have, according to history, frequently caused almost total destruction in areas encompassing 1000 km^2 and have been a threat for inhabitants of this area, which is a relatively densely populated farming area. In spite of open surface faults and measured accelerations higher than 0.8 g no serious injuries were reported and no homes collapsed. In light of the fear which the expected SISZ earthquakes have caused among Icelanders, the relatively minor destruction has lead to some optimism regarding the safety of living in the area. Many of the ideas about the nature of strain release in the area have been confirmed. As far as the epicenter of the first earthquake is concerned, hazard assessments or long-term predictions were confirmed, and in hindsight precursors have been observed. Useful short-term warnings regarding the epicenter, size and time of the second earthquake could be issued beforehand. Signif-

icant observations were made of the earthquakes as well as of their premonitory and following processes which will lead to better models of the SISZ earthquakes as well as to better hazard assessments and warnings in the future. Among significant observational systems are the SIL system, which is especially aimed at retrieving information from microearthquakes, strong motion instruments with a good coverage in the area, continuous GPS measurements, borehole strainmeters and hydrological observations in boreholes. Earlier GPS net measurements were repeated after the earthquakes, and detailed analysis of extensive surface fissures was carried out. It is expected that no more than 1/4 of the moment build-up in the zone has been released in these two earthquakes, and that even larger earthquakes may occur in the zone during the next decades.

The short-term warning, hazard assessment and premonitory activity are further described in Stefánsson et al. (2001).

3.1.6 Task 6: To prepare the SIL system and the alert system for use in other risk areas

The main objective here was, led by Subproject 2, to prepare the SIL system for a possible implementation at Patras in Greece. This has not been carried through because the contact in Patras failed. However, considerable work has been carried out to enhance the SIL system functions (Böðvarsson et al. 1999), as described under Task 1 above. It can also be mentioned here that installation of SIL type network in Sweden includes many refinements based on experiences in operating and continuously developing the SIL system in Iceland within the PRENLAB projects (Böðvarsson et al. 1999).

3.1.7 References

Ágústsson, K. 1998. Jarðskjálftahrina á Hellisheiði og í Hengli í maí-júlí 1998. *Greinargerð Veðurstofu Íslands* VÍ-G98040-JA06. Report, Icelandic Meteorological Office, Reykjavík, 35 pp.

Ágústsson, K., A.T. Linde, R. Stefánsson & I.S. Sacks 2000. Borehole strain observations for the February 2000 eruption of Hekla, South Iceland. In: Abstracts from the AGU spring meeting, Washington D.C., USA, May 30 - June 3, 2000.

Árnadóttir, Þ., S.Th. Rögnvaldsson, K. Ágústsson, R. Stefánsson, S. Hreinsdóttir, K.S. Vogfjörð & G. Þorbergsson 1999. Seismic swarms and surface deformation in the Hengill area, SW-Iceland. *Seismol. Res. Lett.* 70, 269.

Árnadóttir, Þ., H. Geirsson, B.H. Bergsson & C. Völksen 2000. The Icelandic continuous GPS network - ISGPS, March 18, 1999 - February 20, 2000. *Rit Veðurstofu Íslands* VÍ-R00002-JA02. Research report, Icelandic Meteorological Office, Reykjavík, 36 pp.

Árnadóttir, Þ. & K.B. Olsen 2000. Simulation of long-period ground motion and stress changes for the MS=7.1, 1784 earthquake, Iceland. *Rit Veðurstofu Íslands* VÍ-R00003-JA03. Report, Icelandic Meteorological Office, Reykjavík, 31 pp.

Böðvarsson, R., S.Th. Rögnvaldsson, R. Slunga & E. Kjartansson 1999. The SIL data acquisition system - at present and beyond year 2000. *Phys. Earth Planet. Inter.* 113,

89-101.

Crampin, S., T. Volti & R. Stefánsson 1999. A successfully stress-forecast earthquake. *Geophys. J. Int.* 138, F1-F5.

Einarsson, P. & J. Eiríksson 1982. Earthquake fractures in the districts Land and Rangárvellir in the South Iceland seismic zone. *Jökull* 32, 113-120.

Einarsson, P. & K. Sæmundsson 1987. Earthquake epicenters 1982-1985 and volcanic systems in Iceland. In: Þ.I. Sigfússon (editor), *Í hlutarins eðli.* Map accompanying the festschrift, scale 1:750000. Reykjavík, Menningarsjóður.

Erlendsson, P. & P. Einarsson 1996. The Hvalhnúkur fault, a strike-slip fault mapped within the Reykjanes peninsula oblique rift, Iceland. In: B. Þorkelsson (editor), *Seismology in Europe.* Papers presented at the XXV ESC General Assembly, Reykjavík, Iceland, September 9-14, 1996, 498-504.

Geirsson, H., Þ. Árnadóttir & B.H.Bergsson 2000. Samfelldar GPS mælingar við Eyjafjalla- og Mýrdalsjökul. In: Abstracts from the February meeting on Activity in Mýrdals- og Eyjafjallajökull, Reykjavík, Iceland, February 17, 2000. Geoscience Society of Iceland.

Halldórsson, P., R. Stefánsson, B. Þorbjarnardóttir & I. Jónsdóttir 2000. Bráðaviðvaranir um jarðvá – áfangaskýrsla. *Greinargerð Veðurstofu Íslands* VÍ-G00005-JA02. Report, Icelandic Meteorological Office, Reykjavík, 16 pp.

Kjartansson, E. 1996. Databate for SIL earthquake data. In: Abstracts from the XXV ESC General Assembly, Reykjavík, Iceland, September 9-14, 1996.

Rögnvaldsson, S.Th., K. Ágústsson, B.H. Bergsson & G. Björnsson 1998a. Jarðskjálftamælanet í nágrenni Reykjavíkur - lýsing á mælaneti og fyrstu niðurstöður. *Rit Veðurstofu Íslands* VÍ-R98001-JA01. Research report, Icelandic Meteorological Office, Reykjavík, 15 pp.

Rögnvaldsson, S.Th., Á. Guðmundsson & R. Slunga 1998b. Seismotectonic analysis of the Tjörnes fracture zone, an active transform fault in North Iceland. *J. Geophys. Res.* 103, 30117-30129.

Rögnvaldsson, S.Th., G.B. Guðmundsson, K. Ágústsson, S.S. Jakobsdóttir, R. Slunga & R. Stefánsson 1998c. Overview of the 1993-1996 seismicity near Hengill. *Rit Veðurstofu Íslands* VÍ-R98006-JA05. Research report, Icelandic Meterological Office, Reykjavík, 16 pp.

Stefánsson, R. 2000a. Information and warnings to authorities and to the public about seismic and volcanic hazards in Iceland. To appear in a book of papers presented at the Early Warning Conference (EWC98), Potsdam, Germany, September 7-11, 1998, 11 pp.

Stefánsson, R. 2000b. Warnings about seismic and volcanic hazards in Iceland. In: Abstracts from the 4th International Conference of LACDE - Local Authorities Confronting Disasters and Emergencies, Reykjavík, Iceland, August 27-30, 2000.

Stefánsson, R., S.Th. Rögnvaldsson, P. Halldórsson & G.B. Guðmundsson 1998. PRENLAB workshop on the Húsavík earthquake, July 30, 1998. *Greinargerð Veðurstofu Íslands* VÍ-G98032-JA04. Report, Icelandic Meteorological Office, Reykjavík, 5 pp.

Stefánsson, R., K. Ágústsson, G.B. Guðmundsson, B. Þorbjarnardóttir & P. Einarsson

2000a. A successful prediction and warning of an eruption in the Hekla volcano, Iceland. In: Abstracts from the AGU spring meeting, Washington D.C., USA, May 30 - June 3, 2000.

Stefánsson, R., G.B. Guðmundsson & P. Halldórsson 2000b. Jarðskjálfta- og þenslumælingar til eftirlits með Mýrdals- og Eyjafjallajökli – líkur á eldgosi. In: Abstracts from the February meeting on Activity in Mýrdals- og Eyjafjallajökull, Reykjavík, Iceland, February 17, 2000. Geoscience Society of Iceland.

Stefánsson, R., G.B. Guðmundsson & P. Halldórsson 2000c. The two large earthquakes in the South Iceland seismic zone on June 17 and 21, 2000. *Greinargerð Veðurstofu Íslands* VÍ-G00010-JA04. Report, Icelandic Meteorological Office, Reykjavík, 8 pp.

Stefánsson, R., G.B. Guðmundsson & R. Slunga 2000d. The PRENLAB-2 project, premonitory activity and earthquake nucleation in Iceland. In: B. Þorkelsson & M. Yeroyanni (editors), *Destructive earthquakes: Understanding crustal processes leading to destructive earthquakes.* Proceedings of the Second EU-Japan Workshop on Seismic Risk, Reykjavík, Iceland, June 23-27, 1999, 161-172.

Stefánsson, R., Þ. Árnadóttir, G.B. Guðmundsson, P. Halldórsson & G. Björnsson 2001. Two recent M=6.6 earthquakes in the South Iceland seismic zone. A challenge for earthquake prediction research. *Rit Veðurstofu Íslands* VÍ-R01001-JA01. Research report, Icelandic Meteorological Office, Reykjavík, in press.

Tryggvason, A., S.Th. Rögnvaldsson & Ó.G. Flóvenz 2000. Three-dimensional imaging of the P- and S-wave velocity structure and earthquake locations beneath Southwest Iceland. *J. Geophys. Res.*, submitted.

3.2 Subproject 2: Applying new methods using microearthquakes for monitoring crustal instability

Contractor:

Reynir Böðvarsson
Department of Geophysics
Uppsala University
Villavägen 16
S–752 36 Uppsala
Sweden
Tel: +46–471–182378
Fax: +46–471–501110
E–mail: rb@geofys.uu.se

Researcher:

Ragnar Slunga
Department of Geophysics
Uppsala University
Villavägen 16
S–752 36 Uppsala
Sweden
Tel: +46–471–182378
Fax: +46–471–501110
E–mail: ragnar@geofys.uu.se

Researcher:

Björn Lund
E–mail: bl@geofys.uu.se
Department of Geophysics
Uppsala University

Researcher:

Zaher Hossein Shomali
E–mail: hs@geofys.uu.se
Department of Geophysics
Uppsala University

In the first annual report of the PRENLAB-2 project the work on individual tasks of this Subproject were detailed. In the following we report results based on integrating results of those individual tasks.

3.2.1 Real-time mass evaluation of relative locations

One of the successes of the PRENLAB project was development of methods for subcrustal mapping of faults based on the algorithm by Slunga et al. (1995). Location of groups of similar, well correlated microearthquakes with relative accuracy of the order of 10 m,

even at great depth in the crust, made it possible to map with a great accuracy complicated network of faults within active fault zones. The method has been further developed within PRENLAB-2, with applications in some areas of Iceland, where comparison has been made with geological studies. This method together with the fault plane solutions of microearthquakes is also the basis for using microearthquakes to study crustal instability in fault zones.

A new way of handling the multievent locations has been designed within the PRENLAB-2 project, which makes it possible to treat a large mass of data from a complicated fault system.

This method is suited for automatic on-line analysis where the new incoming microearthquake events are located in groups together with the previously located events and where the previous results are used. The analysis of the new events may improve all previous locations successively. This new algorithm consists of three main software programs. One correlates the new event with the previously analyzed and defines the group of events based on both location and signal correlation. The second performs the multievent location based on arrival time differences from the correlations and on the absolute arrival times. The third program fits the absolute locations to the previously achieved absolute locations and stores the results in a library.

This method has been installed for testing and routine application at IMOR.DG.

3.2.1.1 Slungawarning, an algorithm based on microearthquakes for alerting about time and site of impending earthquakes

The Slungawarning algorithm involves to watch in real-time seismicity of microearthquakes as well as of their source dimensions, and to detect anomalies based on a physically established source model and experience of observations of the SIL microearthquake system for 9 years.

The physical basis for developing and testing such an algorithm is a recently evolving rate-and-state dependent model of friction of fault planes. This model suggests that for any given earthquake generating fracture and loading system, there exists a minimum fault radius for earthquakes, again suggesting that different parts of the faults with different minimum fault radius of earthquakes may be active at different stages of the premonitory process leading to large earthquakes. Thus by evaluating microearthquakes it may be possible to resolve a process that sometimes has been assumed and treated as totally chaotic.

Based on such physically based ideas and observations a number of earthquake warning parameters have been defined and an earthquake warning algorithm has been developed which has been tested retrospectively on SW-Iceland (Slunga et al. 2000).

A study of the microseismicity during the 9 years within SW-Iceland where the large earthquakes occurred has been made (Slunga et al. 2000). A detailed description of that work is given in Slunga (2001). Here some main results are summarized.

The most obvious result is the close relation between the microearthquake fault radii and the geodynamic processes (coinciding with large earthquakes, and the large eruption below Vatnajökull glacier in 1996). The 3 largest earthquakes are preceded by large fault radius microearthquakes 3-4 months before the events. In addition the larger earthquakes in the Hengill area are preceded by an increase in microearthquake fault radii one or a few days

before the events.

Most larger earthquakes are also preceded by an increased microearthquake activity culminating with foreshocks within the last day or days before the events. For the largest earthquake of the period the foreshock activity is lacking ML>1 events. For the quiet part of the SIL area with large earthquakes on N-S faults a "sandwich" seismicity ratio method was proposed. It compares the seismicity rate within a N-S strip to the seismicity of the surroundings. It was found that the last month before the large June 17, 2000, earthquake the surroundings became silent while the N-S strip became more active (the microearthquake sizes typically between ML= -0.2 to 0.4).

All these aspects were tested within an EQWA (EartQuake Warning Algorithm) and it was found that during times of warnings (24 hour after each warning and within a distance of 6 km) the probability to have a large earthquake within the warned area was about 500 times larger than the probability based on total randomness.

Finally it was also found that most false warnings were at places of coming earthquakes. Such warnings during the last years before major earthquakes may increase the awareness of the risks.

In general the results of the study (Slunga et al. 2000) are in agreement with other precursory studies of shallow strike-slip earthquakes in other places of the world.

This algorithm is now being installed to be applied routinely for short-term warnings and for testing at IMOR.DG.

A thorough description of the method and of results of tests is found in Slunga (2001).

3.2.2 The Spectral Amplitude Grouping method (SAG) for analyzing crustal stress conditions. A potential for intermediate-term warnings

A new method called Spectral Amplitude Grouping (SAG) has been developed (Lund and Böðvarsson 2000). This method addresses the problem of similarity of focal mechanisms used in stress tensor inversion. SAG has shown to be useful for analysis of temporal evolution of the earthquake grouping patterns. The SIL system calculates spectral amplitudes on three component data rotated into vertical, radial and transverse components. Windows are placed on the direct P- and S-wave arrivals and transforming to the frequency domain the low frequency asymptotes, or DC-level spectral amplitudes, are estimated for the different components (Rögnvaldsson and Slunga 1993). We obtain five amplitude values at each recording station; vertical and radial P (PZ and PR) and vertical, radial and transverse S (SZ, SR and ST), which we refer to as amplitude components. These amplitude components, together with first motion directions, form the basis for the focal mechanism calculation in the SIL system and will be utilized in the spectral amplitude correlation and grouping scheme. In order to assess the similarity of the focal mechanisms of two different events all amplitude components in common for the two events are correlated using linear cross-correlation

$$r = \frac{\sum_i (x_i - \bar{x})(y_i - \bar{y})}{\sqrt{\sum_i (x_i - \bar{x})^2}\sqrt{\sum_i (y_i - \bar{y})^2}}$$

where r is the correlation coefficient, $\bar{x}$, is the mean of the logarithms of one event's amplitude components, x_i, and $\bar{y}$ the mean ofthe logarithms of the other event's amplitude components,

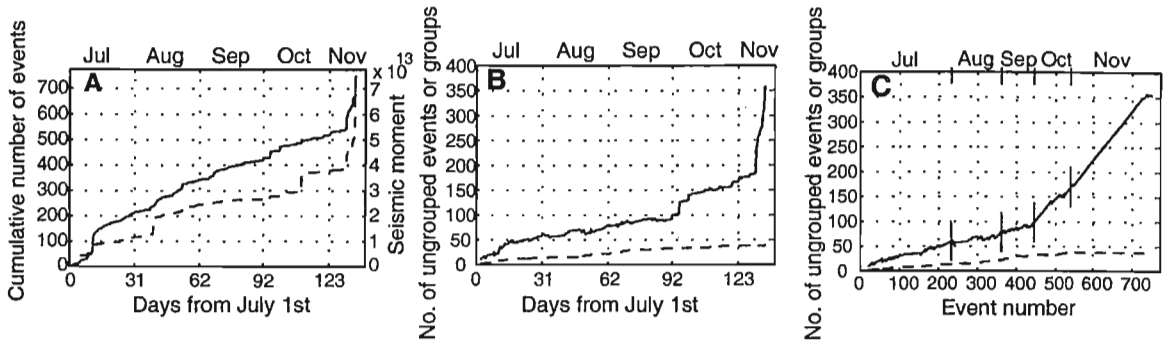

Figure 6. *Correlation results in Ölfus, July 1 to November 13, 1998. A) Plotted versus time in days is the cumulative number of events (solid line, scale to the left) and the cumulative scalar seismic moment (dashed line, scale to the right). B) Number of ungrouped events (solid line) and the number of groups (dashed line) versus time in days. C) Number of ungrouped events (solid line) and number of groups (dashed line) versus the event number.*

y_i. The logarithms are utilized to decrease the importance of the nearest stations, thereby stabilizing the correlation. We use the correlation coefficient as the measure of how similar two events are. All events are correlated with all other events and the events are then grouped according to the correlation coefficients. The grouping is controlled by three parameters; a lower limit on the correlation coefficients, r_{min}, a lower limit on the fraction, f_{min}, of fellow events in the group that a single event is allowed to have below r_{min} and the minimum number of events needed to have a group. After some testing we adopted $r_{min} = 0.9$, $f_{min} = 0.8$ and at least four events in the group, as our parameters for studying larger amounts of seismicity. If a more detailed study on fewer events is desired, the r_{min} and/or f_{min} values should be increased. We define two modes of running the correlation and grouping, the first correlates all events in a catalogue with all other events in one large run, and then performs an iterative grouping that allow us to find the optimal homogeneity within the groups. The second mode starts with a small group of events that are correlated and grouped, and then the events are correlated and grouped one by one with the previous events. This mode will not obtain the optimal group homogeneity but instead it allows us to study the time variations in correlation and grouping. During the development of the correlation and grouping scheme we discovered that it is useful also for applications other than as a preprocessor to stress tensor inversion. If we run the correlation in the second mode the temporal evolution of the earthquake grouping patterns can be studied and the groups of similar events produced by the grouping can be utilized either for composite focal mechanism calculations or as a starting group for relative relocation. We tested the correlation and grouping algorithm on a set of 636 microearthquakes, $0.0 \leq M_L \leq 2.7$, occurring between July 1, 1998, and November 13, 1998, in Ölfus, southwestern Iceland. On November 13 there was a magnitude 5.0 earthquake in the Ölfus area. Cumulative number of events and cumulative seismic moment is plotted in Figure 6.

Studying the Ölfus seismicity using the second mode of correlation and grouping we obtain the plots in Figures 6B and 6C. In Figure 6B we see that the seismicity in July

correlates very well, the rapid increase in number of events is not mirrored by an increase in the number of ungrouped events. Conversely, the increase in seismicity in November has an associated increase in the number of ungrouped events. The grouping pattern becomes clearer if we plot the number of ungrouped events and number of groups as a function of the event number (Figure 6C). We now clearly see a change in the grouping pattern around event 430, which corresponds to late September, where the slope of the curve significantly changes. We interpret the lack of correlation after September as an indication that the microseismicity changed characteristics. Before late September many events occur on the same fault (or a very close, similarly oriented fault) with very similar slip directions. We refer to these events as *repeated* events. After September, spectral amplitude correlation indicates that either the focal mechanisms are different, both compared to earlier and to current seismicity, or the events occur at different locations compared to earlier and current seismicity.

A version of this program program has been installed for real-time monitoring of earthquake grouping patterns.

3.2.3 Real-time inversion of stress tensor

Programs for stress tensor inversion described in the PRENLAB final report and in PRENLAB-2 first annual report (see Lund and Slunga 1999) have being modified for real-time operation. We utilize the SAG method (Lund and Böðvarsson 2000) to preprocess the data prior to the stress tensor inversion. The preprocessor allows for a stable inversion with minimum amount of data thus gives a new measure of the stress tensor at earliest possible time.

3.2.4 References

Lund, B. & R. Slunga 1999. Stress tensor inversion using detailed microearthquake information and stability constraints: application to Ölfus in southwest Iceland. *J.Geophys.Res.* 104, 14947-14964.

Lund, B. & R. Böðvarsson 2000. Correlation of microearthquake body-wave spectral amplitudes. *Bull. Seism. Soc. Am.*, accepted.

Rögnvaldsson, S.Th. & R. Slunga 1993. Routine fault plane solutions for local and regional networks: a test with syntetic data. *Bull. Seism. Soc. Am.* 11, 1247-1250.

Slunga, R. 2001. Foreshock activity, fault radius and silence - earthquake warnings based on microearthquakes. *Greinagerð Veðurstofu Íslands* VÍ-01003-JA03. Report, Icelandic Meteorological Office, Reykjavík, in press.

Slunga, R., S.Th. Rögnvaldsson & R. Böðvarsson 1995. Absolute and relative locations of similar events with application to microearthquakes in southern Iceland. *Geophys. J. Int.* 123, 409-419.

Slunga, R., R. Böðvarsson, G.B. Guðmundsson, S.S. Jakobsdóttir, B. Lund & R. Stefánsson 2000. A simple earthquake warning algorithm based on microearthquake observations - retrospective applications on Iceland. Submitted.

3.3 Subproject 3: Using shear-wave splitting to monitor stress changes before earthquakes and eruptions

Contractor:

Stuart Crampin
Department of Geology and Geophysics
University of Edinburgh, Grant Institute
West Mains Road, Edinburgh EH9 3JW
United Kingdom
Tel: +44-131-650-4908
Fax: +44-131-668-3184
E-mail: scrampin@ed.ac.uk

Researcher:

Theodora Volti
Department of Geology and Geophysics
University of Edinburgh, Grant Institute
West Mains Road, Edinburgh EH9 3JW
United Kingdom
Tel: +44-131-650-8533
Fax: +44-131-668-3184
E-mail: tvolti@ed.ac.uk

3.3.1 Task 1: Continuous monitoring of shear-wave splitting

The basic remit of the project is to respond to any observed changes in shear-wave splitting and analyze data for hazard assessment. The bulk of the activity has been in this task as changes in shear-wave splitting are now observed routinely before larger earthquakes and before volcanic eruptions and subsurface movements of magma.

Shear-wave splitting is sensitive to changes in stress. In anisotropic media, the two shear-waves split into two orthogonally polarized waves that propagate with different velocities. Examination of the seismograms can identify the polarization direction of the first (or faster) shear-wave and the time delay between the two arrivals (Figure 7). Time-delays are particularly sensitive to changes in azimuthal anisotropy induced by stress-induced changes to microcrack distributions (Crampin 1999).

Shear-wave data from earthquakes provided by IMOR.DG are identified and analyzed routinely. Seismic stations in Iceland are shown in Figure 8 with all earthquakes with $M \geq 2$ in the period January 1997 to December 1999. The stations with sufficient shear-wave arrivals for analysis of temporal changes, KRI, BJA, and SAU are marked with red triangles. Stations throughout Iceland with more than 10 polarization measurements during the four years of the PRENLAB projects, 1996-1999, are shown in Figure 9 (after Volti and Crampin 2000). The alignment of polarizations show average directions of the maximum horizontal stress SW-NE.

As in previous years, the stations with sufficient polarization and time-delay data are BJA, SAU and KRI, situated along the South Iceland seismic zone (SISZ) (Figure 8) and

marginally GRI on the island of Grímsey, north of Iceland. During 1998, analysis was concentrated on station BJA, which had the best quality shear-wave arrivals. However, activity near BJA has declined during 1999 and 2000, whereas activity near KRI and SAU has increased (Volti and Crampin 2000).

3.3.1.1 Temporal variations in time-delays

Polarization directions and time-delays were measured during March 1998 - June 2000. The suitable events recorded within the shear-wave window (station-to-epicenter distance less than hypocentral depth) ensures that the shear-waves are not distorted by surface conversions. This constrains the number of events that can be used for shear-wave splitting analysis. There is also need for sufficient activity to show temporal variations. Other constraints include restrictions in focal depths, location errors, and deviations from the mean polarization direction. In the PRENLAB-2 period, these criteria were fulfilled mainly for station BJA, SAU and KRI. Variations in time-delays for the above stations are shown in Figures 10a, 10b and 10c. At each station the mean polarization is calculated and time-delay measurements with polarizations within a standard deviation of this direction are selected. There were 4230 observations at BJA, 5145 at KRI and 44 at SAU. The time-delay measurements are normalized over straight-line path distance and separated into two bands defined by incidence to the vertical plane of symmetry parallel to the mean polarization direction (the average strike of aligned near-vertical cracks). Band-1 (15°-45°) is more sensitive to changes in crack aspect-ratio, the result of gradually increasing stress. Band-2 (0°-15°) is more sensitive to crack density, which does not vary consistently with increasing stress.

Figures 10a, 10b, and 10c show data from March 1998 to June 2000. The middle cartoons show nine-point moving averages through the time-delays in Band-1. The least-squares lines begin before a minima in the nine-point moving average and end when a large earthquake occurs. This is followed by an abrupt decrease in time-delays. The upper cartoons show nine-point moving averages through the time-delays in Band-2. No consistent pattern or relationship to earthquakes can generally be seen in Band-2. The lower cartoons show the magnitudes of all $M \geq 2$ earthquakes within 20 km of the station.

Since 1996, station BJA displayed a relatively simple relationship between the magnitude of an earthquake and the duration (and slope) in the increase of time-delays before the event: the magnitude was proportional to the duration of the increase, and inversely proportional to the slope (Volti and Crampin 2000). In Figure 4a, Band-1 of BJA, variations before two large earthquakes (M=5.1 and 5) are indicated. They both show similar patterns of increase and reach maximum time-delays up to 14 ms/km after an increase of about four months. The second event was stress-forecast (see Subsection 3.3.1.2).

(Note that earthquake magnitudes, written as M, are local magnitudes approximately equivalent to body-wave magnitudes, mb, where in this magnitude range M=5 is approximately equal to surface wave magnitudes, Ms=6).

Three months later, there was a M=4 earthquake, with longer duration and smaller slope from that expected from previous events. The time-delays do not drop immediately afterwards, but show a slight increase. Two months later, July 1999, a volcanic event in Katla took place, after which time-delays started to drop gradually. Also, in contrast with the previous earthquakes, a similar pattern exists in Band-2. In February 2000, there was

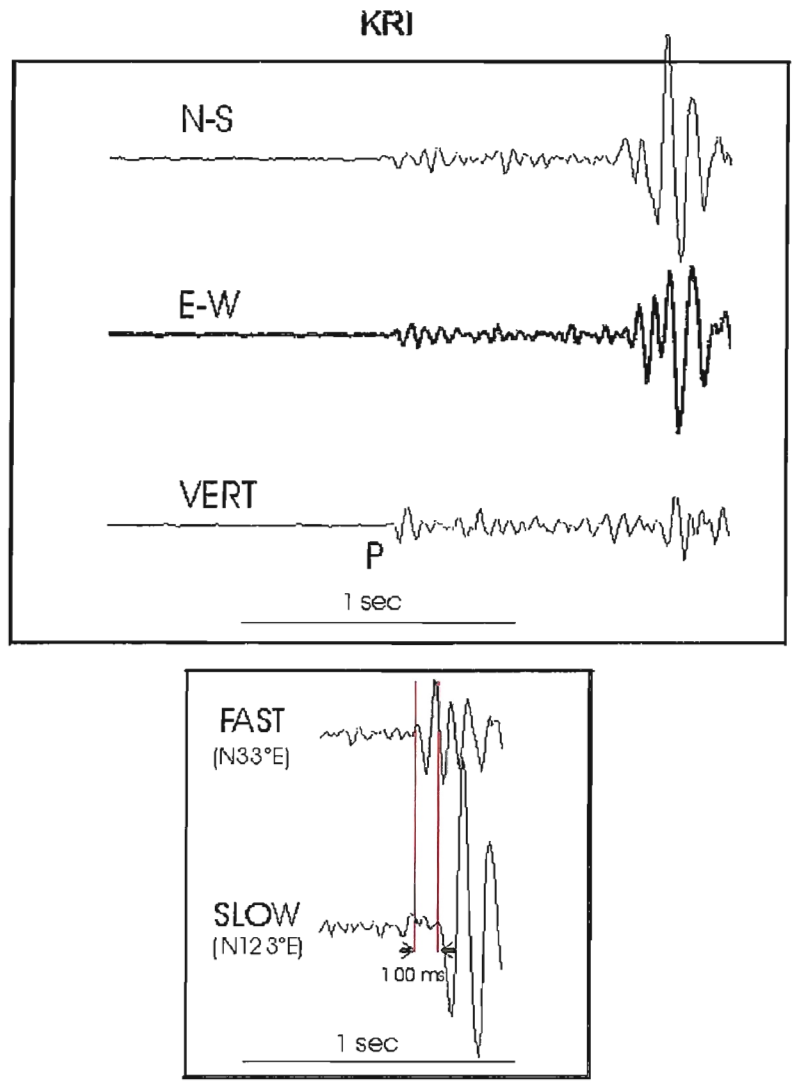

Figure 7. *Example of shear-wave splitting at station KRI. The upper diagram shows the three recorded components. On the bottom the rotated N-S and E-W components show the time-delay between the two shear-wave arrivals. (Event occurred at 03:02:40:6, April 9, 2000, at 5.7 km depth, 4.5 km from KRI).*

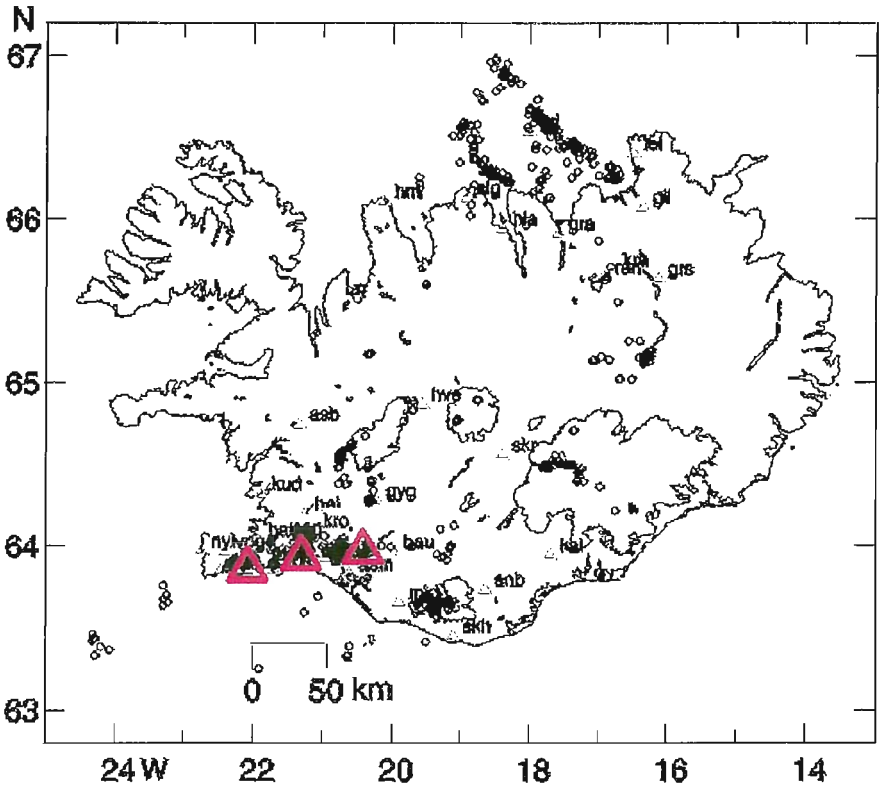

Figure 8. *Map of Iceland showing all earthquakes with $M \geq 2$, during the period March 1998 – June 2000. The small green triangles show the majority of SIL stations, whereas the stations KRI, BJA and SAU (from left to right) are shown with large red triangles.*

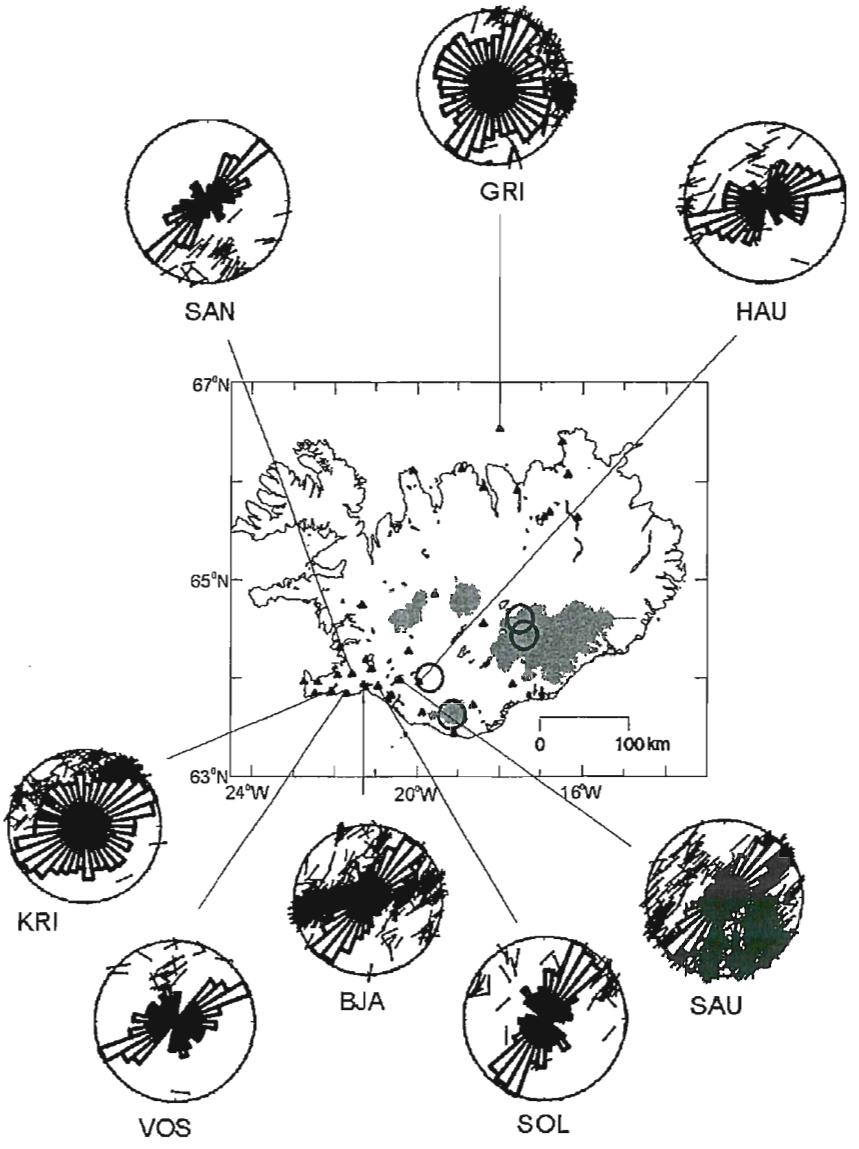

Figure 9. *Map of Iceland, showing the seismic network. Shaded areas are ice fields. Open circles mark the active volcanoes of, from north to south, Bárðarbunga, Grímsvötn, Hekla and Katla. The roundels are equal-area polar plots of polarizations of the faster split shear-wave arrivals in the shear-wave window (out to 45°) and rose diagrams, during 1996-1999. Roundels are shown only for those stations where there are more than 10 arrivals within the shear-wave window. The named stations without roundels (ASM, KRO, MID) have sufficient arrivals but the polarizations are severly disturbed by local rifting and/or local topography (after Volti and Crampin 2000).*

a further eruption at Hekla. It appears that magmatic activity complicates the behaviour of the stress-field, so the simple behaviour before earthquakes in 1997 and 1998 is no longer apparent in 1999 and 2000 (Volti and Crampin 2000).

In Figure 10b, the middle cartoon shows time-delays variations in Band-1 at station SAU. The nine-point moving averages in Band-1 show several broad maxima, one during 1998, three during 1999 and two in 2000. The first can be associated with the M=5.1 event (which is 43 km from SAU). Although during 1999, the peak in March does not seem to correlate with any nearby activity, the other, in July, may be correlated with the event in Katla (75 km SW of SAU). There are two earthquakes of M=4.2 and M=3.8 in September, 1999, but the time-delays do not show any increase. Again, the complications are believed to be due to the combined effects of the build-up of stress before earthquakes and the movement of magma before eruptions.

Recently, (June 17 and 21, 2000) three large earthquakes of M=5.6, M=5 and M=5.3 ($Ms\cong$6.6, M=6, and M=6.3) occurred near SAU. These are the largest earthquakes in Iceland since 1963. Time-delays increased before the events for about four months, with the rate of increase being almost consistent with a M=5.6 earthquake, but the duration was too short. The complication is that there is a period of about seven weeks without source earthquakes to monitor the rockmass. As a consequence the start of the increase in time-delays in Band-1 was not recognized, and the events were consequently not stress-forecast (Volti and Crampin 2000). Such irregularities indicate the need for controlled source seismology, as is proposed in the SMSITES project, even in highly seismic SW-Iceland.

Figure 10c shows variations in station KRI. The there are two increases in time-delays. The first is associated with the M=5 event, November 13, 1998, which was stress-forecast. The second increase is gradual but steady increase in time-delays in Band-1 since December 1998 which may indicate the build-up of stress, and subsequently a future large earthquake.

3.3.1.2 Stress-forecasting earthquakes

Stress-forecasting is based on the assumption that the build-up of stress before earthquakes causes progressive changes in aspect-ratios until a level of cracking, known as fracture criticality, is reached and the earthquake occurs. Therefore, changes in shear-wave splitting in Band-1 are used to monitor crack aspect-ratios and estimate the time and magnitude that crack distributions reach fracture criticality.

It was recognized at the end of October 1998 that the time-delays in Band-1 were increasing since July 1998 at both stations BJA and KRI which are about 38 km apart (Figures 9, 10a and 10c). The increase had approximately the same duration and slope as the increases before the M=5.1 earthquake on June 4, and started at about the lowest level ($\sim$4 ms/km) of any of the increases associated with previous earthquakes. The increase at BJA was already nearly 10 ms/km which was close to the level of fracture criticality of the previous earthquakes. These features suggested that the crust was approaching fracture criticality before an impending larger earthquake. Consequently, the e-mail exchange in Table 1 between UEDIN.DGG and IMOR.DG was initiated. The final specific stress-forecast (November 10, 1998), was that an earthquake could occur any time between now (M=5) and end of February (M=6) if stress kept increasing. Three days later, on November 13, 1998, there was a M=5 earthquake with epicenter 2 km from BJA. This is considered to be a successful

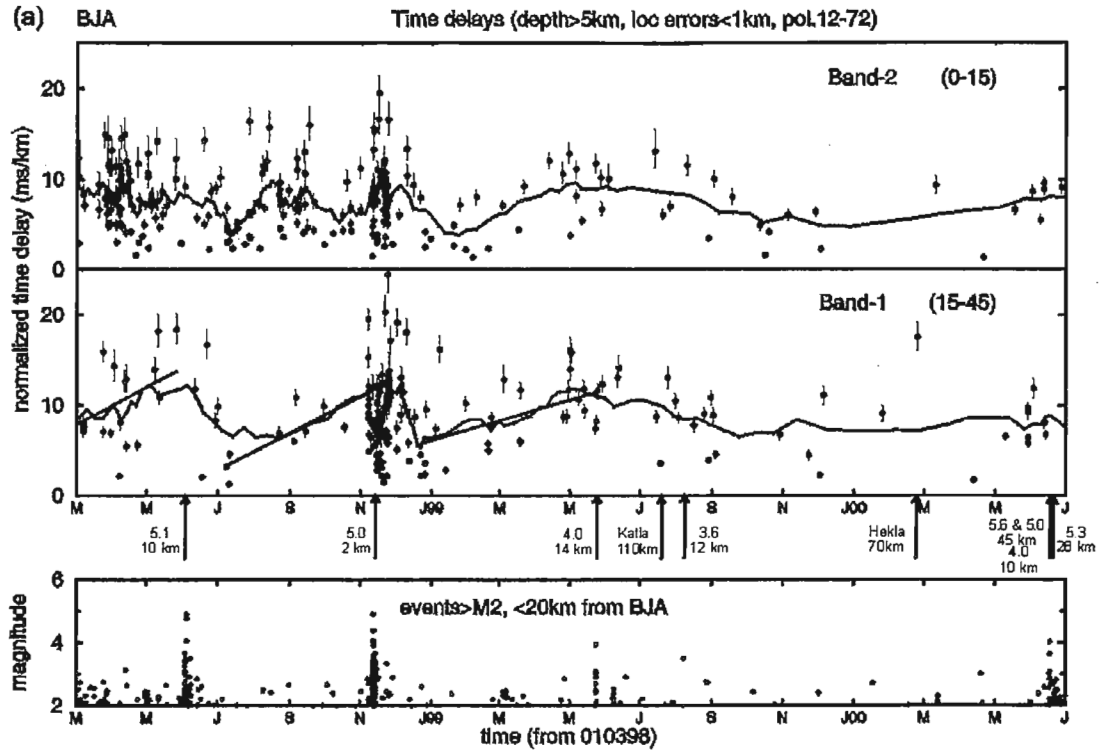
(a) BJA
Time delays (depth>5km, loc errors<1km, pol.12-72)
Band-2 (0-15)
Band-1 (15-45)
normalized time delay (ms/km)
5.1 10 km
5.0 2 km
4.0 14 km
Katla 110km
3.6 12 km
Hekla 70km
5.6 & 5.0 45 km
4.0 10 km
5.3 28 km
events>M2, <20km from BJA
magnitude
time (from 010398)

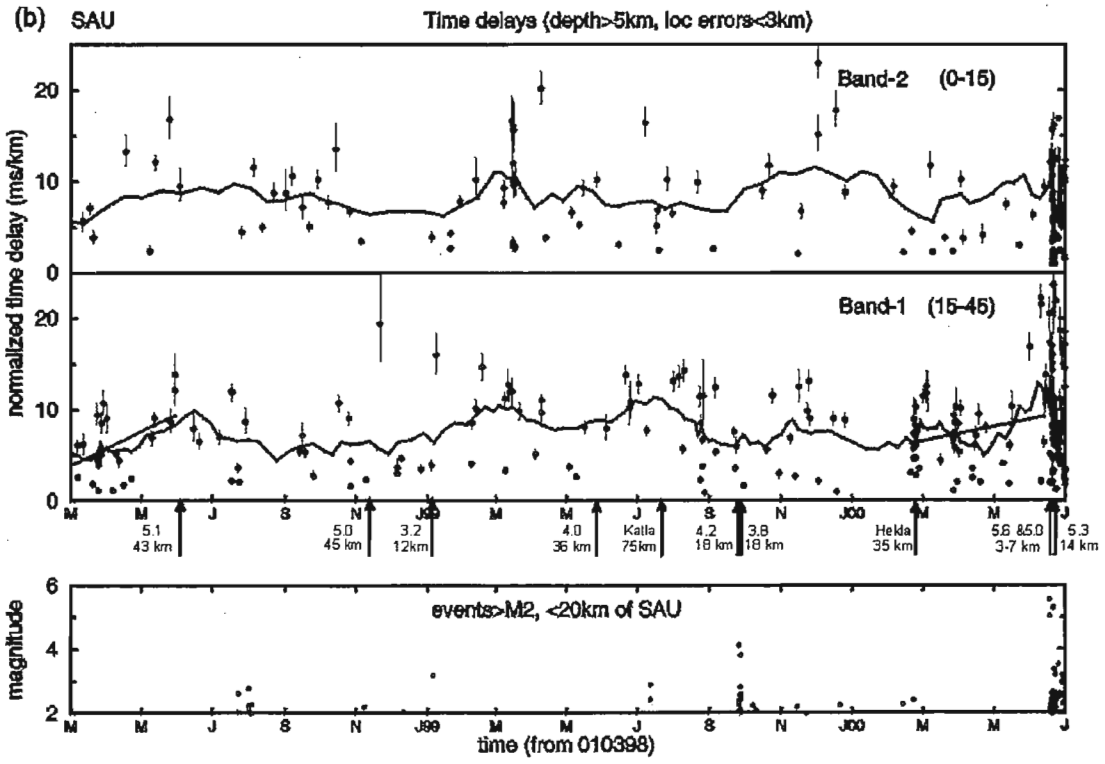
(b) SAU
Time delays (depth>5km, loc errors<3km)
Band-2 (0-15)
Band-1 (15-45)
normalized time delay (ms/km)
5.1 43 km
5.0 45 km
3.2 12km
4.0 36 km
Katla 75km
4.2 18 km
3.8 18 km
Hekla 35 km
5.6 &5.0 3-7 km
5.3 14 km
events>M2, <20km of SAU
magnitude
time (from 010398)

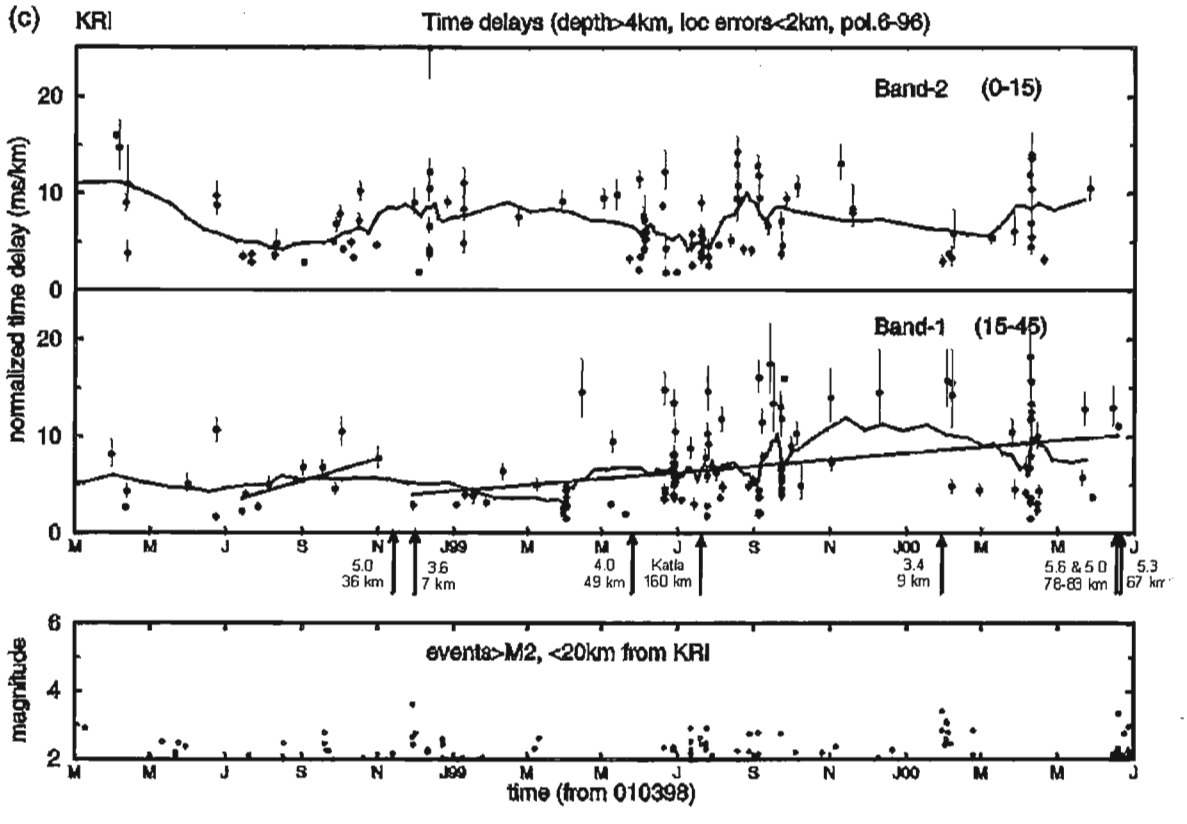

Figure 10. *Shear-wave splitting at BJA (a), SAU (b) and KRI (c) from March 1, 1998 to June 31, 2000. The upper and middle cartoons show variaton of normalized time-delays with time, for ray paths in bands with incidence* 0° *to* 15° *to the crack face (Band-2) and with incidence* 15° *to* 45° *to the crack face (Band-1). Band-2 is sensitive to crack density whereas Band-1 is sensitive to aspect ratio. There are nine-point moving averages through the time-delays. Lines are least square fits to data before a major earthquake. The lower cartoons show the magnitudes of* $M \geq 2$ *earthquakes within 20 km of each station.*

stress-forecast within a comparative narrow time-magnitude window.

During June 2000, three large earthquakes occurred near SAU. Although time-delays in Band-1 seemed to increase about four months before the first event of June 17, these earthquakes were not stress-forecast. The main reason was that before the swarm of activity in February associated with Hekla (Figure 10b), there was a period of about four weeks without any suitable shear-wave source earthquakes, and consequently no reliable time-delay measurements and reliable slopes and durations of the increase could not be identified.

October 27	UEDIN.DGG emails IMOR.DG reporting shear-wave time-delays in Band-1 increasing from July at stations BJA and KRI and suggests: *". . . there was an 80% chance of something significant happening somewhere between BJA and KRI within three months."**
October 28	UEDIN.DGG faxes data for BJA and KRI to IMOR.DG. IMOR.DG suggests M=5.1 earthquake near BJA in June 1998 may be linked to current increase in time-delays.
October 29	UEDIN.DGG updates current interpretation and suggests: *"Shear-wave splitting at both BJA and KRI indicate something is going to happen soon, probably within a month . . ."**
October 30	IMOR.DG sends notice to National Civil Defence (NCD) in Reykjavík suggesting a meeting.
October 31 -November 4	Faxes and emails updating information. UEDIN.DGG refines data and interpretation. IMOR.DG creates local geophysical and geological investigations.
November 5	IMOR.DG presents stress-forecast and other data from surrounding area to scientific advisors of NCD, who conclude no further action was required of them.
November 6-9	Exchange of various faxes and emails updating information and interpretation.
November 10	UEDIN.DGG concludes: *". . . the last plot . . . is already very close to 10 ms/km. This means that an event could occur any time between now (M≥5) and end of February (M≥6) ."**
November 11	UEDIN.DGG faxes updated data for KRI and BJA, with SAU now also suggesting increasing time-delays from September.
November 13	IMOR.DG reports: *". . . here was a magnitude 5 earthquake just near to BJA (preliminary epicenter 2 km west of BJA) this morning at 10:38 GMT."**

Table 1. *Timetable 1998, e-mails, facsimiles, and actions. *Quotations ("italics") are exact texts from e-mails.*

3.3.2 Task 2: Analysis of shear-wave splitting measurements

We had hoped to use several additional stations in the shear-wave window at SAU to investigate why observed time-delays between split shear-waves in Iceland are approximately

twice those usually observed elsewhere, and why time delay values show large scattering. Unfortunately, financial constraints prevented installation of additional SIL stations.

The range of time-delays between split shear-waves is found to vary between different regions worldwide and sometimes between different stations in the same region. Time-delays vary with crack density, crack aspect ratio, and isotropic P- and S-wave velocities. These effects can be calculated, and are reasonably well understood. Time-delays are also observed to be higher in regions with high heat flow (Crampin 1994) and this is believed to be the main reason for the larger values observed in Iceland. Also following the increase in Band-1 time-delays before the Vatnajökull eruption in 1996, the level of time-delays has been decreasing for both Band-1 and Band-2 by approximately 2 ms/km over 1997-1998. It would appear that the crust has been slowly adjusting to the strain released by the eruption as the mid-Atlantic ridge gradually takes up the change in strain.

However, the large scatter of time-delays and polarizations is difficult to explain. During the last two big earthquakes (November 1998 near BJA and June 2000 near SAU) it was observed that the scatter in time-delays increases considerably with the onset of the earthquake and the large scatter continues for several weeks thereafter (Figures 10a and 10b). It is hoped that the controlled source SMSITES project will help to resolve this difficulty.

3.3.3 Task 3: Establish shear-wave splitting map of Iceland

Figure 9 shows a map with roundels and equal-area rose diagrams of shear-wave splitting polarizations at stations with more than about ten arrivals within the shear-wave window out to 45°. Experience suggests that an overall shear-wave splitting map is not particularly useful as was first thought. Optimum procedures seem to require individual studies of shear-wave splitting at individual stations.

3.3.4 Task 4: Calibrate techniques and behaviour if and when changes are identified

Stress-forecasting using small earthquakes as the source of shear-waves is only possible when there is a more-or-less continuous source of small earthquakes. As we have seen, this is extremely rare. To stress-forecast earthquakes without such persistent activity, requires cross-well seismology using a borehole source transmitting orthogonally polarized shear-waves along appropriate ray paths in Band-1 to three-component borehole receivers in further boreholes.

These boreholes exist in northern Iceland near Húsavík close to the Flatey-Húsavík fault of the Tjörnes fracture zone, and an EU project (*SMSITES: Developing stress-monitoring sites and infrastructure for forecasting earthquakes,* contract no. EVR1-CT1999-4000) developing a Stress-Monitoring Site (SMS) has recently started. The SW of Iceland has proved to be a very active seismic area during the last years. However, shear-wave splitting analysis near the Húsavík transform fault and Grímsey zone has not been very productive up to now, due to lack of continuous swarm activity in the shear-wave windows of the northern stations, GRI, SIG, LEI, and others. The new technique of controlled source measurements are expected to monitor changes in shear-wave splitting near Húsavík more efficiently, as well as reduce the scattering in the time-delays.

3.3.5 Task 5: Incorporate shear-wave splitting interpretations into routine analysis

The only successful technique yet established for automatically identifying polarization directions and time-delays from digital records of shear-wave splitting is the Cross-Correlation Function, or CCF technique of Gao et al. (1998). CCF was used on SIL records from SW-Iceland. It was not successful (Volti and Crampin 2000). The reason is thought to be that the data that was used to test CCF was an isolated swarm of small earthquakes, whereas the foci in Iceland are more distributed so that shear-waves propagate along significantly different ray paths. This suggests that reliable automatic reading of shear-wave splitting in Iceland is unlikely to be successful.

3.3.6 Meetings and conferences

PRENLAB contractor meetings:
Stuart Crampin and Theodora Volti: The second PRENLAB-2 workshop, Húsavík, Iceland, July 30, 1998.
Theodora Volti: The fifth PRENLAB-2 workshop, Nice, France, April 27, 2000.

Presentations of PRENLAB results:
Stuart Crampin: 60th annual EAGE meeting, Leipzig, Germany, June 8-12, 1998.
Stuart Crampin: Tenth biennal EUG meeting, Strasbourg, France, March 28 - April 1, 1999.
Stuart Crampin: 61th annual EAGE meeting, Helsinki, Finland, June 7-11, 1999.
Stuart Crampin: The second EU-Japan workshop on seismic risk, Reykjavík, Iceland, June 23-27, 1999.
Stuart Crampin: XXII IUGG General Assembly, Birmingham, United Kingdom, July 18-30, 1999.
Stuart Crampin: 9th International Workshop on Seismic Anisotropy, Houston, Texas, USA, March 26-31, 2000.
Stuart Crampin: 62nd annual EAGE meeting, Glasgow, United Kingdom, June 25-30, 2000.
Stuart Crampin: 70th annual SEG meeting, Calgary, Alberta, Canada, August 6-11, 2000.

3.3.7 References

Crampin, S. 1994. The fracture criticality of crustal rocks. *Geophys. J. Int.* 118, 428-438.

Crampin, S. 1999. Calculable fluid-rock interactions. *J. Geol. Soc.* 156, 501-514.

Gao, Y., P. Wang, S. Zheng, M. Wang & Y.-T. Chen 1998. Temporal changes in shear-wave splitting at an isolated swarm of small earthquakes in 1992 near Dongfang, Hainan Island, Southern China. *Geophys. J. Int.* 135, 102-112.

Volti, T. & S. Crampin 2000. Shear-wave splitting in Iceland: four years monitoring stress changes before earthquakes and volcanic eruptions. *Geophys. J. Int.*, submitted.

3.4 Subproject 4: Borehole monitoring of fluid-rock interaction

Contractor:

Frank Roth
Section: Earthquakes and Volcanism
Division: Solid Earth Physics and Disaster Research
GeoForschungsZentrum Potsdam (GFZ)
Telegrafenberg
D–14473 Potsdam
Germany
Tel: +49–331–288–1210
Fax: +49–331–288–1203
E–mail: roth@gfz-potsdam.de

Subcontractor:

Valgarður Stefánsson
National Energy Authority (Orkustofnun, OS)
Grensásvegur 9
IS–108 Reykjavík
Iceland
Tel: +354–569–6004
Fax: +354–568–8896
E–mail: vs@os.is

3.4.1 Geophysical logging

In the preparatory phase of an earthquake, stress accumulation is expected to be connected with the creation of borehole breakouts (BOs), changes in the number and size of cracks, a possible variation of the stress direction, etc. Therefore it is very important to monitor the following set of geoparameters:

- P–wave travel time.
- electrical conductivity.
- stress information from borehole breakouts (orientation and size).
- crack density.

In the framework of this project, we had the chance to carry out repeated logging to obtain a time series of logs in the South Iceland seismic zone (SISZ). An 1100 m deep borehole (LL–03, Nefsholt) inside the zone (63.92°N, 20.41°W, 7 km south of the seismic station SAU) was used and provided the unique opportunity to perform measurements much nearer to earthquake sources than usual – the hypocenter depths at that location range between 6 and 9 km. Moreover, data could be obtained for a depth interval of more than 1000 m, uninfluenced by the sedimentary cover and less disturbed by surface noise.

This was achieved by repeated logging with tools as: sonic log (BCS), gamma-ray (GR), spectral gamma-ray (SGR), neutron-neutron log, dual induction/latero log (DIL), 16"- and 64"-normal resistivity log, spontaneous potential log (SP), a borehole temperature log (BHT), four-arm-dipmeter (FED), and borehole-televiewer (BHTV).

The neutron-neutron log, the 16"- and 64"-resistivity log, the SP log, and temperature logs were run with the logging equipment of OS, the rest with the Halliburton logging truck of GFZ.

Investigations on the stress field in the SISZ

Besides the repetition of logs in borehole LL-03 (Nefsholt), we performed single logging campaigns at other boreholes to check the state of the regional stress field. This is important for two reasons:

- From the San Andreas fault we know (Zoback et al. 1987) that fault zones may be in a low stress state between earthquakes, which gets visible through stress orientations perpendicular and not pointing at an angle of 30° to 45° to the strike-slip fault. To determine the present state of stress in the SISZ, it is important to see if there are stress components, that are not perpendicular to existing faults and thus favour earthquakes on them.

- The SISZ is no typical transform zone. Looking at the orientation of rift opening and the adjacent rifts, one would expect a left-lateral strike-slip zone in NW-SE direction (N103°E) to connect the Reykjanes ridge and the eastern volcanic zone (EVZ) of Iceland. Instead earthquakes occur on en-echelon N-S striking right-lateral faults. Assuming an angle of 45° between the maximum horizontal compressive stress and the fault (as it is done constructing fault plane solutions) both planes are equivalent. However, from a rock mechanics point of view, expecting an angle of about 30° between fault and maximum horizontal principal stress, the stress orientation at N-S striking faults should be N30°E, compared to N60°E at an E-W striking transform.

3.4.2 Task 1: Repeated logging in borehole Nefsholt

All together 7 logging campaigns took place. The locations are shown in Figure 11. Table 2 lists the logs performed during the project.

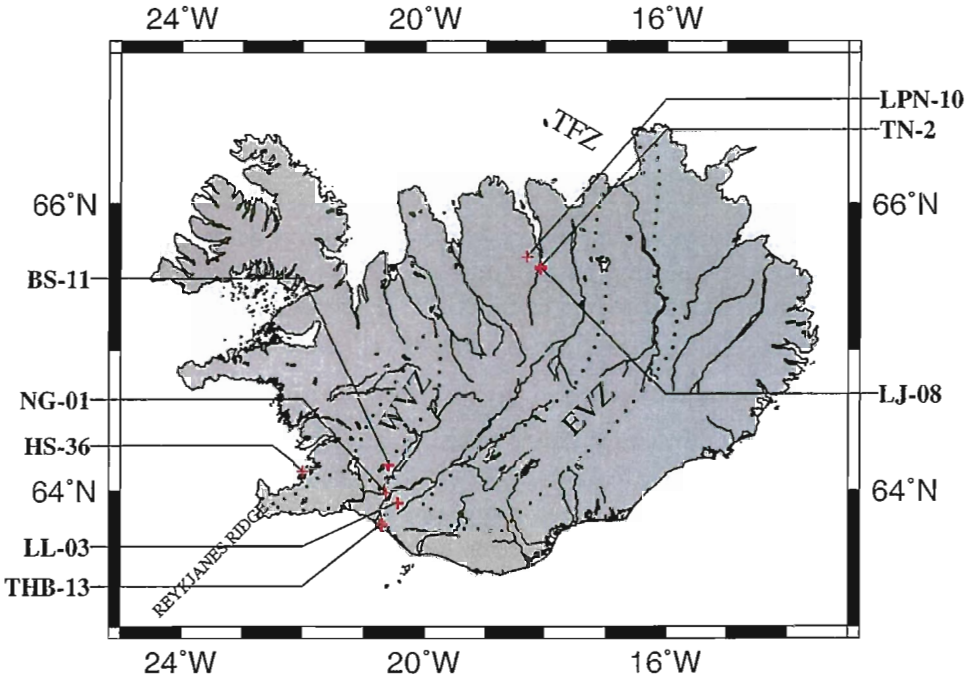

Figure 11. *Map of Iceland showing the location of the site of repeated logging (LL-03) and of the other boreholes, where measurements have been performed. The SISZ extends between the southern ends of the WVZ and EVZ. Wells LL-03 and NG-01 are inside the SISZ, BS-11 is north, THB-13 is south of the zone.*

Altogether, the seven campaigns have contributed to the two aims of this Subproject, that are:

- Observation of changes in physical parameters of the rock, in the degree of fracturing, and in the orientation of principal stresses with respect to seismic activity.
- Indirect measurement of tectonic stress orientation to evaluate the tectonic stress field in the area of the SISZ. For that, the borehole geometry was observed for certain structures, that allow to determinate the orientation of the horizontal principal stress, as there are borehole breakouts and vertical tensile fractures. Borehole breakouts are failures of material of the borehole wall, that result from accumulation of tangential

stress at the borehole wall at the azimuth of the lower horizontal principle stress (σ_h), caused by the free surface produced by drilling. In a linear elastic isotropic theory, this would be perpendicular to the maximum horizontal principal stress (σ_H). Alternatively, at this free surface, the tensile strength of the borehole wall can be exceeded at the azimuth of the maximum principal horizontal stress, what produces vertical fractures along σ_H. These vertical fractures extend in the direction of the maximum and open in the direction of the minimum horizontal principal stress. The occurrence of these tensile fractures can be enhanced by thermal stress caused by cold water pumped into the well.

Orkustofnun provided a lithology log of the well LL-03 at Nefsholt. This log is based on cuttings (rock pieces crushed while drilling), not on cores, what strongly limits its depth resolution. It shows a nearly continuous sequence of altered basalt, interrupted only by a few thin sedimentary layers and some thin layers of dolerite, hyaloclastites and fresh basalt. Different kind of layers show different characteristic sets of logs, that allow to distinguish between the lava flows and the sediments (Figure 12, Table 4). The result, i.e. the correlation with the rock physical parameters, is very reasonable: The sedimentary layers seem to contain more water (larger pore space) entailing higher travel times of elastic waves, lower resistivity and higher absorption of neutrons. The correlation is an important indicator that the log results have good quality.

Name:	Location:	Max. depth:	Logged interval:	Tools used:	Date:
NG-01	Ólafsvellir (inside SISZ)	1070 m	180–1070 m	FED, GR	July 1996
HS-36	Reykjavík	980 m	330–980 m	BHTV, BCS-GR	July 1996
LPN-10	Laugaland near Akureyri, North Iceland	890 m	80–880 m	BHTV, BCS-DIL-GR	July 1996
LJ-08	Syðra-Laugaland near Akureyri	2740 m	120–1890 m 120–1330 m 500–1980 m	FED, BHTV, BCS-DIL-GR, BHTV	July 1996 June 1998
TN-02	Ytri-Tjarnir near Akureyri	1370 m	260–1370 m	BCS, GR	July 1996
LL-03	Nefsholt (inside SISZ, site of repeated logging)	1309 m	80–1100 m	BHTV, BCS-DIL-GR SGR BHT neutron–neutron X-Y-caliper 16"- and 64"-resistivity SP	July 1996 October 1996 September 1997 December 1997 June 1998 September 1997 June 1998 April 1999 August 2000 April 1999 October 1999 September 1996 April 1999 October 1999 August 2000 October 1999
THB-13	Þykkvibær SW of Hella near the south coast	1254 m	466–1225 m	BHTV	December 1997
BS-11	Böðmóðsstaðir near Laugarvatn, north of the SISZ	1193 m	703–1090 m 500–1090 m	BHTV	December 1997 June 1998

Table 2. *All logs performed during both PRENLAB projects. As borehole NG-01 partly collapsed between log runs, the hole was abandoned and well LL-03 was chosen for repeated logging. GR indicates gamma-ray log, SP stands for spontaneous potential, 16" for short normal resistivity tool, and 64" for long normal resistivity tool. FED means four-arm-dipmeter, which includes an oriented four-arm-caliper. BHTV and BHT mean ultrasonic borehole televiewer and borehole temperature, respectively. BCS is borehole compensated sonic log; DIL is dual induction/latero log. The deepest parts of wells LJ-08, LL-03, THB-13, and BS-11 were not accessible anymore.*

Log type:	Date:	Depth range:	File name:	Remarks:
Temperature log (T)	07-07-1977	0–920	T07071977	
Temperature log	18-10-1977	0–1100	T18101977	
Temperature log	17-09-1980	0–1060	T17091980	
Temperature log	25-06-1992	0–1106	T25061992	
Temperature log	23-04-1999	4–1080	21415	
Temperature log	03-08-2000	0–1087	T03082000	
Natural gamma log (GR)	23-04-1999	0–1080	21424	
Natural gamma log	27-10-1999	10–1080	22588	
Neutron-neutron log (NN)	23-04-1999	3–1080	21421	
Neutron-neutron log	27-10-1999	10–1080	22585	+
Neutron-neutron log	03-08-2000	7–1087	N03082000	
Self potential log (SP)	27-10-1999	25–1080	22570	
16" normal resistivity log (SN)	27-10-1999	25–1080	22568	*
16" normal resistivity log	03-08-2000	27–1087	S03082000	*
64" normal resistivity log (LN)	27-10-1999	25–1080	22569	*
64" normal resistivity log	03-08-2000	27–1087	L03082000	*
LL3 of DIL	07-1996	36–1070	LL3-07/96	
LL3 of DIL	12-1997	37–1071	LL3-12/97	

Table 3. *Repeated logging by Orkustofnun in Well LL-03, files used for comparisons. + : depth adjusted to neutron-neutron log of August 2000. * : calibrated and depth adjusted to neutron-neutron log of August 2000.*

Depth interval:	GR:	BCS travel time:	neutron–neutron water content porosity:	DIL, 16", 64" resistivity:	Lithology:
265-275 m	low	low	low	high	altered basalt
275-280 m	low	high	high	low	sediment
280-285 m	low	low	low	high	altered basalt
285-298 m	high	high	high	low	sediment
298-305 m	high	low	low	high	fresh basalt

Table 4. *Characteristic set of log values for different kinds of layers, derived from Figure 12.*

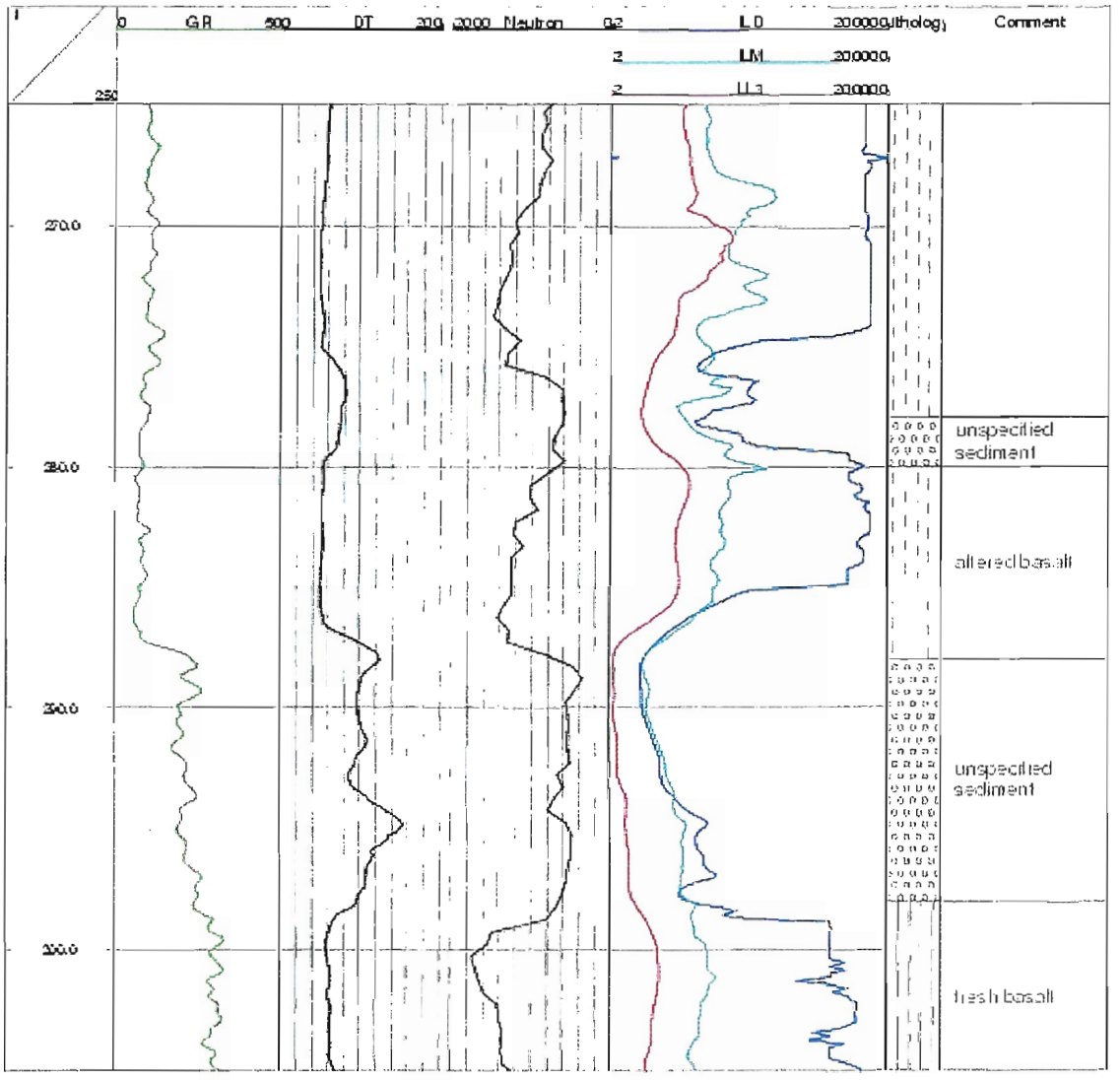

Figure 12. *Data example showing the correlation between the performed logs and the lithology based on the analysis of cuttings provided by Orkustofnun. GR = gamma-ray in API units, DT = compensated travel time in microseconds per foot, Neutron = neutron-neutron log in API units, ILD = induction log of deep penetration in Ωm, ILM = induction log of medium penetration in Ωm, and LL3 = latero log in Ωm.*

3.4.3 Tasks 2, 3, and 4: Cross correlation of logs of the same type from different campaigns and earlier loggings; comparison of changes in logs of different type; comparison of changes in logs with changes in seismicity, etc.

Due to a delay in the year 2000 logging campaign, we had the chance to take at least some data after the two June 2000 earthquakes in the SISZ. Comparing the data of July 1996 to October 1999 with those of August 2000 gives the opportunity to see which parameters have changed across the time from before the event to 6 weeks after.

And there were remarkable changes at the borehole. Our coworker Steinar Þór Guðlaugsson reports: "Water started to flow from well LL-03 on July 20–22 after a rapid rise in the water table from a depth of several meters since the earthquakes. This was probably caused by changes in crustal stress resulting from the earthquakes, although reinjection into the Laugaland geothermal field, which was initiated recently, may also have played some role. On August 3, the flow-rate was 0.5 l/s." The effects seen in the logs will be described below.

Repeated logs in LL–03: borehole temperature

The longest time series of logs is available in the temperature logs (BHT). There are data from the time of the drilling of the well (1977), later from 1980 and 1992, and finally from 1999 and 2000 taken during the work in the PRENLAB projects. The temperature logs are plotted together in Figures 13 and 14. Following a heating phase after drilling, the temperatures went down. The most recent of the logs predating the earthquakes show a regime of inflow into the well at several feed-points and downward flow of this fluid to a depth of 830 m where it re-enters the formation. The new log of August 2000 can be interpreted in two different ways: (1) The fracture at 830 m now feeds water into the well in addition to the other feed-points and above this depth water everywhere flows upwards; (2) Water now flows upwards above the feed-point at 120 m, whereas below this depth water continues to flow down the well to a depth of 830 m as before. In either case, it is evident that water entering the well at feed-points in the 200-250 m depth range is warmer than before. Temperature differences between the feed-points in this depth range also seem to have increased. At present it is unclear whether this is caused by changes in the fracture network feeding this interval or by the reinjection.

In conclusion, a comparison of the August 2000 temperature log with the earlier ones does not reveal any new water-conducting fractures (feed-points), but does show changes in the temperature and flow rate of the water flowing through previously existing fractures. These changes may probably be explained by a combination of stress change (general increase in formation pressure) associated with the earthquakes and reinjection, but do not rule out movements on some of the fractures feeding the well.

Repeated logs in LL-03: latero log and "normal" resistivity tools, self potential
The latero log (the one included in the GFZ DIL tool is of LL3 type) and the "short normal" resistivity tool of OS (16" electrode spacing) are designed for shallow penetration into the formations. Whereas the "induction log medium" and "induction log deep" of the DIL tool and the "long normal" resistivity tool (64") are dedicated for investigations deeper into the rock surrounding the borehole.

The latero log resistivity shows good repeatability (see red curves in Figure 15). So do the 16" and 64" tools, as will be discussed later. Figure 16 gives a comparison of LL3 logs from 2 different campaigns with logs of the short and long normal resistivity tools. The LL3 curves correlate very well besides a small depth shift. They also correlate qualitatively well with the other two logs, but there seems to be a calibration problem in the LL3, leading to much lower values than the other tools. We did not care about this, as only changes in the logs were of interest here. The match between the normal resistivity tools is expected to be moderate as their penetration depths are different. There was no indication of changes in LL3 logs before June 2000.

The resistivity logs from before and after the June 2000 events are plotted together in Figure 17. Two kinds of adjustments were made to the final logs before they were plotted: Firstly, a correction was applied to the logs based on a calibration carried out at the surface with a set of known resistances. Secondly, the origin of the August 2000 neutron-neutron log was taken as a common depth reference and the logs shifted to this datum.

The new logs agree remarkably well with those obtained in 1999. The main change observed is a decrease in the 16" resistivity log above 110 m. This can probably be explained by the increased temperature (and – less likely – salinity) in this depth range caused by the newly established upflow. Too much should not be read from the differences between the 16" logs in the 400-700 Ohmm range, because of the large correction that was applied to the 1999 log as a result of the surface calibration. The differences may simply reflect the inaccuracy of the correction. Keeping this in mind, the only significant difference between the 16" resistivity logs that may require other explanations seems to be a decrease in resistivity in the 465-470 m depth interval.

The main change in the 64" resistivity log is a decrease in resistivity from 150-155 m. This may or may not be associated with the upflow. We also note a slight decrease in the 465-470 m range which correlates spatially with the main anomaly in the 16" log. At the same depth, the spontaneous self potential log (SP) of October 1999 shows an anomaly too (cf. Figure 18), which could indicate a crack, existing already at that time (there is no SP log of August 2000). A possible interpretation of the 3 correlating signals might be a crack that has widened but does not feed-in water with a temperature different from the local temperature in the borehole.

The long normal tool shows variations between October 1999 and August 2000 also at depths other than 465 m and at resistivities lower than 400 Ohmm. They usually display lower values in August 2000, which could mean that water filled cracks have opened. However, none of the variations is also seen in the "short normal" log, which leads to doubts on real changes in rock physical parameters, as new cracks could be formed much more easily near the borehole wall, an area sampled by the 16" tool. See also the discussion on the neutron-neutron log.

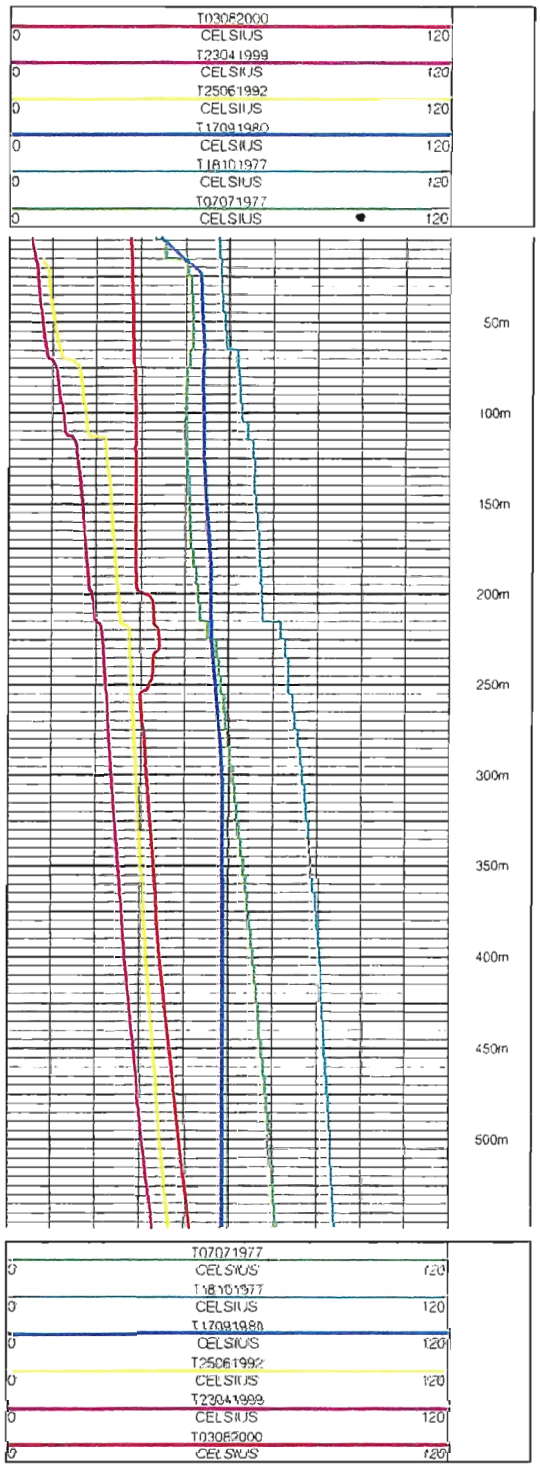

Figure 13. *Borehole temperature logs since the drilling of well LL-03. Numbers following "T" give date of log.*

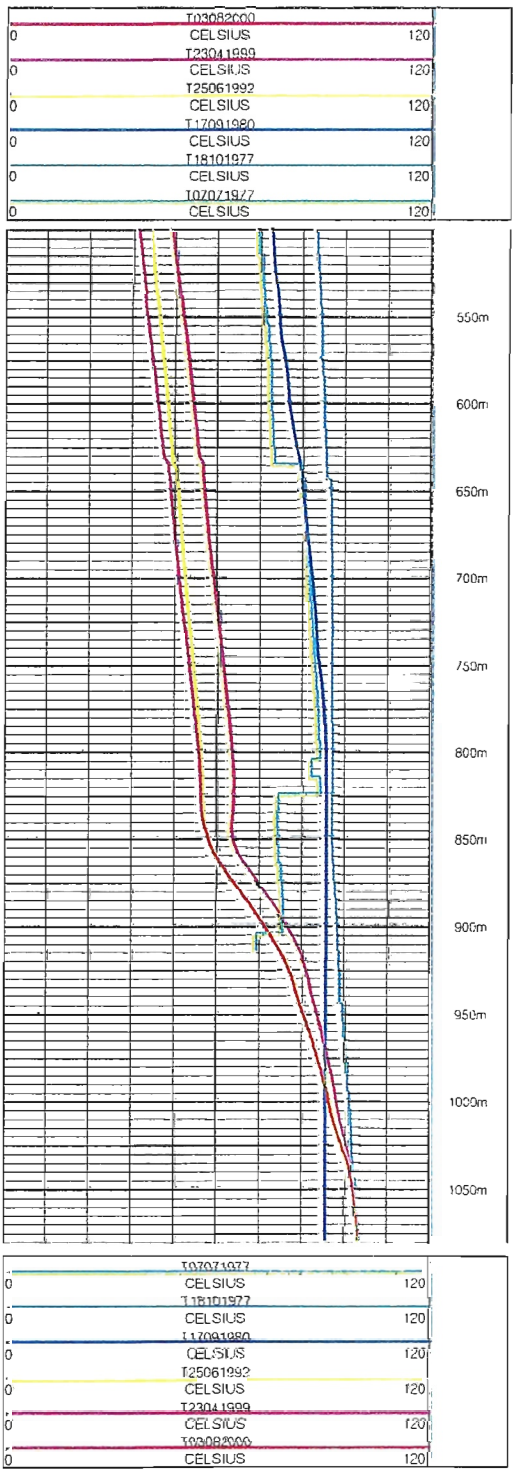

Figure 14. *Borehole temperature logs since the drilling of well LL-03. Numbers following "T" give date of log.*

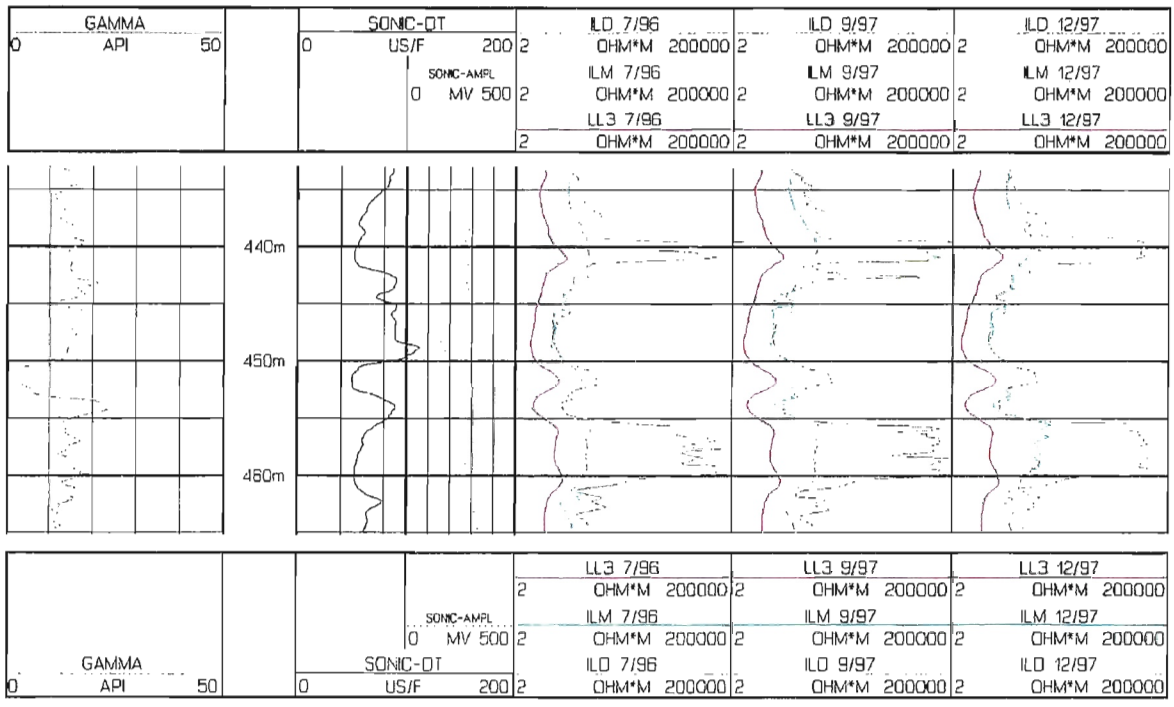

Figure 15. *Data example showing from left to right: gamma–ray log in API units, compensated travel time in microseconds per foot and the sonic amplitude, and three repeated measurements of latero log (LL3), induction log of medium penetration (ILM) and induction log of deep penetration (ILD). Month and year of campaign are given.*

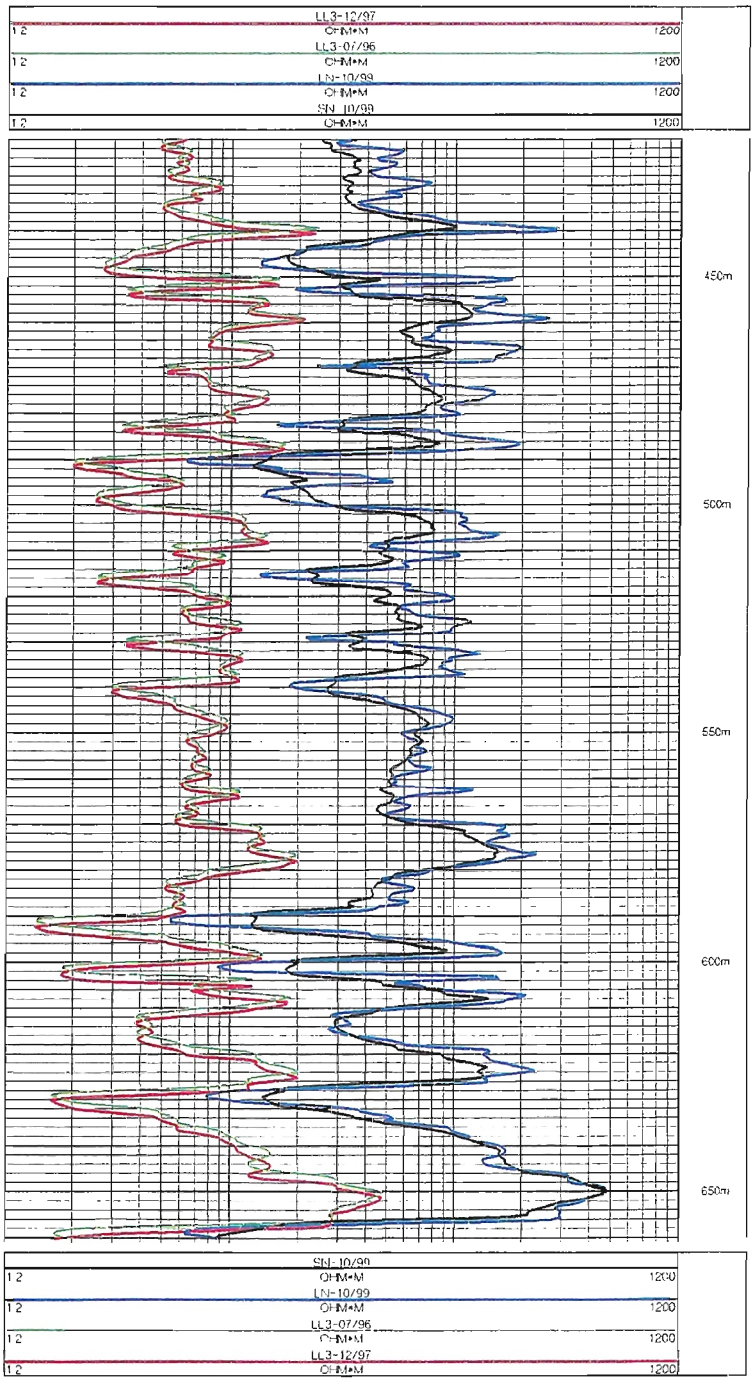

Figure 16. *Data example showing latero log data (LL3) from July 1996 and December 1997 together with short (SN) and long normal (LN) resistivity data from October 1999.*

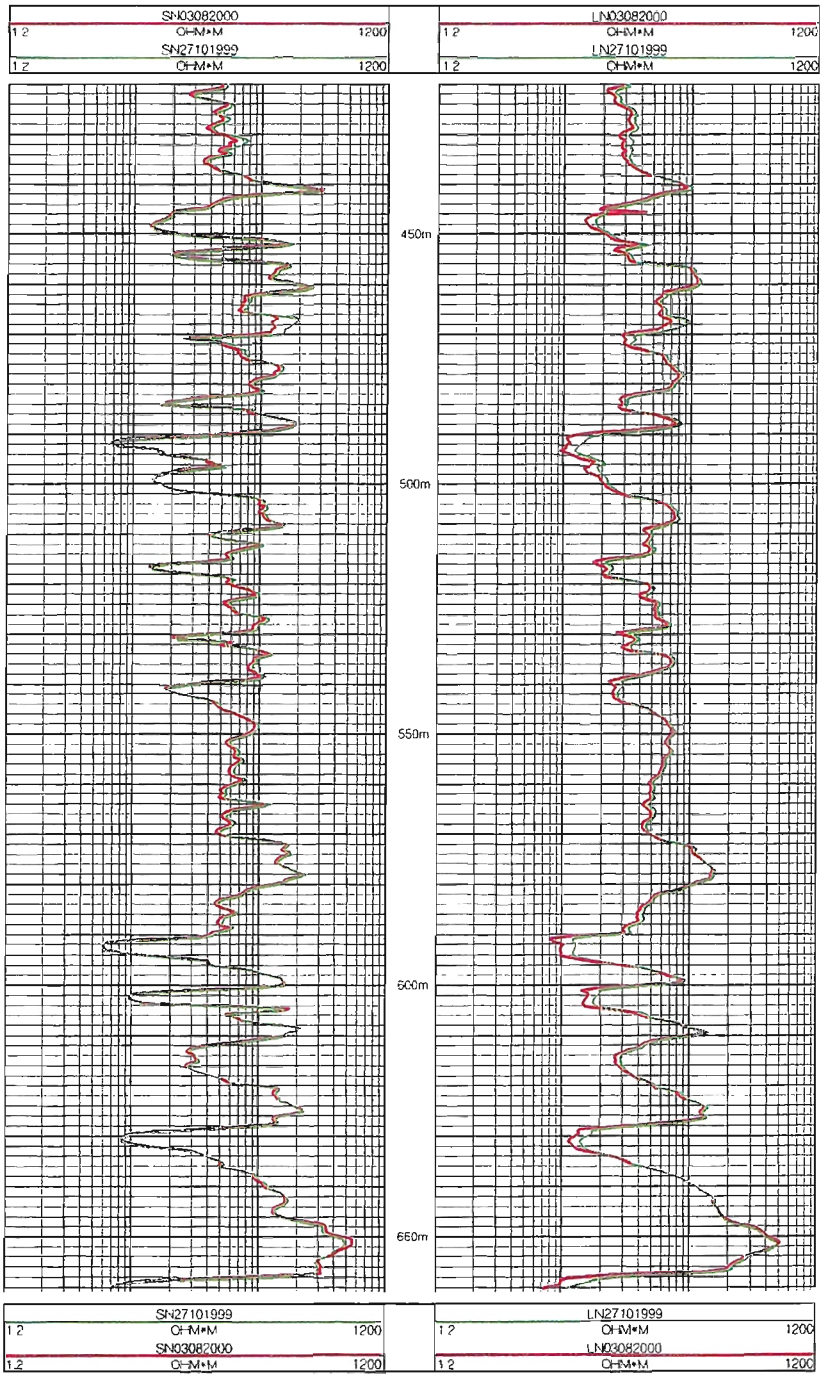

Figure 17. *Data example comparing short (SN) and long normal (LN) resistivity data from October 1999 and August 2000.*

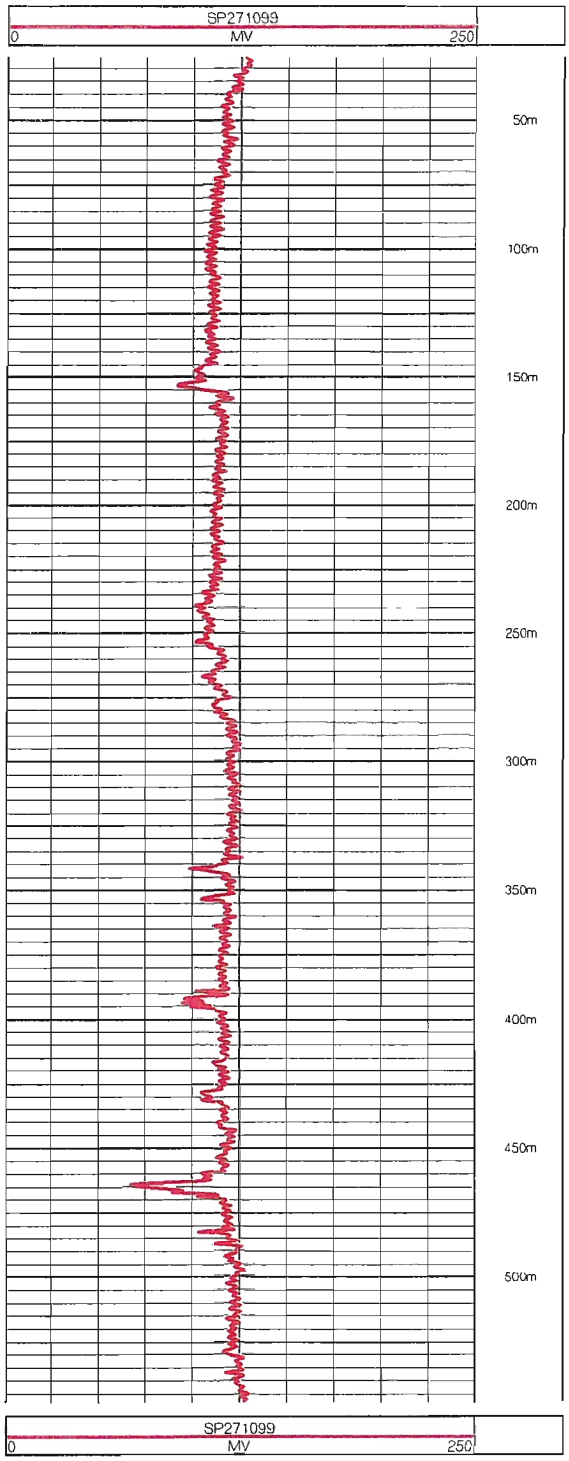

Figure 18. *Data example comparing short (SN) and long normal (LN) resistivity data from October 1999 and August 2000.*

Repeated logs in LL-03: dual-induction log (deep and medium penetration)
The repeated measurements with the dual-induction log (deep and medium penetration) show variations in resistivity even between different logs of one day, therefore these values cannot be used for an analysis of changes. More details can be found in the first annual PRENLAB-2 report.

Repeated logs in LL-03: sonic logs, P-wave travel times
The difference in the sonic velocity of logs measured at one day is in average 3.0% of the average value (Figure 19). At some depth intervals greater differences between repeated logs are caused by inaccurate depth matching, e.g. at 740 m in Figure 19. Depth intervals where the amplitude of the measured signal is very low showed significant variation in the (automatically) picked travel times, thus cannot be considered for an analysis of changes. Greater variations between logs of different logging campaigns could not be found.

Repeated logs in LL-03: neutron-neutron logs
Neutron-neutron logs were run before and after the June 2000 earthquakes. In the environment of borehole LL-03 at Nefsholt they are expected to reflect mainly the water content of the rock. They are plotted together in Figures 20 and 21. The one of April 1999 was measured with a log speed of 40 m/min. Those of October 1999 and August 2000, both were measured with a logging speed of 6 m/min. The April 1999 and the August 2000 logs were measured at 0.5 m depth interval. The 1999 log was measured at a depth interval of 0.1 m. The depth scale was shifted as described above.

Small changes can be found as well as between logs of April and October 1999 as between those of October 1999 and August 2000. The differences in logs of 1999 are larger than between those of October 1999 and August 2000. This might be due to the comparatively high logging speed in April 1999. At the depth of 465 m the neutron logs do not show a difference, as would be expected if a crack would have widened there. Generally, the match between the logs is remarkably good – so good that all of the observed differences can probably be attributed to statistical fluctuations.

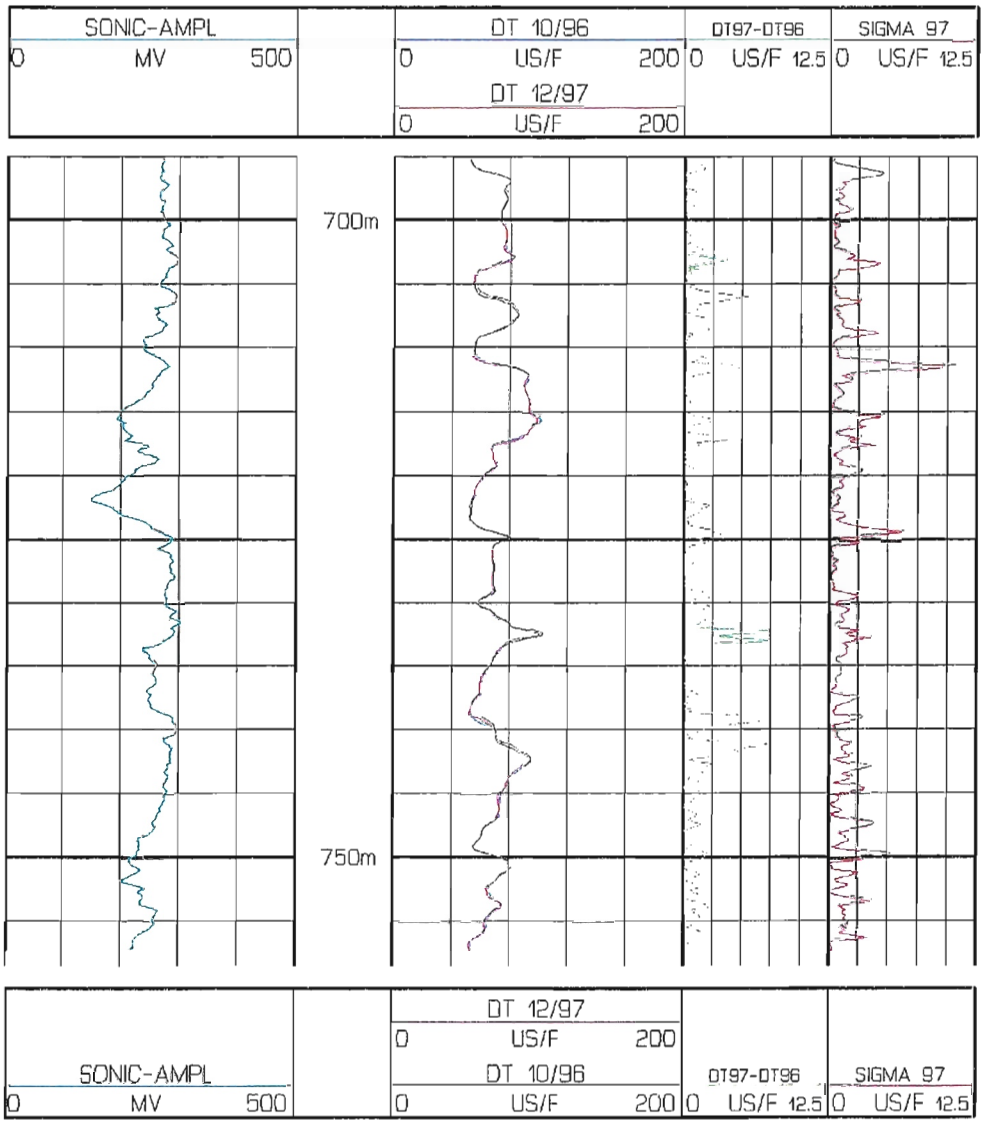

Figure 19. *Data example showing from left to right panel: an average curve of sonic amplitude, a superposition of the average compensated travel times measured in October 1996 and in December 1997 (each averaged over four runs performed immediately one after the other), the difference between these two average travel time curves (absolute value, green curve) and the standard deviation (absolute value) derived from the four runs performed in December 1997. Compensated travel times are given in microseconds per foot. The difference between the average travel times exceeds the standard deviation only in low amplitude intervals (not shown here) or at depths with inaccurate depth–matching (for example around 740 m).*

Borehole-televiewer measurements

Nefsholt:

In drillhole LL-03 (63.92°N, 20.41°W), the orientation of the borehole breakouts found is about 120.5° to 126°, implying a direction of the maximum horizontal principal stress of N30.5°E to N36°E. The circular standard deviation (1σ) is of the order of 10°. The stress direction is in agreement with the expected stress direction from large-scale tectonics (left-lateral strike-slip). The length of picked breakouts sums up to approximately 5.5 m. They are supposed to have formed while drilling, i.e. in 1977.

Þykkvibær:

Borehole breakouts have been found in the depth intervals 925 m to 927 m and 937 m to 941 m in THB-13 (63.77°N, 20.67°W). The breakouts in these two depth intervals sum up to approximately 3.5 m. Data quality is rather poor due to weak reflection amplitudes. Figure 22 shows a data example. The average breakout azimuth is between N105°E (upper depth-interval) and N121°E (lower depth-interval). Statistical analysis over the whole depth range gives a breakout-orientation of N111°E with a circular standard deviation (1σ) of about 10°. This would mean that the larger principal horizontal stress is in average oriented N21°E. This is in agreement with the stress directions expected from the overall tectonics as well as with the results from Nefsholt. The breakouts in THB-13 have most likely formed during drilling in 1997, i.e. just before they were measured.

Böðmóðsstaðir

No breakouts have been observed in borehole BS-11 (64.20°N, 20.55°W), but there are vertical fractures visible between 713 m and 934 m depth. The length of the vertical fractures sums up to 45 m. Vertical fractures are expected to occur in the direction of the maximum horizontal principal stress because of tensile failure of the borehole wall. They are supposed to be not of natural origin but drilling induced; so they stem out of 1992. These fractures occur at an azimuth of N45°E to N90°E. A data example is presented in Figure 23.

Breakout orientations and fracture statistics from the measurements in the SISZ are shown in Table 5 and Figure 24 as an overview. In Subpart 7B stress orientations were calculated for the SISZ using the co-seismic stress release of large earthquakes in the SISZ since 1706 and taking into account the stress build-up by plate motion. For comparison, we give the values for the boreholes where measurements were performed in Figure 25. Both results show stress orientations similar to each other. In general, the modelled values are more oriented to E-W than the measured ones.

Well:	Logged interval:	Interval with BOs / vert. fractures:	Total length of BOs/ vert. fractures:	Orientation of σ_H:	circ. std. devi.:
BS-11	703-1090 m	713-934 m	45.0 m fract.	N45°E–N90°E	—
LL-03	80-1100 m	780-983 m	5.0 m BOs	N30°E	12°
THB-13	466-1225 m	925-941 m	3.5 m BOs	N21°E	10°

Table 5. *Stress orientations found from borehole-televiewer logs.*

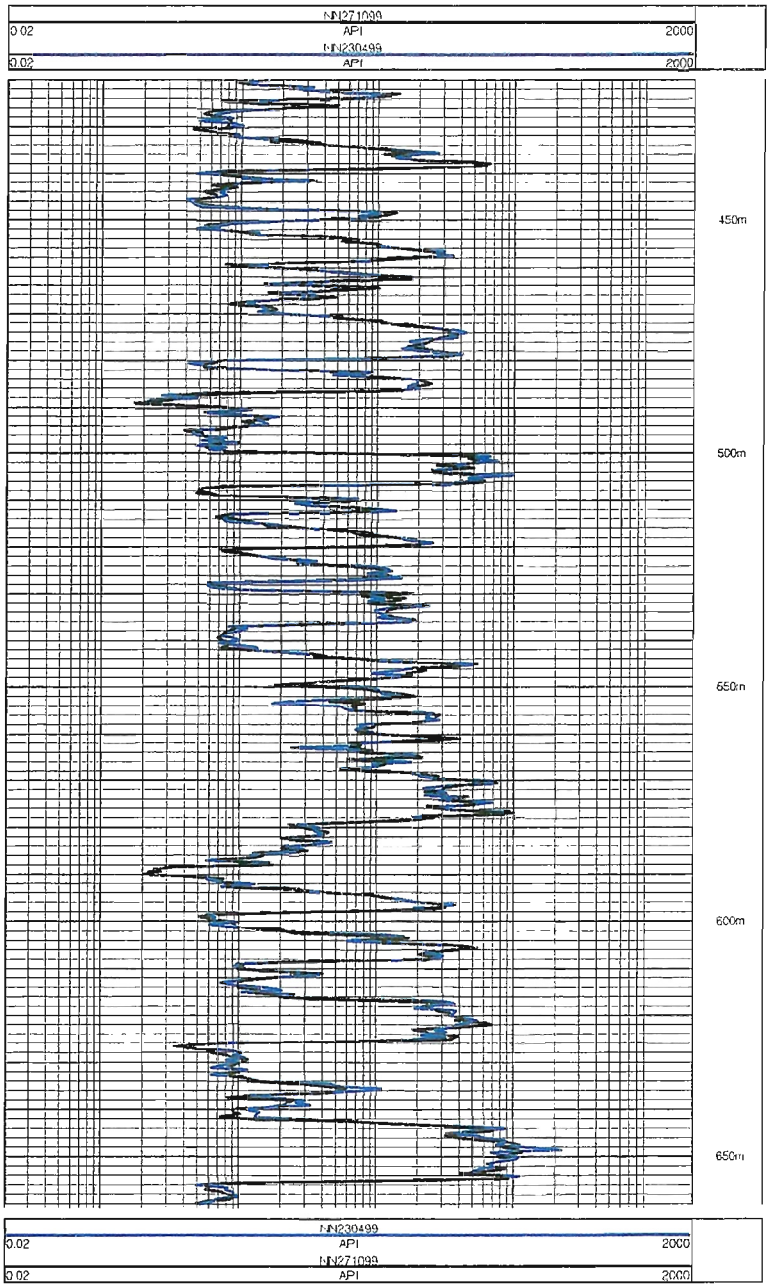

Figure 20. *Data example comparing short (SN) and long normal (LN) resistivity data from April 1999 and October 1999.*

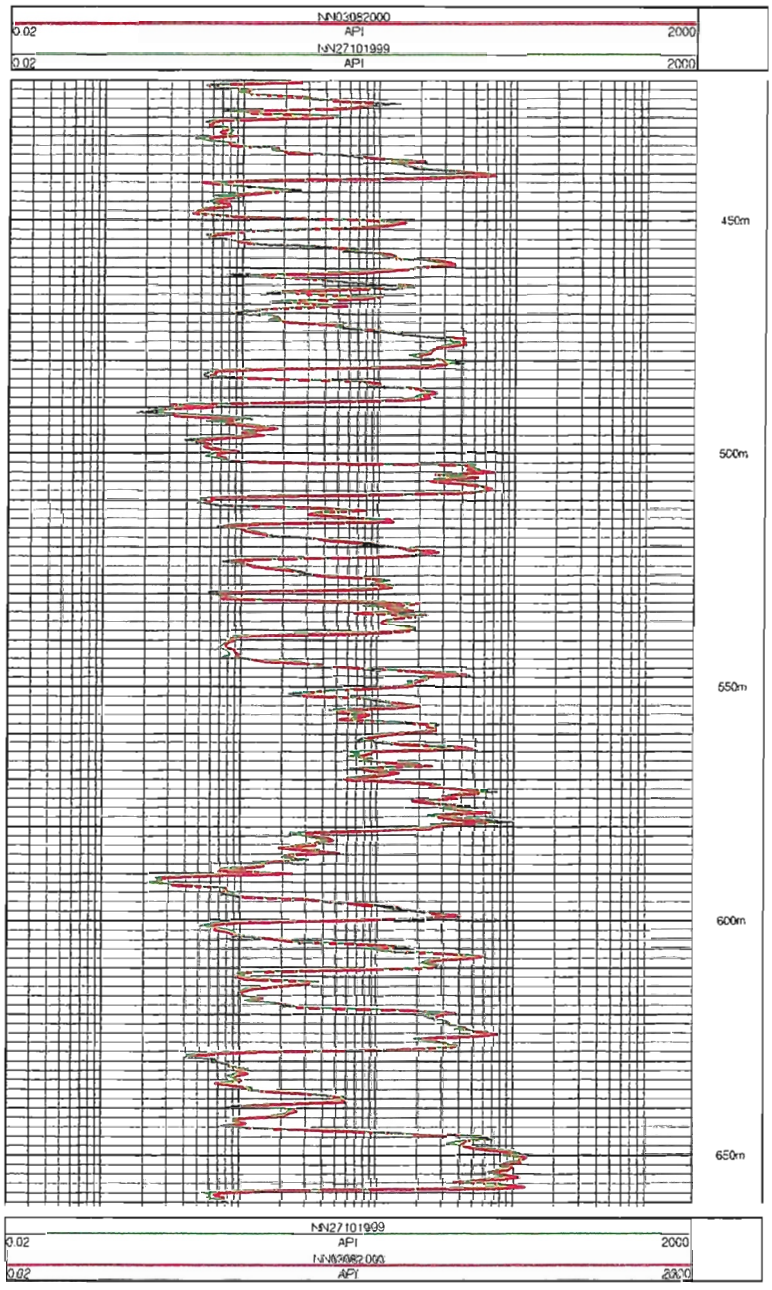

Figure 21. *Data example comparing short (SN) and long normal (LN) resistivity data from October 1999 and August 2000.*

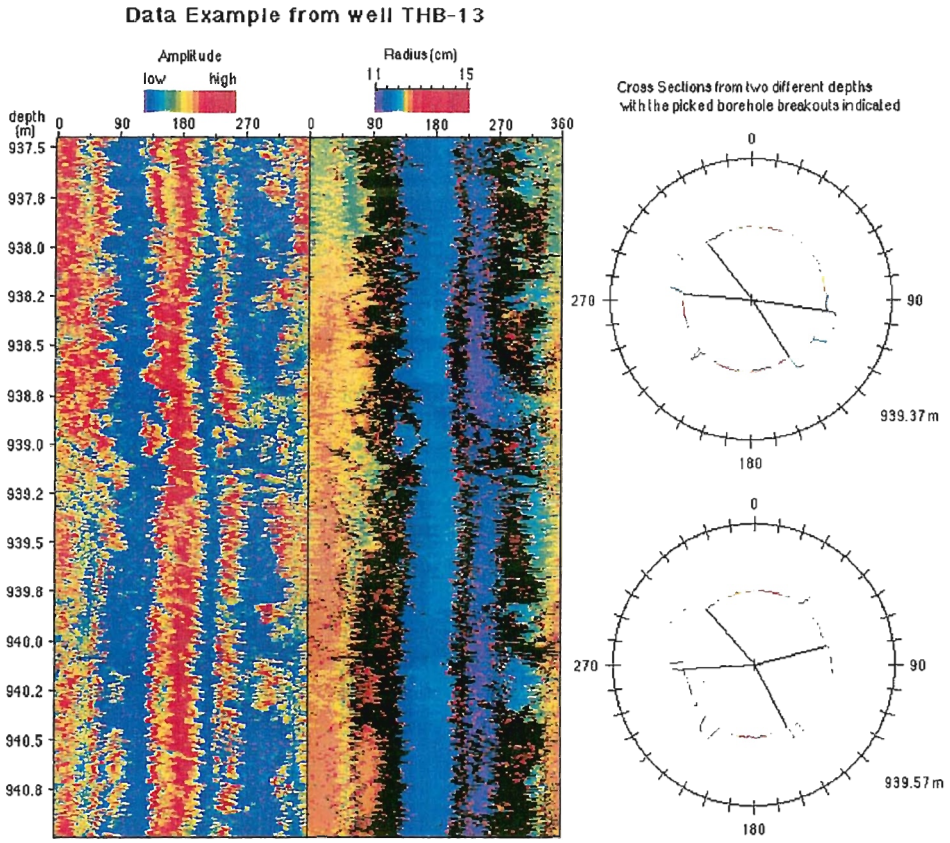

Figure 22. *Example of the borehole breakouts found in well THB-13 with two cross sections. The two panels show the amplitude of the reflected signal (left) and the radius calculated from the travel time (right), both unwrapped from north over east, south, west to north. Vertical axis: depth in meters. Breakouts appear as vertical bands of low reflection amplitudes. Due to poor reflection amplitudes, the values for the radius are often missing in these parts, resulting in black bands. In the two cross sections, the black lines indicate the range in azimuth of the picked breakouts.*

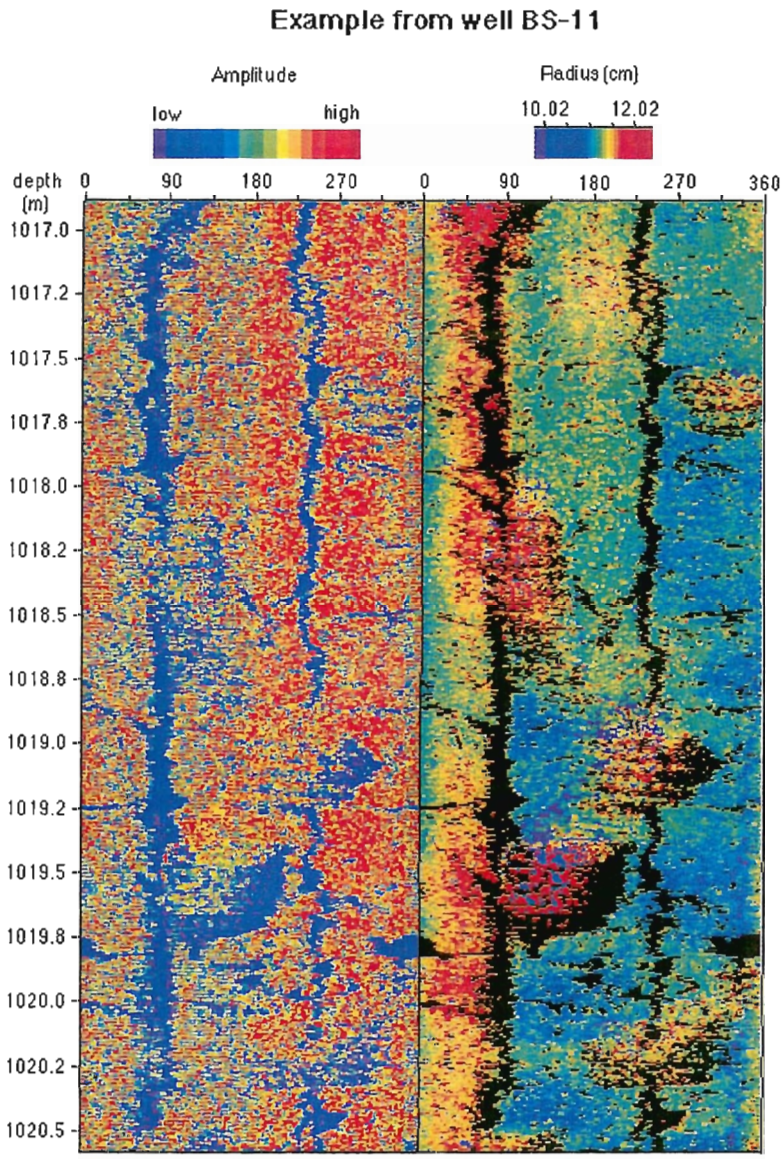

Figure 23. *Example for drilling induced vertical fractures observed in borehole BS-11. The data are displayed as described in Figure 22. The fractures appear as narrow vertical stripes of low reflection amplitude, much narrower than breakouts. Values for the radius calculated from travel time are missing for these stripes due to low amplitudes.*

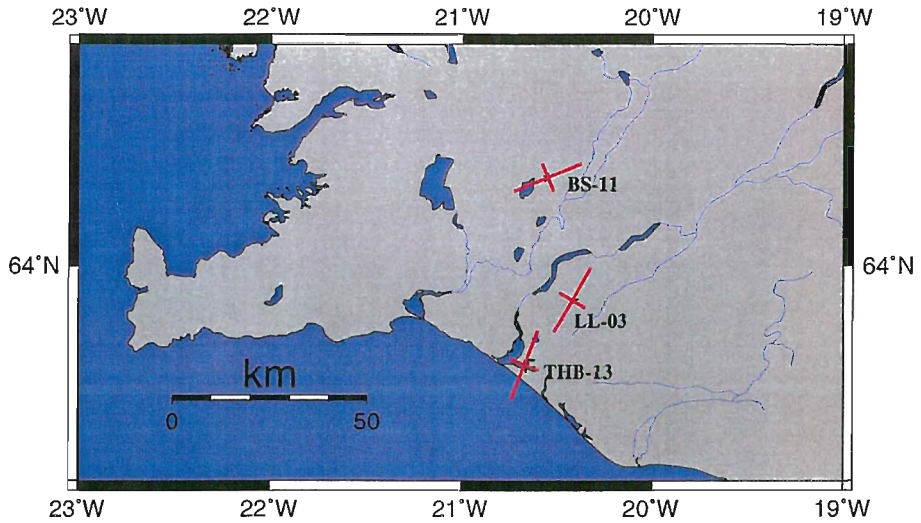

Figure 24. *Stress orientations found in boreholes in the South Iceland seismic zone. Long red lines indicate the orientation of the larger, short ones that of the lower principle horizontal stress.*

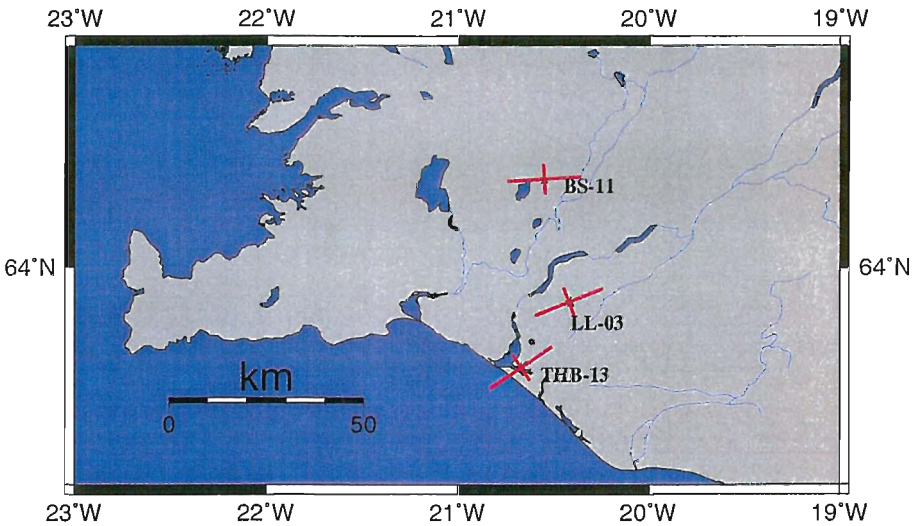

Figure 25. *Stress orientations calculated in Subpart 7B for borehole positions in and near the SISZ.*

Summary:
The results can be summarized as follows:

- The measurements at LL-03 for changes in P–wave velocity with the sonic log, for porosity changes with the neutron-neutron log, and for resistivities with the latero log, 16", and 64" show good repeatability.
- The earthquakes in June 2000 happened two weeks before the end of PRENLAB-2 project. Therefore, the last logging campaign before the events took place 8 months before the events. No clear indication for changes before the events was found. This might be, because the time difference was too long or the signals were below the detection threshold of the tools used.
- Coseismic changes might be visible at about 465 m depth, where both the 16" and the 64" log show a decrease in resistivity. It would be interesting to check whether cracks can be found there and at the other feed-points (visible in the temperature logs) with a high resolution borehole televiewer.
- Non-vertical fractures found down to nearly 1100 m depth show the same dominant strike as those observed at the surface (see first annual PRENLAB-2 report). A dependence of fracture orientation upon depth or upon geographical latitude could not be found.
- The stress orientations found at all three locations are similar and agree with a left–lateral strike-slip regime. They are based on data that are assumed to originate from 1977, 1992 and 1997 and are not perpendicular to existing ruptures found in the SISZ and, therefore indicate, that the SISZ is not a weak fault, as postulated for the San Andreas fault. Instead, it appeared prepared for another earthquake. From a rock mechanics view the stress directions found at LL-03 and THB-13 correlate with N-S striking faults, as they are found in the SISZ. On the other hand the orientation of maximum horizontal principal stress found at BS-11 correlates with the model of an E-W striking strike-slip fault zone. A linear dependency of stress orientation on age, depth or geographical position (in-/outside the SISZ) of the boreholes could not be found. Stress orientations similar to ours were also found by Stefánsson et al. (1993) from fault plane solutions. This was confirmed by other groups in the framework of PRENLAB as by Bergerat and coworkers (Subproject 6), who found a mean orientation of σ_H of N56°E derived from 1916 fault plane solutions selected from 48669 earthquakes in the SISZ of the years 1995 to 1997 (Angelier et al. 2000). A NE–SW orientation of σ_H was also the result of investigations of Crampin and coworkers on shear-wave splitting due to stress anisotropy at four of six seismic stations in the SISZ (Crampin et al. 1999) (Subproject 3).

Participants:
Besides the proposer and the subcontractor, the following scientists and technicians have supported the Subproject:
G. Axelsson (OS), H. Bäßler (Karlsruhe), C. Carnein (GFZ), E.T. Elíasson (OS), H.-J. Fischer (GFZ), P. Fleckenstein (GFZ) S.Þ. Guðlaugsson (OS), K. Henneberg (GFZ; now at

PGS, Oslo), G. Hermannsson (OS), M. Hönig (GFZ), G. Kurz (GFZ; now at NLfB–GGA, Hannover), Fernando J. Lorén Blasco (GFZ), S. Mielitz (GFZ), H. Sigvaldason (OS), Ó. Sigurðsson (OS), and B. Steingrímsson (OS).

3.4.4 Acknowledgements

We are very grateful to all above named participants. We thank Orkustofnun for excellent preparation and support of the logging campaigns. We like to thank the owners of the boreholes for their permission to work in the wells. We are very grateful to GeoSys company and the Geophysical Institute of Karlsruhe University for lending us a BHTV and additional equipment for the logging campaign in June 1998. We also thank the GFZ logging team very much. We are also indebted to F. Lorenzo Martín for assisting in the graphics and checking the text.

3.4.5 References

Angelier, J., F. Bergerat & C. Homberg 2000. Variable coupling explains complex tectonic regimes near oceanic transform fault: Flateyjarskagi, Iceland. *Terra Nova*, in press.

Crampin, S., T. Volti & R. Stefánsson 1999. A successfully stress-forecast earthquake. *Geophys. J. Int.* 138, F1-F5.

Stefánsson, R., R. Böðvarsson, R. Slunga, P. Einarsson, S.S. Jakobsdóttir, H. Bungum, S. Gregersen, J. Havskov, J. Hjelme & H. Korhonen 1993. Earthquake prediction research in the South Iceland seismic zone and the SIL project. *Bull. Seism. Soc. Am.* 83, 696-716.

Zoback, M.D., M.L. Zoback, V.S. Mount, J. Suppe, J. Eaton, J.H. Healy, D. Oppenheimer, P. Reasenberg, L. Jones, C.B. Raleigh, I.G. Wong, O. Scotti & C. Wentworth 1987. New evidence on the state of stress on the San Andreas fault system. *Science* 238, 1105-1111.

3.5 Subproject 5: Active deformation determined from GPS and SAR

Contractor:

Freysteinn Sigmundsson
Nordic Volcanological Institute
Grensásvegur 50
108 Reykjavík
Iceland
Tel: +354-525-4494
Fax: +354-562-9767
E-mail: fs@norvol.hi.is

Associated contractor:

Kurt L. Feigl
Centre National de la Recherche Scientifique
UPR 0234 - Dynamique Terrestre et Planétaire
14 Avenue Edouard Belin
FR-31400 Toulouse
France
Tel: +33-5-6133-2940
Fax: +33-5-6125-3205
E-mail: kurt.feigl@cnes.fr

Subcontractor:

Páll Einarsson
Science Institute
University of Iceland
Hofsvallagata 53
107 Reykjavík
Iceland
Tel: +354-525-4816
Fax: +354-552-8801
E-mail: palli@raunvis.hi.is

Researcher:

Sverrir Guðmundsson
Nordic Volcanological Institute
Grensásvegur 50
108 Reykjavík
Iceland
Tel: +354-525-5868
Fax: +354-562-9767
E-mail: sg@raunvis.norvol.hi.is

Researcher:

Amy E. Clifton
Nordic Volcanological Institute
Grensásvegur 50
108 Reykjavík
Iceland
Tel: +354-525-5481
Fax: +354-562-9767
E-mail: amy@norvol.hi.is

The main end results of this Subproject are described in the following. For details of how individual tasks were carried out, we refer to PRENLAB-2 first annual report.

3.5.1 Subpart 5A: SAR interferometry study of the South Iceland seismic zone

The objective was to measure ongoing crustal deformation in the South Iceland seismic zone (SISZ) and relate it to distribution of faults and seismicity there. We have met that objective at the western edge of the SISZ, around the Hengill volcanic center, and published the results in an international, peer-reviewed scientific journal (Feigl et al. 2000).

We have analyzed synthetic aperture radar (SAR) images acquired by the ERS-1 and ERS-2 satellites between July 1993 and September 1998 using interferometry. In spite of our careful image selection, correlation is poor in the relatively flat and wet lowlands of southern Iceland, which unfortunately includes most of the faults in the SISZ. On the other hand, coherence remains good, even after 4 or 5 years, in the mountainous areas around Hengill.

The predominant signature in all the interferograms spanning at least 1 year, is a concentric fringe pattern centered just south of the Hrómundartindur volcanic center (Figure 26). This we interpret as mostly vertical uplift caused by increasing pressure in an underlying magma source. The volume source that best fits the observed interferograms lies at 7±1 km depth and remains in the same horizontal position to within 2 km. It produces 19±2 mm/year of uplift. This deformation accumulates as elastic strain energy at a rate 2.8 times the rate of seismic moment release.

Under our interpretation, magma is injected at 7 km depth, just below the seismogenic zone formed by colder, brittle rock. There, the inflation induces stresses that exceed the Coulomb failure criterion, triggering earthquakes. Accumulated over 5 years, the deformation increases the Coulomb failure stress by >0.6 bar in an area that includes some 84% of the earthquakes recorded between 1993 and 1998 (Figure 27 and Figure 28).

Our model suggests that magmatic inflation can trigger earthquakes, with stress rising slowly to failure and then dropping instantaneously in an earthquake. Thus a plot of stress as a function of time on a given fault forms a sawtooth pattern. Prior to an earthquake, on the leading edge of the sawtooth, the stress increases at a rate of the order of $\sim$ 1 bar/year. After accumulating for a time interval Δt years, the stress then decreases abruptly in an earthquake with stress drop $\delta\tau$. For the magnitude 5.2 earthquake of June 4, 1998, we take a mean stress drop of the order of $\tau \sim 20$ bars, assuming that μ =33 GPa and $\delta\tau = \mu U(LW)^{1/2}$. If this rupture returns the state of its stress to its initial level, then the accumulation interval is of

the order of $\Delta t \sim 20$ years. If this process is cyclical, then this interval is the recurrence time of a characteristic earthquake. It suggests that inflation of a magma chamber can furnish the primary driving force to actually break rocks on a fault in an earthquake.

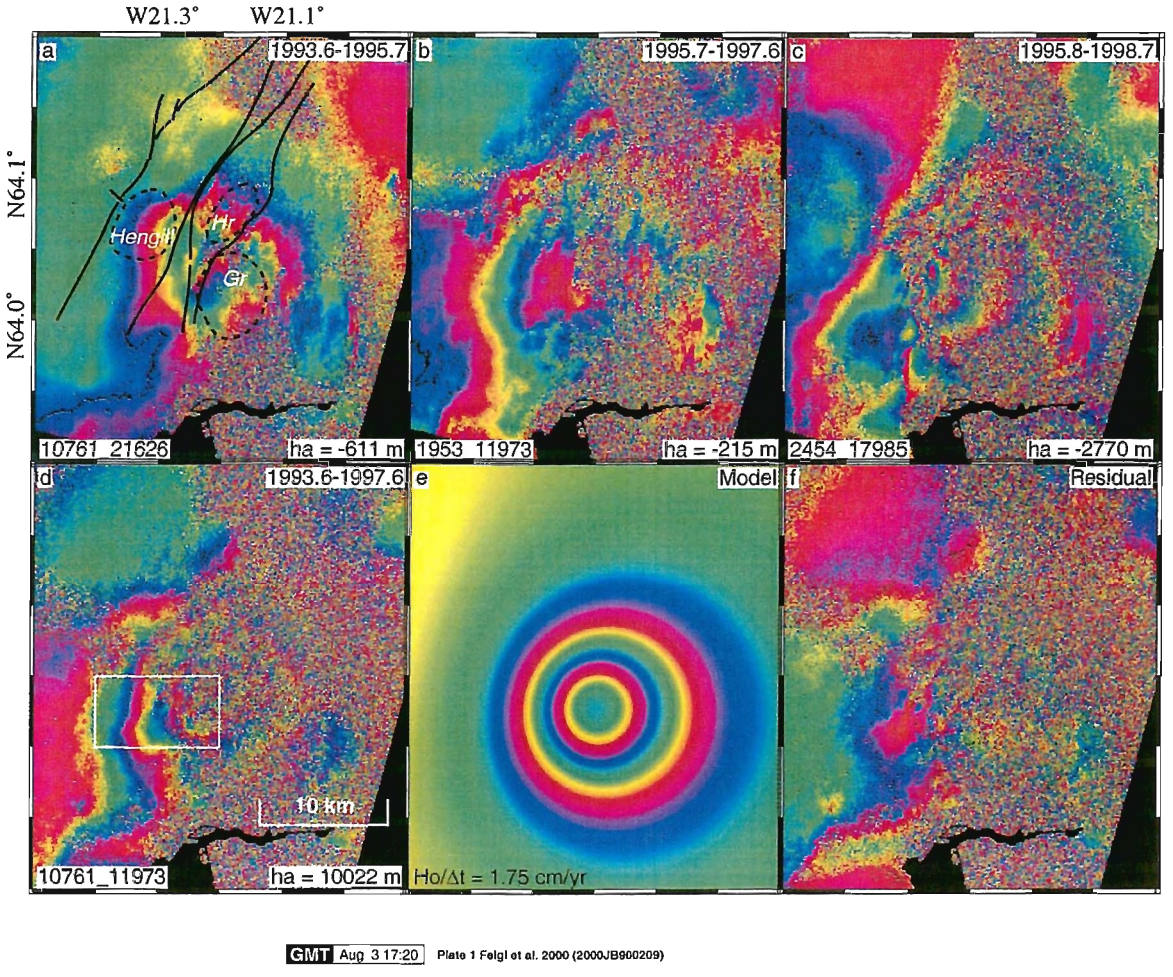

Figure 26. *Observed interferograms of the Hengill area for four different time intervals. The time interval appears in the upper right corner of each panel, the orbit numbers appear at lower left, and the altitude of ambiguity h_a appears at lower right. One fringe represents 28 mm of range change. Two concentric fringes are visible in the 4-year interferogram (d) indicating at least 6 cm of uplift between August 1993 and August 1997. The white box in (d) includes the discontinuity enlarged in (b) and (c).*

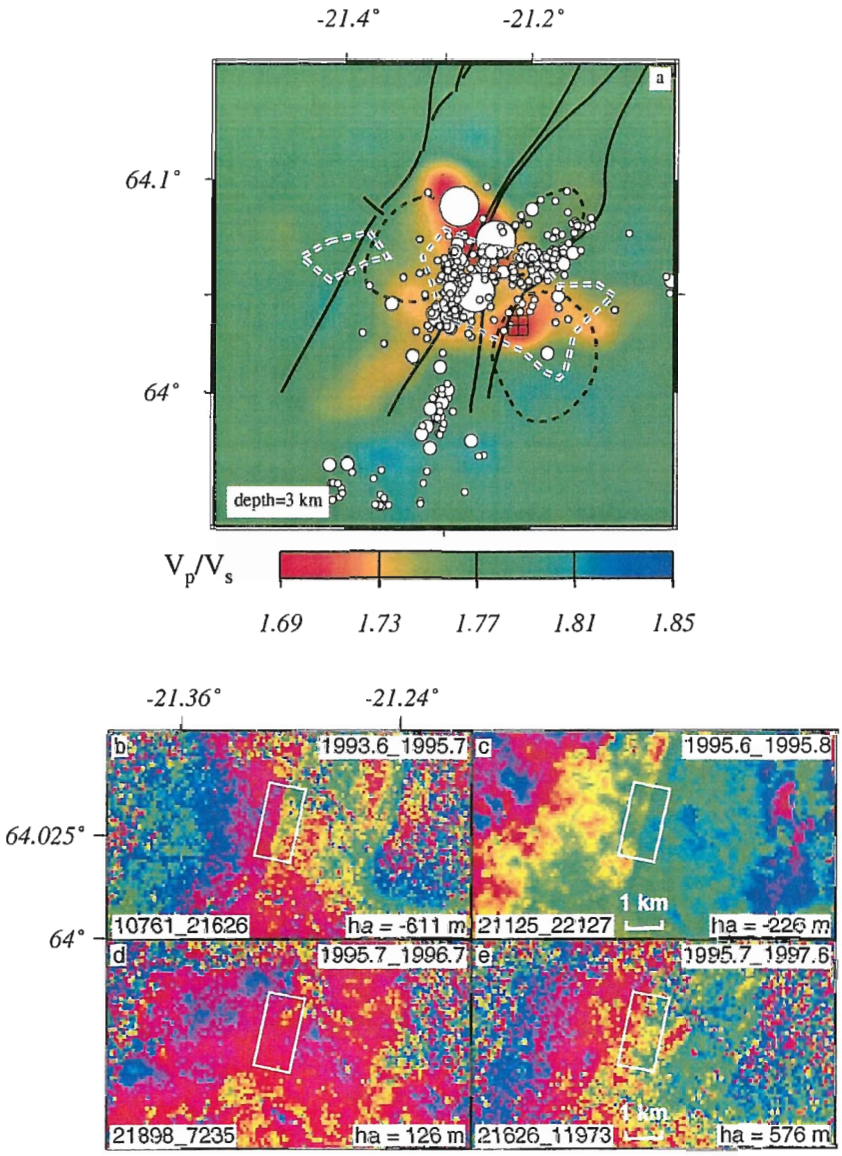

Figure 27. *(a) Structural map showing V_P/V_S wave speed ratio at 4 km depth (Miller et al. 1998); our best fitting volume source (crossed square); contours of P-wave speed velocity anomaly $\delta V_P = +1\%$ at 4 km depth (dashed white lines); contours of Miller et al. (1998); limits of volcanic system (solid black lines); outlines of three central volcanos (dashed black lines). Circles and dots show earthquake hypocenters for events between 1993 and 1998 (Rögnvaldsson et al. 1998a; Rögnvaldsson et al. 1998b). The largest circle is the M_w=5.2 event of June 4, 1998. Events with magnitude smaller than 2.5 plot as dots. (b-e) Enlargement of two interferograms that span August 1995 [b) and c)], and two which do not [d) and e)]. A discontinuity is clearly visible in b) and c) and is interpreted as a fault rupturing. We cannot discern a discontinuity in Figures d) and e).*

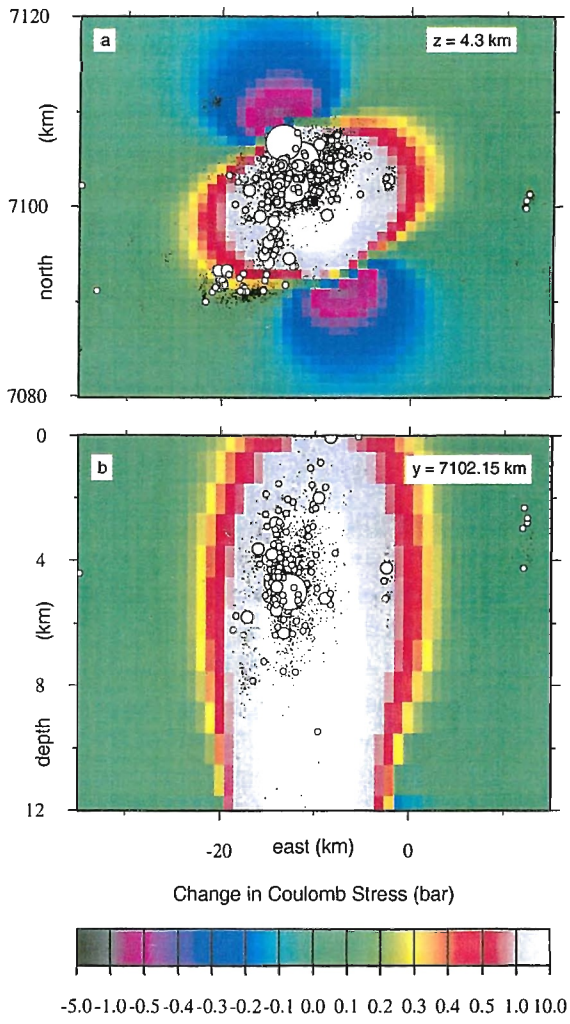

Figure 28. *(a) Coulomb failure stress change on optimally oriented vertical faults shown in a horizontal slice at 4.3 km depth. White color denotes where the stress increase is >1 bar but <10 bar. Source parameters include: latitude* 64.032°*N, longitude* 21.213°*W, depth 7.0 km, tensile opening 12.1 m on each of three dykes with length L=1 km and width W=1 km; the apparent coefficient of friction* μ'_f*=0.4, the azimuth* ϕ*=70° (measured clockwise from north) of the most compressive principal value of the stress tensor, and its magnitude* $|\sigma_1|$*=1 bar, and the two Lame' constants* $\mu=\lambda$*=33 GPa. Hypocenters of the earthquakes (circles and dots) are as in Figure 27. (b) Coulomb failure stress change on optimally oriented vertical faults shown in a vertical cross section passing E-W through the center of the modelled volcanic point source (crossed square). Model parameters and plotting conventions as in Figure 27a.*

3.5.2 Subpart 5B: GPS measurements of absolute displacements

The objective was to measure absolute plate motions near the South Iceland seismic zone (SISZ), in order to help with improved understanding of the mechanism of faulting in the seismic zone. The objective has been met by developing a new technique to combine GPS and satellite radar interferograms into three-dimensional motion maps, that give an unprecedented view of the absolute plate motions (Guðmundsson et al. 2000). The methodology has been applied to the western continuation of the SISZ, the Reykjanes peninsula.

The original plan was to operate one semi-continuous GPS station and interpret data from this station. Rather than doing that, we participated in the installation of network of continuously recording stations in S-Iceland. These results are described in Subproject 1. Additional work was conducted on two topics: Development of a new technique to combine GPS and satellite radar interferometry results (work lead by Sverrir Guðmundsson), and secondly, fault mapping was conducted in the Hengill region in order to advance further the understanding of interferograms collected in Subpart 5A (work lead by Amy Clifton).

The new technique developed to efficiently produce high-resolution three-dimensional surface motion maps, relies on combining information about motion of the earth's surface from interferometric observations of synthetic aperture radar images and repeated Global Positioning System geodetic measurements. Unwrapped interferograms showing pixel-wise change in range from ground to satellite, and sparse values of three-dimensional movements are required as input. The problem of finding the full three-dimensional motion field is separated into two two-dimensional problems. Initially the vertical component of the deformation field, and its horizontal component in the look-direction of the satellite are found. Later the look-direction component is resolved into north and east components. Initial values for the motion fields are assigned to each pixel of interferograms from ordinary kriging of available GPS observations. These values are then updated and optimized by comparison with the interferograms and the GPS observations. Additional constraint is the smoothness of motion field. Markov random field based regularization, and simulated annealing algorithm are used for the optimization. The technique has been applied to create surface motion maps for the Reykjanes peninsula (Figure 29). Although separate interpretation of GPS and InSAR data from the area (Hreinsdóttir et al. 2000; Vadon and Sigmundsson 1997) have shown the main components of deformation, the three-dimensional motion maps provide an unprecedented view of the three-dimensional deformation. The largest signals are plate movements causing large gradients in the east motion field, and circular subsidence centered on the Svartsengi and Eldvörp geothermal area. The north and east motion field images show also clearly that the subsidence is associated with horizontal movements towards the subsidence center, a pattern that is imprinted on the background plate movements. The motion maps form the basis of a future project on conducting a detailed study of strain accumulation in the area and how it correlates with seismicity.

A related effort was the study of faulting and surface rupture that has taken place in the Hengill volcanic area (Clifton and Sigmundsson 2000). It is the same area as studied by satellite radar interferometry under Subpart 5A. The Hengill and Hrómundartindur volcanic systems in SW-Iceland are considered to comprise the Hengill triple junction at which the oblique Reykjanes peninsula rift zone, the western volcanic (rift) zone and the South Iceland seismic (transform) zone meet. It is therefore experiencing both tectonic extension and left-

lateral shear causing seismicity related to both strike-slip and normal faulting. Between 1994 and 1998, the area experienced episodic swarms of enhanced seismicity attributed to magma moving within the system. Activity culminated in a magnitude 5.1 earthquake on June 4, 1998, and a magnitude 5 earthquake on November 13, 1998. Geodetic measurements using GPS, levelling and InSAR detected uplift and expansion of the volcanic edifice above a point source of pressure beneath the Hrómundartindur volcanic system. Magma accumulation elevated the volcanic edifice 2 cm/year and is believed to have triggered motion along strike-slip faults that were near to failure due to tectonic stresses. A number of faults in the area generated small-scale surface breaks. Geographic information system has been used to integrate aerial photographs, field data and geophysical data to determine how the crust breaks in response to deformation along this plate boundary, and to see how much of the recent activity focussed on pre-existing weaknesses in the crust. Our data indicates that all surface rupture has occurred along or adjacent to old faults, several of which were previously unmapped. The most prominent surface breaks occurred along NE- and NNE-trending faults adjacent to the epicenter of the June 4 earthquake. Maximum opening observed along a single fault segment was 1.2 m. Styles of rupture include fresh rockfall into pre-existing fissures and along old scarps, subsidence along and possible widening of old fissures, tears in turf and gashes in soil, shattering of lava blocks and loosening of push-up structures related to strike-slip faulting (Figure 30). Although all geophysical data agree that rupture occurred along a shallow, right-lateral strike-slip fault, no clear evidence of lateral offset was observed at the surface. Foreshocks and aftershocks from the November 13 earthquake define a broad E-W zone that intersects the southern end of the June 4 fault. The only surface rupture observed in this zone was found at that intersection.

In addition to fault mapping in the Hengill area, then Páll Einarsson at UICE.SI worked as a subcontractor on preparing a digitized fault map of the South Iceland seismic zone, as described in the PRENLAB-2 first annual report. That work is still in progress.

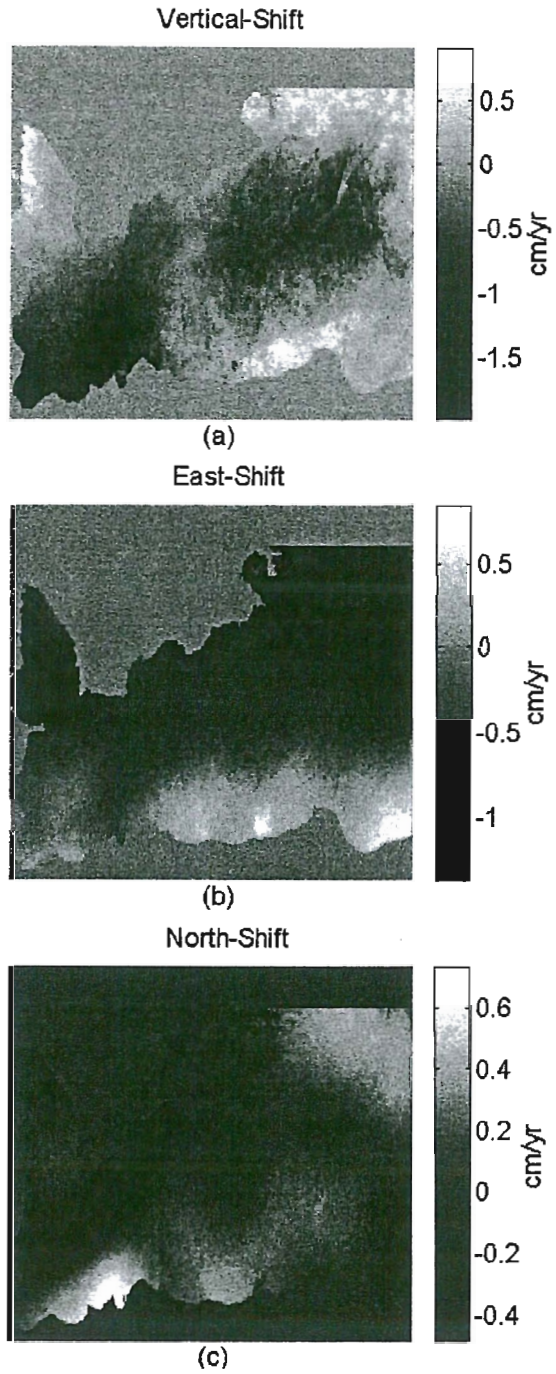

Figure 29. *Estimated one-year average motion field maps at the Reykjanes peninsula. (a), (b) and (c): Average vertical, east and north motion maps, respectively, inferred by the 1992-1993, 1992-1995, 1992-1996 and 1993-1995 InSAR data, and the 1993-1998 GPS data (Guðmundsson et al. 2000).*

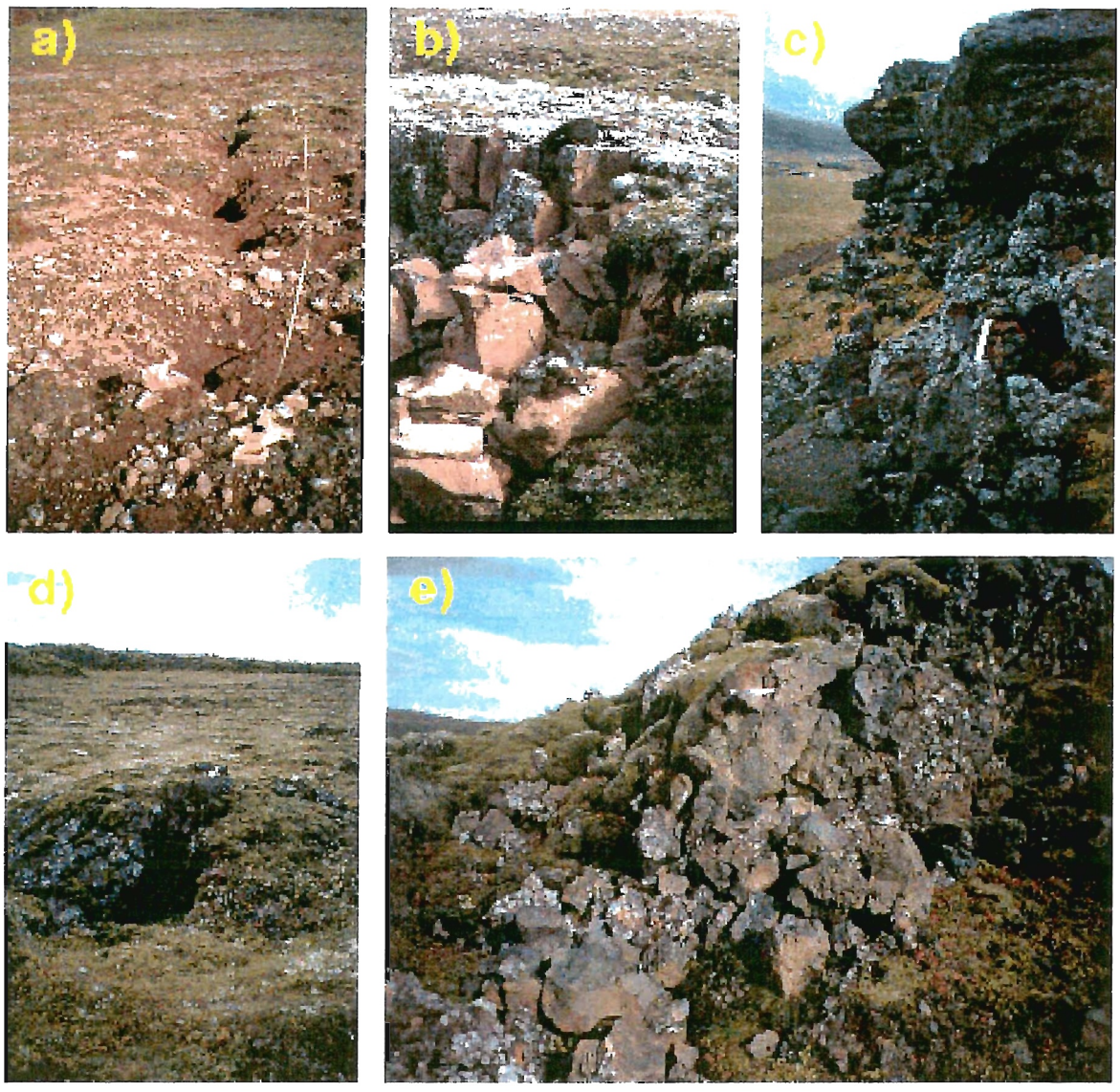

Figure 30. *Different styles of surface rupture observed in the Hengill area in response to uplift, and the June 4, 1998, M=5.1 earthquake. a) Gashes in soil: Ellipital segments up to 1.5 m wide, 2 m long, more than 1 m deep, en-echelon and along-strike arrangement. b) Rock fall along old fissures: Unweathered surfaces of broken rock, free of vegetation, plant roots freshly exposed. c) Rock fall along old fault scarps: Large fallen blocks, exposing freshly torn plant roots and soil, large rocks dislodged from slope leaving gaps between rocks and soil. d) Loosened push-up structures: Piles of rock with gaps of up to several centimeters between rock and soil; individual rocks may show evidence of rotation. e) Shattered aa lava: Broken blocks up to 1 m in diameter, aligned along strike and at flow margins near the June earthquake epicenter (Clifton 2000).*

3.5.3 References

Clifton, A. 2000. Surface deformation related to volcanic uplift and seismicity in SW-Iceland. Poster presented at the Nordvulk-Ridge summer school, Iceland, August 20-30, 2000.

Clifton, A. & F. Sigmundsson 2000. Faulting and deformation resulting from magma accumulation at the Hengill triple junction, SW-Iceland. In: Abstracts from the AGU fall meeting, San Francisco, California, USA, December 15-19, 2000.

Feigl, K.L., J. Gasperi, F. Sigmundsson & A. Rigo 2000. Crustal deformation near Hengill volcano, Iceland, 1993-1998: coupling between magmatic activity and faulting inferred from elastic modeling of satellite radar interferograms, *J. Geophys. Res.* 105, 25655-25670.

Guðmundsson, S., F. Sigmundsson & J.M. Carstensen 2000. Three-dimensional surface motion maps estimated from combined InSAR and GPS data. *J. Geophys. Res.*, submitted.

Hreinsdóttir, S., P. Einarsson, & F. Sigmundsson 2000. Crustal deformation at the oblique spreading Reykjanes peninsula, SW-Iceland: GPS measurements from 1993 to 1998. *J. Geophys. Res.*, submitted.

Miller, A.D., B.R. Julian & G.R. Foulger 1998. Three dimensional seismic structure and moment tensors of non-double-couple earthquakes at Hengill-Grensdalur volcanic complex, Iceland. *Geophys. J. Int.* 133, 309-325.

Rögnvaldsson, S.Th., G.B. Guðmundsson, K. Ágústsson, S.S. Jakobsdóttir, R. Slunga & R. Stefánsson 1998a. Overview of the 1993-1996 seismicity near Hengill. *Rit Veðurstofu Íslands* VÍ-R98006-JA05. Research report, Icelandic Meterological Office, Reykjavík, 16 pp.

Rögnvaldsson, S. Th., Þ. Árnadóttir, K. Ágústsson, Þ. Skaftadóttir, G.B. Guðmundsson, G. Björnsson, K.S. Vogfjörð, R. Stefánsson, R. Böðvarsson, R. Slunga, S.S. Jakobsdóttir, B.S. Þorbjarnardóttir, P. Erlendsson, B.H. Bergsson, S. Ragnarsson, P. Halldórsson, B. Þorkelsson & M. Ásgeirsdóttir 1998b. Skjálftahrina í Ölfusi í nóvember 1998. *Greinargerð Veðurstofu Íslands* VÍ-G98046-JA09. Report, Icelandic Meteorological Office, Reykjavík, 19 pp. In Icelandic.

Vadon, H., & F. Sigmundsson 1997. Crustal deformation from 1992 to 1995 at the mid-Atlantic ridge, Southwest Iceland, mapped by satellite radar interferometry. *Science* 257, 194-197.

3.6 Subproject 6: Effects of stress fields and crustal fluids on the development and sealing of seismogenic faults

Contractor:

Françoise Bergerat
Département de Géotectonique, Boite 129
Université Pierre et Marie Curie
4, place Jussieu
FR-75252 Paris Cedex 05
France
Tel: 33-1-4427-3443
Fax: 33-1-4427-5085
E-mail: bergerat@lgs.jussieu.fr

Subcontractor:

Jacques Angelier
Département de Géotectonique, Boite 129
Université Pierre et Marie Curie
4, place Jussieu
FR-75252 Paris Cedex 05
France
Tel: 33-1-4427-5857
Fax: 33-1-4427-5085
E-mail: jacques.angelier@lgs.jussieu.fr

Subcontractor:

Ágúst Guðmundsson
Geological Institute
University of Bergen
Allégaten 41
N-5007 Bergen
Norway
Tel: 47-5558-3503
Fax: 47-5558-9416
E-mail: agust.gudmundsson@geol.uib.no

Subcontractor:

Thierry Villemin
Laboratoire de Geodynamique des Chaines Alpines
Université de Savoie
Batiment Belledonne
Domaine Universitaire
73376 Le Bourget du Lac Cedex
France
Tel: 33-4-7975-8735
Fax: 33-4-7975-8777

E-mail: Thierry.Villemin@univ-savoie.fr

Subcontractor:

Philip Meredith
Department of Geological Sciences
University College London
Gower Street
London WC1E 6BT
United Kingdom
Tel: 44-171-380-7822
Fax: 44-171-387-1612
E-mail: p.meredith@ucl.ac.uk

3.6.1 Task 1: Determination of the paleostress fields associated with the test areas from fault-slip data

3.6.1.1 Task 1.1: The South Iceland seismic zone (SISZ)

We carried out a structural study in this area, including analysis of aerial photographs, local observation of major faults and collection of minor fault slip data in outcrops, as well as an analysis of the focal mechanisms of earthquakes (Bergerat et al. 1998; Bergerat et al. 1999; Bergerat and Angelier 2000). At the regional scale, the main fault trends are approximately NNE-SSW and NE-SW. ENE-WSW, NW-SE and WNW-ESE trending faults are also detected in aerial photographs and in the field. All these faults are normal or strike-slip in character. Some of the historical major earthquake fractures are observed in the post-glacial lava flows in the SISZ: most are right-lateral and trend roughly N-S. We analyzed more than 700 minor faults at 25 sites. Most sites are located in rocks of Upper Pliocene-Pleistocene age. Inversion of fault-slip datasets enabled us to reconstruct local paleostress tensors, hence to define the major tectonic regimes which have prevailed in the SISZ. Two main groups of faulting mechanisms reveal two distinct stress regimes, with perpendicular directions of extension, NW-SE (primary) and NE-SW (secondary). Both groups, however, display inhomogeneous datasets, related to extensional and to strike-slip faulting. The primary stress regime is in agreement with both the general behaviour of the SISZ as a left-lateral transform zone and the opening of the rift segments. The secondary stress regime, incompatible with the primary stress regime, is interpreted in terms of stress permutations. A population of 231 double-couple focal mechanisms (M>1 and depth>2 km) was also analyzed in terms of stress states. The results show great similarity in terms of stress directions. Figure 31 gives an example of a characteristic fault-slip data site and a comparison with focal mechanisms of earthquakes.

The present-day stress field mainly inferred from analyses of earthquake focal mechanisms is consistent with the present behaviour of the SISZ as a left-lateral transform zone. However, the proportion of strike-slip faulting within the present-day seismic activity (71%) is significantly higher than that revealed by the geological observation of Quaternary faults (50%). This contrast is interpreted in terms of development and evolution of the transform fault zone. Figure 32 schematically presents a comparison between the paleostress results obtained from faulting analysis and the present day activity based on focal mechanisms of

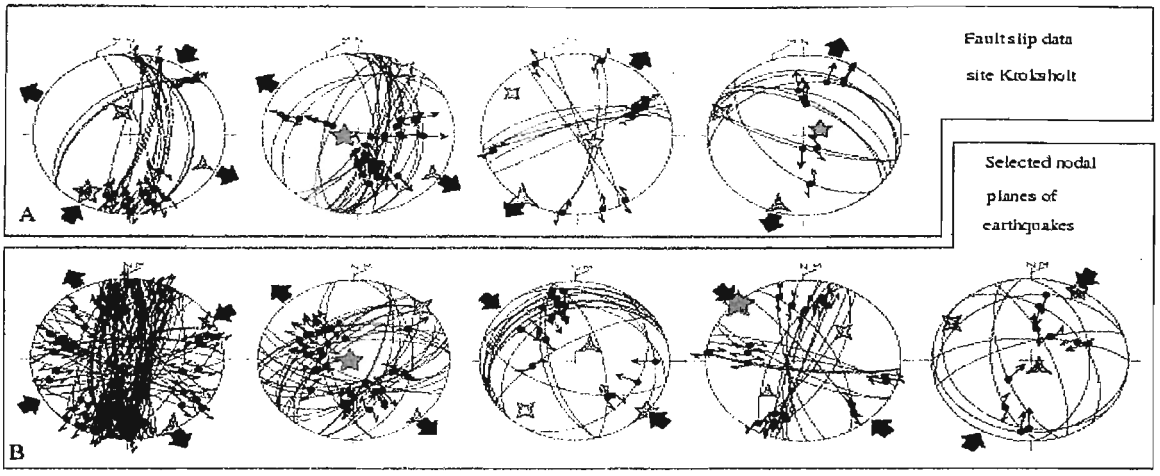

Figure 31. *Comparison between the main stress regimes as indicated by fault–slip datasets and focal mechanisms of earthquakes in the SISZ, based on two case examples (after Bergerat and Angelier 2000). (A) Striated faults at site Króksholt. (B) Selected nodal planes and slip vectors of earthquakes throughout the SISZ for the years 1991-1994 and 1996, at crustal depths larger than 2 km, with magnitudes larger than 1.*

earthquakes analysis. Stress permutations between different regimes are shown as couples of open arrows. The paleostress fields identified in the Upper Pliocene-Pleistocene formations of the SISZ reflect both the previous behaviour of the area, when it was located inside the rift zone, and its present behaviour as a transform zone, thus illustrating the local evolution from rifting to transform motion.

3.6.1.2 Task 1.2: The Tjörnes fracture zone (TFZ)

The inversion of about 1000 fault-slip data collected in 20 sites in the Flateyjarskagi peninsula allows reconstruction of eight normal and strike-slip regimes (Angelier et al. 2000b; Bergerat et al. 2000) related to the general behaviour of the Húsavík-Flatey fault (HFF), a major structure of the Tjörnes fracture zone connecting the Kolbeinsey ridge and the North Icelandic rift. The two most important regimes (E-W and NE-SW extensions), consistent with the right-lateral motion along the Húsavík-Flatey fault, constitute the main tectonic group. The two others (NW-SE and N-S extensions), forming the subordinate tectonic group, are incompatible and result from drastic stress permutations (as a probable result of stress drop, elastic rebound and dyke injection). Figure 33 summarizes the local paleostress determinations made in Flateyjarskagi.

The relationships between these stress regimes imply not only σ_1/σ_2 and σ_2/σ_3 stress permutations, but also σ_1/σ_3 reversals. An important factor controlling the transform mechanism is the variation of coupling along the HFF. The obliquity between the direction of transform motion and the trend of extension for the two main regimes may vary between 25° and 85°, reflecting repeated changes of the coefficient of friction along the HFF (Figure

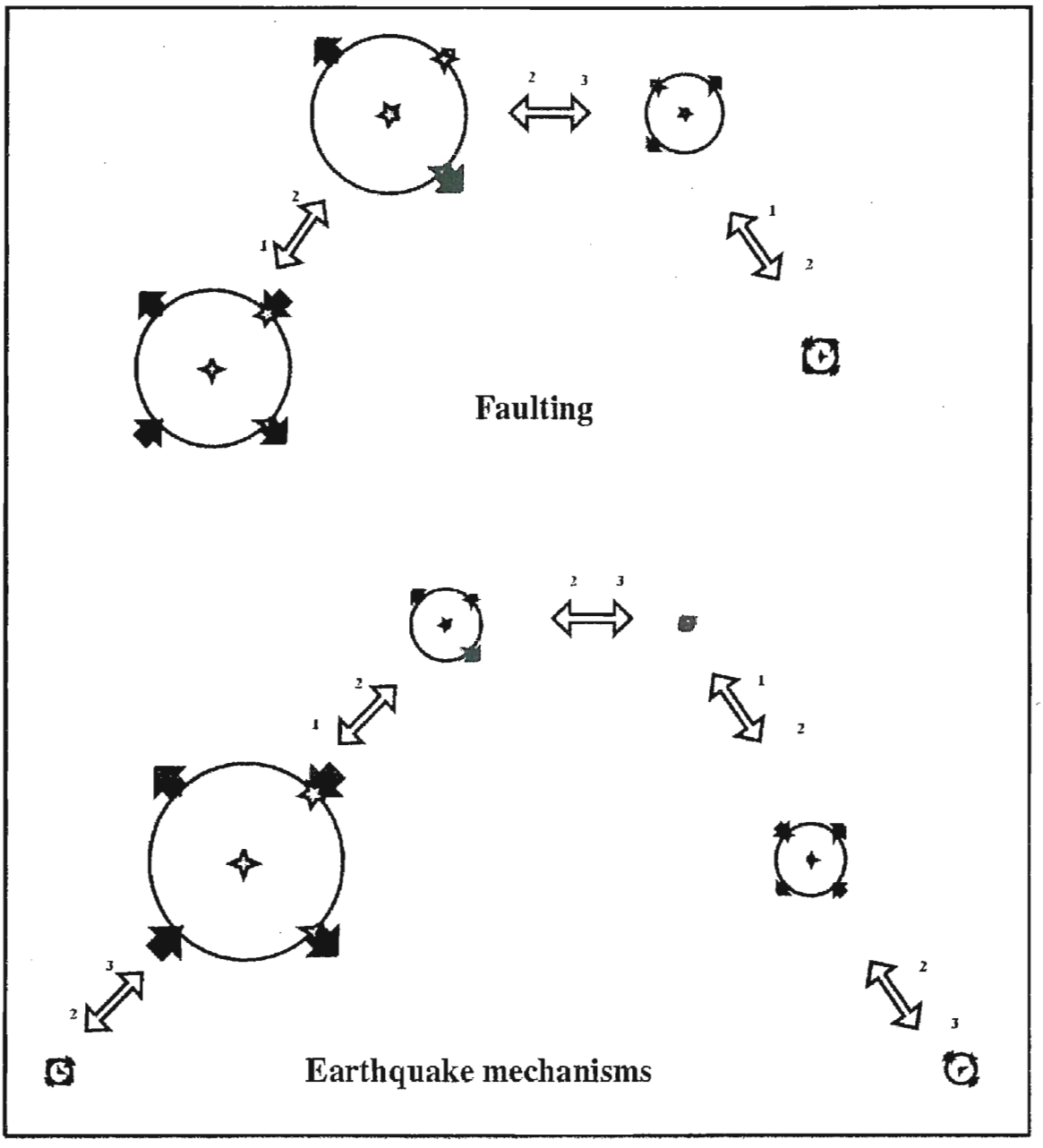

Figure 32. *The different stress tensors obtained from analyses of sets of fault-slip data and earthquake focal mechanisms in the SISZ (after Bergerat et al. 1999). Size of diagrams proportional to numbers of data. Three-, four-, and five-branched stars: regional axes of σ_3, σ_2 and σ_1 respectively (schematic). Couples of black arrows: directions of compression (convergent) or extension (divergent). Couples of open arrows: stress permutations (σ_1/σ_2 or σ_2/σ_3 modes) between the different regimes.*

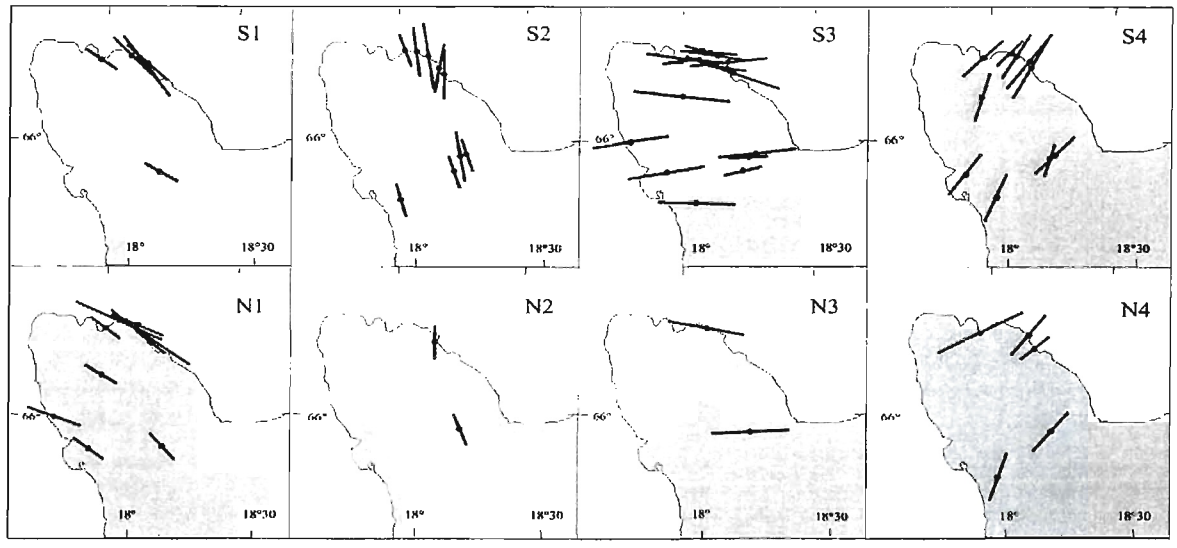

Figure 33. *Summary of local paleostress determinations made in Flateyjarskagi using Angelier's inversion (1990) (after Angelier et al. 2000b). Solid bars: trends of minimum compressive stress, σ_3. Bar size increases with quality of paleostress tensor determination. Nature of brittle tectonic regime: S-type for nearly vertical σ_2, N-type for nearly vertical σ_1.*

34). Such changes from very low mechanical coupling (weak fault) to moderate friction may occur very rapidly since it takes place several times in a few years, as shown by focal mechanisms of earthquakes analysis. Thus, the tectonic regimes need not be interpreted in terms of numerous tectonic episodes, but rather as a consequence of variable coupling across the transform zone.

3.6.2 Task 2: Reconstruction of the current stress field associated with the test areas

3.6.2.1 Task 2.1: Inversion of large sets of focal mechanisms of earthquakes

Using a new inversion technique suitable for focal mechanisms of earthquakes (in that it does not require the choice of a nodal plane as the actual fault plane) was particularly worthwhile in order to process the very large numbers of focal mechanisms of earthquakes determined within the SIL network set-up and monitored by IMOR.DG. This was because of the mathematical aspects which imply analytical resolution so that at the core of the inversion process itself the runtime does not depend on the quantity of data (Angelier 1998).

The inversion was carried out with a total dataset of about 50000 double–couple focal mechanisms of earthquakes (Angelier et al. 2000a). It revealed regional deviations as large as 40° in the direction of extension near the major transform zones (clockwise for the South Iceland seismic zone, counterclockwise for the Tjörnes fracture zone), relative to the N104°E trend of plate separation across the mid-Atlantic ridge. However, the mean axis of minimum stress obtained from these inversions for the whole of Iceland is quite consistent with the

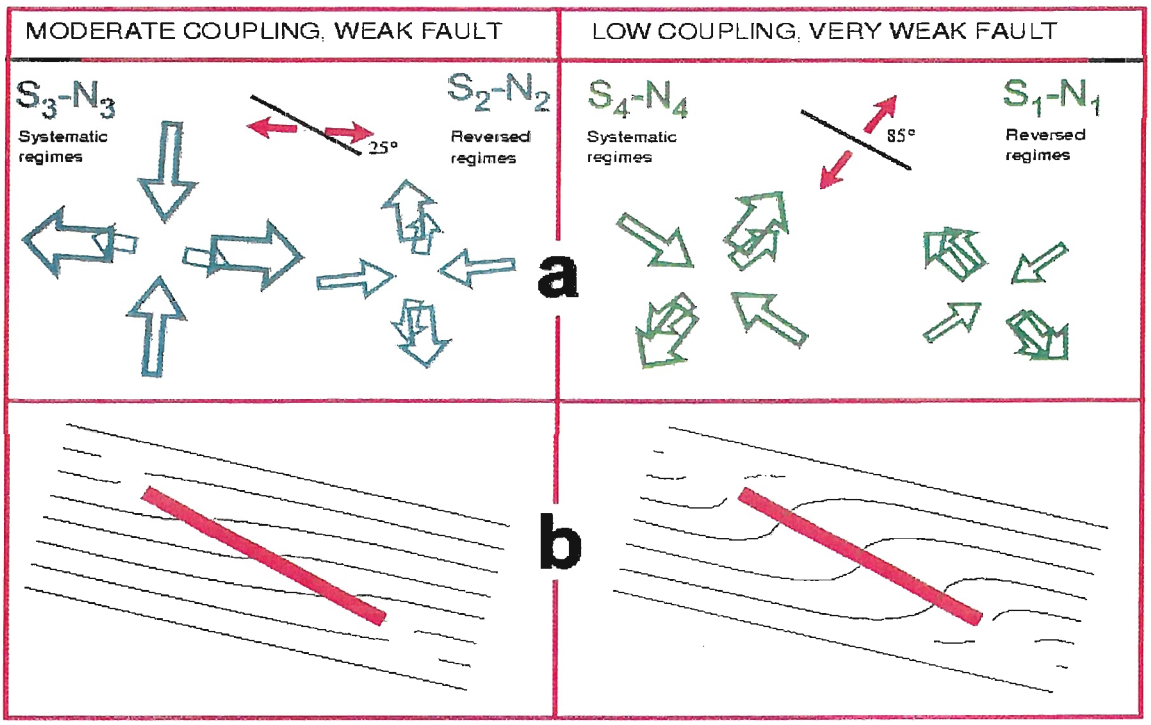

Figure 34. *Interpretation of tectonic regimes in terms of variable coupling near transform zone (after Angelier et al. 2000b). (a) Groups of tectonic regimes. Angles between transform direction (dotted lines) and averaged trends of extension (black arrows) indicated. (b) Schematic pattern of minimum compressive stress trajectories (thin lines) due to tensile loading parallel to spreading vector in North Iceland around oblique dextral transform fault zone (thick line).*

trend of plate separation independently reconstructed by DeMets et al. (1990).

3.6.2.2 Task 2.2: Seismotectonic analysis of individual faults

The Tjörnes fracture zone

The study of the Húsavík–Flatey fault in the Tjörnes fracture zone includes a tectonic analysis (see Subsection 3.6.1.2) and also a seismotectonic analysis in order to obtain a reconstruction of the stress patterns in accordance with the mechanisms of the transform zone since about 7 million years to the present (Garcia 1999; Garcia et al. 2000; Garcia et al., in preparation). We carried out an analysis of 669 double-couple earthquake mechanisms (period 1995-1997, magnitude ranging between 1 and 4.8). Three main sets of stress regimes have been identified, each including three individual stress regimes (Figure 35). The major one corresponds to an ENE-WSW trending right-lateral transtension. The two other regimes, less important, correspond to transform-parallel (WNW-ESE) and transform-perpendicular extensions (NNE-SSW).

Considering the angle between the trends of the rift and of the transform zone involves an extension occurring throughout the transform zone. This extension is accommodated by the transtensional regime, as well as, locally, by the extension sub-perpendicular to the transform direction. The extension sub-parallel to the transform direction may express by pull-apart process or by locking of part of the transform fault. The analysis of focal mechanisms of earthquakes indicates that most of these regimes currently occur, invalidating as well the hypothesis of polyphase tectonism (see Subsection 3.6.1.2). It suggests that transform motion along an oceanic fault zone may induce a variety of tectonic regimes. A major point of the transform mechanism is the variation of coupling along the HFF. These changes may correspond, at least partly, to the necessity of extension in this area because of the obliquity of the transform zone versus the rifts zones of N–Iceland and of Kolbeinsey, but the occurrence of magmatism at depth probably plays an important role also in such a phenomenon.

The Leirubakki fault

The Leirubakki fault is one of the large N-S seismic faults of the South Iceland seismic zone, located in its eastern part, a few kilometers west of the 1912 earthquake major earthquake. The Leirubakki rupture occurred earlier during historical times (maybe before the settlement of Iceland). Our work included the reconnaissance of the fault trace based on aerial photograph analysis and field study, a GPS mapping to reconstruct the morphology of the rupture zone, and some measurements of structures along the fault, including orientations and amplitudes (Bergerat et al. 2000; Bergerat et al., in preparation). We thus identify a pattern of dextral segments that connect typical push-up structures, with specific angular relationships between these features and the general trend of the earthquake fault (Figure 36). The fracturing process involved development of near-surface strike-slip segments, oblique relative to the underlying shear zone (Figure 36). We computed the shortening amounts and rock volumes involved in push-up development and estimated the magnitude of the Leirubakki fault to more than 7.

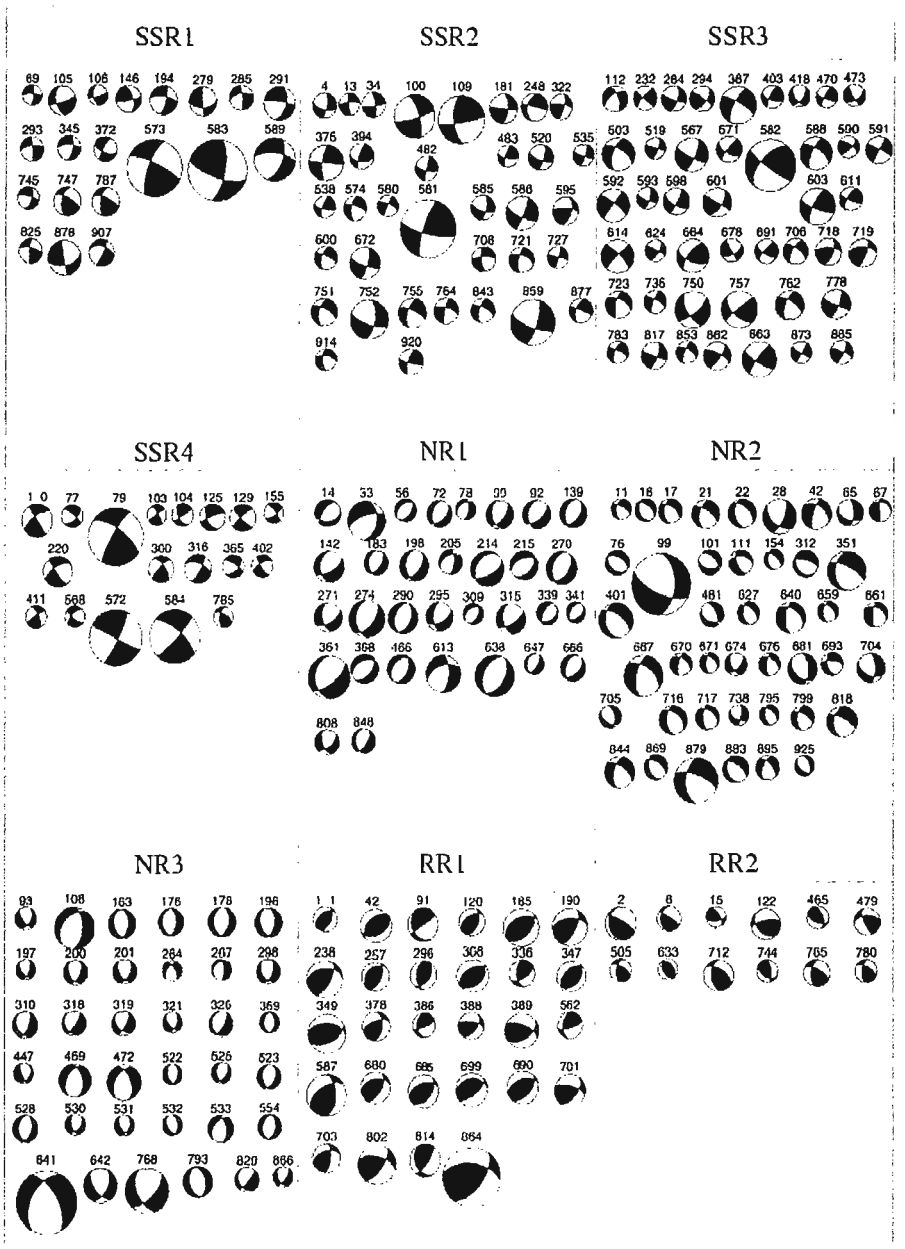

Figure 35. *Focal mechanisms of earthquakes characterizing the nine stress regimes in the Tjörnes fracture zone (SSR: strike-slip regime, NR: normal regime, RR: reverse regime) (after Garcia 1999; Garcia et al., in preparation). For the SSR2, SSR3, NR3 and RR4, only the focal mechanisms with M>1.8 are shown, for the other regimes all the focal mechanisms (M>1) are shown.*

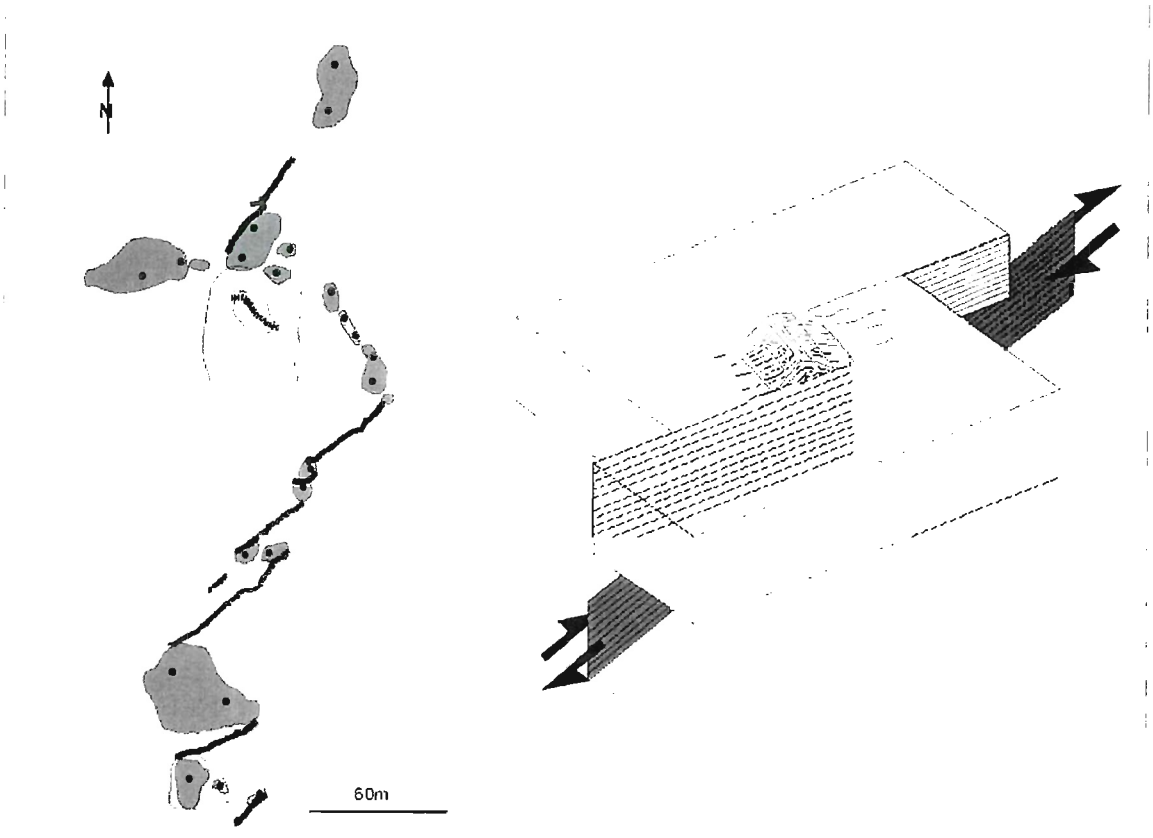

Figure 36. *The Leirubakki fault in the SISZ. On the left: detailed part of the map (drawn after GPS measurements) showing a typical array of individual fractures and individual push-ups. On the right: schematic view of a push-up and en-echelon fractures in the uppermost part of the crust and a single right-lateral strike-slip fault at depth (after Bergerat et al. 2000; Bergerat et al., in preparation).*

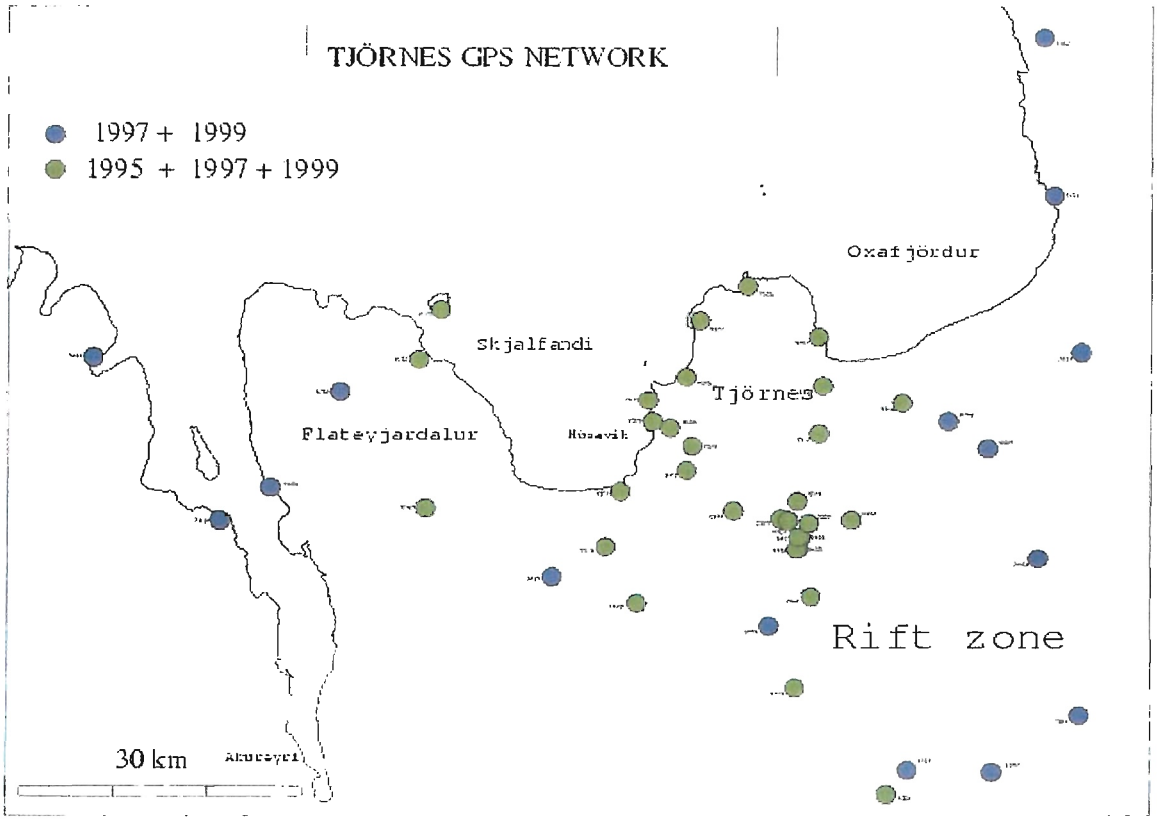

Figure 37. *The Tjörnes GPS network. 32 points have been measured in 1995, 1997 and 1999. The whole network has been measuring both in 1997 and 1999.*

3.6.3 Task 3: Present–day deformation from GPS network and interferograms of ERS-SAR scenes

3.6.3.1 Task 3.1: Measuring the present–day crustal displacements in the Tjörnes fracture zone and adjacent areas

The Tjörnes GPS network

The network consists of about 45 sites distributed in the northern Iceland seismic zone (Figure 37). It completes the geodetic networks already installed over the whole Iceland at a smaller scale. The TGN has been designed to measure the surface displacement field on each side of the Húsavík-Flatey fault (HFF). It has been done in order to estimate if there are locked fault segments in the area and how these segments can contribute to increase the seismic risk.

1995–1997 velocity field

The velocities (Figure 38) have been computed by reference to a point located in the southern part of the network. Two tendencies can be distinguished on the Tjörnes peninsula: eastward velocities reaching 13 mm/year for the most northern points of the peninsula and NNE velocities up to 15 mm/year for the points located on both sides of the HFF. Displacements

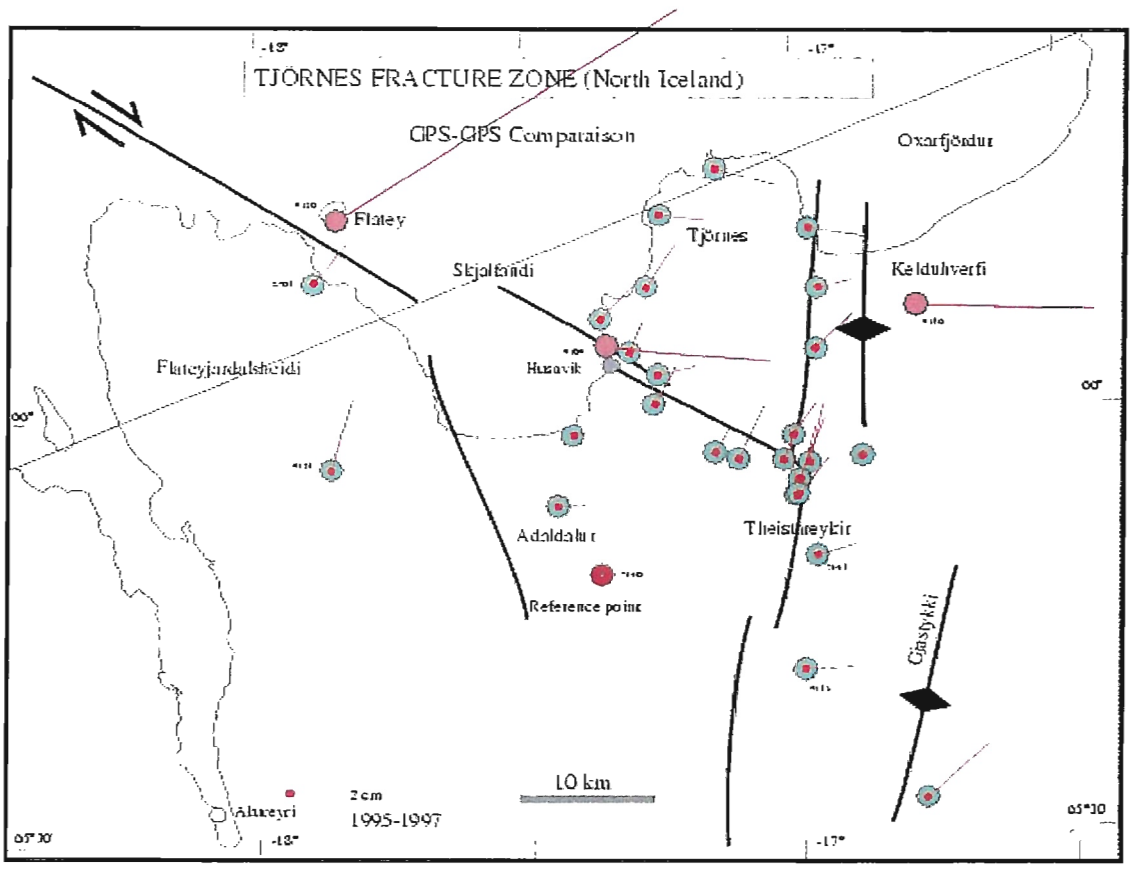

Figure 38. *1995-1997 horizontal displacements on the TGN.*

to the east have been computed for the points located in the fissure swarms. Points on Flateyjardalur move to the north. The point on the Flatey island reveals a large displacement to the NE that could be due to a local instability.

The assumption of an interseismic strain has been tested by using a simple dislocation model. This model assumes that a set of buried planar fault surfaces are locked above a given depth and are affected by uniform aseismic creep below this depth. In order to determine this brittle/ductile transition we used the microseismicity recorded by the SIL network from 1995 to 1997. We assume that most earthquakes are localized in the brittle crust. Thus gives us a limit at a 10 km depth in average. We founded a solution that minimizes the differences between simulated and observed velocities.

The model (Figure 39) assumes: (1) a dyke opening of 20 mm/year affecting all the brittle crust along the Kolbeinsey ridge; (2) two dyke openings of 30 mm/year and 20 mm/year respectively along the Krafla and Þeistareykir fissure swarms; (3) a dextral strike–slip fault striking N100°E between the two previous rift segments with a velocity of 50 mm/year below a depth of 10 km and completely locked above the brittle/ductile transition; (4) a 15 mm/year opening zone striking N140°E south of the HFF; (5) a fault along the Grímsey lineament with both a 15 mm/year opening and 20 mm/year dextral strike–slip movements.

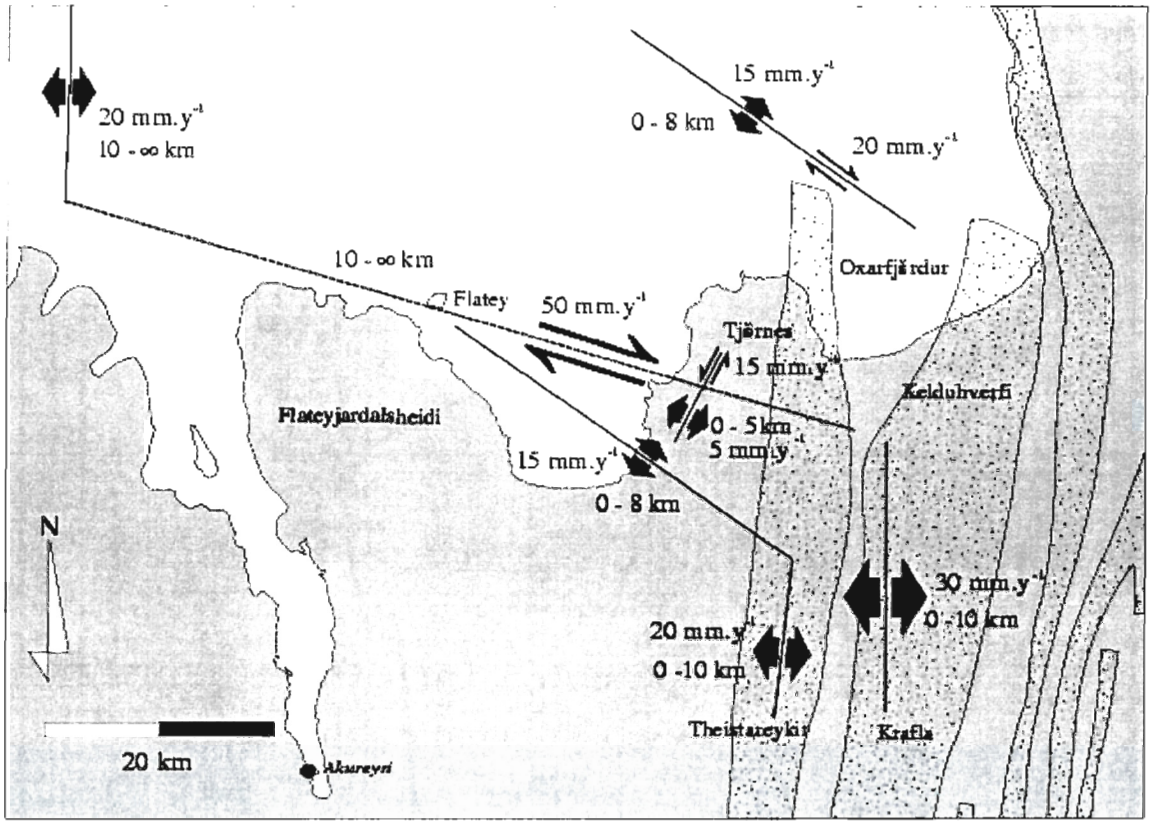

Figure 39. *Dislocations used in the simulation of the 1995-1997 displacement field (after Jouanne et al. 1999). Two main kinds of dislocation can be distinguished: superficial dislocations that affected the upper crust with mainly aseismic opening or strike-slip (Kolbeinsey ridge) and a major dislocation simulating a fault locked at 10 kilometers depth and affected by a constant slip below this limit simulating ductile slip at depth.*

In addition small wavelength tendencies has been adjusted by superficial faults.

This model based on our 1995-1997 TGN comparison revealed extension and strike–slip movements 3 to 4 times larger than the average velocity. The transform motion is locked on a large (150x10 km) fault surface and this represents the main risk for destructive earthquakes in the near future. From a mechanical point of view, the lockage could be due to the increase of normal stress on this surface following the double opening north and south of the fault zone.

1997-1999 velocity field

Comparison with the 1995–1997 velocity field

32 common points have been measured during the 3 campaigns (1995, 1997 and 1999). In comparison with to the first period and using the same reference point located in the southern part of the network, the 1997-1999 velocity field has the following main characteristics:

The eastward tendencies north of Tjörnes are always present but the average velocity

has been divided by 2. We observed less than 1 cm/year of dextral displacement north of Tjörnes. The NNE displacements observed in 1995-1997 on both side of the Húsavík fault are always observed but their component are in the opposite direction of those observed during the first period. These points are now moving to the south also with smaller velocities. Similar conclusions are drawn with the 2 points on Flateyjardalur. The large displacement observed in 1995-1997 for Flatey is no more observed.

From this comparison we can argue that the displacements on Tjörnes have varied significantly in sense and size in less than 2 years. A model compatible with both period is presently being elaborated.

Velocities for the points added to the 1995 network

13 new points have been added to the 1995 network both to the east and to the west to the first study area. All eastern points shows very similar ESE azimuth of displacements. A difference of 1 cm/year has been observed between the points respectively inside and outside the Krafla fissure swarm. This demonstrates the activity of the eastern margin of this swarm. The points added to the west of the network show similar displacements to those located on Flateyjardalur, which mean a general sinistral displacement of the SW area, relatively to a point located in the southern middle part of the network.

3.6.3.2 Task 3.2: 1992-1998 deformation of the Krafla volcano

The Krafla fissure swarm, in the North Iceland rift zone, last underwent rifting between 1975 and 1984. Activity mostly concentrated at the Krafla volcano although it occurred all along the fissure swarm. We formed interferograms of ERS-SAR scenes (Figure 40) covering the area of Krafla with time span values of up to six years (1992–1998). This long period interferograms have been revealed steady rate of deformation at Krafla volcano, N–Iceland. The deformation rate at Krafla and within the fissure swarm, has values reaching +2.1 cm/year in the ground to satellite direction, at the volcano. The area affected by deformation extends 20 km both north and south of the volcano. The best fit dislocation model consists of sills, to the north and south of the volcano, and a magma chamber, located below the volcano, all of them undergoing contraction. The contraction of the magma chamber induced a subsidence that has been constant in rate during all of the studied period (Figure 41).

3.6.4 Task 4: Effects of fluid pressure on faulting

It is well known that seismogenic faulting is normally associated with zones of fluid overpressure (Guðmundsson 1999; Guðmundsson 2000a; Guðmundsson 2000b); in absence of fluids there would be hardly any tectonic earthquakes. The origin and magnitude of the fluid overpressure are, however, uncertain. For example, for the San Andreas fault, there are two models; one assuming the fluids to be of local and shallow origin, the other assuming the fluids to be of deep origin.

In order to throw light on the potential fluid overpressure in a major fault zone, as a part of a general study on the effects of fluid pressure on the probability of fault-slip, field measurements were made of 1717 mineral-filled veins in the damage zone in deeply eroded and

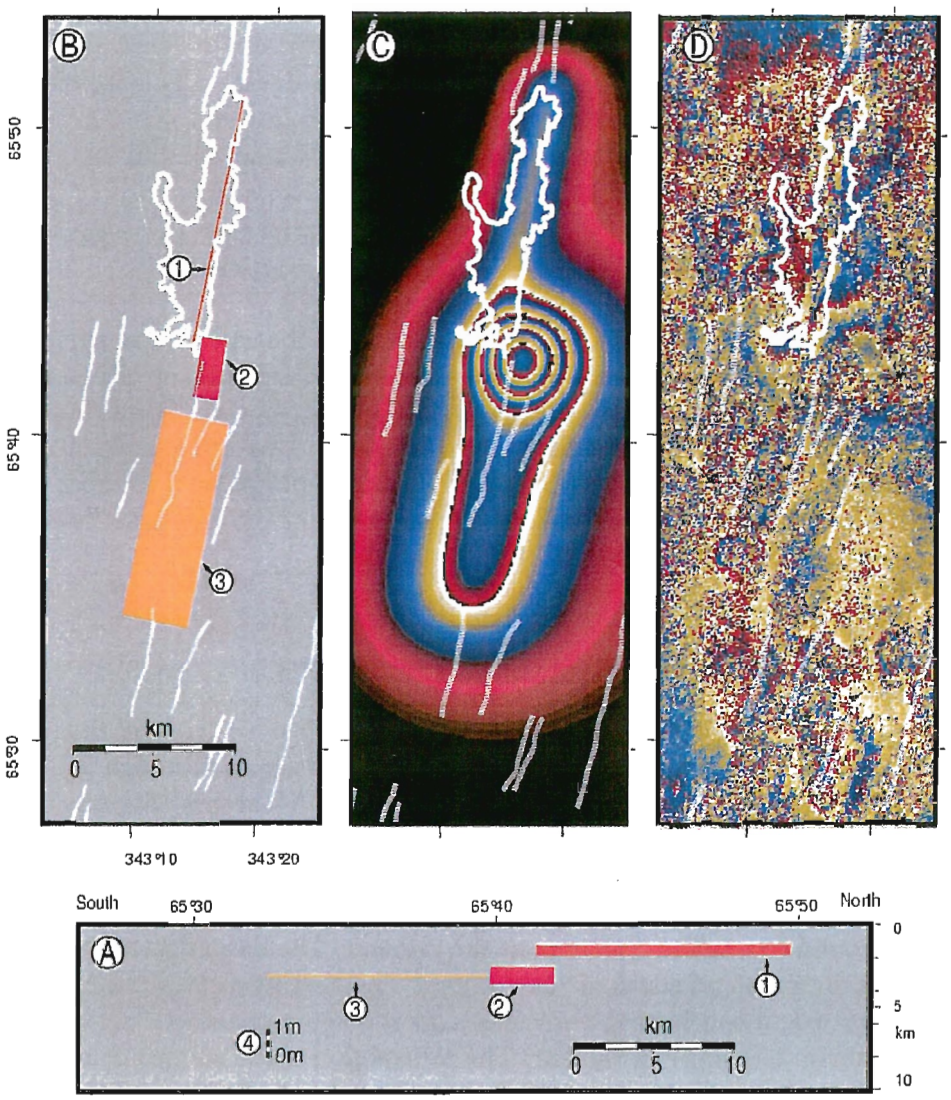

Figure 40. *Model geometry in cross section (A) and plan view (B), best fit model for the 6 year interferogram (C) and residual interferogram, i.e. model minus 6 year interferogram, (D) for the 6 year interferogram (after Henriot et al. 2000). Model elements represented in (A) and (B) are the northern sill (1), the magma chamber (2) and the southern sill (3). The model element dimensions represent their real geometries. The thickness of the lines in the cross-section (A) is proportional to the amount of contraction applied to the discontinuity in the model. The scale for the contraction in the 6 year interferogram model is given in (4).*

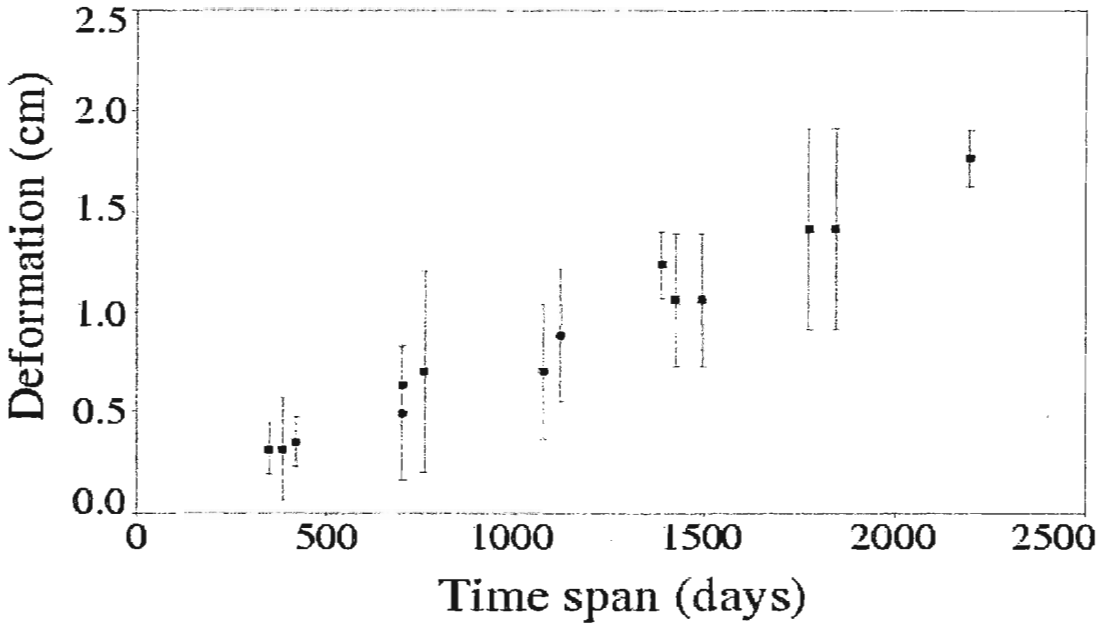

Figure 41. *Deformation at Leirhnjúkur, in the ground to satellite direction, with respect to the time span of the corresponding interferogram (after Henriot et al. 2000). The error is a function of the visual quality (Q) of the interferogram, 0 for no readability, 9 for perfect readability. It has been estimated as 1/Q of a fringe.*

well-exposed parts of the Tjörnes fracture zone, particularly on the Flateyjarskagi peninsula (Guðmundsson 1999; Guðmundsson 2000c; Guðmundsson et al. 2000). Most veins are composed of quartz, chalcedony and zeolites, strike roughly parallel or perpendicular to the fault zone, and are members of dense palaeo–fluid transporting networks. A common vein frequency in these networks is 10 veins per meter. Cross-cutting relationships indicate that 79% of the veins are extension (mode I) cracks; 21% are shear cracks. The apertures of most veins, measured as mineral-fill thicknesses, are from 0.1 mm to 85 mm, and the aperture frequency distribution is a power law. The outcrop trace lengths of 384 veins (of the 1717) could be measured accurately. These 384 veins are mostly small and range in length from 2.5 cm to 400 cm, in aperture from 0.01 cm to 0.9 cm, and have an average length/aperture ratio of about 400. Using simple fracture mechanics models, and the appropriate elastic properties of the host rock, this length/aperture ratio indicates and average fluid overpressure during vein formation of 20 MPa. If this fluid pressure acted on a potential fault plane, the effective normal stress across that plane would be zero or negative and, therefore, reduce the driving shear stress needed to trigger slip on that plane to only 4-6 MPa. This compares well with the most common stress drops, estimated at 3-6 MPa, for earthquakes worldwide.

Another potentially strong effect of fluid pressure on the probability of fault-slip in seismic zones is dyke emplacement in the nearby volcanic zones (Guðmundsson 2000d). In this model, dyke injection (and normal faulting) in the volcanic systems can lock or unlock the Húsavík-Flatey fault and the central parts of the South Iceland seismic zone. Dyke injection in the parts of the North and East volcanic zones between the Húsavík-Flatey fault and the South Iceland seismic zone tends to open (unlock) these zones and trigger seismogenic faulting. By contrast, dyke injection south of the South Iceland seismic zone and north of the Húsavík-Flatey fault tends to lock these faults and suppress their seismogenic faulting. Similarly, dyke injection in the north part of the West volcanic zone tends to lock, but dyke injection in its south part (including the Reykjanes peninsula) to unlock, the South Iceland seismic zone. Locking by dyke injection, however, is always temporary because plate pull gradually relaxes the compressive stresses generated by the dykes.

In terms of this model, the largest historical eruption in Iceland, Laki 1783, may have triggered the largest known earthquake sequence in S-Iceland, that of 1784. Conversely, the Húsavík-Flatey fault has recently experienced locking by dyke injection. There was considerable seismicity associated with the Húsavík-Flatey fault until early 1976. Then dyke injection and normal faulting in the northernmost part of the Krafla volcanic systems generated horizontal compressive stresses encouraging sinistral movement on the otherwise dextral Húsavík-Flatey fault, thereby locking the fault. Renewed seismicity on the Húsavík-Flatey fault, since February 1994, indicates that the Húsavík-Flatey fault is currently being unlocked by normal plate-pull movements which gradually relax the horizontal compressive stresses generated by the 1976 dyke. The unlocking began at the westernmost part of the Húsavík-Flatey fault, at the greatest distance from the 1976 dyke.

3.6.5 Task 5: Numerical models on faults and fault populations

Part of this work has focussed on quantitative field studies and modelling of the linking up of fractures into normal faults (Acocella et al. 2000) and strike-slip faults (Belardinelli et al. 2000). Part of the work, however, has focussed on the general evolution of the seismic

zones, exploring the model of a stress-field homogenization being a necessary condition for the generation of large earthquakes (Guðmundsson and Homberg 1999). The work on the South Iceland seismic zone made in collaboration with Maria Elina Belardinelli and Maurizio Bonafede (Belardinelli et al. 2000) is described in Subproject 7.

Detailed, quantitative field and photogeological studies were made of the interaction and linkage of extension fractures and normal faults (Acocella et al. 2000), a fault type that is common in the South Iceland seismic zone and the Tjörnes fracture zone. 90 zones of interacting fracture segments in Holocene pahoehoe lava flows of the rift zone of Iceland were studied, each zone being located between a pair of extension fractures or a pair of normal faults, with lengths from tens of meters to several kilometers. Of all the zones, only 7% are underlapping, whereas 93% are overlapping and mostly with hook-shaped fracture pairs. The length/width ratios of most overlapping zones are from 2-6, with a mean value of 3.5. In the overlapping zones, most fracture pairs show moderate shear (strike-slip) components which are related to local variations in the extension (opening) directions. Vertical displacements on normal faults decrease as the overstep and length of overlapping zone increase; both, in turn, are proportional to the total lengths of the faults forming the pair. During their evolution, these zones develop from an underlapping stage, through an overlapping stage (the most common configuration) and, finally, to a linkage stage. The geometrical features of overlapping spreading centres at mid-ocean ridges show great similarities to those reported here. These similarities indicate that the architecture and evolution of overlapping zones are scale independent.

It is proposed that on entering crustal parts where the state of stress is unfavourable to any particular type of seismogenic faulting, the fault propagation becomes arrested (Guðmundsson and Homberg 1999). This model is supported by field and numerical studies on the propagation of fractures of various types (Guðmundsson 2000e). It follows that prior to the propagation of an earthquake fracture, the stress conditions in the zone along the whole potential rupture plane must be homogenized. The proposed homogenization of the stress field in a large rock volume as a precursor to large earthquakes implies that by monitoring the state of stress in a seismic zone, its large earthquakes may possibly be forecasted.

3.6.6 Task 6: Analyzing the fracture properties of Icelandic rocks in the laboratory

Our main overall objective has been to determine changes in the strength, deformability and physical properties of rocks subjected to elevated temperatures. In order to achieve this objective, we have designed and constructed an apparatus for the measurement of rock fracture and deformation properties at high temperatures and pressures, and performed a series of experiments to measure these properties.

3.6.6.1 Task 6.1: Apparatus development

We previously reported on the design and manufacture of an environmental cell for the measurement of fracture mechanics parameters under high-temperature/high-pressure conditions (PRENLAB–2 first annual report). We have now extended the range of capabilities of this apparatus so that it can perform four different types of experiment: (1) rock fracture mechan-

ics experiments, (2) confined compression experiments, (3) confined extension experiments, and (4) direct tension experiments. The extended operating conditions are: (i) confining pressure up to 70MPa, (ii) test temperatures up to 500°C with water as the confining/pore fluid, (iii) test temperatures up to 900°C with dry nitrogen as the confining/pore fluid, and (iv) sample diameters from 25 mm to 60 mm. A schematic diagram of the apparatus and its operating modes is given in Figure 42.

3.6.6.2 Task 6.2: Experimental results and discussion

Starting material

The measurements reported here were made on samples of a macroscopically isotropic basalt collected from a roadstone quarry located southeast of Reykjavík, Iceland. Microscopically it has an aphyric texture, comprising euhedral laths of unaltered plagioclase averaging 0.2 mm in length, and anhedral augite microphenocrysts averaging 0.1 mm in diameter, with accessory anhedral oxides up to 0.1 mm in diameter. No free quartz was visible under either optical or SEM microscopy.

Summary of previously reported results

We previously reported results of measurements made at room temperature on samples that have previously been heat-treated to temperatures up to a maximum of 900°C in order to induce thermal crack damage. In a shallow crustal environment where the geothermal gradient is anomalously high, such as in Iceland, thermal stresses may well be large enough to induce such fracturing. Furthermore, where enough fractures propagate and link up to provide an interconnected network, they can provide permeable pathways for fluid flow which can in turn lead to embrittlement and weakening of the rock. The thermal cracking was monitored by measuring the compressional (P) and shear (S) wave velocities through the samples both prior to and following heat-treatment. Both P-wave and S-wave velocities remained essentially constant up to 400°C, with values of about 5.3 km/s and 3.0 km/s respectively. For higher temperatures the velocities decrease rapidly, so that by 800° they decreased to about 3.4 km/s and 2.2 km/s repectively.

We presented results from a series of fracture toughness measurements on heat-treated specimens of Icelandic basalt using the ISRM recommended methodology. Fracture toughness at ambient temperature was 2.71 MPa/m^2, and this remained essentially constant up to 400°C. There was then a very rapid decrease in fracture resistance between 400°C and 600°C, with relatively little change between 600°C and the highest heat-treatment temperature of 900°C. This pattern of behaviour was considered to be entirely consistent with the wave velocity data.

Finally, we presented the results of permeability measurements on heat-treated cores of basalt. The mean permeability of the basalt prior to heat-treatment was 9.4 nanodarcy (9.4 x $10^{-21}m^2$). Similar to the previous results, the permeability remained essentially constant after heat treatment to temperatures up to 300°C, and showed only a slight increase after treatment to 400°C. At higher temperatures, however, the normalized permeability changed dramatically, increasing by an order of magnitude at 700°C and by a factor of 40 by 800°C. We concluded that such a large increase in permeability was unlikely to result merely from the increase in the number or size of thermally-induced cracks, but from crack linkage processes

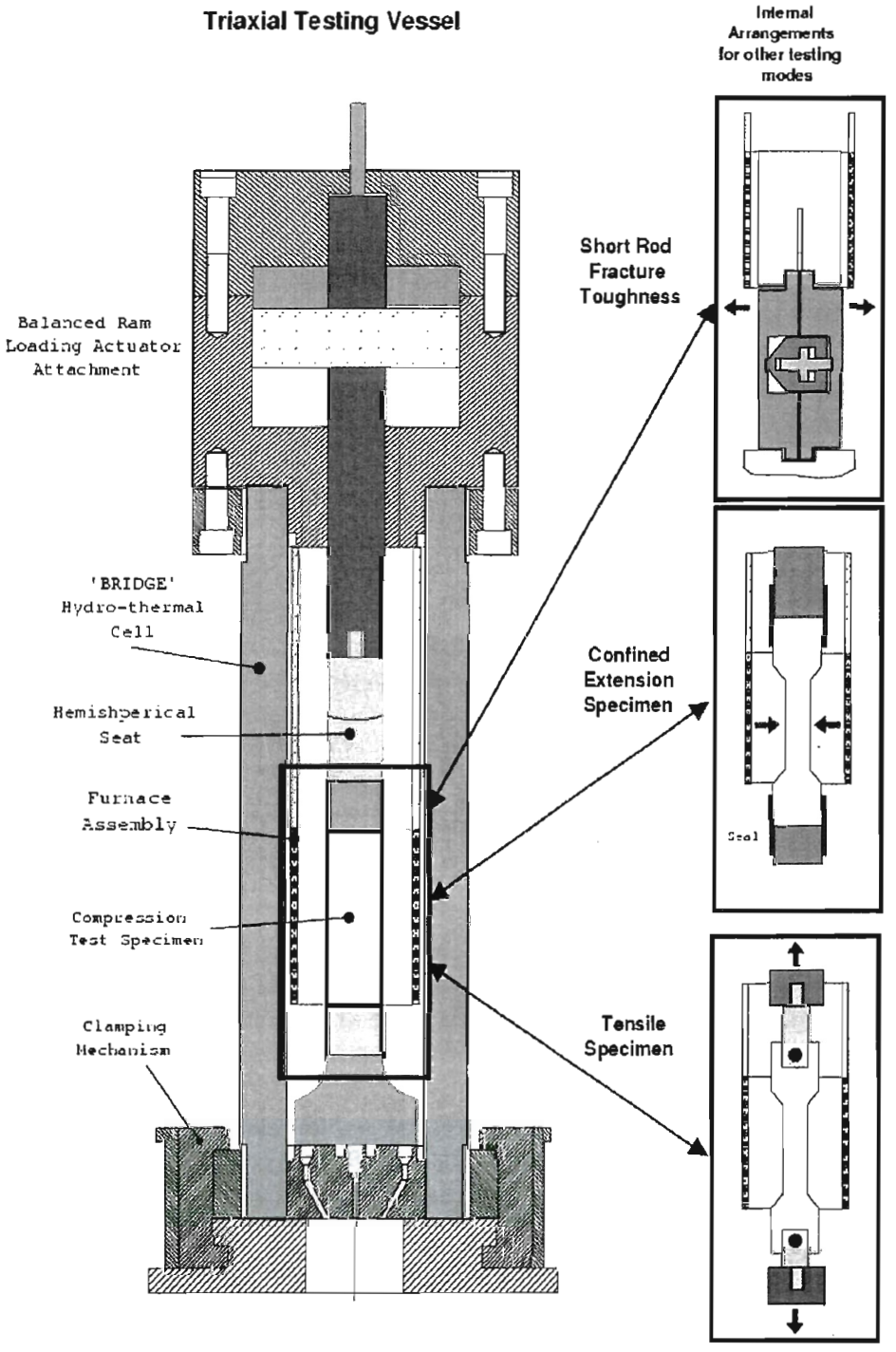

Figure 42. *Schematic diagram of the apparatus and its operating modes.*

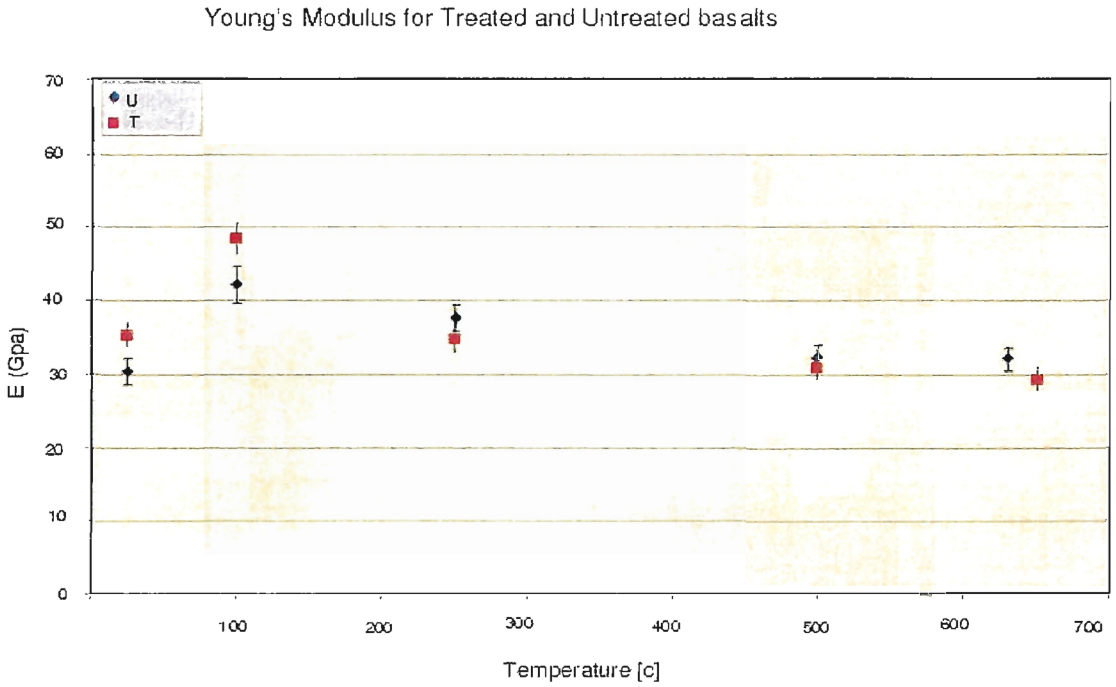

Figure 43. *Results of measurements of Young's modulus of elasticity for both PHT and NHT specimens up to 650° C.*

above some percolation threshold to form extensive sample-spanning permeable pathways for fluid flow.

New experimental results

In our most recent programme, we have performed suites of experiments on both pre-heat treated (PHT) and non-heat-treated (NHT) specimens of basalt. The reason for this is that when a measurement is made at elevated temperature, there are two potential effects on the measurement, which act simultaneously. First, the high temperature can lead to thermal cracking and hence in a change to the microstructure of the material being tested. Second, the temperature can influence the actual deformation mechanism. By performing these two suites of experiments, we hope to be able to discriminate betwen these two effects.

Figure 43 shows the results of measurements of Young's modulus of elasticity for both PHT and NHT specimens up to 650°C (all PHT specimens were pre-heated to 750°C). The two datasets show very similar trends and values, suggesting that the pre–heat treatment has relatively little effect on this parameter. As the temperature is raised from room temperature to 100°C, there is a significant increase in the modulus. This may appear counterintuitive, but is consistent with previously reported data on deformation properties of brittle rocks over this temperature interval (e.g. Meredith and Atkinson 1985). It is considered to be due to thermal expansion leading to microcrack closure and hence higher stiffness and crack resistance. At all higher temperatures, the modulus decreases monotonically with increasing

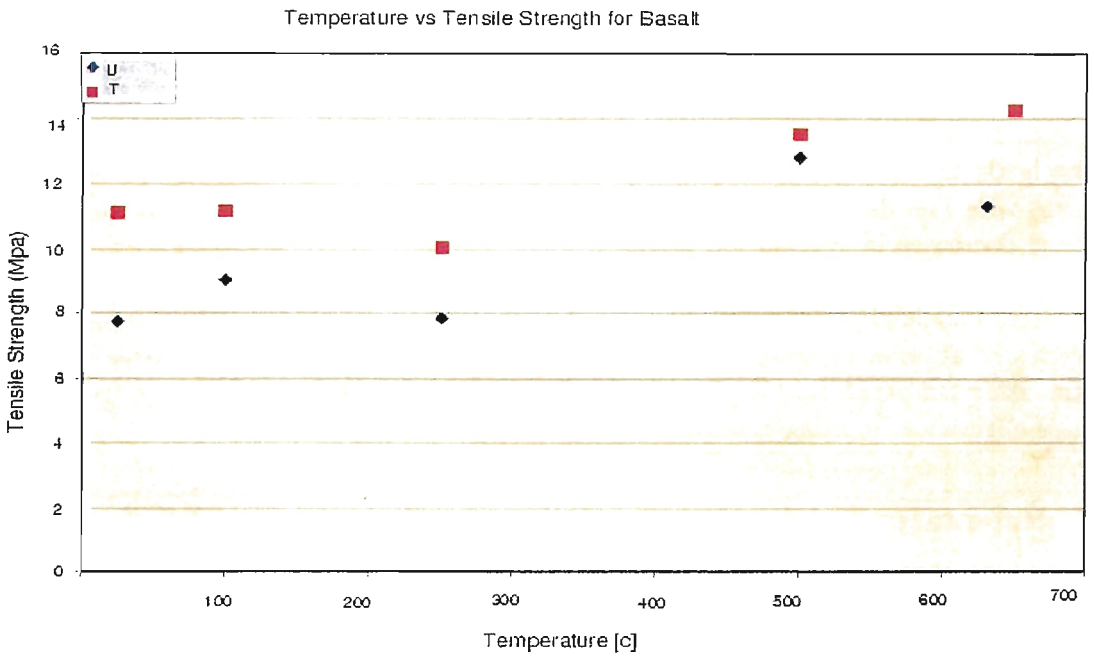

Figure 44. *Results of measurements of tensile strength up to 650°C for both PHT and NHT specimens.*

temperature.

Figure 44 shows the results of measurements of tensile strength up to 650°C, again for both PHT and NHT specimens. Here, the strength values for both datasets at first decreases for temperatures up to 250°C, and then actually increases for temperatures up to 650°C. Furthermore, tensile strength values for the PHT specimens are consistently higher than for the NHT specimens. The reasons for these variations are not fully understood at present, but we consider that it is likely to be due to local microplasticity at crack tips. Microplasticity is generally enhanced by high stresses, and hence is more likely to occur at crack tips than elsewhere in the rock because of the high stress concentrations at these sites. Microplasticity acts to blunt crack tips and therefore make crack propagation more difficult. If this is the case, then we could expect specimens to be less susceptible to tensile crack growth at higher temperatures. Furthermore, we might also expect the PHT specimens to exhibit higher strength because they have previously been subjected to a higher temperature (750°C) and hence potentially to more microplasticity. This explanation is consistent with the observation of little difference in modulus between PHT and NHT specimens. The modulus is controlled by the mere presence of cracks and not by their growth, and hence crack tip blunting is not likely to affect modulus values.

These are very new results, and we will be investigating this possible explanation microstructurally with a combination of scanning electron and optical microscopy.

3.6.7 Conclusions

Due to the high temperature gradient and low lithostatic stress, thermal cracking may be an important process in controlling fracture in Icelandic crust. In the absence of confining stress, such cracking starts in the temperature range 300° to 400°C in fresh basalt. Thermal cracking leads to increased fluid permeability above about 300°C, with the permeability increasing very non-linearly with temperature. Thermal cracking also appears to lead to significant decreases in mechanical strength and resistance to crack propagation of PHT specimens when tested after cooling at room temperature.

However, a somewhat different picture emerges when both PHT and NHT specimens are actually tested at elevated temperatures. There appears to be an increase in tensile strength with increasing temperature. We attribute this to enhanced microplasticity at highly stressed crack tips effectively blunting cracks.

3.6.8 References

Acocella, V., Á. Guðmundsson & R. Funiciello 2000. Interaction and linkage of extension fractures and normal faults: examples from the rift zone of Iceland. *Journal of Structural Geology* 22, 1233–1246.

Angelier, J. 1998. A new direct inversion of earthquake focal mechanisms to reconstruct the stress tensor. In: *Annales Geophysicae.* Abstracts from the XXIII EGS General Assembly, Nice, France, April 20–24, 1998.

Angelier, J., F. Bergerat, H.-T. Chu, Á. Guðmundsson, J.-C. Hu, J.-C. Lee, C. Homberg, H. Kao & S.Th. Rögnvaldsson 2000a. Active faulting, earthquakes and deformation–stress fields: from mid–Atlantic ridge spreading (Iceland) to collision in Southeast Asia (Taiwan). In: B. Þorkelsson & M. Yeroyanni (editors), *Destructive earthquakes: Understanding crustal processes leading to destructive earthquakes.* Proceedings of the second EU–Japan workshop on seismic risk, Reykjavík, Iceland, June 23–27, 1999. European Commission, 48–61.

Angelier, J., F. Bergerat & C. Homberg 2000b. Variable coupling explains complex tectonic regimes near oceanic transform fault: Flateyjarskagi, Iceland. *Terra Nova*, in press.

Belardinelli, M.E., M. Bonafede & Á. Guðmundsson 2000. Secondary earthquake fractures generated by a strike–slip fault in the South Iceland seismic zone. *J. Geophys. Res.* 105, 13613–13629.

Bergerat, F., Á. Guðmundsson, J. Angelier & S.Th. Rögnvaldsson 1998. Seismotectonics of the central part of the South Iceland seismic zone. *Tectonophysics* 298, 319–335.

Bergerat, F., J. Angelier & S. Verrier 1999. Tectonic stress regimes, rift extension and transform motion: the South Iceland seismic zone. *Geodin. Acta* 12(5), 303–319.

Bergerat, F. & J. Angelier 2000. The South Iceland seismic zone: tectonic and seismotectonic analyses revealing the evolution from rifting to transform motion. *Journ. Geodynamics* 29(3–5), 211–231.

Bergerat, F., J. Angelier & C. Homberg 2000. Tectonic analysis of the Húsavík–Flatey fault (northern Iceland) and mechanisms of an oceanic transform zone, the Tjörnes fracture

zone. *Tectonics*, in press.

Bergerat, F., J. Angelier & Á. Guðmundsson. The Leirubakki earthquake rupture: a large fault of the South Iceland seismic zone. In preparation.

DeMets, C., R.G. Gordon, D.F. Argus & S. Stein 1990. Current plate motions. *Geophys. J. Int.* 101, 425–478.

Garcia, S. 1999. *De sismotectonique d'un segment transformant en domaine océanique: la Zone de Fracture de Tjörnes, Islande.* Unpublished master thesis. Universite Pierre & Marie Curie, Paris.

Garcia, S., J. Angelier, F. Bergerat & C. Homberg 2000. Etude sismotectonique d'un segment transformant: la Zone de Fracture de Tjörnes, Islande. 18^{me} RST, Paris, France, April 2000.

Garcia, S., J. Angelier, F. Bergerat & C. Homberg. Tectonic behaviour of an oceanic transform fault zone from fault–slip data and focal mechanisms of earthquakes analyses: the Tjörnes fracture zone, Iceland. In preparation.

Guðmundsson, Á. 1999. Fluid pressure and stress drop in fault zones. *Geophys. Res. Lett.* 25, 115–118.

Guðmundsson, Á. 2000a. Active fault zones and groundwater flow. *Geophys. Res. Lett.*, in press.

Guðmundsson, Á. 2000b. Fluid overpressure and flow in fault zones: field measurements and models. *Tectonophysics*, in press.

Guðmundsson, Á. 2000c. Fracture dimensions, displacements and fluid transport. *Journal of Structural Geology* 22, 1221–1231.

Guðmundsson, Á. 2000d. Dynamics of volcanic systems in Iceland: Example of tectonism and volcanism at juxtaposed hot spot and mid–ocean ridge system. *Annual Review of Earth and Planetary Sciences* 28, 107–140.

Guðmundsson, Á. 2000e. Displacement and stresses of arrested hydrofractures. *Tectonophysics*, in preparation.

Guðmundsson, Á. & C. Homberg 1999. Evolution of stress fields and faulting in seismic zones. *Pure and Applied Geophysics* 154, 257–280.

Guðmundsson, Á., S.S. Berg, K.B. Lyslo & E. Skurtveit 2000. Fracture networks and fluid transport in active fault zones. *Journal of Structural Geology*, in press.

Henriot, O., T. Villemin & F. Jouanne 2000. Long period interferograms reveal 1992–1998 steady rate of deformation at Krafla volcano (North Iceland). *Geophys. Res. Lett.*, in press.

Jouanne, F., T. Villemin, V. Ferber, C. Maveyraud, J. Ammann, O. Henriot & J.-L. Got 1999. Seismic risk at the rift–transform junction in North Iceland. *Geophys. Res. Lett.* 26(24), 3689.

Meredith, P.G. & B.K. Atkinson 1985. Fracture toughness and subcritical crack growth during high-temperature deformation of Westerly granite and Black gabbro. *Phys. Earth & Planet. Ints.* 39, 33–51.

3.7 Subproject 7: Theoretical analysis of faulting and earthquake processes

Contractor:

Maurizio Bonafede
Department of Physics
University of Bologna
Viale Berti-Pichat 8
40127 Bologna
Italy
Tel: +39-051-630-5001/5017
Fax: +39-051-630-5058
E-mail: bonafede@ibogfs.df.unibo.it

Associated contractor:

Frank Roth
Section: Earthquakes and Volcanism
Division: Solid Earth Physics and Disaster Research
GeoForschungsZentrum Potsdam
Telegrafenberg
D–14473 Potsdam
Germany
Tel: +49–331–288–1210
Fax: +49–331–288–1203
E–mail: roth@gfz-potsdam.de

3.7.1 Subpart 7A: Ridge-fault interaction in Iceland employing crack models in heterogeneous media

3.7.1.1 Task 1: Magma upwelling as driving mechanism for the stress build-up in the elastic lithosphere

Tensile cracks are often employed to model magma migration in rift zones or within volcanic edifices, through lateral or feeding dykes. In a crack model, the overpressure of magma Δp with respect to the horizontal stress in the host rock, is assumed to be responsible for dyke opening and propagation. Most crack models of dykes have been developed so far in homogeneous media. The most simple heterogeneous medium has been considered, made up of two welded half-spaces, characterized by different elastic parameters. The analytical solutions available for the elementary dislocation problem in such a medium (Bonafede and Rivalta 1999) have been employed to set up an integral equation with generalized Cauchy kernel, representing the condition for static equilibrium. The unknown in such a problem is the dislocation density distribution, whose singular behaviour has been studied near the crack tips and near the intersection with the interface between the two media. When the crack is in half-space 1 but touches the interface, the order of singularity of the dislocation density distribution at the interface changes from the classical behaviour $\sim r^{-1/2}$ to $\sim r^{-b}$

(where r is the distance from the interface) and the order of infinity b is obtained solving a trascendental compatibility equation; some results are shown in Table 6.

$m = \mu_1/\mu_2$	∞	10	5	2	1	0.5	0.2	10^{-1}
b	0.255	0.312	0.352	0.430	0.500	0.576	0.678	0.752

Table 6. *Crack touching the interface.*

A crack crossing the interface $z = 0$ between the two half-spaces with rigidities μ_1 (in $z > 0$) and μ_2 (in $z < 0$) has been considered in detail. A system of generalized Cauchy equations is obtained, which is solved for the dislocation density distributions of each crack section. An internal singularity in the dislocation density distribution appears at the intersection between the crack plane and the interface. This singularity is again of the type r^{-b} on both sides of the interface and its order b depends only upon the elastic parameters of the media in welded contact and the ratio between the crack lengths in the two half-spaces (see Table 7). More specifically, the order of singularity b does not depend on the stress drop.

$m = \mu_2/\mu_1$	1	0.5	0.1	0.05	0.001
b	0	0.030	0.170	0.208	0.245

Table 7. *Crack crossing the interface.*

The horizontal stress component induced by crack opening is plotted in Figure 45, assuming 5 MPa overpressure within the crack. From a comparison with solutions pertinent to a homogeneous medium, it appears that layering can be responsible of stress changes, localized along the the interface, which may be considerably higher than the overpressure within the dyke. These results provide useful hints for the interpretation of induced seismicity in rift zones and in volcanic areas. The detailed results of this research are reported in Bonafede and Rivalta (1999).

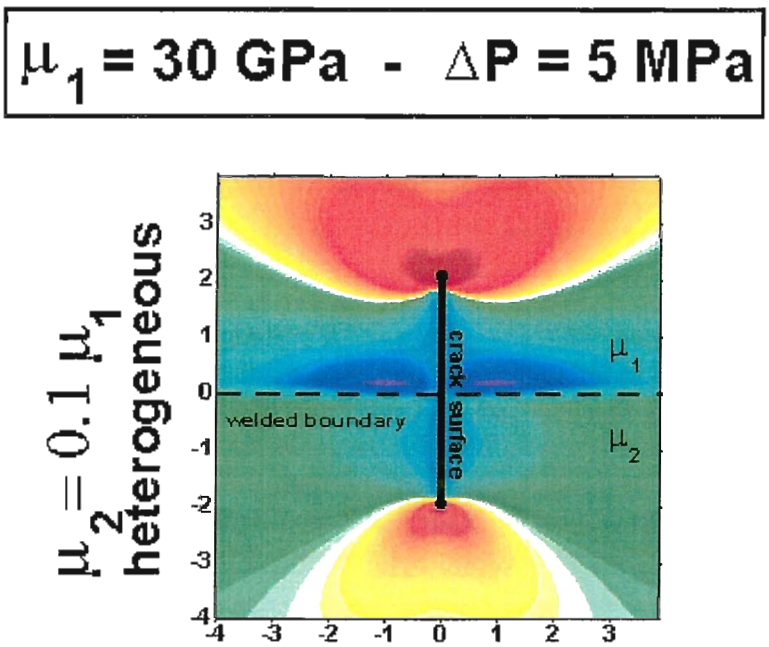

Figure 45. *Horizontal normal stress induced by rifting in proximity of a structural discontinuity (horizontal dashed line). The harder side of the interface is affected by strong compressive stresses. Other stress components (not shown) are also affected by layering, but to a lesser extent. Rifting is modelled as a tensile crack with overpressure* Δp.

3.7.1.2 Task 2: Space-time evolution of the stress field following earthquakes and episodes of magma upwelling

Mechanical effects left by an earthquake on its fault plane, in the post-seismic phase, were investigated employing the "displacement discontinuity method" and imposing the release of a constant, uni-directional shear traction. Due to unsymmetric interaction between the fault plane and the free surface, significant normal stress components are left over the shallow portion of the fault surface after the earthquake (Figure 46): these are compressive for normal faults, tensile for thrust faults, and are typically comparable to the stress drop. In Figure 46 the s-axis is along the strike of the fault, the d-axis is along the dip (positive upwards). Several observations can be explained from the present model: low-dip thrust faults and high-dip normal faults are found to be favoured, according to the Coulomb failure criterion, in repetitive earthquake cycles; the shape of dip-slip faults near the surface is predicted to be upward-concave; the shallow aftershock activity commonly observed in the hanging block of a thrust event is easily explained. The detailed results of this research are reported in Bonafede and Neri (2000).

The study of the effects induced by structural inhomogeneities on the stress and displacement fields around strike-slip faults has been recently completed. An elastic medium is considered, made up of an upper layer bounded by a free surface and welded to a lower

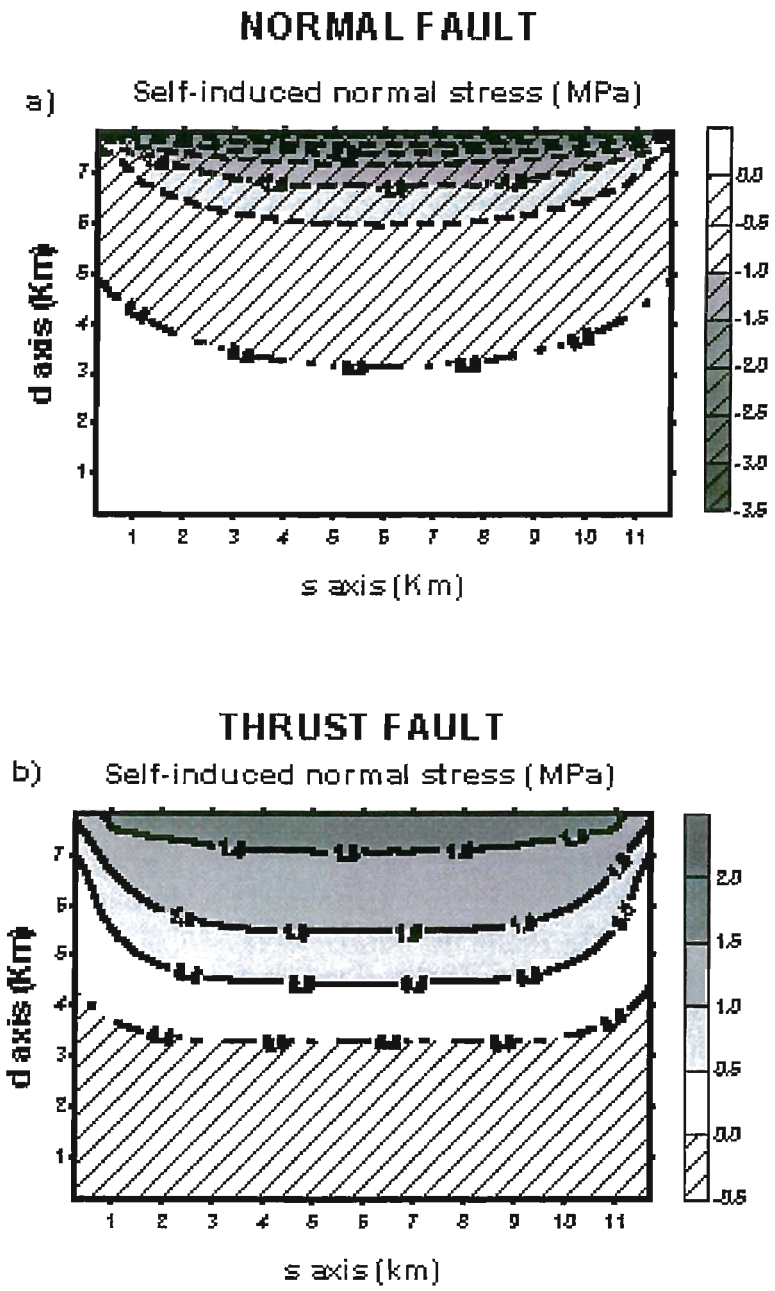

Figure 46. *Normal stress induced by uniform stress drop over a high-dip normal fault and a low-dip thrust fault. The near-surface part of a normal fault is affected by compressive stress, while tensile stresses act there for a thrust fault.*

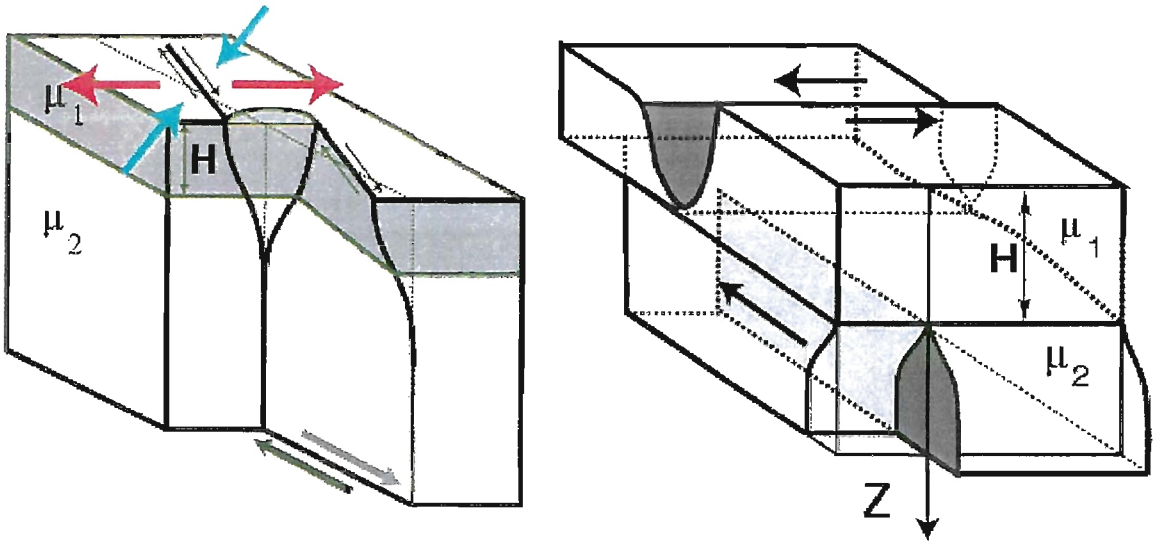

Figure 47. *According to the stress-drop-discontinuity condition, en-echelon fault segments, rotated in the direction of the tensile principal stress axis, must accompany brittle faulting at depth (left). On the contrary, anelastic deformation at depth is preferably accompanied by antithetic faulting in brittle surface layers (right).*

half-space characterized by different elastic parameters. Shear cracks with assigned stress drop are employed as mathematical models of strike-slip faults which are considered as vertical and planar. If the crack is entirely embedded within the lower medium (case A), a Cauchy-kernel integral equation is obtained, which is solved by employing an expansion of the dislocation density in Chebyshev polynomials. If the crack is within the lower medium but it terminates at the interface (case B), a generalized Cauchy singularity appears in the integral kernel. This singularity affects the singular behaviour of the dislocation density at the crack tip touching the interface. Finally, the case of a crack crossing the interface is considered (case C). The crack is split into two interacting sections, each placed in a homogeneous medium and both open at the interface. Two coupled generalized Cauchy equations are obtained and solved for the dislocation density distribution of each crack section. An asymptotic study near the intersection between the crack and the interface shows that the dislocation densities for each crack section are bounded at the interface, where a jump discontinuity appears. As a corollary, the stress drop must be discontinuous at the interface, with a jump proportional to the rigidity contrast between the adjoining media. This finding is shown to have important implications for the development of geometrical complexities within transform fault zones: planar strike-slip faults cutting across layer discontinuities with arbitrary stress drop values are shown to be admissible only if the interface between different layers becomes unwelded during the earthquake. Planar strike-slip faulting may also take place in mature transform zones, where a repetitive earthquake cycle has already developed. Otherwise, the fault cannot be planar: we infer that strike-slip faulting at depth is plausibly accompanied by en-echelon surface breaks (Figure 47) in a shallow sedimentary layer (where the stress drop is lower than prescribed by the discontinuity condition), while

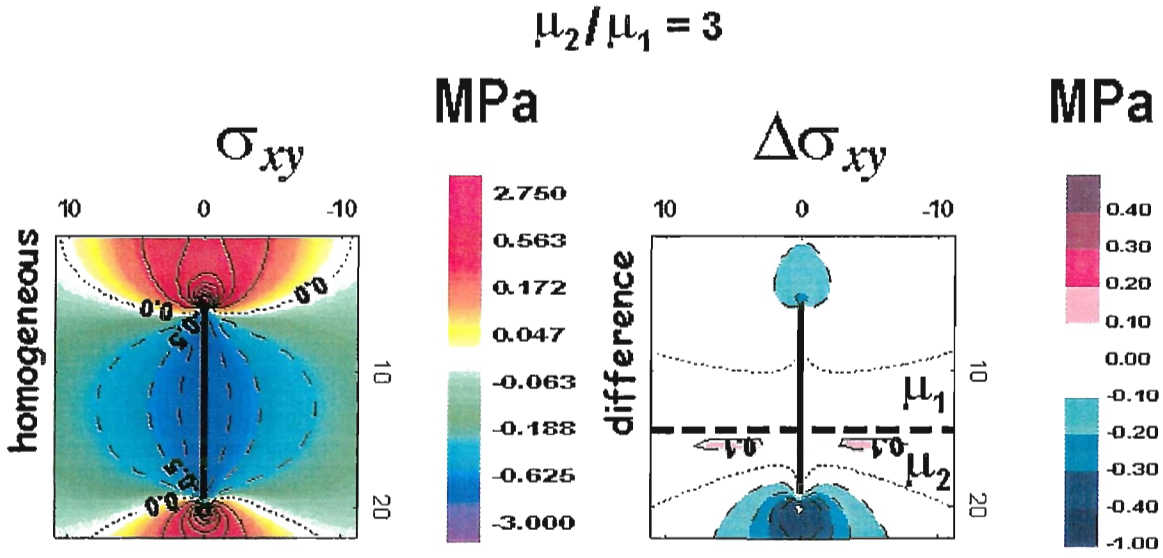

Figure 48. *Stress concentration induced by strike-slip faulting across layer interfaces. The panel on the right shows the incremental stress present in the layered model compared to the homogeneous half-space model (on the right). Accurate re-location of aftershocks in several areas of the world actually show a sharp concentration of events along bedding planes.*

ductile deformation (or steady sliding) at depth is preferably accommodated by antithetic faulting in the upper brittle layer (endowed with lower rigidity but higher stress), giving rise to bookshelf faulting (Figure 47). Results of this research were presented at several international conferences. A paper has been submitted for publication (Bonafede et al. 2000). The South Iceland seismic zone provides several instances of application of both types of complexities.

3.7.1.3 Task 3: Secondary earthquake fractures generated by a strike-slip fault in the South Iceland seismic zone

Most earthquakes in the South Iceland seismic zone occur on N-S trending dextral strike-slip faults. The resulting rupture zones display complex en-echelon patterns of secondary structures including NNE-trending arrays of (mostly) NE-trending open fractures (O.F.) and hillocks.

Three spatial scales characterize the surface faulting pattern: the length of the main fault (M.F. 104 m), the arrays here interpreted as surface evidence of secondary faults (102 m) and the individual O.F. (10 m). In order to improve our understanding of the genetic relationship between the O.F. and the M.F. we computed the stress field induced by slip on a buried M.F. using a dislocation model in a layered half-space: the fault surface is assumed to be embedded in the basement rock, topped by a softer near-surface layer. The O.F. were preliminarily considered as pure mode-I cracks opening in the near surface layer in the direction of the maximum (tensile) principal stress. Alternatively, secondary fractures were interpreted, as

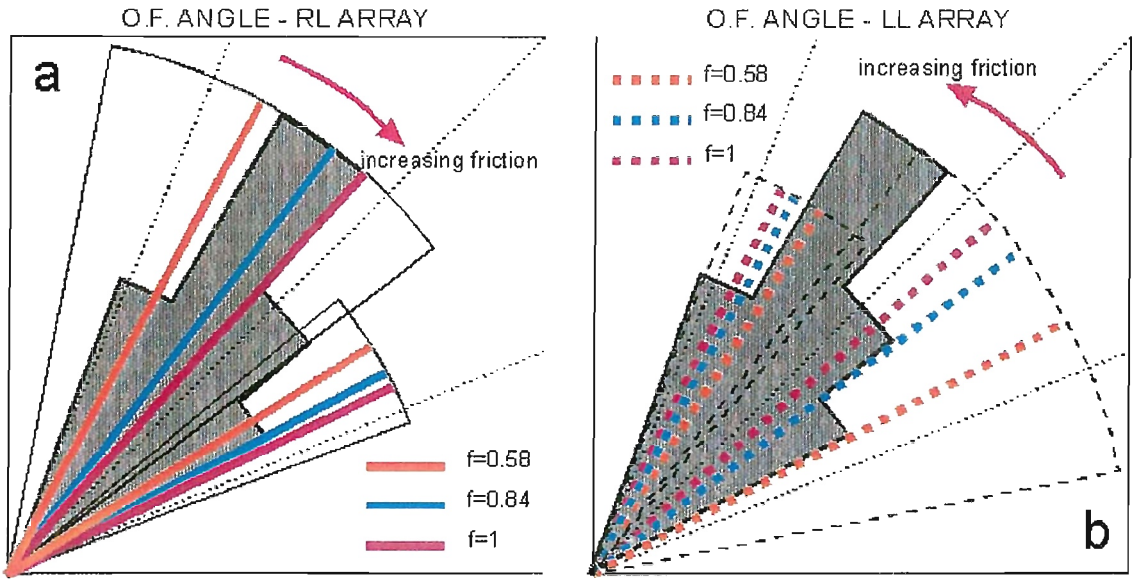

Figure 49. *Open fractures (O.F.) angles predicted from the combined effect of the main fault rupture and secondary fault (S.F.) rupture along the strike direction. The observed range and relative frequency of O.F. angles is shown shaded (from Bjarnason et al. 1993). If the friction coefficient f varies between 0.2 and 1.5 predicted O.F. angles vary within the circular sectors contoured in black. Solid lines in panel (a) represent the angle expected for O.F. belonging to dextral arrays. Dashed lines in panel (b) represents the angle expected for O.F. belonging to sinistral arrays. In both panels, longer lines indicate the predicted mixed-mode O.F. trends, while shorter lines indicate pure tensile trends. Mixed-mode O.F. are assumed to share the same style of faulting (sinistral or dextral) with the array to which they belong. The dotted lines indicate 22.5°, 45° and 67.5° directions (for reference). Coloured lines refer to particular friction values (indicated). Friction increases as indicated by the red arrow.*

mixed-mode cracks, slipping at depth as shear cracks and opening near the surface due to low confining pressure. The Coulomb failure function after the earthquake (obtained summing the M.F. stress change and the lithostatic stress) suggests that secondary faulting (S.F.) can be expected to occur in response to the main rupture below the upper soft layer down to few hundreds of meter depth. The total stress change induced by the M.F. and the S.F. (of smaller scale) is shown to yield quantitative explanations of the complex geometry observed in the fault region in terms of simple frictional laws and friction coefficients very close to those measured in the lab (Figure 48).

3.7.1.4 Meetings and conferences

XXIII EGS General Assembly, Nice, France, April 20-24, 1998.
LXXXIV Congresso Nazionale Societa Italiana di Fisica, Salerno, Italy, September 28 - October 2, 1998.
The third PRENLAB-2 workshop, Strasbourg, France, March 31, 1999.
XXIV EGS General Assembly, The Hague, The Netherlands, April 19-23, 1999.
XXV EGS General Assembly, Nice, France, April 25-29, 2000.
The fifth PRENLAB-2 workshop, Nice, France, April 27, 2000.
International School of Solid Earth Geophysics, Erice, Italy, June 17-23, 2000. 17^{th} course: Fault interaction by stress transfer: new horizons for understanding earthquake occurrence.

3.7.2 Subpart 7B: Modelling of the earthquake related space–time behaviour of the stress field in the fault system of southern Iceland

In the framework of the PRENLAB-2 project a model study which started during the PRENLAB project was continued to obtain forward models of the stress field and stress changes in the South Iceland seismic zone (SISZ).

This proposal has the target to model the space–time development of the stress field using data on strain and stress changes from the other experiments and from databases.

Two models were prepared during PRENLAB-1 and PRENLAB-2:

- a model of the South Iceland seismic zone and the adjacent part of the eastern volcanic zone.
- a scheme comprising the main ridge parts on Iceland and the North Atlantic ridge to the North and to the South of the island, including both the faults and the load due to Katla and Hekla volcanoes.

It was modelled:

- the changes in crustal strain and stress due to earthquakes and aseismic movement in the fault system of the South Iceland seismic zone.
- the interaction of faults.
- the mutual influence between volcanic and earthquake activity, e.g. magmatic upwelling and shearing at fault zones.

3.7.2.1 The model for the earthquake sequence at the SISZ

During PRENLAB-2, this model was further improved. The main features of this model are given again to ease comparison with the new results.

The method

The forward modelling of stress fields is done by applying static dislocation theory to geodetic data and data obtained through the seismic moments from seismograms. It allows to calculate displacements, strain and stresses due to double-couple and extensional sources in layered elastic and inelastic earth structures. Besides the change in displacement during the event, the changes caused by the movement of plates are included (for further details see e.g. Roth 1989).

Usually, for earthquake hazard estimation, the location, the magnitude and the statistically estimated recurrence period of former events is used. To improve this, here the rupture length and width as well as the tectonic setting and the crustal deformation rates are considered while calculating the space time development of the stress field.

The targets

In general, with these models, Subpart 7B aims:

- to achieve a better understanding of the distribution of seismicity in space and time, its clustering and migration in Iceland.

- to provide models for the joint interpretation of the data gathered in the whole research programme, of which this is one part.
- to compare models of stress fields at SISZ to those for stress fields in other regions, e.g. the North Anatolian fault zone.
- to make a contribution to the intermediate-term earthquake prediction in this populated and economically important region of Iceland.

The tectonic setting
The SISZ is situated between two sections of the mid-Atlantic ridge, the Reykjanes ridge (RR) and the eastern volcanic zone (EVZ). Even though the angle between the SISZ and the neighbouring ridges is far from 90°, it is considered as a transform fault. Following the transform fault hypothesis, left-lateral shear stress is expected along the E-W striking zone. This is equivalent to right-lateral shear stress on N-S oriented rupture planes. In fact, earthquakes seem to occur on N-S trending en-echelon faults (cf. Einarsson et al. 1981; Hackman et al. 1990), They are located side by side between the Hengill-Ölfus triple junction, where the RR meets the low activity western volcanic zone (WVZ) and Hekla volcano, in the EVZ (cf. Einarsson et al. 1981) (Figure 50). As we further know from Subprojects 4 and 5, the orientation of the larger horizontal principal stress is NE–SW, i.e. fits to an active N-S or E-W trending fault, which is (at least for the period of those investigations) not a weak fault like the San Andreas fault (cf. Zoback et al. 1987). Moreover, the stress orientation seems to have been constant since Pliocene time.

In detail, the questions to be solved are:

- Do these events, placed on parallel faults, release all the energy stored in the 3-D volume of the SISZ?
- Do the earthquakes always take place in areas of high stress?
- What is the critical stress level? How large is its variability?
- Where are the highest stresses nowadays?

The area investigated extends from 18° to 24°W and from 63° to 65°N. The origin is set to 24°W, 64°N (cf. Figure 51) it includes the SISZ, ±1° north and south of 64°N, the SW edge of the EVZ, and the northeasternmost part of the RR.

The initial stress field
The initial stress field is determined as follows: A tensional stress acting N103°E (nearly parallel to the SISZ; cf. DeMets et al. 1990) is assumed, due to the opening of the mid-Atlantic ridge in the region adjacent to the transform fault. While this rifting induces mainly shear stresses in the SISZ with a small opening component, the rift segments (RR and EVZ) are modelled with tensional stress and a small shear stress contribution. Tensional stresses at both ridges are modelled as constantly being released to end up with zero values at the rifts. This induces additional stress in the transform zone. The stress magnitude, which is unknown, is set to a value that produces left-lateral shear stresses in E-W direction as

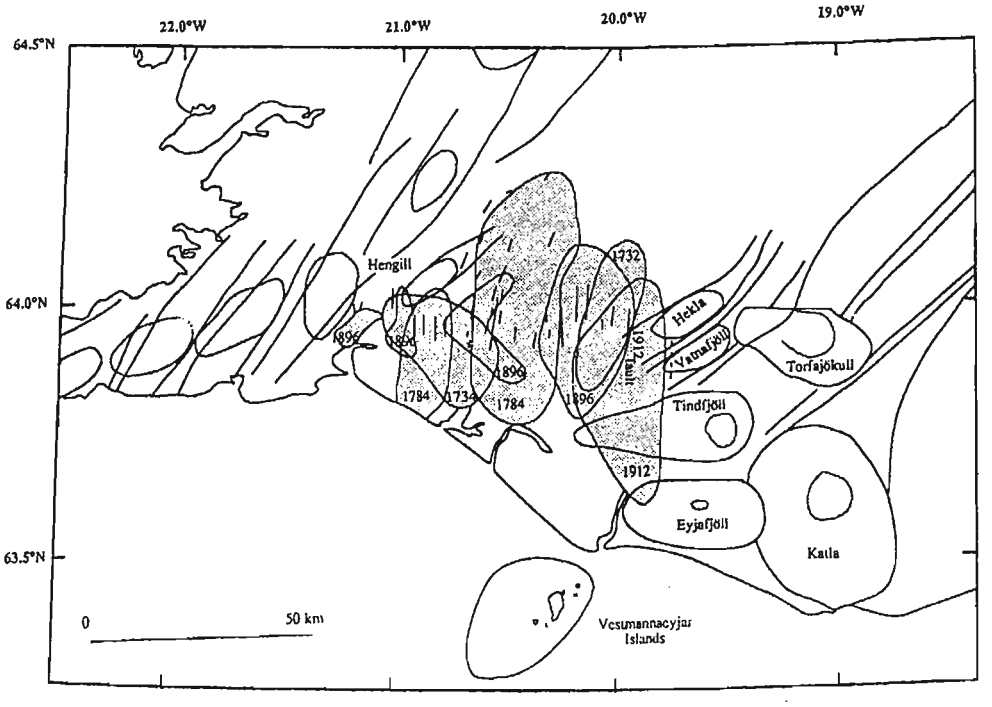

Figure 50. *The South Iceland seismic zone showing mapped surface breaks and regions in which over half of the buildings were destroyed in historic seismic events (after Einarsson et al. 1981). The north-south dashed line near Vatnafjöll indicates the estimated location of the fault on which the May 25, 1987, earthquake occurred (after Bjarnason and Einarsson 1991). The structural features and the coastline are after Einarsson and Sæmundsson (1987).*

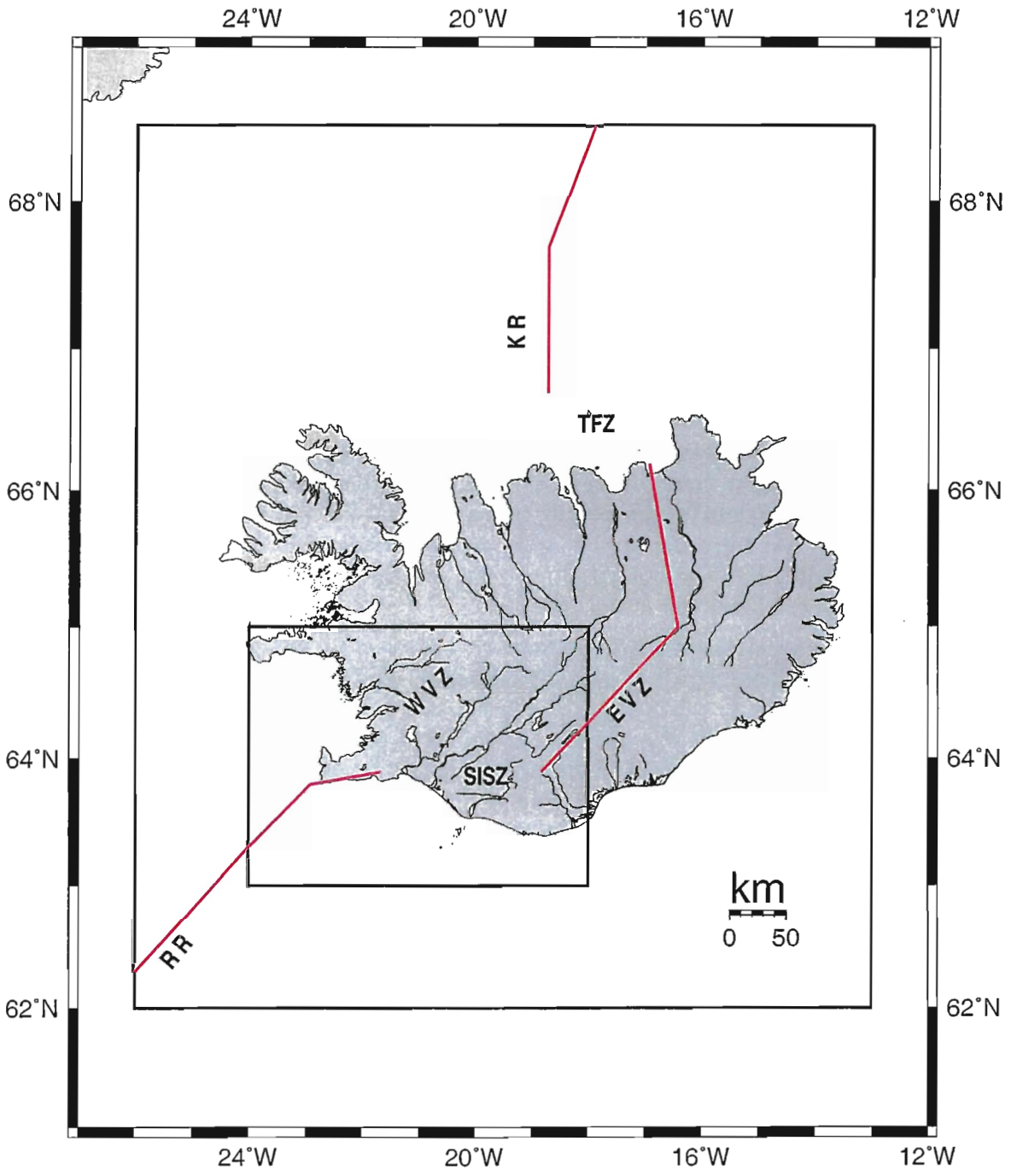

Figure 51. *Map of Iceland and surrounding area. Thick red lines indicate mid-Atlantic ridge segments, as used in the models. The smaller box shows the region of the model on the SISZ. The SISZ extends approximately between 21.4° W, 63.95° N to 18.8° W, 64° N. The large box gives the region for the Iceland rift model. RR: Reykjanes ridge, KR: Kolbeinsey ridge, WVZ/EVZ: western/eastern volcanic zone, SISZ: South Iceland seismic zone, TFZ: Tjörnes fracture zone.*

large as the stress drop determined for the largest event (M=7.1) in the studied earthquake sequence.

On this initial field, the stress changes due to earthquakes are iteratively superposed as well as the stress changes due to further spreading at the ridge segments. From global geodetic measurements an opening of 2 cm/year is found, e.g. in DeMets et al. (1990). This was used as a zero-th order approach but was reduced to only 1 cm/year, as discussed later. Further, as the simplest assumption, lacking other data, the spreading rate is taken to be constant during the modelled time period, even though this can be questioned as for instance the present debate on the stress increase in the New Madrid seismic zone shows (cf. Schweig and Gomberg 1999; Newman and Stein 1999) The stress field before every event is thus the sum of the initial field, the stress drop of all preceding events, and the plate tectonic stress build-up since the starting time of the model, which is set to 1706, when the first event in the series occurred.

Results were calculated for 280x220 test-points covering 280 km in E-W direction and 220 km in N-S direction. Stresses were computed for a homogeneous half-space, as a starting model. Although surface stress changes are calculated, these should be representative for crustal stresses using values for the moduli, that are typical for oceanic crust (see Dziewonski et al. 1975) and not for sedimentary layers at the surface. Moreover, as the faults are introduced vertically into the unlayered environment, the stresses do not vary much with depth, besides at the lower end of the fault.

Changes and improvements in PRENLAB-2

In the first phase of PRENLAB-2, the models developed in PRENLAB-1 were improved:

A The test-point density was increased from 56x44 (5 km distance) to 280x220 (1 km distance) to get more details of the stress field and to reduce interpolation errors.

B At the western end of the SISZ, segments with aseismic oblique slip (mainly normal faulting with a smaller component of left-lateral strike-slip) were introduced, to better fit the Reykjanes ridge (RR) between the southwest tip of the Reykjanes peninsula to Hengill-Ölfus triple junction (Figure 51).

C At the eastern and western tips of the SISZ two areas with steady stress release were introduced (see dashed lines in Figure 52). This could occur by a high rate of small events and maybe by creep. This is likely as these areas did never show strong events ($M \geq 6$) in the seismic history of Iceland, with the exception of possible events in 1546 and 1632 at the western end (about 21.3°W) and one event in 1311 (about 18.9°W) (cf. Halldórsson 1991). See under Task 2 for a discussion of this.

D To investigate the model resolution a set of different models is produced: Besides the main model, several extreme cases are assumed and the variation of the main results under these assumptions is observed.

E The stress field was extrapolated to 1999 and was now updated to the situation after the June 21, 2000, event.

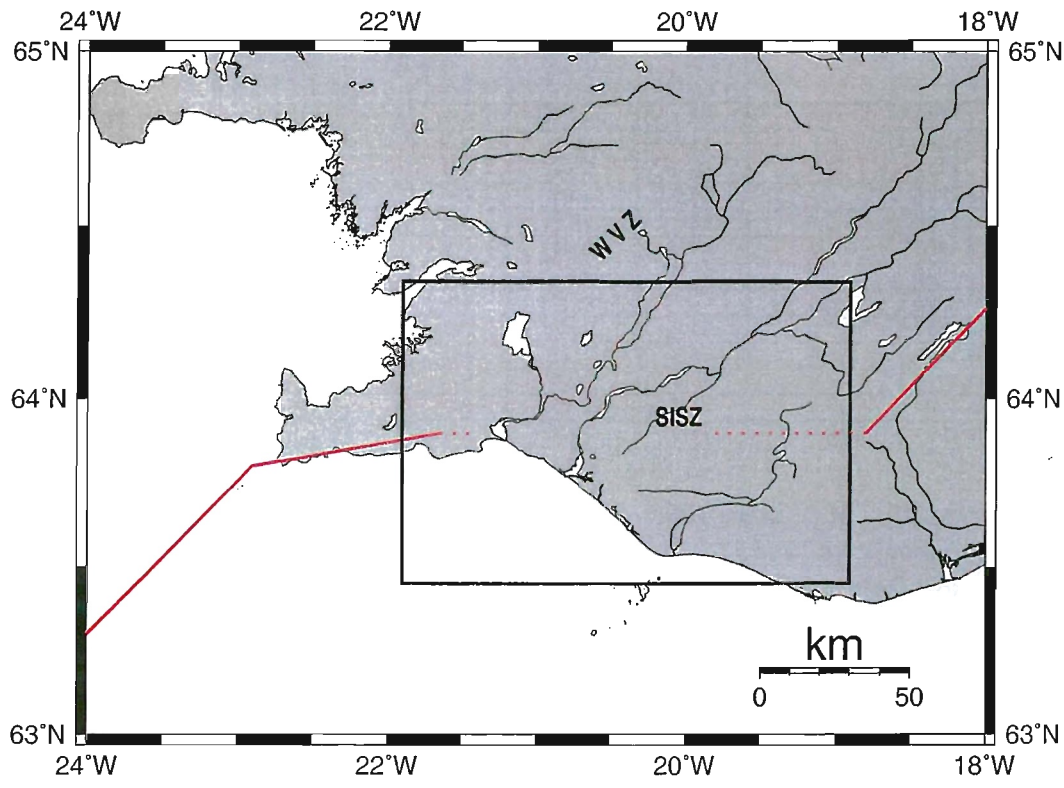

Figure 52. *The box gives the area in SW-Iceland used in the modelling as indicated with the small box in Figure 51.*

The earthquake data

All events with M $\geq$ 6 since 1706 were used (listed in Table 8., following Halldórsson et al. 1984; after Hackman et al. 1990; Stefánsson and Halldórsson 1988; and Stefánsson et al. 1993). The catalogue is supposed to be complete from 1706 for these earthquakes.

All ruptures were set to be oriented N-S, according to the isolines of damage intensity and surface ruptures shown in Figure 50. As only the events in 1912 and 2000 were instrumentally recorded, the source parameters are not very accurate – a problem to be discussed further below. The position of the epicenters and the rupture planes used in the models are given in Figure 53 and Figure 54, respectively.

Date[1]	Magnitude[1]	Epicenter[1]		South end of rupture[2]		Co-seismic slip[3]	Rupture length[4]
		Lat. °N	Long. °W	x [km]	y [km]	U_0 [m]	L [km]
1706	6.0	64.0	21.2	131	-5	0.30	10
1732	6.7	64.0	20.1	183	-11	0.77	22
1734	6.8	63.9	20.8	150	-23	0.96	25
14.08.1784	7.1	64.0	20.5	164	-18	1.9	35
16.08.1784	6.7	63.9	20.9	145	-22	0.77	22
26.08.1896	6.9	64.0	20.2	178	-14	1.2	28
27.08.1896	6.7	64.0	20.1	183	-11	0.77	22
05.09.1896	6.0	63.9	21.0	140	-16	0.30	10
05.09.1896	6.5	64.0	20.6	159	-9	0.48	18
06.09.1896	6.0	63.9	21.2	131	-16	0.30	10
06.05.1912	7.0	63.9	20.0	187	-27	1.5	32
17.06.2000	6.5	64.0	20.4	169	-12	0.9	16
21.06.2000	6.4	64.0	20.7	154	-13	1.1	18

Table 8. *Earthquakes M$\geq$6 since 1706 in the South Iceland seismic zone. 1) Data taken from Stefánsson et al. (1993); for the events in 1706, 1732, and 1734 no exact date is known. Data on the events of June 2000 are from Stefánsson, Guðmundsson and Halldórsson (pers. comm.), with magnitudes as moment magnitudes. 2) Position in the model coordinate system with origin at 64° N, 24° W. 3) Calculated via the magnitude moment relationship log M_0 [dyne cm] = 1.5M_S+(11.8 - log(σ_a/μ)) with the apparent stress σ_a = 1.5 MPa and the shear modulus μ = 39 GPa (after Kanamori and Anderson 1975), followed by using the values of μ above, the rupture length as given in the table as well as a vertical fault width of 14 km east of 21° W and 7 km between 21° W and 21.2° W. Finally, the values for all events before those in 2000 were reduced by a factor of 2, following the discussion of Hackman et al. (1990). All this does not apply to the June 17 and 21, 2000, earthquakes, for which good instrumental data are available, and e.g. a maximum rupture depth of 9 and 7 km were given, respectively. 4) Besides for the June 2000 events, calculated using log L [km] = 0.5 M - 2 (after Qian 1986) which results in slightly lower values compared to e.g. Schick (1968).*

The results

The stress fields at 20 dates were calculated: the pre- and post-seismic situation for all 13 events. The time before 6 events was too short to accumulate appreciable plate tectonic stresses since the preceding event. In these cases, the post-seismic stress field of the preceding

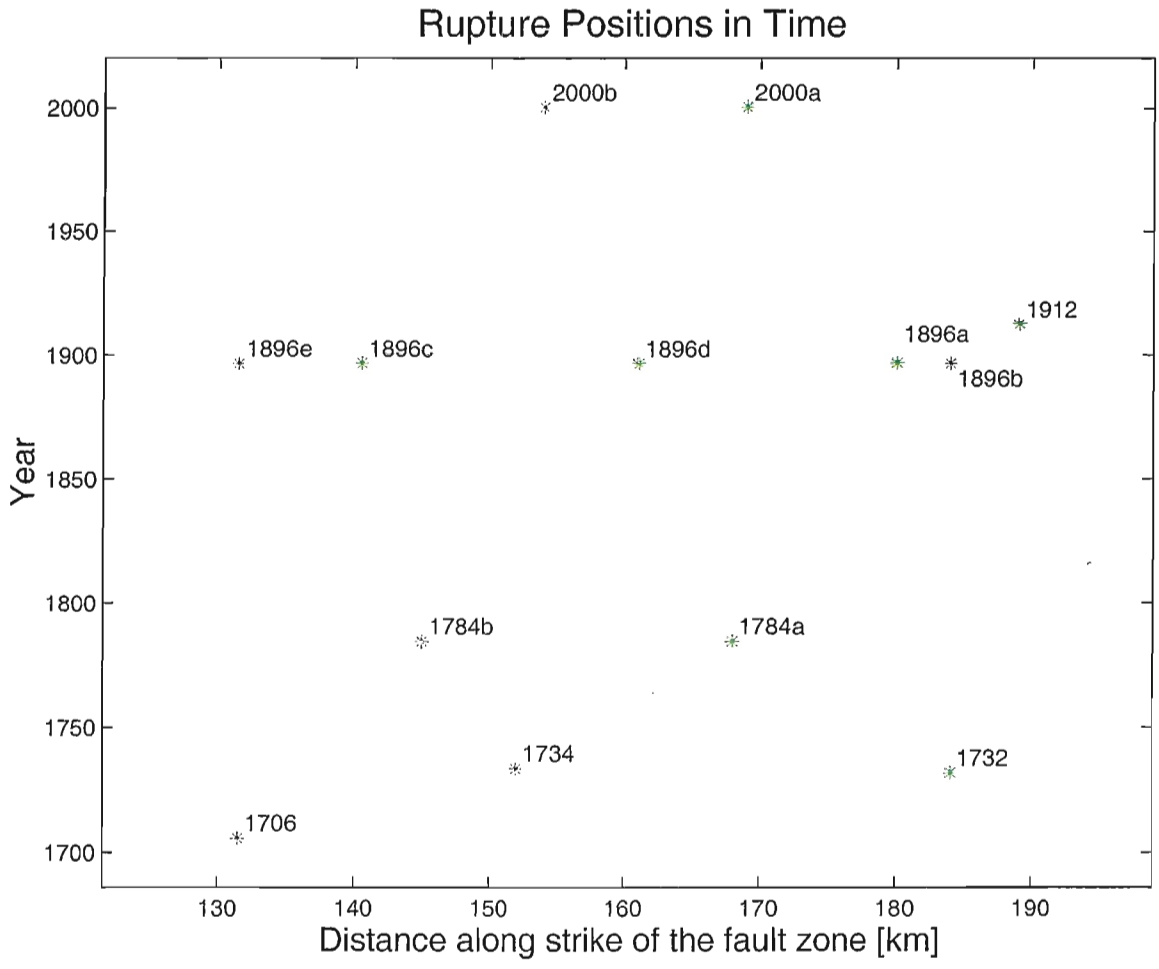

Figure 53. *Location of the earthquakes in space and time (cf. Table 8). As the events have been located on N-S trending faults in an E-W trending fault zone, their location is very accurately displayed in this graph.*

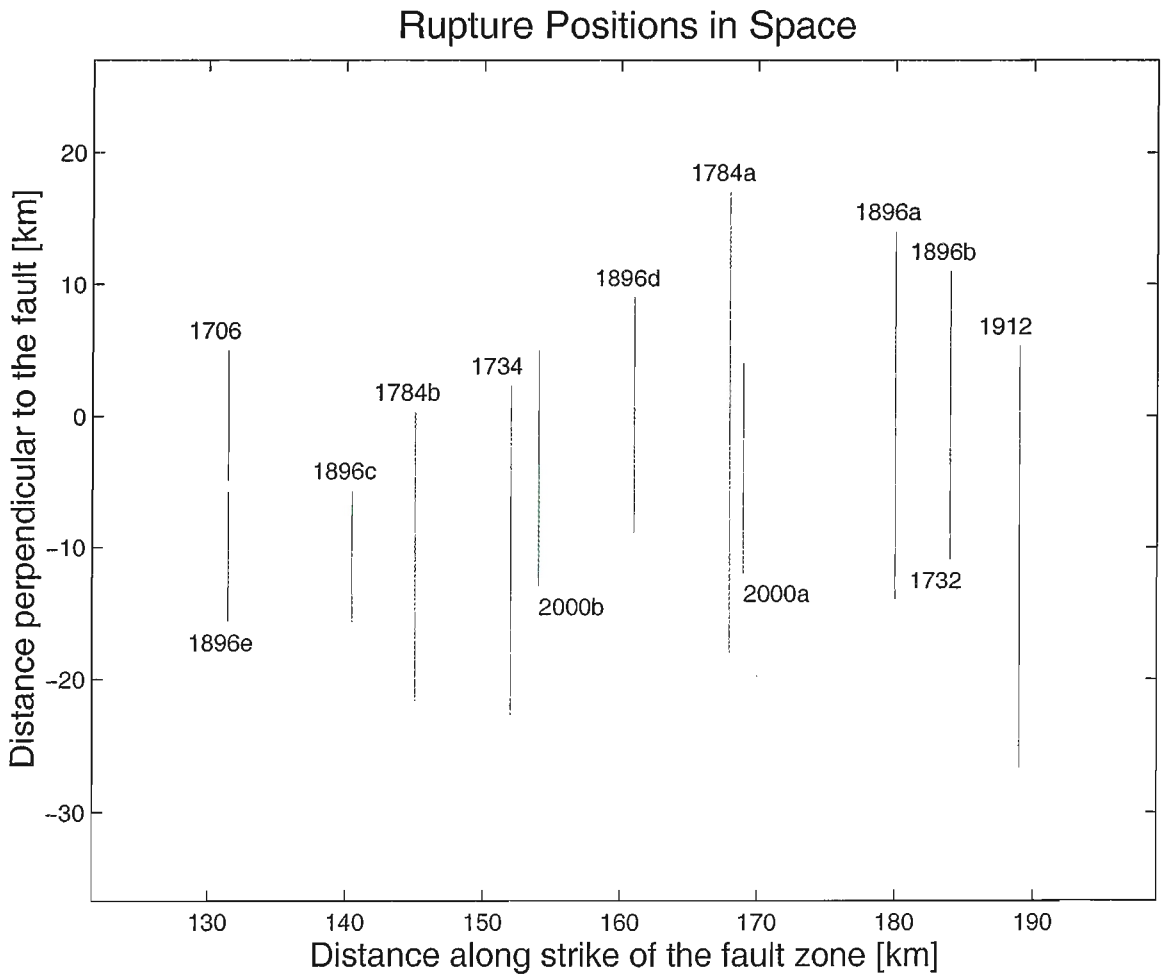

Figure 54. *The position of the rupture planes of the earthquake sequence as used in the models (cf. Table 8).*

event was set equal to the pre-seismic stress field of these earthquakes.

Originally, an extrapolation was done from the 1912 earthquake to spring 1999. After the two earthquakes happened this June, it was updated to June 17, 2000 (Figure 56) and the effect of both events were determined (see Figure 57 and Figure 58).

As a simple assumption, one might expect, that earthquakes in a certain fault zone usually occur at about the same critical shear stress level. We examine here if such an expectation matches the known facts about the earthquakes, given above, and the stress field in the SISZ from knowledge about plate motion and the modelling here. Figure 59 summarizes the mean shear stress level before each of the earthquakes at the area of the impending event. The stress level is near the average (1.8 MPa) or higher for most of the events. The highest value (for 1896e) is mainly influenced by the fact that the rupture area for the event in 1706 was located completely north of that in 1896 (cf. Figure 54). The second 1784 earthquake (two days after the first, 0.4 in magnitude smaller, 19 km away) might have been an aftershock and therefore situated in a lower stress area (1.6 MPa). The same might apply to the second of the 1896 events. The forth event in 1896 and the first shock in 2000 are both influenced by the largest event in the series, i.e. the first one in 1784. Thus, the accuracy of the source parameter of this 1784 earthquake strongly influences the whole model. Concerning the first event in June 2000, it has to be noted that it took place in a very inhomogeneous stress field, i.e. there are low stresses in the north of the rupture plane and high ones in the south (see Figure 56). Calculating an average pre-seismic stress level might be especially misleading for this event, when all the test-points around the rupture plane are considered equally.

Checking the performance of the model in a qualitative way, we examined if the earthquakes hit the high stress area and how large the high stress areas with no event were at the same time (the range in longitude with high stresses was summed when the N-S extension of the area was at least 5 km and the longitude range for the event that occurred was subtracted, usually 0.1 to 0.2 degrees in longitude). The results can be found in Table 9 and are quite satisfying with respect to the named question. Almost all events hit high stress areas and the size of high stress areas with no event was rather small after the earthquakes in the eighteenth century. Nevertheless, the problem remains, why some events did not occur earlier (at lower stress), just passing the "limit in pre-seismic stress" (i.e. here: the average pre-seismic stress).

As stated earlier, the plate velocity used in the model was set to 1 cm/year, only half of that what is measured. The reason can be seen in Figure 59 in comparison with Figure 60. The higher plate velocity leads to a steady and strong increase in the pre-seismic stress level, which is very unlikely, while the reduced rate entails an almost constant level. As the model cannot change the geodetic results, the reason for the discrepancy might be that only 50% of the stress build-up by plate tectonics is released seismically. For the rest, stable sliding or aseismic creep could be responsible.

Two problems were addressed next: (i) To see how sensitive the results depend on the model parameters, it was begun to check extreme cases and their outcome. (ii) The average stress level before some events is considerably lower than for others (cf. the discussion on Figure 59). This is, among other reasons, due to the fact that the rupture planes, used until now, extend rather far to the north and south of the SISZ. The damage areas from historical records are not gathered by scientists and are usually biased by uneven population density.

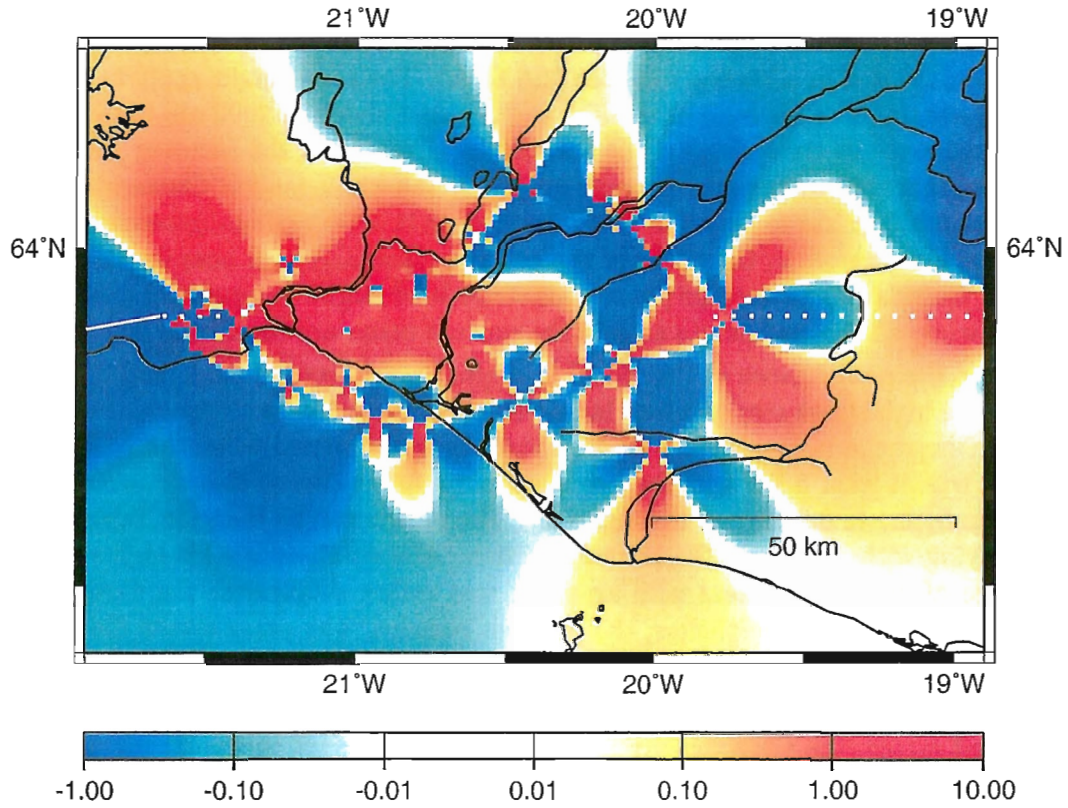

Figure 55. *The stress field after the May 6, 1912 earthquake.*

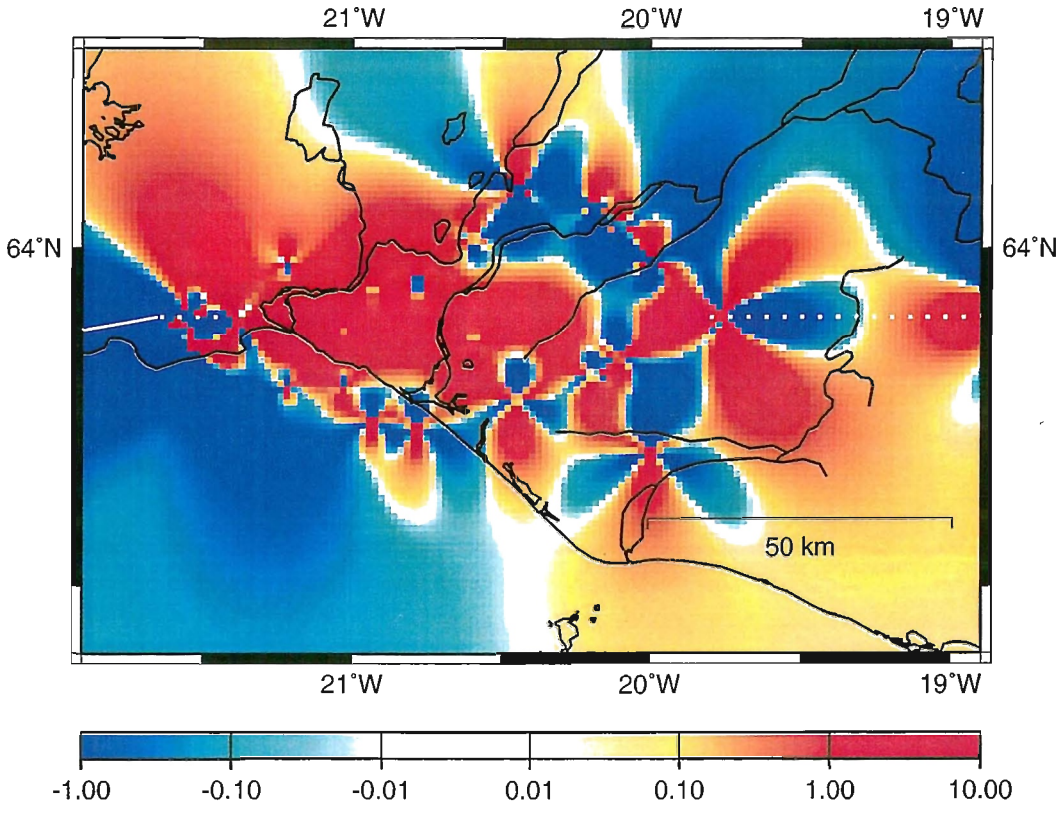

Figure 56. *The stress field before the June 17, 2000, M=6.5 earthquake occurring at 20.4° W, 64.0° N, i.e. (169, -12 — +4).*

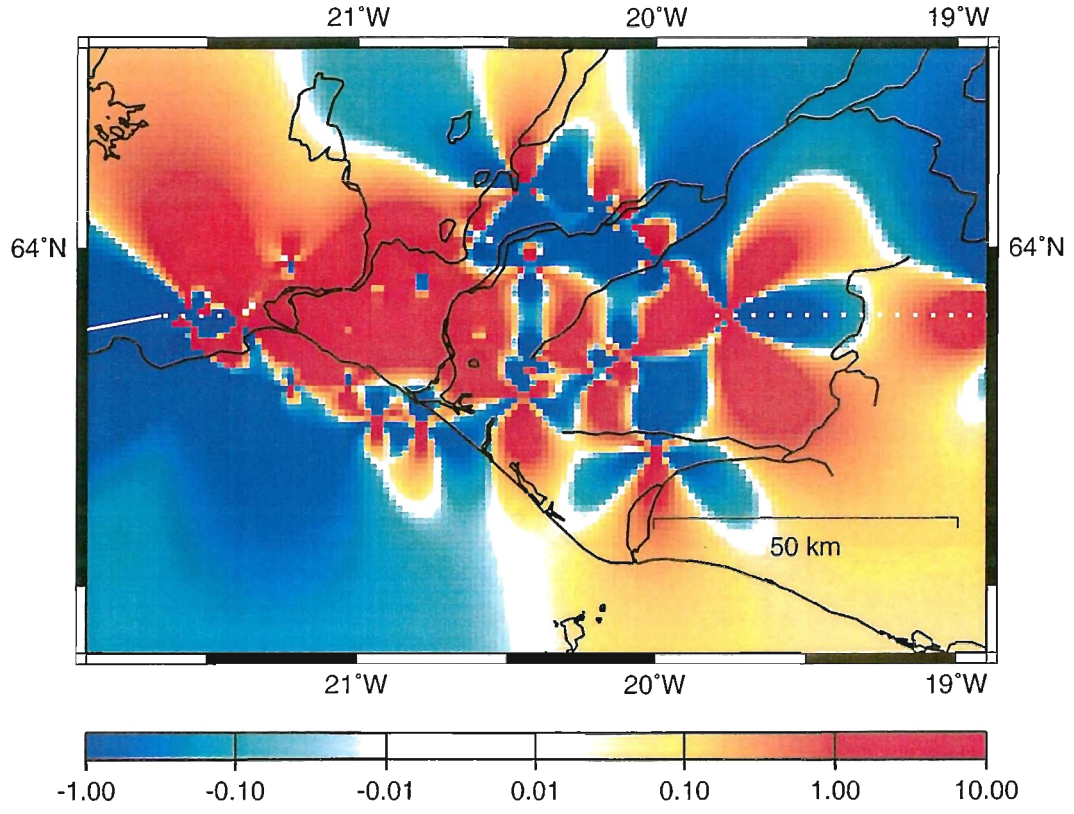

Figure 57. *The stress field after the June 17, 2000, M=6.5 earthquake occurring at 20.4° W, 64.0° N), i.e. (169, -12 — +4).*

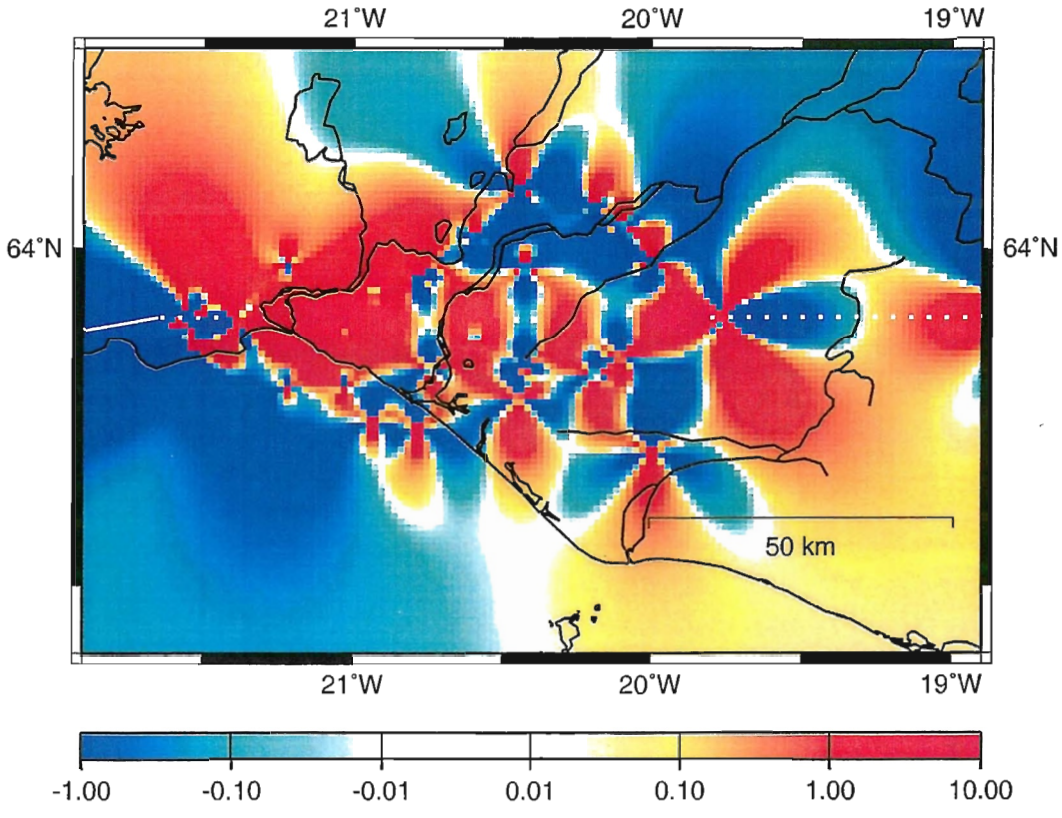

Figure 58. *The stress field after the June 21, 2000, M=6.4 earthquake occurring at 20.7° W, 64.0° N, i.e. (154, -13 — +5).*

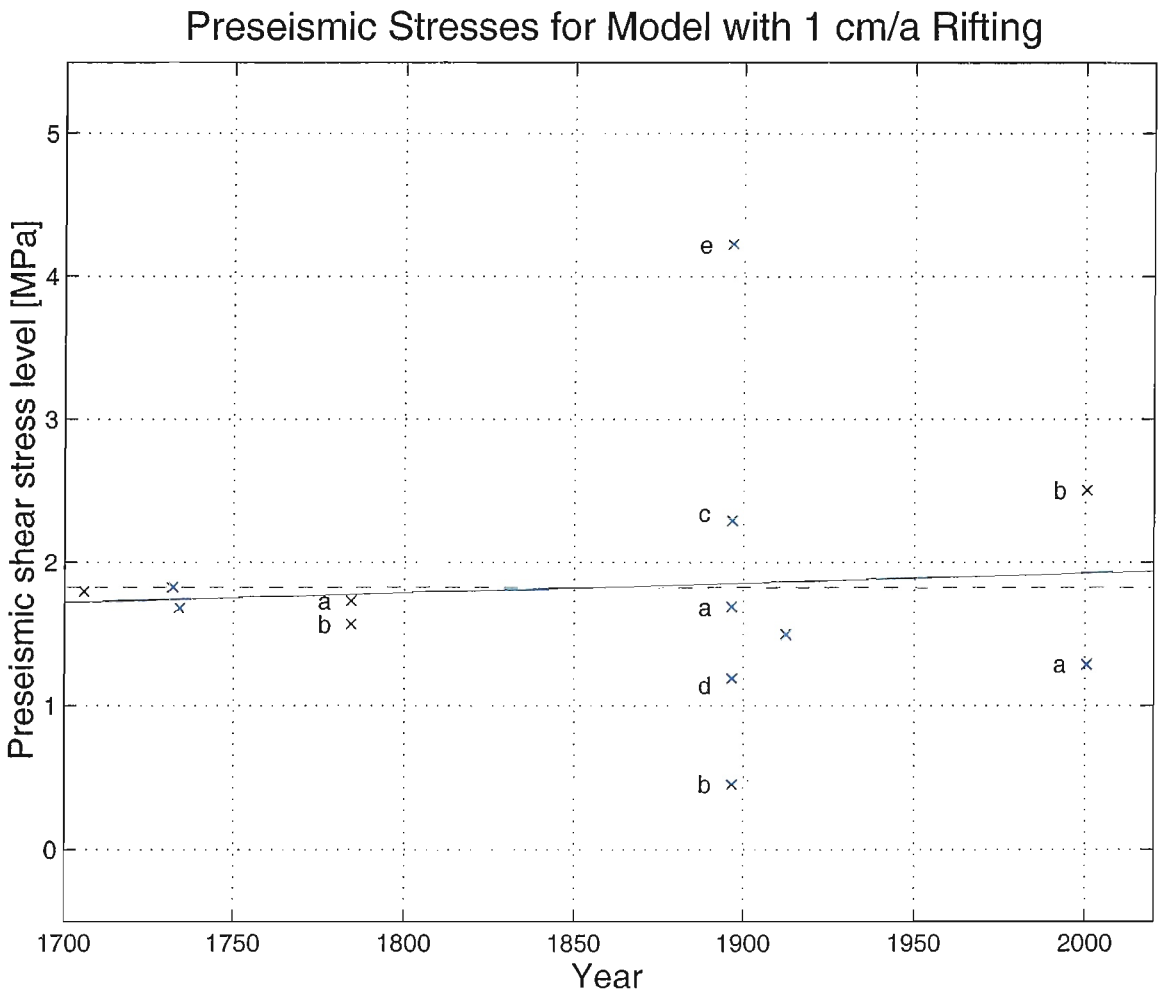

Figure 59. *Cross plot of the pre-seismic shear stress level at the site of the impending earthquakes vs. occurrence time. The stress values at 2 to 14 test-points at 0.5 km distance to the surface trace of the rupture plane were averaged. Instead of a plate velocity of 2 cm/year only 1 cm/year was used (see text). Letters "a" through "e" denote the events in one year in temporal sequence. The dashed line gives the average stress, the solid line represents the trend found by a linear least squares fit.*

Event time:	Pre-seismic stress high at °W:	Earth-quake at °W:	Hit high stress area?	Size of other areas with high stress:	Remarks:
1706	19.8 – 21.2	21.2	yes	large	tuning phase[1]
1732	19.8 – 21.1	20.1	yes	large	tuning phase
1734	19.8 – 20.0, 20.2 – 21.1	20.8	yes	large	tuning phase
1784a	19.8 – 20.0, 20.2 – 20.7, 20.8 – 21.1	20.5	yes	medium	tuning phase
1784b	19.8 – 20.0, 20.9 – 21.1	20.9	yes	small	tuning phase
1896a	19.8 – 20.3, 20.8 – 21.2	20.2	yes	medium	other high stress area hit 10 days later
1896b	19.8 – 20.0, ± 20.6, 20.8 – 21.2	20.1	no	medium	other high stress area hit 9 days later
1896c	19.8 – 20.0, ± 20.6, 20.8 – 21.2	21.0	yes	medium	other high stress area hit next day
1896d	19.8 – 20.0, ± 20.6, 20.8 – 21.2	20.6	yes	medium	other high stress area hit at the same day
1896e	19.8 – 20.0, 20.8 – 21.2	21.2	yes	small	
1912	19.8 – 20.0, 20.8 – 21.2	20.0	yes	small	
2000a	± 19.9, 20.5 – 21.2	20.4	no/ yes	small	hit short (N-S) high stress area[2]
2000b	± 19.9, 20.6 – 21.2	20.7	yes	small	

Table 9. *Qualitative evaluation of the model performance. 1) As the initial stress field is unknown, it was assumed to be homogeneous. So the first series of events that ruptures all across the fault zone is very strongly influenced by this assumption. 2) The stress field before the first earthquake in June 2000 is very inhomogeneous, i.e. there are low stresses in the north of the rupture plane and high ones in the south (see Figure 56). Looking at the development of the stress distribution, this situation is still influenced by the rupture position and magnitude of the first event in 1784 (cf. Figure 54). These historical data have some uncertainty (cf. Figure 50).*

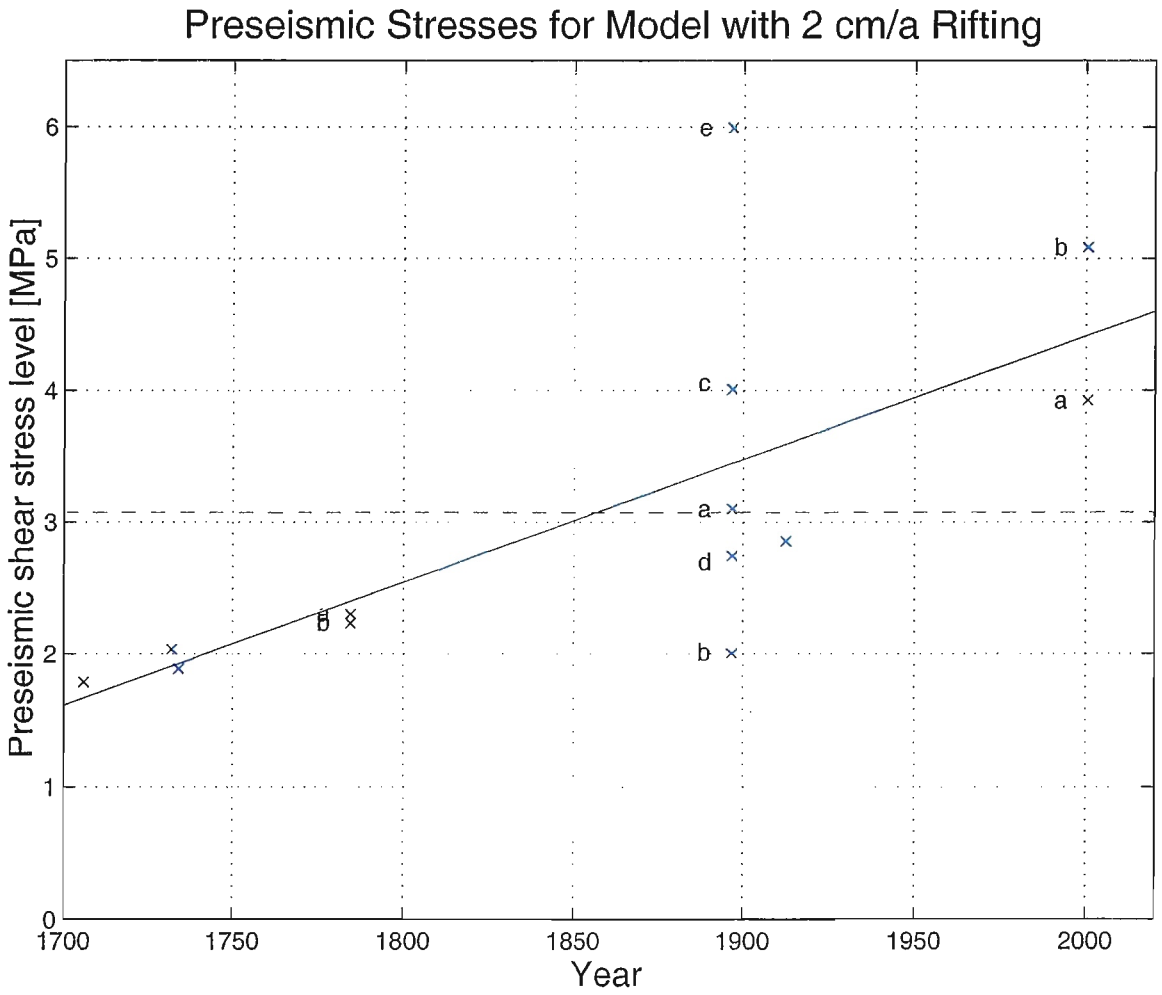

Figure 60. *Cross plot of the pre-seismic shear stress level at the site of the impending earthquakes vs. occurrence time. A plate velocity of 2 cm/year was used. For further explanations see Figure 59.*

So the magnitudes and locations are not very accurate, as stated earlier. And as mentioned in the footnotes of Table 9, there are doubts on the correct rupture size from global relations between magnitude and rupture length.

From both reasons given here, a model was calculated that uses the same seismic moment of the events, but cuts the fault length to 50% while doubling the co-seismic displacement. It will be termed "short rupture model". One side-effect of this change is an increase of the stress level, as the moment release is concentrated to a smaller area. The initial stress field amplitude was increased accordingly, because – as described above – this field is adjusted to the average stress change of the strongest event. It is important to note that the increase in stress level does not change the stress pattern of the initial stress field; as we are not looking for specific stress amplitudes but for stress concentrations, the change in level is not important. The resulting variation of the pre-seismic stress level is – as expected – smoother than before due to the concentration of stress release to high stress areas. However, this approach could only be used, once the historical events are re-evaluated with the result of shorter ruptures.

The processing of the recent earthquakes last June led to maximum rupture depth of less than ten kilometres. Even though there are smaller events located down to 13 km (cf. Stefánsson et al. 1993), the assumption that all ruptures extend to no more than a depth of 10 km seems to be reasonable. Such a model was calculated too, replacing the maximum depth of 14 km for most events (cf. Table 9) by 10 km. In this case too, the stress release by the events is higher, as it is concentrated to an area closer to the rupture plane. Moreover, the interaction of the events is lower due to this concentration in space. However, the stress level before the main events remains in a similar range as before (average now 2.1 MPa instead of 1.8 MPa), and the variation in the pre-seismic stress does not differ much (the standard deviation is 0.87 MPa instead of 0.88 MPa) from the model with deeper ruptures (cf. Figure 61).

In general, the variation of the model parameters shows that the models are stable, i.e. small changes in the parameters do not lead to totally different results. Therefore, they fulfill this important quality criterium.

3.7.2.2 Task 1: Extrapolation of the stress field for the next years

Originally, the stress field for the new models was extrapolated to spring 1999, with the additional stresses due to plate motion since 1912. This became obsolete when the earthquakes in June 2000 occurred. As presented above, the stress field before and after these events was determined. To examine if the stresses were high before the events was a good check for the model results. The present situation is essentially that after the second earthquake in June (see Figure 58). For more details see the discussion below.

3.7.2.3 Task 2: Pin-pointing of stress concentrations in space and time

At present, stresses are concentrated around 19.9°W and at 20.8–21.2°W. As there have not been earthquakes since 1912 and 1896, respectively, this is to be expected and was reproduced by the model.

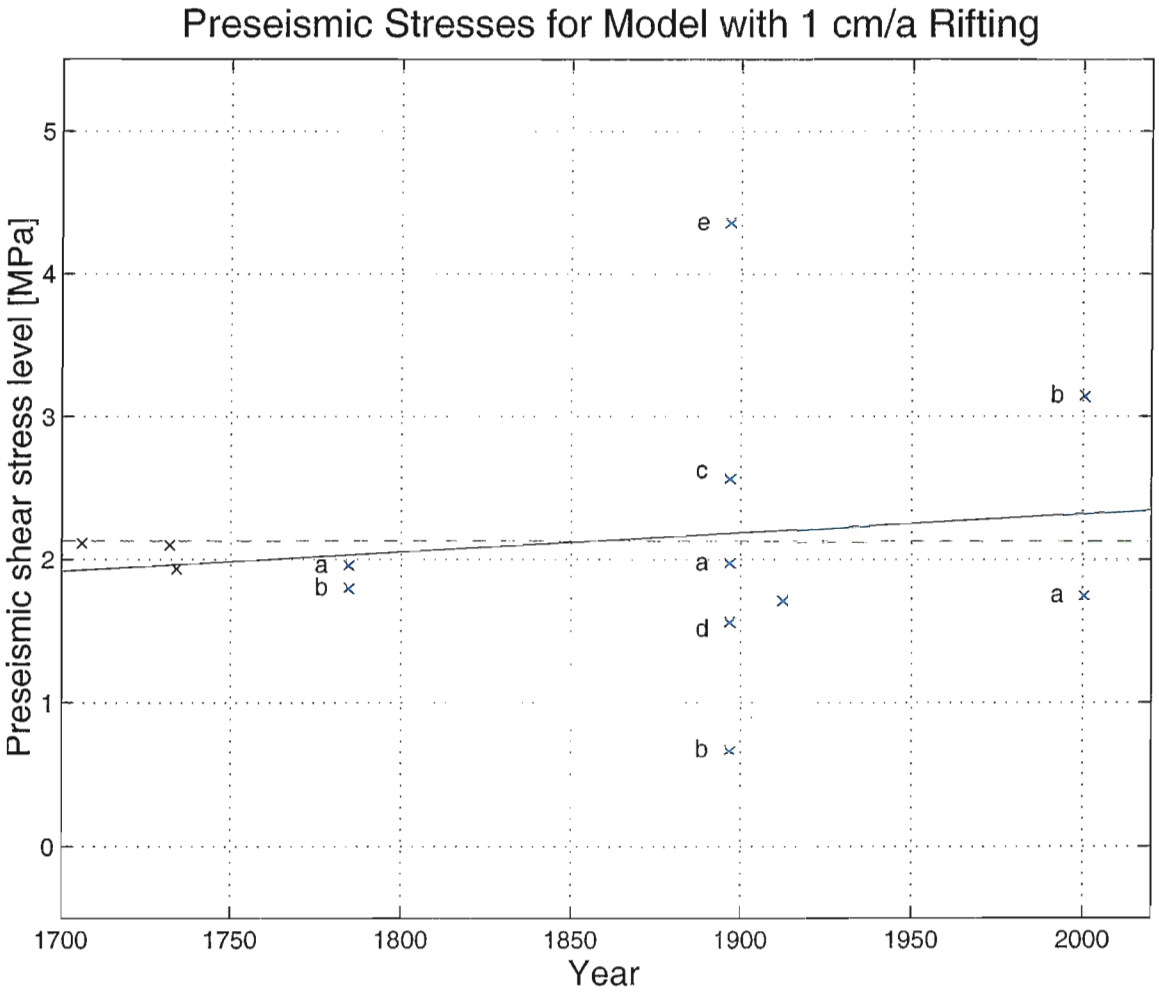

Figure 61. *Cross plot of the pre-seismic shear stress level at the site of the impending earthquakes vs. occurrence time. A maximum rupture depth of 10 km was used. For further explanations see Figure 59.*

Once more, we would like to point to the fact that, in the model, stresses are steadily released at those areas (marked with dashed lines) where the SISZ approaches the ridge segments, as noted under item "C" of the list of improvements above. It are sections of the SISZ between the high stress areas just mentioned and the rift tips.

Is this a weakness of the models or is it the real situation? Could these high stress areas be excluded from the model? The answer is essentially "no". The origin of the stress concentrations at the end of the SISZ, i.e. at the tips of the adjoining ridges, is the fact that the ridges do not extend to infinite depth, but are assumed to reach only 7 km depth and enter than an inelastic, hot region not capable of supporting stresses for time periods of years. Deeper penetration of the brittle layer there would homogenize the stress field between rift tips at some average value. Although this is not very likely, a similar effect would be produced by drag at the base of the adjacent plates. Nevertheless, such a redistribution of stress would not lead to low stresses at the ends of the SISZ.

Possibly, there might have been stronger events in 1546 and 1632 at the western end (about 21.3°W) and one event in 1311 (about 18.9°W) (cf. Halldórsson 1991). But all other evidence only shows small and medium sized events there. The main argument against high seismogenic stress release there is, that there was no large event ($M \geq 6$) since 1706. There are several indications that the stress release indeed mainly takes place in small and medium events at the ends of the SISZ. In 1987, there was a medium sized earthquake (M_S=5.8) at 63.91°N 19.78°W (198, -9) near Vatnafjöll (see Figure 50) at the east end of the SISZ. And in 1998, there were 2 similar events at the Hengill-Ölfus triple junction at the western end of the SISZ: June 4 (M=5.1) and November 13 (M=5) both accompanied by a lot of smaller events.

Therefore, we believe that the tips of the SISZ might only be the place where medium sized events take place and the stress concentrations given around 19.9°W and at 20.8–21.2°W represent those for future strong earthquakes.

As the stress build-up by plate motion is very low in these models (compare the stress field in 2000 in Figure 56 with that of 1912 in Figure 55), the uncertainty in time is very large in the occurrence time, see also the discussion below.

3.7.2.4 Task 3: Search for characteristic preseismic stress level

As a simple assumption, one might expect, that earthquakes in a certain fault zone usually occur at about the same critical shear stress level. Here, we tried to find out, if such an expectation matches the known facts about the earthquakes and the stress field in the SISZ.

In all models, the pre-seismic stress level for most main shocks is high and fairly stable. This is also true for the events at the end of the sequence, namely those of 1912, of June 20, 2000, and – with minor reservations – of June 17, 2000. It indicates that the rather simple model can already explain the main features of the behaviour of the SISZ. This is especially astonishing, when the fact is kept in mind, that most (all but one) events used are not instrumentally recorded. Before the June 2000 events the SISZ seems to have been prepared for rupturing at the specific locations. This fits very well to the findings from stress measurements in wells (see Subproject 4) that E-W left-lateral shear stress was acting on the fault zone. To improve the model further, the initial unknown stress field of 1706 could be reduced in the eastern part and the central part, where the first events did not occur before

1732 and 1734, respectively. Another improvement might be to include more basal drag as the source of plate tectonic stress increase as compared to ridge push.

Nevertheless, the problem remains, why some events, as those of September 6, 1896, or June 21, 2000, did not occur earlier (i.e. at lower stress), just passing the "threshold in pre-seismic stress" (here e.g. the average pre-seismic stress (cf. Figure 59). Only if this would be the case, a prediction of the occurrence time might be at reach.

Even though the earthquake rupture planes strike N-S, the stress changes calculated here affect the whole area of the SISZ.

A tendency with time towards higher values of pre-seismic stress was found. It is an indication that the stress increase due to rifting might have been assumed too high, i.e. not all of the stress increase due to the spreading rate of 2 cm/year (assumed to be constant between 1706 to 2000) was released by earthquakes. The assumption that only half of the accumulated stress is seismically released led to a rather constant pre-seismic stress level.

The variation in model parameters does not lead to totally different results, i.e. the model is rather stable.

In general, the models go beyond the standard earthquake moment release and hazard analysis as they include the spatial location and extension of the events, quantify the amplitudes of stress release and that of plate motion on the faults, as well as providing an extrapolation to the present stress situation. This report will be submitted for publication in an appropriate form.

3.7.2.5 Meetings and conferences

A meeting between Maurizio Bonafede and coworkers with Frank Roth took place in March 1999 in Strasbourg, France, parallel to the tenth biennal EUG meeting. Another meeting with Bonafede and Ragnar Stefánsson took place at the GeoForschungsZentrum Potsdam in June 1999.

3.7.2.6 Acknowledgements

I like to thank the staff of IMOR.DG, especially Páll Halldórsson, for great support on the seismicity of Iceland. I am also indebted to F. Lorenzo Martín and Fernando J. Lorén Blasco for assisting in the graphics and checking the text.

3.7.3 References

Bjarnason, I.Þ. & P. Einarsson 1991. Source mechanism of the 1987 Vatnafjöll earthquake in South Iceland. *J. Geophys. Res.* 96, 4313-4324.

Bjarnason, I.Þ., P. Cowie, M.H. Anders, L. Seeber & C.H. Scholz 1993. The 1912 Iceland earthquake rupture: growth and development of a nascent transform system. *Bull. Seism. Soc. Am.* 83, 416-435.

Bonafede, M. & E. Rivalta 1999. The tensile dislocation problem in a layered elastic medium. *Geophys. J. Int.* 136, 341-356.

Bonafede, M. & A. Neri 2000. Effects induced by an earthquake on its fault plane: a boundary element study. *Geophys. J. Int.* 141, 43-56.

Bonafede, M., B. Parenti & E. Rivalta 2000. Strike-slip faulting in layered media. *Geophys. J. Int.*, submitted.

DeMets, C., R.G. Gordon, D.F. Argus & S. Stein 1990. Current plate motions. *Geophys. J. Int.* 101, 425-478.

Dziewonski, A.M., A.L. Hales & E.R. Lapwood 1975. Parametrically simple earth models consistent with geophysical data. *Phys. Earth Plan. Int.* 10, 12.

Einarsson, P., S. Björnsson, G.R. Foulger, R. Stefánsson & Þ. Skaftadóttir 1981. Seismicity pattern in the South Iceland seismic zone. In: D. Simpson & P. Richards (editors), Earthquake prediction - an international review. *Maurice Ewing Series* 4. American Geophysical Union, 141-151.

Einarsson, P. & K. Sæmundsson 1987. Earthquake epicenters 1982-1985 and volcanic systems in Iceland. In: Þ.I. Sigfússon (editor), *Í hlutarins eðli.* Map accompanying the festschrift, scale 1:750000. Reykjavík, Menningarsjóður.

Hackman, M.C., G.C.P. King & R. Bilham 1990. The mechanics of the South Iceland seismic zone. *J. Geophys. Res.* 95, 17339-17351.

Halldórsson, P. 1991. Historical earthquakes in Iceland until 1700. In: K. Kozák (editor), *Proceedings of the third international symposium on historical earthquakes in Europe.* Prague, Czechoslovakia, 115-125.

Halldórsson, P., R. Stefánsson, P. Einarsson & S. Björnsson 1984. *Mat á jarðskjálftahættu: Dysnes, Geldinganes, Helguvík, Vatnsleysuvík, Vogastapi og Þorlákshöfn.* Veðurstofa Íslands, Raunvísindastofnun Háskólans, Reykjavík.

Kanamori, H. & D.L. Andersson 1975. Theoretical basis of some empirical relations in seismology. *Bull. Seism. Soc. Am.* 65, 1073-1096.

Newman, A. & Stein 1999. Reply: New results justify open discussion of alternative models. *EOS, Trans. Am. Geophys. Un.* 80, 197 and 199.

Qian, H. 1986. Recent displacements along Xianshuihe fault belt and its relation with seismic activities. *J. Seism. Res.* 9, 601-614.

Roth, F. 1989. A model for the present stress field along the Xian-shui-he fault belt, NW Sichuan, China. In: M.J. Berry (editor), Earthquake hazard assessment and prediction. *Tectonophysics* 167, 103-115.

Schick, R. 1968. A method for determining source parameters of small magnitude earth-

quakes. *Zeitschr. f. Geophys.* 36, 205-224.

Schweig, E.S. & J.S. Gomberg 1999. Comment: Caution urged in revising earthquake hazards estimates in New Madrid seismic zone. *EOS, Trans. Am. Geophys. Un.* 80, 197.

Stefánsson, R. & P. Halldórsson 1988. Strain release and strain build-up in the South Iceland seismic zone. *Tectonophysics* 152, 267-276.

Stefánsson, R., R. Böðvarsson, R. Slunga, P. Einarsson, S.S. Jakobsdóttir, H. Bungum, S. Gregersen, J. Havskov, J. Hjelme & H. Korhonen 1993. Earthquake prediction research in the South Iceland seismic zone and the SIL project. *Bull. Seism. Soc. Am.* 83, 696-716.

Zoback, M.D., M.L. Zoback, V.S. Mount, J. Suppe, J. Eaton, J.H. Healy, D. Oppenheimer, P. Reasenberg, L. Jones, C.B. Raleigh, I.G. Wong, O. Scotti & C. Wentworth 1987. New evidence on the state of stress on the San Andreas fault system. *Science 238*, 1105-1111.

Chapter 4

Publications

Papers directly associated with PRENLAB–2

Subproject 1

Ágústsson, K. 1998. Jarðskjálftahrina á Hellisheiði og í Hengli í maí–júlí 1998. *Greinargerð Veðurstofu Íslands* VÍ–G98040–JA06. Report, Icelandic Meteorological Office, Reykjavík, 35 pp.

Ágústsson, K., A.T. Linde, R. Stefánsson & S. Sacks 1998. Strain changes for the 1987 Vatnafjöll earthquake in South Iceland and possible magmatic triggering. *J. Geophys. Res.* 104, 1151–1161.

Ágústsson, K., S.Th. Rögnvaldsson, B.H. Bergsson & R. Stefánsson 1998. Jarðskjálftamælanet Veðurstofu Íslands og Hitaveitu Suðurnesja – lýsing á mælaneti og fyrstu niðurstöður. *Rit Veðurstofu Íslands* VÍ–R98002–JA02. Research report, Icelandic Meteorological Office, Reykjavík, 17 pp.

Árnadóttir, Þ. & K.B. Olsen 2000. Simulation of long–period ground motion and stress changes for the Ms=7.1, 1784 earthquake, Iceland. *Rit Veðurstofu Íslands* VÍ–R00003–JA03. Research report, Icelandic Meteorological Office, Reykjavík, 31 pp.

Bergerat, F., Á. Guðmundsson, J. Angelier & S.Th. Rögnvaldsson 1998. Seismotectonics of the central part of the South Iceland seismic zone. *Tectonophysics* 298, 319–335.

Böðvarsson, R., S.Th. Rögnvaldsson, R. Slunga & E. Kjartansson 1998. The SIL data acquisition system – at present and beyond the year 2000. *Rit Veðurstofu Íslands* VÍ–R98005–JA04. Research report, Icelandic Meteorological Office, Reykjavík, 22 pp.

Böðvarsson, R., S.Th. Rögnvaldsson, R. Slunga & E. Kjartansson 1999. The SIL data acquisition system – at present and beyond year 2000. *Phys. Earth Planet. Inter.* 113, 89–101.

Crampin, S., T. Volti & R. Stefánsson 1999. A successfully stress–forecast earthquake. *Geophys. J. Int.* 138, F1-F5.

Halldórsson, P., R. Stefánsson, B. Þorbjarnardóttir & I. Jónsdóttir 2000. Bráðaviðvaranir um jarðvá - áfangaskýrsla. *Greinargerð Veðurstofu Íslands* VÍ–G00005–JA02. Report, Icelandic Meteorological Office, Reykjavík, 16 pp.

Rögnvaldsson, S.Th. 1999. Frammistaða SIL kerfisins frá ágúst 1998 til mars 1999. *Greinargerð Veðurstofu Íslands* VÍ–G99004–JA01. Report, Icelandic Meteorological Office, Reykjavík, 14 pp.

Rögnvaldsson, S.Th. 2000. Kortlagning virkra misgengja með smáskjálftamælingum - yfirlit. *Rit Veðurstofu Íslands* VÍ–R00001–JA01. Research report, Icelandic Meteorological Office, Reykjavík, 15 pp.

Rögnvaldsson, S.Th., K. Ágústsson, B.H. Bergsson & G. Björnsson 1998. Jarðskjálftamælanet í nágrenni Reykjavíkur - lýsing á mælaneti og fyrstu niðurstöður. *Rit Veðurstofu Íslands* VÍ–R98001–JA01. Research report, Icelandic Meteorological Office, Reykjavík, 15 pp.

Rögnvaldsson, S.Th., Þ. Árnadóttir, K. Ágústsson, Þ. Skaftadóttir, G.B. Guðmundsson, G. Björnsson, K.S. Vogfjörð, R. Stefánsson, R. Böðvarsson, R. Slunga, S.S. Jakobsdóttir, B.S. Þorbjarnardóttir, P. Erlendsson, B.H. Bergsson, S. Ragnarsson, P. Halldórsson, B. Þorkelsson & M. Ásgeirsdóttir 1998. Skjálftahrina í Ölfusi í nóvember 1998. *Greinargerð Veðurstofu Íslands* VÍ–G98046–JA09. Report, Icelandic Meteorological Office, Reykjavík, 19 pp.

Rögnvaldsson, S.Th., Á. Guðmundsson & R. Slunga 1998a. Seismotectonic analysis of the Tjörnes fracture zone, an active transform fault in North Iceland. *J. Geophys. Res.* 103, 30117–30129.

Rögnvaldsson, S.Th., Á. Guðmundsson & R. Slunga 1998b. Seismotectonic analysis of the Tjörnes fracture zone, an active transform fault in North Iceland. *Rit Veðurstofu Íslands* VÍ–R98004–JA03. Research report, Icelandic Meteorological Office, Reykjavík, 23 pp.

Rögnvaldsson, S.Th., G.B. Guðmundsson, K. Ágústsson, S.S. Jakobsdóttir, R. Slunga & R. Stefánsson 1998. Overview of the 1993–1996 seismicity near Hengill. *Rit Veðurstofu Íslands* VÍ–R98006–JA05. Research report, Icelandic Meterological Office, Reykjavík, 16 pp.

Rögnvaldsson, S.Th., K.S. Vogfjörð & R. Slunga 1999. Kortlagning brotflata á Hengilssvæði með smáskjálftum. *Rit Veðurstofu Íslands* VÍ–R99002–JA01. Research report, Icelandic Meterological Office, Reykjavík, 22 pp.

Stefánsson, R. 1998. Earthquake–prediction research in a natural laboratory – PRENLAB. In: C.P. Providakis & M. Yeroyanni (editors), *Earthquake strong ground motion evaluation.* Proceedings of the EU–Japan workshop on seismic risk, Chania, Crete, Greece, March 24–26, 1998. European Commission, 113–122.

Stefánsson, R. 1999. A tentative model for the stress build–up and stress release in and around the SISZ.
URL: http://hraun.vedur.is/ja/prenlab/symp-mar-1999/ragnar/index2.html. Last modified March 31, 1999.

Stefánsson, R. 2000. Information and warnings to authorities and to the public about seismic and volcanic hazards in Iceland. To appear in a book of papers presented at the Early Warning Conference (EWC98), Potsdam, Germany, September 7-11, 1998, 11 pp.

Stefánsson, R., S.Th. Rögnvaldsson, P. Halldórsson & G.B. Guðmundsson 1998. PRENLAB workshop on the Húsavík earthquake, July 30, 1998. *Greinargerð Veðurstofu Íslands* VÍ–G98032–JA04. Report, Icelandic Meteorological Office, Reykjavík, 5 pp.

Stefánsson, R., F. Bergerat, M. Bonafede, R. Böðvarsson, S. Crampin, P. Einarsson, K.L. Feigl, Á. Guðmundsson, F. Roth & F. Sigmundsson 1999. Earthquake–prediction research in a natural laboratory – PRENLAB. In: M. Yeroyanni (editor), *Seismic risk in the European Union II.* Proceedings of the review meeting, Brussels, Belgium, Novem-

ber 27–28, 1997, European Commission, 1–39.

Stefánsson, R., G.B. Guðmundsson & P. Halldórsson 2000a. The two large earthquakes in the South Iceland seismic zone on June 17 and 21, 2000. *Greinargerð Veðurstofu Íslands* VÍ-G00010-JA04. Report, Icelandic Meteorological Office, Reykjavík, 8 pp.

Stefánsson, R., G.B. Guðmundsson & P. Halldórsson 2000b. Jarðskjálftarnir miklu á Suðurlandi 17. og 21. júní, 2000. *Greinargerð Veðurstofu Íslands* VÍ–G00011–JA05. Report, Icelandic Meteorological Office, Reykjavík, 8 pp.

Stefánsson, R., G.B. Guðmundsson & R. Slunga 2000. The PRENLAB-2 project, premonitory activity and earthquake nucleation in Iceland. In: B. Þorkelsson & M. Yeroyanni (editors), *Destructive earthquakes: Understanding crustal processes leading to destructive earthquakes.* Proceedings of the second EU-Japan workshop on seismic risk, Reykjavík, Iceland, June 23–27, 1999. European Commission, 161–172.

Stefánsson, R., Þ. Árnadóttir, G.B. Guðmundsson, P. Halldórsson & G. Björnsson 2001. Two recent M=6.6 earthquakes in the South Iceland seismic zone. A challenge for earthquake prediction research. *Rit Veðurstofu Íslands* VÍ-R01001-JA01. Research report, Icelandic Meteorological Office, Reykjavík, in press.

Tryggvason, A., S.Th. Rögnvaldsson & Ó.G. Flóvenz 2000. Three–dimensional imaging of the P- and S-wave velocity structure and earthquake locations beneath Southwest Iceland. *J. Geophys. Res.*, submitted.

Vogfjörð, K.S & S.Th. Rögnvaldsson 2000. Identification and modelling of secondary phases in short–period seismograms from local earthquakes in the South Iceland seismic zone. *Geophys. J. Int.*, accepted.

Subproject 2

Böðvarsson, R., S.Th. Rögnvaldsson, R. Slunga & E. Kjartansson 1998. The SIL data acquition system – at present and beyond year 2000. *Rit Veðurstofu Íslands* VÍ–R98005–JA04. Research report, Icelandic Meteorological Office, Reykjavík, 22 pp.

Böðvarsson, R., S.Th. Rögnvaldsson, R. Slunga & E. Kjartansson 1999. The SIL data acquisition system – at present and beyond year 2000. *Phys. Earth Planet. Inter.* 113, 89–101.

Lund, B. & R. Slunga 1999. Stress tensor inversion using detailed microearthquake information and stability constraints: application to Ölfus in southwest Iceland. *J. Geophys. Res.* 104, 14947–14964.

Lund, B. & R. Böðvarsson 2000. Correlation of microearthquake body–wave spectral amplitudes. *Bull. Seism. Soc. Am.*, accepted.

Shomali, Z.H. & R. Slunga 2000. Body wave moment tensor inversion of local earthquakes: an application to the South Iceland seismic zone. *Geophys. J. Int.*, 63–70.

Slunga, R. 2001. Foreshock activity, fault radius and silence - earthquake warnings based on microearthquakes. *Greinagerð Veðurstofu Íslands* VÍ-01003-JA03. Report, Icelandic Meteorological Office, Reykjavík, in press.

Slunga, R., R. Böðvarsson, G.B. Guðmundsson, S.S Jakobsdóttir, B. Lund & R. Stefánsson

2000. A simple earthquake warning algorithm based on microearthquake observations - retrospective applications on Iceland. Submitted.

Subproject 3

Crampin, S. 1998a. Stress–forecasting: a viable alternative to earthquake prediction in a dynamic Earth. *Trans. R. Soc. Edin. Earth Sci.* 89, 121–133.

Crampin, S. 1998b. Shear–wave splitting in a critical crust: the next step. In: P. Rasolofosaon (editor), *Rev. Inst. Franc. Pet.* 53. Proceedings of Eighth International Workshop on Seismic Anisotropy, Boussens, France, 749–763.

Crampin, S. 1999a. A successful stress–forecast: an addendum to "Stress–forecasting: a viable alternative to earthquake prediction in a dynamic Earth". *Trans. R. Soc. Edin. Earth Sci.* 89, 231.

Crampin, S. 1999b. Calculable fluid–rock interactions. *J. Geol. Soc.* 156, 501–514.

Crampin, S. 2000a. The "New Geophysics": a critical, compliant, calculable, and controllable reservoir. In: Extended abstracts from the 62nd EAGE meeting, Glasgow, United Kingdom.

Crampin, S. 2000b. The potential of shear–wave splitting in a stress–sensitive compliant crust: a new understanding of pre–fracturing deformation from time–lapse studies. In: Expanded abstracts from the 70th Annual International SEG Meeting, Calgary, Alberta, Canada, 1520–1523.

Crampin, S. 2000c. Shear–wave splitting in a critical self–organized crust: the New Geophysics. Expanded abstracts from the 70th Annual International SEG Meeting, Calgary, Alberta, Canada, 1544–1547.

Crampin, S. 2000d. Stress–monitoring sites (SMSs) for stress–forecasting the times and magnitudes of future earthquakes. *Tectonophysics*, in press.

Crampin, S., T. Volti & R. Stefánsson 1999. A successfully stress–forecast earthquake. *Geophys. J. Int.* 138, F1–F5.

Crampin, S. & S. Chastin 2000. Shear–wave splitting in a critical crust: II - compliant, calculable, controllable fluid–rock interactions. In: L. Ikelle (editor), *Proceedings of the Ninth International Workshop on Seismic Anisotropy*, Cape Allen, Houston, Texas, USA, 2000, submitted.

Crampin, S., T. Volti & P. Jackson 2000. Developing a stress–monitoring site (SMS) near Húsavík for stress–forecasting the times and magnitudes of future large earthquakes. In: B. Þorkelsson & M. Yeroyanni (editors), *Destructive earthquakes: Understanding crustal processes leading to destructive earthquakes.* Proceedings of the second EU–Japan workshop on seismic risk, Reykjavík, Iceland, June 23–27, 1999, 136–149.

Gao, Y., P. Wang, S. Zheng, M. Wang & Y.-T. Chen 1998. Temporal changes in shear–wave splitting at an isolated swarm of small earthquakes in 1992 near Dongfang, Hainan Island, Southern China. *Geophys. J. Int.* 135, 102–112.

Volti, T. & S. Crampin 2000. Shear–wave splitting in Iceland: four years monitoring stress changes before earthquakes and volcanic eruptions. *Geophys. J. Int.*, submitted.

Subproject 4

Henneberg, K., F. Roth, H. Sigvaldason, S.Þ Guðlaugsson & V. Stefánsson 1998. Ergebnisse von Bohrlochmessungen in der Südisländischen Seismizitätszone in den Jahren 1996 und 1997. Paper presented at the third meeting of the FKPE working group on Borehole Geophysics and Rock Physics, Hannover, Germany, 1998.

Roth, F. 1999a. Erforschung von Erdbeben auf Island. Invited talk at the Faculty of Geosciences, University of Hamburg, Germany, 1999.

Roth, F. 1999b. Bohrlochmessungen zum Spannungsfeld und zu Aquifären. Invited talk at the Faculty of Geosciences, Geotechniques and Mining, Technische Universität Bergakademie Freiberg, 1999.

Roth, F. & P. Fleckenstein 1999a. Report on repeated logging in the framework of PRENLAB–2. PRENLAB–2 workshop, Strasbourg, France, March 31, 1999.

Roth, F. & P. Fleckenstein 1999b. Ergebnisse von Bohrloch–Spannungsmessungen in der Südisländischen Seismizitätszone. Paper presented at the fifth meeting of the FKPE working group on Borehole Geophysics and Rock Physics, Hannover, Germany, 1999.

Roth, F., K. Henneberg, P. Fleckenstein, J. Palmer, V. Stefánsson & S.Þ. Guðlaugsson 2000. Ergebnisse von Bohrloch–Spannungsmessungen in der Südisländischen Seismizitätszone. In: *Trans. Dt. Geophys. Ges.* III. Extended abstracts from the fifth meeting of the FKPE working group on Borehole Geophysics and Rock Physics, Hannover, Germany, 1999, 49–50.

Subproject 5

Clifton, A. 2000. Surface deformation related to volcanic uplift and seismicity in SW–Iceland. Poster presented at the Nordvulk–Ridge summer school, Iceland, August 20–30, 2000.

Clifton, A. & F. Sigmundsson 2000. Faulting and deformation resulting from magma accumulation at the Hengill triple junction, SW–Iceland. Abstract submitted the AGU fall meeting, San Francisco, California, USA, December 15–19, 2000.

Feigl, K.L., J. Gasperi, F. Sigmundsson & A. Rigo 2000. Crustal deformation near Hengill volcano, Iceland 1993–1998: coupling between magmatic activity and faulting inferred from elastic modeling of satellite radar interferograms. *J. Geophys. Res.* 105, 25655–25670.

Guðmundsson, S., F. Sigmundsson & J.M. Carstensen 2000. Three–dimensional surface motion maps estimated from combined InSAR and GPS data. *J. Geophys. Res.*, submitted.

Hreinsdóttir, S., P. Einarsson & F. Sigmundsson 2000. Crustal deformation at the oblique spreading Reykjanes peninsula, SW–Iceland: GPS measurements from 1993 to 1998. *J. Geophys. Res.*, submitted.

Johnson, D.J., F. Sigmundsson & P.T. Delaney 2000. Comment of "Volume of magma accumulation or withdrawal estimated from surface uplift or subsidence, with application to the 1960 collapse of Kilauea volcano" by P.T. Delaney and D.F. McTigue. *Bull.*

Volc. 61, 491–493.

Vadon, H. & F. Sigmundsson 1997. Crustal deformation from 1992 to 1995 at the mid-Atlantic ridge, Southwest Iceland, mapped by satellite radar interferometry. *Science* 257, 194–197.

Subproject 6

Acocella, V., Á. Guðmundsson & R. Funiciello 1999. The interaction between extensional segments at the Icelandic mid-oceanic ridge. In: Abstracts from the tenth biennial EUG meeting, Strasbourg, France, March 28 - April 1, 1999.

Acocella, V., Á. Guðmundsson & R. Funiciello 2000. Interaction and linkage of extension fractures and normal faults: examples from the rift zone of Iceland. *Journal of Structural Geology* 22, 1233–1246.

Angelier, J. 1998. A new direct inversion of earthquake focal mechanisms to reconstruct the stress tensor. In: *Annales Geophysicae.* Abstracts from the XXIII EGS General Assembly, Nice, France, April 20–24, 1998.

Angelier, J. & F. Bergerat 1998. Stress fields and mechanisms of seismogenic faults: the South Iceland seismic zone as a case example. In: Abstracts from the international workshop on the Resolution of geological analysis and models for earthquake faulting studies, Camerino, Italy, June 3–6, 1998.

Angelier, J., F. Bergerat & S.Th. Rögnvaldsson 1998. Seismogenic stress field in the South Iceland seismic zone. In: *Annales Geophysicae.* Abstracts from the XXIII EGS General Assembly, Nice, France, April 20–24, 1998.

Angelier, J., F. Bergerat , H.-T. Chu, Á. Guðmundsson, C. Homberg, J.-C. Hu, H. Kao, J.-C. Lee & S.Th. Rögnvaldsson 1999. Active faulting, earthquakes and deformation-stress fields: from the mid–Atlantic ridge (Iceland) to a collision boundary of Southeast Asia (Taiwan). Abstracts from the second EU–Japan workshop on seismic risk, Reykjavík, Iceland, June 23–27, 1999.

Angelier, J., F. Bergerat & C. Homberg 1999. Variations in mechanical coupling as a source of apparent polyphase tectonism: the case of the Tjörnes transform zone, North Iceland. In: *Annales Geophysicae.* Abstracts from the XXIV EGS General Assembly, The Hague, The Netherlands, April 19–23, 1999.

Angelier, J., F. Bergerat & S.Th. Rögnvaldsson 1999a. Using inversion of large population of earthquake focal mechanisms to derive the regional seismotectonic field: Iceland. In: Abstracts from the tenth biennial EUG meeting, Strasbourg, France, March 28 - April 1, 1999.

Angelier, J., F. Bergerat & S.Th. Rögnvaldsson 1999b. Perturbation of late–scale extension across oceanic rift and transform faults revealed by inversion of earthquake focal mechanisms in Iceland. In: *Annales Geophysicae.* Abstracts from the XXIV EGS General Assembly, The Hague, The Netherlands, April 19–23, 1999.

Angelier, J., F. Bergerat, H.-T. Chu, Á. Guðmundsson, J.-C. Hu, J.-C. Lee, C. Homberg, H. Kao & S.Th. Rögnvaldsson 2000. Active faulting, earthquakes and deformation–stress fields: from mid–Atlantic ridge spreading (Iceland) to collision in Southeast

Asia (Taiwan). In: B. Þorkelsson & M. Yeroyanni (editors), *Destructive earthquakes: Understanding crustal processes leading to destructive earthquakes.* Proceedings of the second EU–Japan workshop on seismic risk, Reykjavík, Iceland, June 23–27, 1999. European Commission, 48–61.

Angelier, J., F. Bergerat & C. Homberg 2000. Variable coupling explains complex tectonic regimes near oceanic transform fault: Flateyjarskagi, Iceland. *Terra Nova*, in press.

Belardinelli, M.E., M. Bonafede & Á. Guðmundsson 1999. Multiscale surface faulting generated by strike–slip earthquakes in Iceland. In: *Annales Geophysicae.* Abstracts from the XXIV EGS General Assembly, The Hague, The Netherlands, April 19–23, 1999.

Belardinelli, M.E., M. Bonafede & Á. Guðmundsson 2000. Secondary earthquake fractures generated by a strike–slip fault in the South Iceland seismic zone. *J. Geophys. Res.* 105, 13613–13629.

Bergerat, F. & J. Angelier 1998. Neotectonic evidences from field studies of recent faulting in the South Iceland seismic zone (SISZ). In: *Annales Geophysicae.* Abstracts from the XXIII EGS General Assembly, Nice, France, April 20–24, 1998.

Bergerat, F., Á. Guðmundsson, J. Angelier & S.Th. Rögnvaldsson 1998. Seismotectonics of the central part of the South Iceland seismic zone. *Tectonophysics* 298, 319–335.

Bergerat, F. & J. Angelier 1999a. Géométrie des failles et régimes de contraintes à différents stades de développement des zones transformantes océaniques: exemple de la Zone Sismique Sud–Islandaise et de la Zone de Fracture de Tjörnes (Islande). *Sciences de la terre et des planètes* 329. C. R. Acad. Sc. Paris, 653–659.

Bergerat, F. & J. Angelier 1999b. Fault and stress patterns at different stages of development of oceanic transform zones: examples in Iceland. In: *Annales Geophysicae.* Abstracts from the XXIV EGS General Assembly, The Hague, The Netherlands, April 19–23, 1999.

Bergerat, F., J. Angelier & C. Homberg 1999. Field studies of recent faulting along the Húsavík–Flatey fault (Tjörnes transform zone, northern Iceland): complex tectonic regimes and variable coupling. In: Abstracts from the tenth biennial EUG meeting, Strasbourg, France, March 28 - April 1, 1999.

Bergerat, F., J. Angelier & S. Verrier 1999. Tectonic stress regimes, rift extension and transform motion: the South Iceland seismic zone. *Geodin. Acta* 12(5), 303–319.

Bergerat, F. & J. Angelier 2000. The South Iceland seismic zone: tectonic and seismotectonic analyses revealing the evolution from rifting to transform motion. *Journ. Geodynamics* 29(3–5), 211–231.

Bergerat, F., J. Angelier & C. Homberg 2000. Tectonic analysis of the Húsavík–Flatey fault (northern Iceland) and mechanisms of an oceanic transform zone, the Tjörnes fracture zone. *Tectonics*, in press.

Bergerat, F., J. Angelier & Á. Guðmundsson 2000. The Leirubakki fault, a large earthquake rupture of the South Iceland seismic zone. In: *Annales Geophysicae.* Abstracts from the XXV EGS General Assembly, Nice, France, April 25–29, 2000.

Bergerat, F., J. Angelier & Á. Guðmundsson. The Leirubakki earthquake rupture: a large fault of the South Iceland seismic zone. In preparation.

Dauteuil, O., J. Angelier, F. Bergerat, S. Verrier & T. Villemin 2000. Deformation partitioning inside a fissure swarm of the northern Icelandic rift. *Journal of Structural Geology*, accepted, in revision.

Garcia, S. 1999. *De sismotectonique d'un segment transformant en domaine océanique: la Zone de Fracture de Tjörnes, Islande.* Unpublished master thesis. Universite Pierre & Marie Curie, Paris.

Garcia, S., J. Angelier, F. Bergerat & C. Homberg 2000. Etude sismotectonique d'un segment transformant: la Zone de Fracture de Tjörnes, Islande. $18^{ème}$ RST, Paris, France, April 2000.

Garcia, S., J. Angelier, F. Bergerat & C. Homberg. Tectonic behaviour of an oceanic transform fault zone from fault–slip data and focal mechanisms of earthquakes analyses: the Tjörnes fracture zone, Iceland. In preparation.

Guðmundsson, Á. 1998a. Development of permeability in fault zones. In: *Annales Geophysicae* Abstracts from the XXIII EGS General Assembly, Nice, France, April 20–24, 1998.

Guðmundsson, Á. 1998b. Rift–zone and off–rift earthquakes in Iceland. In: *Annales Geophysicae.* Abstracts from the XXIII EGS General Assembly, Nice, France, April 20–24, 1998.

Guðmundsson, Á. 1999a. Fluid pressure and stress drop in fault zones. *Geophys. Res. Lett.* 25, 115–118.

Guðmundsson, Á. 1999b. Fluid flow in fractured rocks: application to the hydrogeology of Norway. In: Abstracts from the General Meeting of the Geological Society of Norway, Stavanger, Norway.

Guðmundsson, Á. 1999c. Extensional veins used to estimate overpressure and depth of origin of fluids in fault zones. In: Abstracts from the tenth biennial EUG meeting, Strasbourg, France, March 28 - April 1, 1999.

Guðmundsson, Á. 1999d. Fluid pressure and stress for large earthquakes. In: *Annales Geophysicae.* Abstracts from the XXIV EGS General Assembly, The Hague, The Netherlands, April 19–23, 1999.

Guðmundsson, Á. 1999e. Injection and arrest of water–filled fractures. In: *Annales Geophysicae.* Abstracts from the XXIV EGS General Assembly, The Hague, The Netherlands, April 19–23, 1999.

Guðmundsson, Á. 1999f. Flow of groundwater into and along fault zones. In: *Annales Geophysicae.* Abstracts from the XXIV EGS General Assembly, The Hague, The Netherlands, April 19–23, 1999.

Guðmundsson, Á. 1999g. Similarities in the structural evolution of rift basins and rift–zone grabens. In: Abstracts from the Norwegian Petroleum Society Meeting on Sedimentary Environments Offshore Norway, Bergen, Norway.

Guðmundsson, Á. 1999h. Fluid overpressure and flow in fault zones: field measurements and models. Workshop on Fluids and Fractures in the Lithosphere, Nancy, France. Tectonic Study Group of Nancy, Geological Society of France.

Guðmundsson, Á. 2000a. Active fault zones and groundwater flow. *Geophys. Res. Lett.*,

in press.

Guðmundsson, Á. 2000b. Fluid overpressure and flow in fault zones: field measurements and models. *Tectonophysics*, in press.

Guðmundsson, Á. 2000c. Fracture dimensions, displacements and fluid transport. *Journal of Structural Geology* 22, 1221–1231.

Guðmundsson, Á. 2000d. Dynamics of volcanic systems in Iceland: Example of tectonism and volcanism at juxtaposed hot spot and mid–ocean ridge system. *Annual Review of Earth and Planetary Sciences* 28, 107–140.

Guðmundsson, Á. 2000e. Fault slip and groundwater transport. In: Abstracts from the XXIV Nordic Geological Winter Meeting, Trondheim, Norway.

Guðmundsson, Á. 2000f. Propagation of hydrofractures in a layered rock mass. In: Abstracts from a Meeting on Hydrogeology and Environmental Geochemistry, Trondheim, Norway. The Geological Survey of Norway.

Guðmundsson, Á. 2000g. Effect of fault slip on the flow of crustal fluids. In: *Annales Geophysicae*. Abstracts from the XXV EGS General Assembly, Nice, France, April 25–29, 2000.

Guðmundsson, Á. 2000h. Magma flow beneath the volcanic zones of Iceland. In: *Annales Geophysicae*. Abstracts from the XXV EGS General Assembly, Nice, France, April 25–29, 2000.

Guðmundsson, Á. Displacement and stresses of arrested hydrofractures. *Tectonophysics*, in preparation.

Guðmundsson, Á. & C. Homberg 1999. Evolution of stress fields and faulting in seismic zones. *Pure and Applied Geophysics* 154, 257–280.

Guðmundsson, Á., S.S. Berg, K.B. Lyslo & E. Skurtveit 2000. Fracture networks and fluid transport in active fault zones. *Journal of Structural Geology*, in press.

Henriot, O., T. Villemin & F. Jouanne 1998a. Surface deformation at the Tjörnes rift–transform junction (North Iceland) computed from SAR images. In: *Annales Geophysicae*. Abstracts from the XXIII EGS General Assembly, Nice, France, April 20–24, 1998.

Henriot, O., T. Villemin & F. Jouanne 1998b. Cartographie de la déformation de surface par interférométrie radar: l'exemple de la jonction rift transformante de Tjörnes. Colloque Mouvements Actuels de la Surface Terrestre, October 5–6, 1998. Ecole de Physique des Houches.

Henriot, O., T. Villemin & F. Jouanne 1999a. Seismic risk in northern Iceland: (2) deformation maps of the Tjörnes peninsula computed from INSAR. In: Abstracts from the tenth biennial EUG meeting, Strasbourg, France, March 28 - April 1, 1999.

Henriot, O., T. Villemin & F. Jouanne 1999b. Seismic risk in northern Iceland: Deformation maps of Tjörnes computed from INSAR. Fringe'99, Liège, Belgium, November 10–12, 1999.

Henriot, O., T. Villemin & F. Jouanne 2000. Long period interferograms reveal 1992–1998 steady rate of deformation at Krafla volcano (North Iceland). *Geophys. Res. Lett.*, in

press.

Henriot, O. & T. Villemin. The Krafla fissure swarm, northern Iceland: the end of the subsidence due to the postrifting cooling of magma? In preparation.

Jouanne, F., T. Villemin, V. Ferber, C. Maveyraud, J. Ammann, O. Henriot & J.-L. Got 1999. Seismic risk at the rift–transform junction in North Iceland. *Geophys. Res. Lett.* 26(24), 3689.

Lyslo, K.B. & Á. Guðmundsson 2000. Permeability and stress concentration around active faults. In: Abstracts from a Meeting on Hydrogeology and Environmental Geochemistry, Trondheim, Norway. The Geological Survey of Norway.

Skurtveit, E. & Á. Guðmundsson 1999. Hydromechanical infrastructure of a major fault zone in Iceland. In: Abstracts from a Meeting on Hydrogeology and Environmental Geochemistry, Trondheim, Norway. The Geological Survey of Norway.

Villemin, T., F. Jouanne & GPS–TFZ Team 1998. 1995–1997 surface deformation along the Húsavík–Flatey transform fault and around its junction with the northern volcanic zone in Iceland. In: *Annales Geophysicae.* Abstracts from the XXIII EGS General Assembly, Nice, France, April 20–24, 1998.

Villemin, T., F. Jouanne & O. Henriot 1999. Seismic risk in northern Iceland: (1) locking of the Húsavík fault deduced from GPS. In: Abstracts from the tenth biennial EUG meeting, Strasbourg, France, March 28 - April 1, 1999.

Villemin, T. & O. Henriot. Active faulting in the Theistareykir fissure swarm, northern Iceland. In preparation.

Villemin, T. & F. Jouanne. Active deformation in northern Iceland at the rift transform junction: a dynamic system in rapid evolution. In preparation.

Villemin, T., G. Ouillon & V. Ferber 2000. Processes of fractures pattern evolution deduced from field data: the Krafla fissure swarm and the last rifting episode in North Iceland. *J. Geophys. Res.*, submitted.

Subproject 7

Belardinelli, M.E., M. Bonafede & Á. Guðmundsson 2000. Secondary earthquake fractures generated by a strike–slip fault in the South Iceland seismic zone. *J. Geophys. Res.* 105, 13613–13630.

Bonafede, M. & N. Cenni 1998. A porous flow model of magma migration within Mt. Etna: the influence of extended sources and permeability anisotrophy. *J. Volcanol. Geotherm. Res.* 81, 51–68.

Bonafede, M. & M. Mazzanti 1998. Modelling gravity variations consistent with ground deformation in the Campi Flegrei caldera. *J. Volcanol. Geotherm. Res.* 81, 137–157.

Bonafede, M. & E. Rivalta 1999a. The tensile dislocation problem in a layered elastic medium. *Geophys. J. Int.* 136, 341–356.

Bonafede, M. & E. Rivalta 1999b. On tensile cracks close to and across the interface between two welded elastic half–spaces. *Geophys. J. Int.* 138, 410–434.

Bonafede, M. & A. Neri 2000. Effects induced by an earthquake on its fault plane: a

boundary element study. *Geophys. J. Int.* 141, 43–56.

Bonafede, M., B. Parenti & E. Rivalta 2000. Strike–slip faulting in layered media. *Geophys. J. Int.*, submitted.

Bonafede, M. & E. Rivalta. The stress–drop discontinuity condition: implications for fault complexities in transform boundaries. In preparation.

Bonafede, M. & E. Rivalta. Dip–slip faulting in layered media. In preparation.

Roth, F. 1998. Modellrechnungen zu den plattentektonischen, insbesondere seismotektonischen Spannungen auf Island (model calculations on plate tectonic and especially seismotectonic stresses on Iceland). Paper presented at the 4th workshop of the FKPE working group on Borehole Geophysics and Rock Physics, Hannover, Germany.

Roth, F. 1999a. Stress changes in space and time at the South Iceland seismic zone - model calculations. Poster on the Workshop on Recurrence of Great Interplate Earthquakes and its Mechanism, Kochi, Shikoku, Japan, January 20–22, 1999. Japan Science and Technology Agency.

Roth, F. 1999b. Entwicklung des tektonischen Spannungsfeldes im Süden Islands - Modellierung einer Erdbebenserie (development of the tectonic stress field in the south of Iceland - modelling of an earthquake series). In: *Proceedings of the 59th Annual Meeting of the German Geophysical Society*, Braunschweig, Germany.

Roth, F. 1999c. Stress changes in space and time at the South Iceland seismic zone - model calculations. In: Abstracts from the tenth biennial EUG meeting, Strasbourg, France, March 28 - April 1, 1999.

Roth, F. 1999d. Erforschung von Erdbeben auf Island (research about earthquakes on Iceland). Paper presented at the Institute of Geophysics, University of Hamburg, Germany.

Roth, F. 1999e. Stress changes in space and time at the South Iceland seismic zone - model calculations. In: *Proceedings of the Workshop on Recurrence of Great Interplate Earthquakes and its Mechanism*, Kochi, Shikoku, Japan, January 20–22, 1999. Japan Science and Technology Agency, 22–32.

Roth, F. 1999f. Stress changes at the South Iceland seismic zone - a model from 1706 up to the present for better hazard estimation. In: Abstracts from the XXII IUGG General Assembly, Birmingham, United Kingdom, July 18–30, 1999.

Roth, F. 2000. Stress changes in the South Iceland transform zone due to strong earthquakes and forcing from the adjacent rifts. In: Abstracts from the XXVII ESC General Assembly, Lisbon, Portugal, September 10–15, 2000.